Poly(ether block amide)-based Composite Membranes for Carbon Capture

by

Silu Chen

A thesis

presented to the University of Waterloo

in fulfillment of the

thesis requirement for the degree of

Doctor of Philosophy

in

Chemical Engineering

Waterloo, Ontario, Canada, 2020

Author's Declaration

I hereby declare that I am the sole author of this thesis. This is a true copy of the thesis, including any required final revisions, as accepted by my examiners.

I understand that my thesis may be made electronically available to the public.

Abstract

A great amount of anthropogenic CO_2 emissions has caused the greenhouse effect which impacts the living environment of creatures on the planet. Effective carbon capture technologies need to be developed to reduce CO_2 emissions. Membrane separation technology can be applied in carbon capture due to its advantages in energy conservation and pollution prevention. Poly(ether block amide)-based (PEBAX 1657) composite membranes were developed for carbon capture in separating CO_2/N_2, CO_2/CH_4, and CO_2/H_2 mixtures in this study.

Polyvinylamine/PEBAX (PVAm/PEBAX) blend membranes were prepared for carbon capture by a solution casting method. The presence of PVAm enhanced membrane hydrophilicity and gas solubility. When the mass ratio of PVAm to PEBAX reached 0.025, the blend membrane showed a CO_2 permeability of 600 Barrer at 298 K and a feed gas pressure of 400 kPa, while the CO_2/N_2, CO_2/CH_4, and CO_2/H_2 ideal gas selectivity remained comparable with pristine PEBAX membrane.

Diethanolamine/PVAm/PEBAX (DEA/PVAm/PEBAX) composite membranes were fabricated on polysulfone substrate membranes. The structures of the composite membranes not only improved gas permeance due to reducing the thickness of the permselective layer but also provided great mechanical strength. DEA can increase membrane hydrophilicity. The DEA/PVAm/PEBAX composite membrane with a mass fraction of DEA in the membrane of 0.2 exhibited a CO_2 permeance of 12.5 GPU which was higher than the PEBAX composite membrane (6.24 GPU). The CO_2/N_2, CO_2/CH_4, and CO_2/H_2 selectivity was 42.3, 22.9, and 12.1 at room temperature and 700 kPa.

NH_4F/PEBAX membranes were developed by a solution casting method. The introduction of F^- affected the permeabilities of N_2, CH_4, and H_2 in the membranes more significantly than CO_2 permeability due to the salting-out effect. On the other hand, F^- made water molecules more basic owing to the hydrogen bonds, which was more favorable for CO_2 dissolution in the membranes. Compared to pristine PEBAX membrane, the selectivities CO_2/N_2, CO_2/CH_4, and

CO_2/H_2 in the NH_4F/PEBAX(0.1) membrane were 54%, 13%, and 22% higher, respectively, and the CO_2 permeability was 372 Barrer at room temperature and 700 kPa.

Mixed matrix membranes were fabricated by embedding amino-modified multi-walled carbon nanotubes (MWCNTs) as a dispersed phase in a PEBAX polymer matrix. After acid treatment, MWCNTs were modified by polydopamine (PDA) through self-polymerization of dopamine (DA). The catechol groups can react with amine groups on branched polyethylenimine (PEI) by the Michael addition reaction and Schiff base reaction. The addition of MWCNT-PDA-PEI can facilitate CO_2 transport and adjust membrane structures. When the mass ratio of MWCNT-PDA-PEI to PEBAX was 0.08, the CO_2 permeability of the prepared MMM was 2.4-fold of that of the PEBAX membrane, while the selectivities of CO_2/N_2, CO_2/CH_4, and CO_2/H_2 at room temperature and 300 kPa were 107, 26, and 11, respectively.

Keywords: PEBAX; carbon capture; water-swollen membranes; salting-out effect; mixed matrix membranes; solution-diffusion mechanism; facilitated transport of CO_2

Acknowledgments

It takes at least 13 hours to fly from Beijing to Toronto, and the distance between Shanxi province and Ontario province is around 10027 km. It takes 4 years to complete a Ph.D. program, but the distance between the beginning and the ending of this journey can not be measured easily. It is a quite valuable and meaningful experience for me to study and live in this country. Many people accompany and support me on this journey, and I would love to give my sincere gratitude to them.

I want to thank Dr. Xianshe Feng for giving me this precious chance to study at the University of Waterloo. During the four-year study, he teaches me lots of knowledge, guides my research works, and broadens my scientific visions in membrane separation. His invaluable advice and encouragement helped me solve problems and get through the difficult time. A great teacher not only teaches you knowledge but also how to be a good person. Dr. Feng is always responsible and his attitudes to work affect me a lot. I am so honored and lucky to have him as my supervisor in my Ph.D. study.

I want to express my gratitude to my Ph.D. examination committee members: Prof. Shuhui Sun of the Institut National de la Recherche Scientifique (INRS), Prof. John Wen of Mechanical Engineering, and Prof. Christine Moresoli and Prof. Boxin Zhao of Chemical Engineering, for providing valuable suggestions regarding my research.

I am deeply thankful to all the people who helped me in my study at UW. When I joined the lab, Dr. Dihua Wu, Dr. Boya Zhang, Dr. Shuixiu Lai, and Bo Qiu helped me set up my experiments. Xiaotong Cao, Xuezhen Wang, Jiaxin Xu, Dr. Elnaz Halakoo, Dr. Yijie Hu, Prof. Miaoqing Liu, Yiran Wang, and Zhelun Li offered me numerous help and support in my research. I would like to thank all my friends for their encouragement and being accompanied in my life in UW.

Financial support from the China Scholarship Council and the University of Waterloo is deeply acknowledged. The research was supported by the Natural Sciences and Engineering

Last but not least, I would like to express my great gratitude to my dearest parents and brothers for their selfless love. They are always supportive in my life, standing by me, and giving me the power to move forward.

The kindness of all people named or not named here will be always in my mind and heart. Although we might be apart or together sometimes, I hope we all can live in the way you really want to live. The Ph.D. study at UW finished, and I will start a new journey and be a better man.

Dedication

This is dedicated to my dearest parents and brothers.

Table of Contents

List of Tables

List of Figures

xv

List of Symbols

Chemicals

A	Membrane area, cm^2
c	Concentration
D	Diffusion coefficient, $cm^2\ s^{-1}$
$E_{p,i}$	Activation energy for permeation of component i, $kJ\ mol^{-1}$
J	Permeance, GPU (1 GPU = $10^{-6}\ cm^3\ (STP)\ cm^{-2}\ s^{-1}\ cm\ Hg^{-1}$)
l	Membrane thickness, cm
P	Permeability coefficient, Barrer
	(1 Barrer = $10^{-10}\ cm^3\ (STP)\ cm\ cm^{-2}\ s^{-1}\ cm\ Hg^{-1}$)
$P_{0,i}$	Pre-exponential factor, Barrer
p	Gas pressure, $cmHg$
p_{feed}	Feed gas pressure, $cm\ Hg$
p_{perm}	Permeate gas pressure, $cm\ Hg$
Q	Gas flow rate, $cm^3\ s^{-1}$
q	Amount of gas flow per unit area per unit time
R	Ideal gas constant, $kJ\ mol^{-1}\ K^{-1}$
S	Solubility coefficient, $cm^3(STP)\ cm^{-3}\ cm\ Hg$
T	Temperature, K
X	Position in the membrane

$x_{feed,i}$	Mole fraction of component i in the feed gas
$x_{perm,i}$	Mole fraction of component i in the permeate gas

Greek letters

$\alpha_{i/j}$	Selectivity or separation factor between gas component i and j
Δp	Pressure difference across the membrane, $cm\ Hg$

Subscripts

1	Position of the feed side
2	Position of the permeate side
$feed$	Feed gas
i	Gas component i
j	Gas component j
$perm$	Permeate gas

List of Abbreviations

AMP 2-Amino-2-methyl-1-propanol

CMCS Carboxymethyl chitosan

CNT Carbon nanotube

COF Covalent organic framework

DA Dopamine

DEA Diethanolamine

EDA Ethanediamine

GO Graphene oxide

MDEA N-methyldiethanolamine

MEA Monoethanolamine

MMM Mixed matrix membrane

MOF Mental organic framework

MWCNT Multi-walled carbon nanotubes

PA6 Polyamide, Nylon-6

PAA Polyallylamine

PAN Polyacrylonitrile

PANI Polyaniline

PC Polycarbonate

PDA Polydopamine

PDMS	Polydimethylsiloxane
PE	Polyether
PEBAX	Poly(ether block amide)
PEG	Polyethylene glycol
PEGDA	Poly(ethylene glycol) diacrylate
PEGMEA	Poly(ethylene glycol) methyl ether acrylate
PEI	Polyethylenimine
PEO	Poly(ethylene oxide)
PEP	Poly(2,3-epoxy- 1-propanol)
PI	Polyimide
PIP	Piperazine
PSf	Polysulfone
PTFE	Polytetrafluoroethylene
PTMEO	Poly(tetramethylene oxide)
PU	Polyester
PVA	Polyvinyl alcohol
PVAm	Polyvinylamine
PVP	Poly(vinylpyrrolidone)
SWCNT	Single-walled carbon nanotubes
TDI	2,4-Toluylene diisocyanate
ZIF	Zeolite imidazole framework

Chapter 1

Introduction

1.1 Background

The CO_2 content in the atmosphere has increased dramatically in recent years due to the increased consumption of fossil fuels including petroleum, coal, and natural gas. The greenhouse effect results in an increasing temperature on the planet which impacts the survival of creatures in many aspects. These CO_2 emissions are mainly from human activities, and it is necessary to apply carbon capture technologies to reduce anthropogenic CO_2 emissions. Natural gas sweetening, oxy-combustion, pre-combustion and post-combustion are effective strategies for carbon capture in industries [MacDowell et al. (2010); Kunze and Spliethoff (2012)]. Adsorption, absorption, and membrane separation technologies can be utilized in carbon capture. Membrane separation technology possesses great advantages and has demonstrated its strong vitality and competitiveness in terms of technological advancement, energy conservation, and pollution prevention and control [Bernardo et al. (2009)]. The separation of different components is achieved because of the different permeation rates of components through a membrane under a certain driving force which is pressure difference across the membrane. Membrane materials are the core of membrane separation technology. There are two important parameters for separation

1

membranes: permeability and selectivity. Permeability is a measure of the permeable properties of a gas, while the selectivity shows preferential permeation of one gas component over the other. Membranes with a large gas permeability and high selectivity are considered as high-performance membranes. These properties are determined by the chemical and physical nature and the structure of the membrane materials [Rezakazemi et al. (2014)].

Membranes can be divided into symmetric and asymmetric membranes based on their structures. Symmetric membranes are isotropic, while asymmetric membranes contain a thin permselective layer and a substrate. Asymmetric membranes include Loeb-Sourirajan membranes and composite membranes. In terms of membrane materials, membranes can be classified as inorganic, organic and mixed matrix membranes (MMMs). Zeolite-based inorganic membranes can withstand the harsh chemical environment and exhibit excellent gas selectivity. However, large scale manufactures are still difficult. Organic membranes are made of various polymeric materials and show great flexibility and potential industrial application. Based on a large number of experimental data of the gas separation performance of the polymer membranes in the literatures, Robeson (1991) summarized the empirical upper limit relationship between gas permeability and selectivity and updated this upper limit in 2008 [Robeson (2008)]. This is so-called the Robeson's upper bound. The trade-off relationship between permeability and selectivity often restricts the further improvement of gas separation performance. MMMs are utilized to break the Robeson's upper bound by combining more than one material with distinct properties. Polymeric materials are usually selected as a matrix and other materials are embedded into it as a dispersed phase. In spite of various advantages, MMMs suffer from many issues, *e.g.*, filler dispersion, interfacial compatibility, high capital cost [Chung et al. (2007)]. To design a high-performance membrane material, it is necessary to understand the transport mechanism within the membrane. The transport of gas molecules in porous membranes mainly includes Knudsen diffusion, surface diffusion, and molecular sieving separation. The transport mechanism of gas molecules in dense membranes is divided into the solution-diffusion mechanism and facilitated transport of CO_2 [Wijmans and Baker (1995); Meldon et al. (2011)]

Poly(ether block amide) copolymers are easy to synthesize and some have been commercialized (trade name PEBAX$^{®}$) [Chen et al. (2004)]. They are composed of soft polyether (PE) segments and hard polyamide (PA) segments. PE segments are responsible for gas selectivity due to dipole-quadrupole interactions with CO_2, while PA segments provide favorable mechanical properties. Various types of PEBAX polymers have been used in preparing gas separation membranes. Among them, PEBAX 1657 contains around 60 wt% poly(ethylene oxide) (PEO) segments and around 40 wt% Nylon-6 (PA6) segments and shows profound application prospects. In addition, PEBAX 1657 has good hydrophilicity and mechanical property [Car et al. (2008b); Chen et al. (2017); Li et al. (2013)]. Hence, all PEBAX-based membranes used in this thesis were prepared in the lab. Polyvinylamine (PVAm) contains numerous amine groups on its polymer chains and can be dissolved in water easily. Amine groups on the polymer chains can act as CO_2 carriers via reversible reaction with CO_2 to facilitate its transportation. PVAm membranes are brittle owing to high crystallinity, and high crystallinity could decrease gas permeability [Yi et al. (2006)]. Thus, they are usually used along with other polymers by physical blending or chemical crosslinking to reduce the crystallinity of PVAm [Yi et al. (2006); Deng and Hagg (2010); Qiao et al. (2015)]. Hence, PEBAX and PVAm can be combined to prepare water-swollen membranes. Water-swollen membranes are hydrophilic, which is favorable to gas permeability especially when the gas is humid. The structures of water-swollen membranes are loosened, which is beneficial for gas diffusion. Liu et al. (2008) studied the permselectivity of various water-swollen membranes and showed that water molecules in the membrane can not only act as a plasticizer to make polymer chains flexible but also provide pathways for gas transport. Deng and co-workers studied the relationship between gas permeance and relative humidity in the feed gas. The swelling behavior was found to depend on the relative humidity of the operating environment. Membrane swelling was beneficial not only to the diffusion of gas molecules and solutes which were dissolved in the membranes but also to the solubility of gas molecules in the membranes [Deng and Hagg (2010)]. As a result, the enhancement of membrane hydrophilicity with the addition of PVAm can reinforce gas permeability.

3

However, water-swollen membranes can lose mechanical strength when the amounts of water are excessive. Composite membranes can maintain a good mechanical property because the substrate provides a support to the permselective layer. Thinner selective layer can provide higher gas permeance which is important for practical applications. With a high content of PVAm in the membranes, the crystallinity of PVAm could be severe due to strong intermolecular interactions. Small molecule amines can be an alternative option instead of polymeric amines. Similar to PVAm, small molecule amines can serve as mobile CO_2 carriers. Thus, they move more flexibly than PVAm due to the low molecular weights. Small molecule amines (*e.g.*, monoethanolamine (MEA), diethanolamine (DEA), N-methyldiethanolamine (MDEA), 2-amino-2-methyl-1-propanol (AMP), ethanediamine (EDA), and piperazine (PIP) were blended into polymer membranes to facilitate CO_2 transport [Francisco et al. (2007, 2010); Qiao et al. (2015)]. However, the solution-diffusion mechanism dominates the gas permeation in the water-swollen membranes. The addition of small molecule amines can still reduce the crystallinity of PVAm and enhance membrane hydrophilicity.

Membrane swelling is beneficial for gas diffusion but difficult to achieve a high selectivity. The loosen and swollen structures of membranes make polymer chains less compacted and decrease the molecule-sieving ability. In order to reduce membrane swelling, polymers are always crosslinked to reinforce membrane selectivity. The alkali or alkaline-earth metal salts in polymer electrolyte membranes were used as crosslinking agents due to complexation interaction between salts and polymer chains [Li et al. (2014)]. The interactions were weaker than chemical bonds, so the hydrophilicity of the membrane is not compromised dramatically. F^- ions have been treated as CO_2 carriers in some facilitated transport membranes [Kim et al. (2004); Zhang and Wang (2012); Ji et al. (2010); Quinn et al. (1997)]. The strong interactions between F^- and H_2O due to the high electronegativity of F^- resulted that water molecules became more basic, which increased CO_2 solubility in the membranes. Moreover, the salting-out effect caused by F^- could effectively reduce the solubility of non-polar gases [Zhang and Wang (2012)]. Thus, F^- has multiple effects that can be used to adjust membrane structures and improve gas selectivity.

MMMs offer a novel approach to breaking the Robeson's upper bound and extending the choices of membrane materials. The fillers in the polymer matrix include graphene oxide [Shen et al. (2016); Li et al. (2015a)], carbon nanotubes [Murali et al. (2010); Wang et al. (2014)], zeolites [Suer et al. (1994); Husain and Koros (2007)], mental organic frameworks (MOFs) [Basu et al. (2011); Ordonez et al. (2010)], covalent organic frameworks (COFs) [Kang et al. (2016); Biswal et al. (2016)]. Carbon nanotubes have high flexibility, low density, large aspect ratio (>1000) as well as good mechanical, thermal, and electrical properties. There are multi-walled carbon nanotubes (MWCNTs) and single-walled carbon nanotubes (SWCNTs). Murali et al. (2010) embedded MWCNTs into PEBAX membranes to improve gas permeability, and the 2,4-toluylene diisocyanate crosslinked MWCNT/PEBAX could further improve gas selectivity. MWCNTs tend to form bundles owing to the van der Waals interactions between MWCNTs. The surface of MWCNTs can be modified for improved dispersion in the matrix to improve the interfacial compatibility between polymer and fillers [Zhao et al. (2017); Wang et al. (2016); Habibiannejad et al. (2016)]. Dopamine (DA) can self-polymerize to form polydopamine (PDA) on the surface of MWCNTs, and it is an easy and feasible method to achieve amino-modification. The introduction of amine groups can facilitate CO_2 transport, but the amounts of amine groups on PDA are limited. Hence, branched polyethylenimine (PEI) with abundant amine groups can be modified on MWCNTs by the Michael addition reaction and Schiff base reaction between amine groups on PEI and the catechol groups on PDA. The amine-modified MWCNTs can not only improve interface interaction but also facilitate CO_2 transport in the membranes.

1.2   Research objectives

The main purpose of this research was to fabricate PEBAX-based composite membranes with high gas permeability and selectivity in CO_2/N_2, CO_2/CH_4, and CO_2/H_2 separations. The composite membranes in this project were not only referred to as the membranes which were prepared using different materials but also the asymmetric structure of the membrane which was composed of a

selective layer and a substrate. As shown in Figure 1.1, three directions were selected to break the Robeson's upper bound. Improving membrane hydrophilicity is benefit for gas diffusion in the membranes, so the water-swollen membranes with polymeric amines (PVAm) and small molecule amines (DEA) were prepared to increase CO_2 permeability. The salting-out effect caused by the addition of NH_4F can reduce gas solubility in the membranes, but the hydrogen bonds between F^- and H_2O can make water molecules become more basic to increase CO_2 solubility in the membranes. Hence, the $NH_4F/PEBAX$ membranes were prepared to improve gas selectivity. Due to the reversible reaction between CO_2 and amine groups, the amine-modified MWCNTs can be blended in the membranes to facilitate CO_2 transport to improve both gas permeability and selectivity.
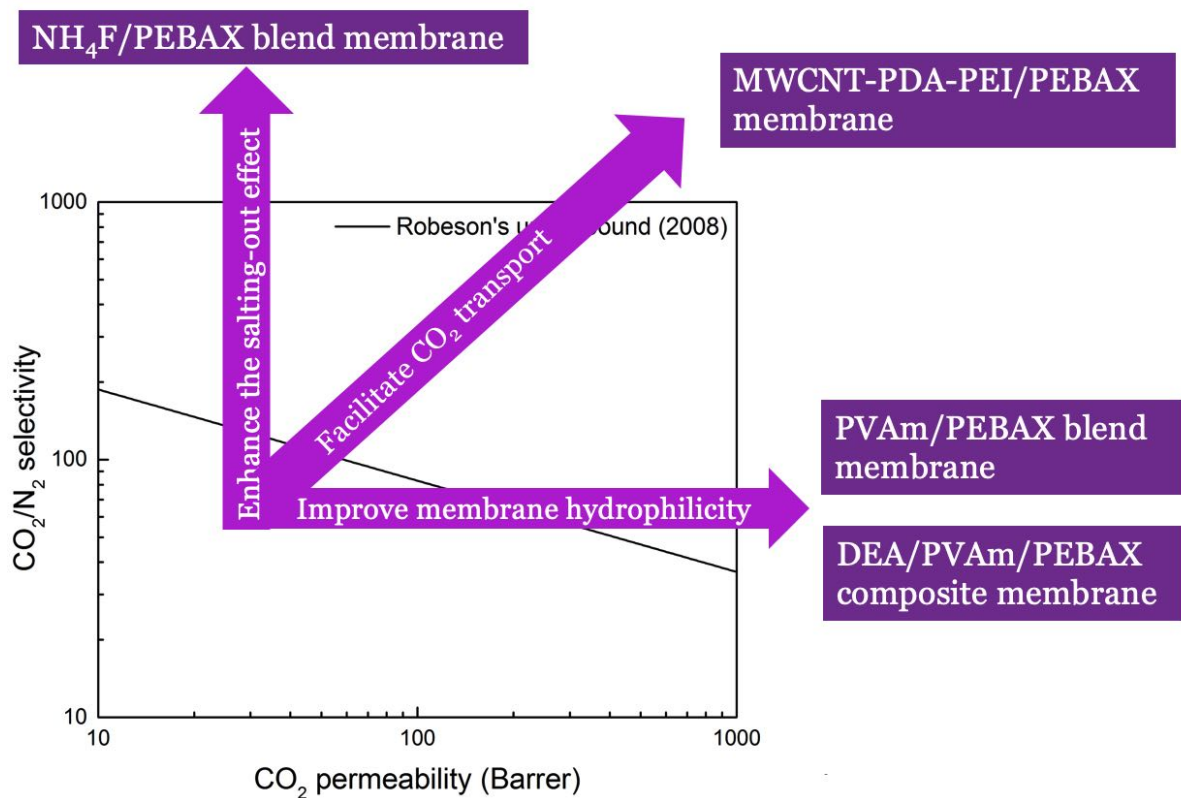
Figure 1.1: Objectives of the thesis

6

1.3 Outline of the thesis

The thesis consists of seven chapters as follows:

Chapter 1 introduces the background of this study. The improvement of different aspects of the PEBAX membranes through various approaches is described. The objectives of this study are presented as well.

Chapter 2 presents a literature review of membranes for gas separation. Carbon capture technologies are introduced. The structures, transport mechanisms, and materials of gas separation membranes are described. Besides, the research work based on PEBAX membranes is discussed.

Aiming at the enhancement of membrane hydrophilicity and gas permeability, water-swollen membranes were prepared in Chapters 3 and 4. Chapter 3 studies the PVAm/PEBAX blend membranes for carbon capture. Chapter 4 shows the gas permeation performance of the PEBAX/PVAm/DEA composite membranes. Membranes with polymeric amines and small molecule amines improved gas permeability but little gas selectivity. Hence, Chapter 5 develops polymer electrolyte membranes with PEBAX and NH_4F in order to enhance the gas selectivity of the membranes. Facilitated transport of CO_2 can enhance the gas selectivity of the membranes as well. Chapter 6 presents the preparation of PDA and PEI modified MWCNTs. MMMs composed of amine-modified MWCNTs as a dispersed phase and PEBAX as a polymeric matrix were fabricated. In these four chapters, the effects of membrane composition and operating conditions (*e.g.*, temperature and feed pressure) on pure gas permeation performance of N_2, CH_4, H_2, and CO_2 were studied. The mixture gas permeation and stability of the prepared membranes for CO_2/N_2, CO_2/CH_4, and CO_2/H_2 separations were investigated as well.

Chapter 7 summarizes the general conclusions and contributions from this study. Some recommendations for future works are included as well. In order to have a clear understanding of this thesis, Figure 1.2 shows the structure of this thesis:
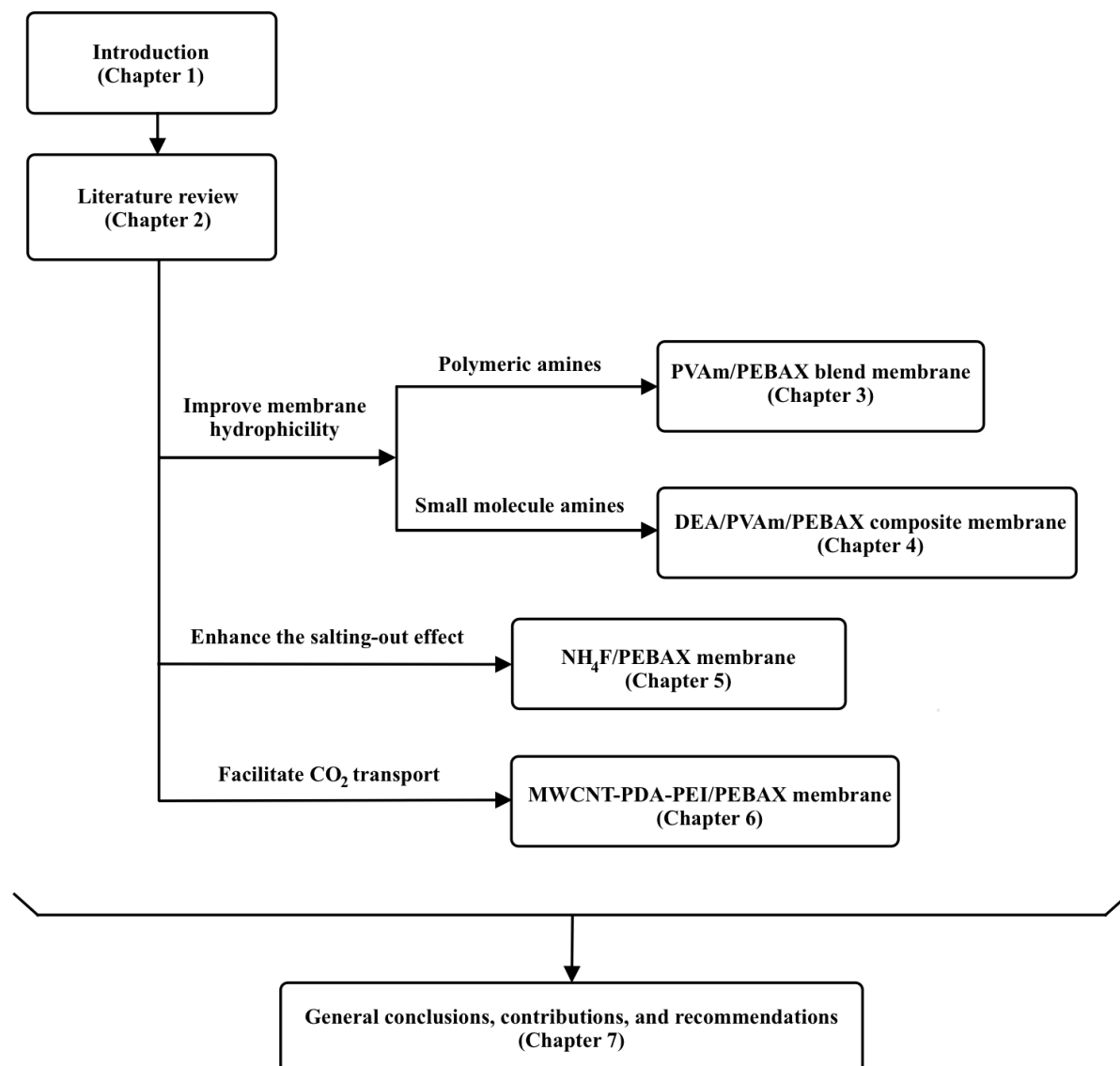
Figure 1.2: Thesis structure illustrated in terms of chapters and content relevance

Chapter 2

Literature review

2.1 Greenhouse effect

CO_2 is the main greenhouse gas produced by human activities. It's predicted that the intensification of human activities would increase CO_2 concentration in the atmosphere from 270 ppm before the industrial revolution to 550 ppm in 2050. CO_2 emissions and accumulation cause global warming. CO_2 emissions come from a variety of human activities, the most important of which is the burning of fossil fuels [Bernardo et al. (2009); Jeon and Lee (2015); Yang et al. (2008)]. 44% of emissions come from the consumption of fossil fuels such as oil, coal, and natural gas. However, it is unlikely to have a huge change in the global energy consumption structure in the coming decades [MacDowell et al. (2010); Raupach et al. (2007)]. The greenhouse effect becomes severe with a large amount of anthropogenic CO_2 emissions. On the one hand, global warming will have an impact on the environment. For example, extreme weather has become frequent in recent years, the ecological environment both on land and in the sea has been destroyed at different levels, sea levels have risen, the living environment has deteriorated, and species diversity has decreased. On the other hand, the greenhouse effect also has an impact on human health. For example, some microorganisms will multiply faster in a high-temperature

environment, which in turn will lead to some uncontrollable infectious diseases [McMichael et al. (2006)]. Therefore, the greenhouse effect has brought many challenges to the survival of all creatures on the planet. It is necessary and urgent to take action to save energy and reduce the amount of CO_2 emissions.

2.2 Carbon capture from gas sources

2.2.1 Gas sources

CO_2 emissions from various gas sources need to be controlled and reduced to mitigate the impact of the greenhouse effect on global ecosystems. CO_2 capture technologies can be applied in natural gas sweetening and power generation processes that involve fossil fuels.

In the exploitation of natural gas, the raw natural gas mainly contains CH_4, C_2H_6, C_3H_8, C_4H_{10} and other hydrocarbons. It also contains such impurities as CO_2 (usually 5-30%), H_2S, N_2, and heavier hydrocarbons. The presence of these compounds will affect the combustion quality of natural gas and must be removed to meet the requirements of pipeline transportation. Therefore, CO_2/CH_4 separation is necessary to meet practical production requirements [Bernardo et al. (2009)].

Post-combustion carbon capture can be applied to the removal of CO_2 from flue gas (Figure 2.1). At present, the power plant uses air for combustion. After combustion, flue gas containing about 15% of CO_2 is generated. The partial pressure of CO_2 is usually less than 0.15 atm, so the driving force for separation is low. Despite all the difficulties, two-thirds of the CO_2 emissions can be reduced at least if the post-combustion carbon capture can be fully applied and integrated into the power plant process [Kunze and Spliethoff (2012); Figueroa et al. (2008); Ramasubramanian et al. (2013)]. Oxy-combustion is another an important carbon capture technology [Kunze and Spliethoff (2012)]. As shown in Figure 2.2, the fuel is burned in the environment composing purified O_2 and recycled flue gas. O_2 is separated from air to prevent N_2 in the system. This

combustion process mainly generates CO_2 and H_2O. The water can be easily removed by condensation, and the remaining CO_2 can be further separated or stored [Ramasubramanian et al. (2013)]. The CO_2 concentration in the pre-combustion carbon capture is high (about 40%) and the operating pressure is high (about 6500 kPa). As shown in Figure 2.3, the coal-fired power plant uses oxygen as an oxidant, and the coal is first gasified and converted into a mixture of CO and H_2 (syngas). After the CO_2 and H_2 are separated, H_2 is mixed with the O_2 produced by the previous air separation unit before entering the combustion system [Descamps et al. (2008); Kunze and Spliethoff (2012); Ramasubramanian et al. (2013)].
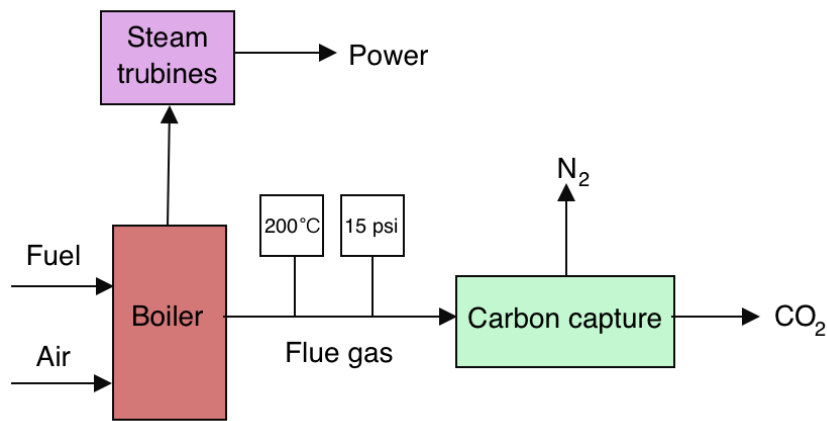
Figure 2.1: Post-combustion carbon capture system [Figueroa et al. (2008)]
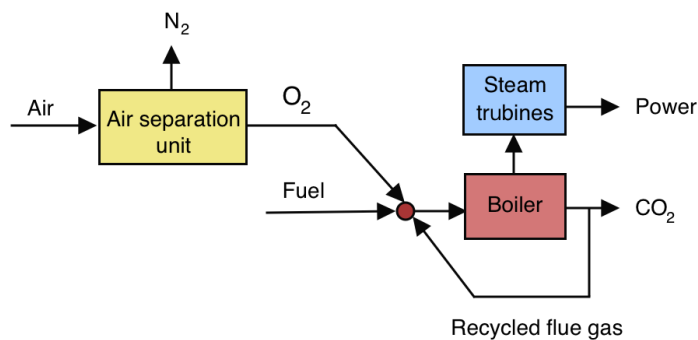
Figure 2.2: Oxygen-combustion system [Figueroa et al. (2008)]

11
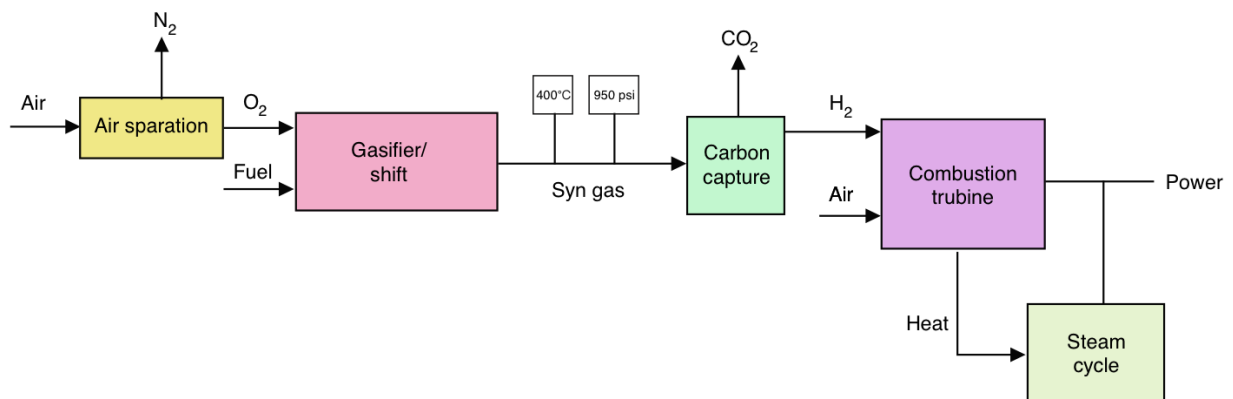
Figure 2.3: Pre-combustion carbon capture system [Figueroa et al. (2008)]

2.2.2 Carbon capture technology

Based on all these strategies, gas separation methods including adsorption, absorption, and membrane separation have been developed. Many materials for carbon capture have been applied and studied. These three technologies for carbon capture are introduced below.

Adsorption

Most of the adsorbents have a large specific surface area, a loose and porous structure, and an easy regeneration property. Zeolites, carbon materials, and metal organic framework (MOF) can be used in adsorption [D'Alessandro et al. (2010)]. Gas separation properties of zeolite adsorbents depend on the size, charge density, and distribution of metal cations in the porous structure [Zhao et al. (1998)]. Comparing with zeolite materials, activated carbon materials possess an advantage of low raw material cost which have the potential for large scale industrial applications [Choi et al. (2009)]. Besides, metal organic framework (MOF) has a very high porosity, large specific surface area, ordered porous structure, and can be chemically modified easily [Millward and Yaghi (2005)]. Although MOF materials have significant adsorption capacity and gas separation performance, their costs are high and not suitable for industrial applications at present.

Absorption

Absorption may be based on physical absorption or chemical absorption, and it is a relatively mature technology for CO_2 separation [MacDowell et al. (2010); Yu et al. (2012)]. Physical absorption utilizes absorbents, such as water and methanol in the Rectisol process, to separate CO_2 from a gas mixture. Chemical absorption is based on the reversible chemical interaction between the absorbents (*e.g.*, ethanolamines or ionic liquids) and CO_2. Monoethanolamine (MEA) is the most widely used CO_2 absorbent among all organic amines [Rochelle (2009)]. Absorption has a high capacity and separation performance, but both the operating costs and the energy consumption for CO_2 desorption are high. Besides, liquid amine absorbents are highly corrosive to the absorption equipment.

Membrane separation

Membrane separation has been developed in the past decades and is widely applied in wastewater treatment, seawater desalination, and gas separation. The concept of gas separation membrane was first proposed by Graham in 1866. Loeb and Sourirajan first prepared asymmetric membranes for reverse osmosis in 1961 [Kentish et al. (2008); Koros and Fleming (1993)]. The first industrial application of the gas separation membrane was commercialized for hydrogen recovery in 1977 [Koros and Fleming (1993)]. With technological advances, membrane separation technology has become more and more commercially competitive as compared with conventional separation processes. At present, gas separation membranes are mainly used in air separation (greater than 99.5% of N_2 production and O_2 enrichment), recovery of hydrogen from ammonia purge gas, and removal of CO_2 from natural gas [Rezakazemi et al. (2014); Du et al. (2012); Lin and Freeman (2005); Yu et al. (2008)]. In general, membranes are assembled as an element which is called a membrane module or a permeator. There are different membrane modules: plate and frame, spiral-wound, and hollow fiber membrane modules. The hollow fiber module is widely used in industrial applications due to the high membrane area per unit volume. Cellulose acetate-based

CO_2 separation membranes were developed in the 1960s, and the membrane plants were installed and operated in the 1980s [Koros and Fleming (1993)]. Companies involving gas separation membranes include Air Products, Air Liquide, and Praxair, and the membranes are not only for air separation but also for the generation of high-purity hydrogen. UOP, Natco, Kvaerner and other companies are mainly developing membrane processes related to the separation of natural gas.

Compared with traditional gas separation technology, membrane separation provides a green, low operating cost, low energy consumption, and advanced technology without phase change [Rezakazemi et al. (2014)]. In order to make the membrane separation more industrially competitive, the development of high permeability and selectivity membrane materials is crucial. Therefore, membrane separation for carbon capture was investigated in this study.

2.3   Gas separation membranes

Membrane separation is a process in which gas mixture permeates through a membrane under a pressure difference. Initially, each component contacts and dissolves on the surface of the membrane in the upstream side. Due to the difference in the transport rates of the components in the membrane, each gas reaches the downstream side at different time so that mixture gas separation can be achieved. In this process, the gas reached the downstream side of the membrane is called permeate gas, and the gas retained on the upstream side of the membrane is called retentate gas (Figure 2.4).
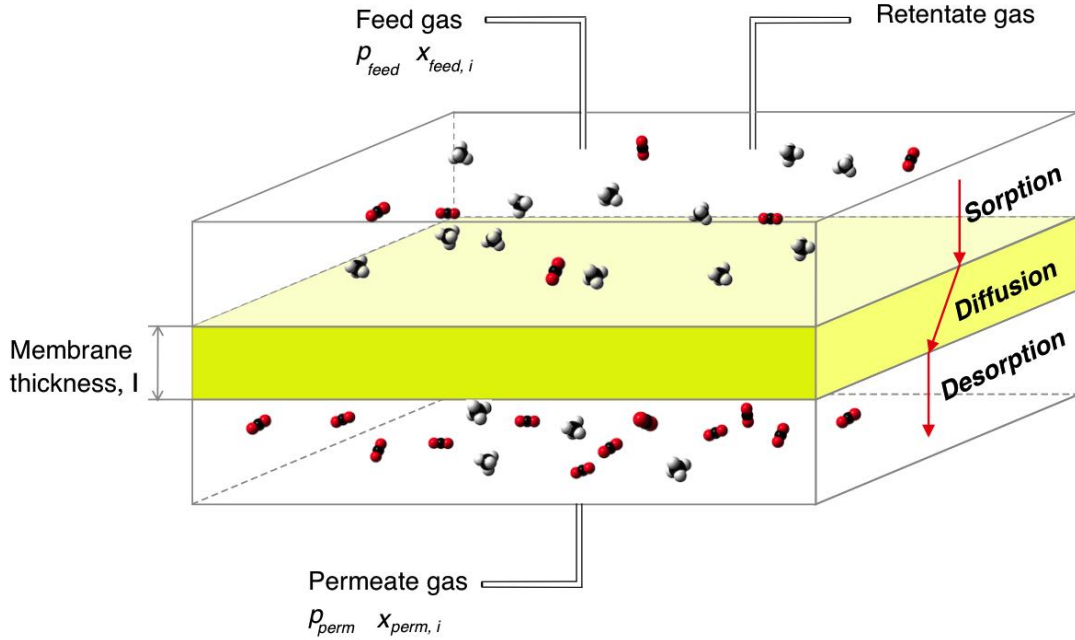
Figure 2.4: Diagram of membrane separation process

The permeability of a membrane can be characterized by permeance (J) and permeability coefficient (P). The unit of permeance is GPU ($1\ GPU\ =\ 10^{-6}\ cm^3\ (STP)\ cm^{-2}\ s^{-1}\ cm\ Hg^{-1}$), while the unit of permeability coefficient is $Barrer$ ($1\ Barrer = 10^{-10}\ cm^3\ (STP)\ cm\ cm^{-2}\ s^{-1}\ cm\ Hg^{-1}$). For pure gas, permeability and permeance can be calculated by following equations:

$$P = \frac{Q \times l}{\Delta p \times A} = \frac{Q \times l}{(p_{feed} - p_{perm}) \times A} \tag{2.1}$$

$$J = \frac{Q}{\Delta p \times A} = \frac{Q}{(p_{feed} - p_{perm}) \times A} \tag{2.2}$$

where Q represents gas permeation rate ($cm^3(STP)\ s^{-1}$), A is the membrane area (cm^2), Δp is the pressure difference across the membrane ($cm\ Hg$), p_{feed} is the feed gas pressure ($cm\ Hg$), and p_{perm} is the permeate gas pressure ($cm\ Hg$). For mixture gas, permeability and permeance can be calculated by following equations:

$$P_i = \frac{Q_i \times l}{\Delta p_i \times A} = \frac{Q \times l \times x_{perm,i}}{(p_{feed}x_{feed,i} - p_{perm}x_{perm,i}) \times A} \tag{2.3}$$

15

$$J_i = \frac{Q_i}{\Delta p_i \times A} = \frac{Q \times x_{perm,i}}{(p_{feed}x_{feed,i} - p_{perm}x_{perm,i}) \times A} \tag{2.4}$$

where i represents the gas component i, $x_{feed,i}$ represents the mole fraction of component i in the feed gas, and $x_{perm,i}$ represents the mole fraction of component i in the permeate gas. Another important factor is selectivity (or separation factor), $\alpha_{i/j}$, can be described as:

$$\alpha_{i/j} = \frac{P_i}{P_j} = \frac{J_i}{J_j} = \frac{D_i}{D_j} \cdot \frac{S_i}{S_j} \tag{2.5}$$

where i and j represent different gas components. The ideal gas selectivity is calculated by the ratio of two gas permeability coefficients from pure gas permeation test. $\frac{D_i}{D_j}$ and $\frac{S_i}{S_j}$ represent diffusivity selectivity and solubility selectivity, respectively. These two ratios indicate the contributions of sorption and diffusion process to overall selectivity.

2.3.1   Membrane structures

Membranes can be classified as symmetric and asymmetric membranes based on membrane structures. Symmetric membranes include porous membranes and dense membranes (Figure 2.5). The pore structures of symmetric porous membranes stay almost unchanged at different depth, *i.e.*, they have isotropic structures. Due to the highly voided structures, the flux of gas is high. Dense membranes are nonporous and homogeneous, and the transport of gas molecules in the membranes is by the force of pressure. Compared with porous membranes, dense membranes usually exhibit higher selectivity of gases due to compacted structures. Therefore, multiple dense membranes were developed in this study.

Asymmetric membranes can be divided into composite membranes and Loeb-Sourirajan type of membranes (Figure 2.6). Composite membranes include a dense surface layer which mainly contributes to the permselectivity of the membranes and a porous support layer which provides the mechanical properties of the membranes [Liu et al. (2004)]. The Loeb-Sourirajan membranes, based on cellulose acetate, had a thin layer with a thickness of around 0.2 μm [Loeb (1981)]. The ultimate structure and properties of the Loeb-Sourirajan membranes are determined by the

16

thermodynamics of the casting solution and the transport dynamics of solvent and non-solvent in the membrane formation process. In conclusion, membrane structures have an influence on the permselectivity of membranes, and thin membranes with enough mechanical properties are desired [Chung et al. (2007)].

(a) Porous symmetric membrane

(b) Dense symmetric membrane
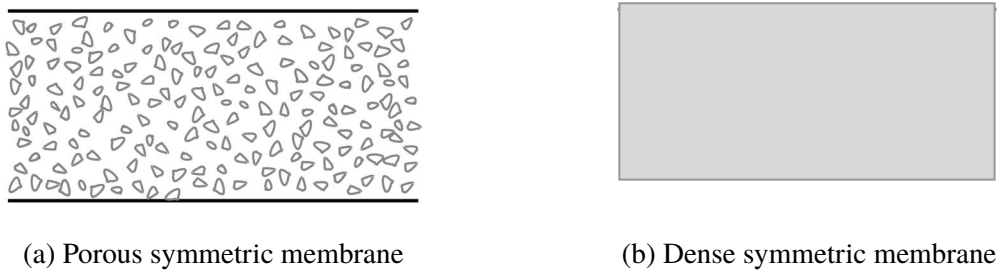
Figure 2.5: Schematic diagram of symmetric membrane [Baker (2012)]

(a) Composite membrane

(b) Loeb-Sourirajan membrane
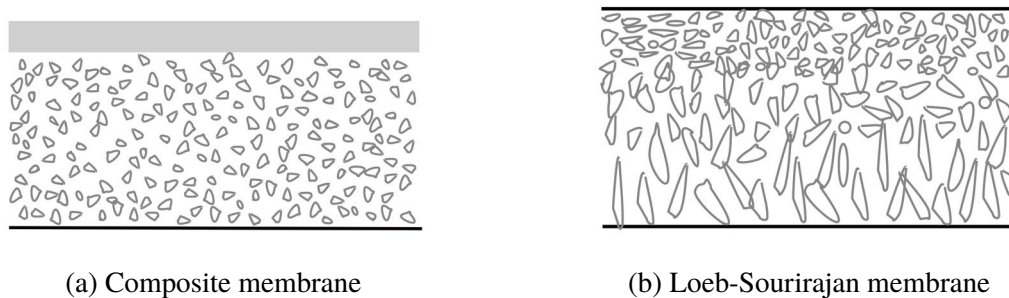
Figure 2.6: Schematic diagram of asymmetric membrane [Baker (2012)]

2.3.2   Transport mechanism in membranes

Porous membranes

As shown in Figure 2.7, the gas separation mechanisms in porous membranes include Knudsen diffusion, viscous flow, surface diffusion, capillary condensation, and molecular sieving [Baker (2012)]. The difference between Knudsen diffusion and viscous flow results from the difference

between the size of the pores (d) and the mean free path (λ) of the gas molecule. In Knudsen diffusion, d is smaller than λ. On the contrary, d is larger than λ in the viscous flow. When gas molecules are adsorbed on the surface of the pore walls, they tend to move along the pore walls and surface diffusion occurs. The capillary condensation mechanism is due to the fact that the condensable gas aggregates in the pore whose diameter is larger than the diameters of the gas components, thereby blocking the passage of other molecules and achieving separation. The molecular sieving mechanism is based on the difference in the kinetic diameters of gas molecules. When the pore size decreases to a range of 0.3-0.52 *nm*, the pores allow the passage of molecules with specific sizes due to the molecule sieving effect [Lewis (2018)].
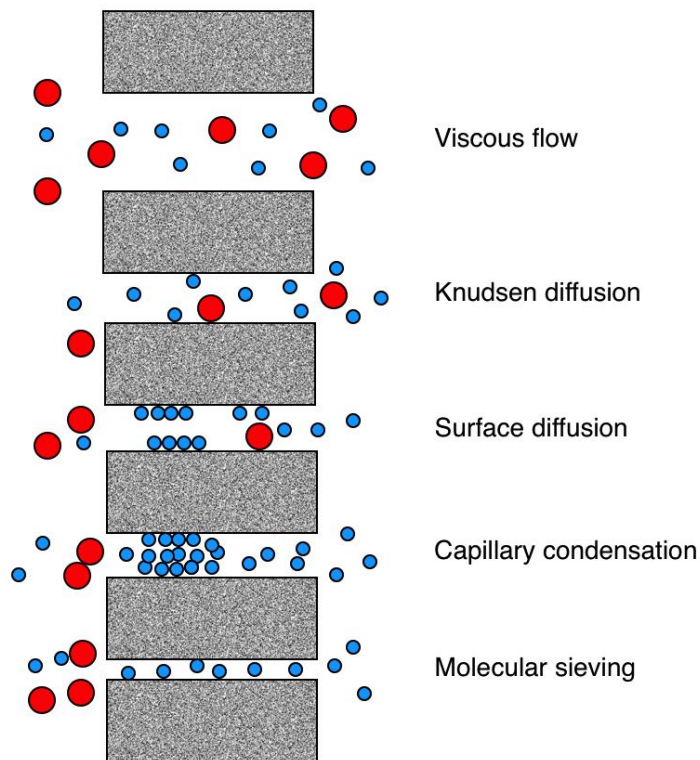
Figure 2.7: Gas transport in porous membranes

18

Solution-diffusion mechanism

Gas transport in nonporous membranes can be described by the solution-diffusion model [Wijmans and Baker (1995); Baker (2012)]. As shown in Figure 2.8, when the gas molecules penetrate through membranes, they come in contact with membrane surface first and then dissolve on the membrane surface. As a result, there is a concentration gradient between the two sides of the membranes. After penetrating to the other side of the membranes, the gas molecules desorb from the membrane surface and then come to the bulk of the permeate gas. Due to the different transport rates in membranes, different gas molecules reach the permeate side at different time leading to the achievement of gas separation.
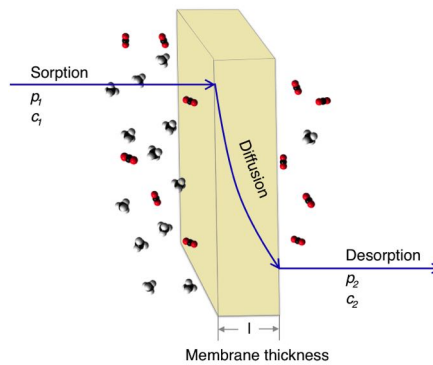
(a) Unsteady state
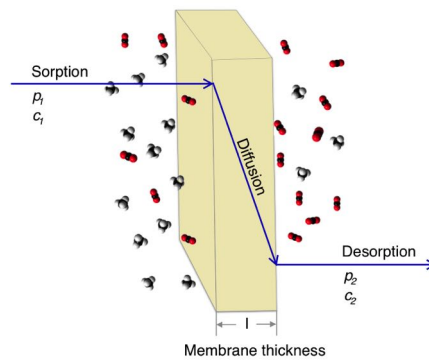
(b) Steady state

Figure 2.8: Gas transport in nonporous membranes by the solution-diffusion mechanism

In the beginning, the diffusion process is unsteady and the concentration of the gas molecules in the membrane exhibits non-linear distribution (Figure 2.8 (a)). When reaching a steady state, the gas concentration gradient along the membrane thickness does not change with time (Figure 2.8 (b)). According to Fick's first law, the gas diffusion flux is:

$$q = -D\frac{dc}{dx} \tag{2.6}$$

where q is the amount of gas permeated per unit area per unit time, D is the diffusivity coefficient, c is concentration, and x is the position in the membrane, $\frac{dc}{dx}$ is the concentration gradient, and the negative sign represents the transport direction is opposite to the concentration gradient direction. After integrating Equation 2.6, the following equation can be obtained:

$$q = D\frac{(c_1 - c_2)}{l} \tag{2.7}$$

where c_1 and c_2 represent concentrations in upstream and downstream sides, respectively. Usually, the concentration of gas dissolved in a polymer (c) is proportional to its pressure in the gas phase in contact with the polymer when the concentration of gas is low, and the proportionality constant is called the solubility coefficient, expressed as S, then

$$c = Sp \tag{2.8}$$

Substituting Equation 2.8 into Equation 2.7, yield

$$q = \frac{DS(p_1 - p_2)}{l} = \frac{P}{l}\Delta p = J\Delta p \tag{2.9}$$

$$P = DS \tag{2.10}$$

$$q = \frac{P}{l}\Delta p = J\Delta p \tag{2.11}$$

where P is permeability, p_1 and p_2 represent pressure of upstream and downstream side, respectively. Gas transport mechanism through the nonporous membrane is described by the solution-diffusion mechanism (Equation 2.10).

S is the ratio of the concentration of gas dissolved in the membrane to the gas pressure. The dissolution process is closely related to the solubility of gas molecules in the membrane. The boiling points of CO_2, N_2, CH_4 and H_2 are shown in Table 2.1. CO_2 has the highest boiling point among the gases, which indicates CO_2 can be dissolved more easily than the other gases. The critical temperature also can indicate gas condensability. The highest critical temperature of CO_2 among them implies that it is more condensable than the other three gases [Lin and Freeman (2005)]. Besides, the interaction between gas molecules and polymer can impact gas solubility as well. Theoretically, if there are more polar groups in the membrane, it is more conducive to the dissolution of CO_2. However, if too many polar groups are present in the membrane, it will lead to an increase in cohesive energy, which hinders the rapid penetration of molecules. When the membrane stays in humid conditions, different gas solubility in water can affect the gas dissolution process. CO_2 can dissolve in water more easily than the other three gases. Besides, when some ionic species exists in the membranes, it tends to decrease gas solubility in the membranes, which is so-called the salting-out effect.

D is a measure of the mobility of a gas molecule through free volume between polymer chains. The diffusion coefficient is related to the size and shape of the gas molecule. The kinetic diameter of CO_2 is smaller than those of N_2 and CH_4, but larger than that of H_2. As a result, CO_2 usually can diffuse faster in membranes than N_2 and CH_4. The diffusivity of H_2 was larger than CO_2 in membranes [Shao et al. (2009)]. The free volume of the polymer can also have an influence on diffusion coefficient. Higher free volume favors the gas permeation generally [Du et al. (2012)]. For CO_2-philic membranes, the strong sorption of CO_2 can make polymer chains become flexible, which is so-called the CO_2-induced plasticization. The more flexible polymer chains are, the more easily gas molecules can penetrate. Due to the difference in diffusivity and solubility of gas molecules, gas permeability in the membranes is different. Hence, various membranes haven been designed and fabricated to enhance diffusivity selectivity, solubility selectivity, or both of them.

Table 2.1: Properties of CO_2, N_2, CH_4 and H_2 [Rumble (1977)]

Gas molecule	Molecular weight (g/mol)	Kinetic diameter (nm)	Critical temperature (K)	Boiling point (K)	Solubility in water $(g/kg\ water$, at 293 K and 1 Bar)	Diffusivity in water $(cm^2\ s^{-1}$, at 298 K)
CO_2	44.01	0.33	304.2	194.7	1.25	1.91×10^{-5}
N_2	14.01	0.364	126.2	77.4	1.6×10^{-2}	2.0×10^{-5}
CH_4	16.04	0.38	190.8	111.6	1.8×10^{-2}	1.84×10^{-5}
H_2	2.02	0.289	33.2	20.3	1.6×10^{-3}	5.11×10^{-5}

Facilitated transport mechanism

Facilitated transport utilizes CO_2-philic groups in the membrane to have reversible reactions or interactions with CO_2. These CO_2-philic groups are called carriers, which increase the reaction selectivity and allow CO_2 to diffuse rapidly. According to the mobility of the carrier in the membrane, it can be divided into mobile carrier membranes, where the carriers can be freely diffused; semi-mobile carrier membranes, where the carriers move with a high diffusion activation energy; and fixed site carrier membranes, where the carriers only vibrate in a limited area, but can't move freely. The interaction between gas molecules and the facilitated transport carriers is based on nucleophilic addition reactions and π-complexation reactions [D'Alessandro et al. (2010)].

The nucleophilic addition reaction often occurs on the carbon atoms of the asymmetric double bonds. The shift of the electron cloud makes the positively charged carbon atoms more vulnerable to nucleophile attack such as H_2O, OH^-, $-NH_2$, $-COOH$ [Li et al. (2012); Francisco et al. (2007); Huang et al. (2008); Yegani et al. (2007)]. According to Bronsted and Lowry's acid-base theory, the conjugate base of a weak acid is usually a strong base. For example, OH^- can react with CO_2 to produce HCO_3^-, so in polyelectrolyte membranes, CO_2 can diffuse in the form of HCO_3^- in the membrane [Xiong et al. (2014)].

The facilitated transport of CO_2 as a result of amino groups is also based on the nucleophilic addition reaction with CO_2. Amino groups are also a typical non-ionic CO_2 carrier and can be covalently attached to the polymer chain. The reactions between primary and secondary amines and CO_2 are as follows [Caplow (1968)]:

$$CO_2 + RNH_2 \rightleftharpoons RNHCOOH$$
$$RNHCOOH + RNH_2 \rightleftharpoons RNHCOO^- + RNH_3^+$$
$$CO_2 + R_2NH \rightleftharpoons R_2NH^+COO^-$$
$$R_2NH^+COO^- + R_2NH \rightleftharpoons R_2NCOO^- + R_2NH_2^+$$
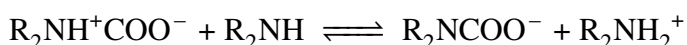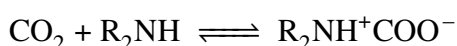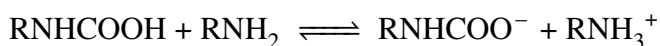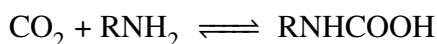
where R can be the same or different groups. Among them, the nucleophilic addition reaction is

a rate-control step, and water molecules also play an irreplaceable role in this process in humid conditions:

$$2\ CO_2 + 2\ RNH_2 + H_2O \rightleftharpoons RNHCOOH + RNH_3^+ + HCO_3^-$$

$$2\ CO_2 + 2\ R_2NH + H_2O \rightleftharpoons R_2NCOOH + R_2N_2^+ + HCO_3^-$$
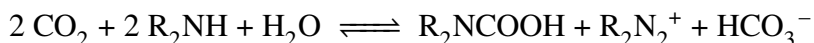
Due to the stronger electron donation effect, secondary amines exhibit stronger alkalinity and higher reaction selectivity in general. It also should be mentioned that the steric hindrance effect of secondary amines should be considered as well. Shen *et al.* used carboxymethyl chitosan (CMCS) and polyethylenimine (PEI) to prepare a gas separation membrane by a blending method. Because of the hydrogen bonding between PEI and CMCS, they can be blended uniformly, and the blend membranes have excellent gas separation performance. When the PEI content is 30 wt.%, the CO_2/N_2 selectivity reaches 325 in the wet state [Shen et al. (2013)]. Deng *et al.* prepared PVAm/PVA facilitated transport composite membranes with a CO_2/N_2 separation factor of up to 174 at 2 *Bar*. The addition of PVA can improve the mechanical properties of the blend membrane, and an ultra-thin selective layer can be formed to enhance the gas permeance [Deng et al. (2009)].

Unlike primary and secondary amine groups, tertiary amine groups and CO_2 hardly react in the dry state. Donaldson and Nguyen (1980) believed that tertiary amines can participate in the hydration reaction of CO_2 as a weak base catalyst to form bicarbonates in the presence of water. They also thought that the tertiary amine catalyzed CO_2 hydration reaction is more efficient than the primary and secondary amines. The reaction of the tertiary amine (R_3N) with CO_2 to produce HCO_3^- is as follows:

$$CO_2 + R_3N \rightleftharpoons R_3N^+ + HCO_3^-$$
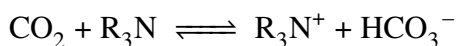
where R can be the same or different kinds of organic groups. In summary, the facilitated transport carriers for CO_2 is achieved in the form of carbamate and bicarbonate.

Another major class of facilitated transport mechanisms is based on π-complexation interaction. The carrier is usually a transition metal carrier. The empty orbit of the transition metal complexes with the π-electrons in CO_2, thereby accelerating CO_2 transport. Facilitated transport carriers that have such effects include Ag^+, Zn^{2+}, K^+, and polarized copper nanoparticles [Ismail

et al. (2011); Li et al. (2007); Li and Chung (2008); Oh et al. (2013); Lee et al. (2012)]. Saeed and Deng (2015) synthesized mimic enzymes using 1,4,7,10-tetraazacyclododecane and Zn^{2+} and successfully introduced Zn^{2+} into the membrane. Although aza-macrocyclic compounds also contain a large number of amino groups, the authors believed that their contribution to facilitating the transport of carriers was limited, and the main contribution should be the complexation interaction. The CO_2 molecule was adsorbed on the Zn^{2+} active site to form a metastable complex, Lewis base OH^- will attack the complex, resulting in HCO_3^-. Water is necessary for the reaction process, and the author selected polyvinyl alcohol (PVA) which has good hydrophilicity and can maintain a water environment. The diffusion of CO_2 in the membrane is in the form of ions (HCO_3^-), and its transportation rate is more than twice as fast as the gas molecule penetration through the polymer in a molecular form.

2.4 Membrane materials for gas separation

2.4.1 Inorganic membranes

Base on the structures of membranes, inorganic membranes can be classified as dense and porous membranes. Palladium and its alloys, silver, nickel and stabilized zirconia are used as dense metal membrane materials, while alumina, zeolite, silica-based, and carbon-based materials are served as porous membrane materials [Chung et al. (2007)]. Inorganic membrane materials can not only tolerate high temperature and pressure environments but also resist corrosion by aggressive chemicals. The excellent selectivity of inorganic membranes attracts a lot of attention. However, they are usually brittle, difficult to handle and expensive to manufacture due to poor mechanical properties, all of which limit their large-scale industrial application [Chung et al. (2007); Pera-Titus (2014)].

2.4.2 Organic membranes

Organic membranes which are also known as polymer membranes have attracted attention due to their flexibility and permselectivity [Du et al. (2012)]. However, polymer membranes cannot stand the high operating temperature and aggressive chemical circumstances. A large number of polymers have been investigated and developed for gas separation. In terms of glass transition temperatures (T_g), polymers are divided into glassy polymers and rubbery polymers. Common glassy polymer membrane materials include polyimide (PI), polyetherimide (PEI), and polycarbonate (PC) [Xiao et al. (2007); Shieh et al. (2001); Ward et al. (1976)]; common rubbery organic membrane materials include polydimethylsiloxane (PDMS), poly(ethylene oxides) based polymers[Firpo et al. (2015); Lin and Freeman (2004)]. Rubbery polymers exhibit high permeability, while glassy polymers exhibit high gas selectivity.

Robeson (1991) predicted the gas separation performance of the polymer membranes based on a large number of experimental data and empirical relationships in 1991 (Figure 2.9) and summarized the empirical upper limit relationship in the diagram. Then, he updated this upper limit in 2008 (Figure 2.10) [Robeson (2008)]. Most of the gas separation performance of the membranes is below this upper bound. It can be observed from the figures that there is often a trade-off effect between permeability and selectivity, that is, when the permeability of the membrane is high, the selectivity is usually low, and *vice versa*. Therefore, the current development of gas separation membranes focuses on breaking Robeson's upper bound, trying to break the trade-off effect, and gaining both high permeability and selectivity.
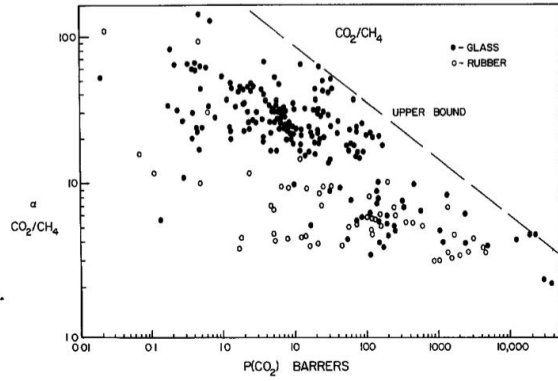
(a) Literature data for α_{CO_2/CH_4} versus P_{CO_2}
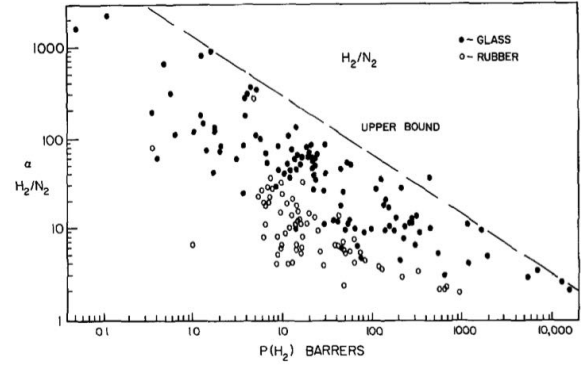
(b) Literature data for α_{H_2/N_2} versus P_{H_2}

Figure 2.9: The relationship between selectivity and permeability for different gas pairs in 1991 [Robeson (1991)]
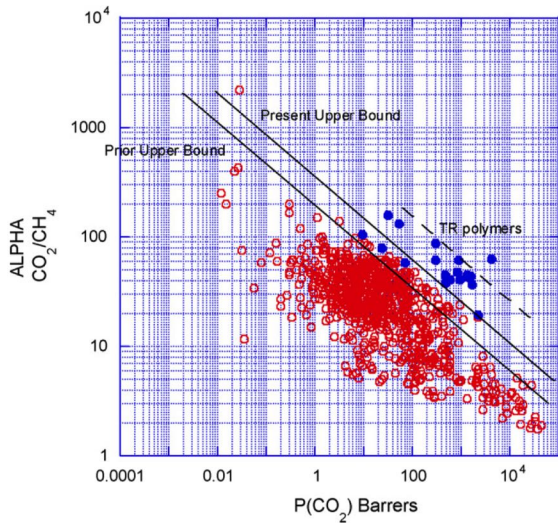
(a) Literature data for α_{CO_2/CH_4} versus P_{CO_2}
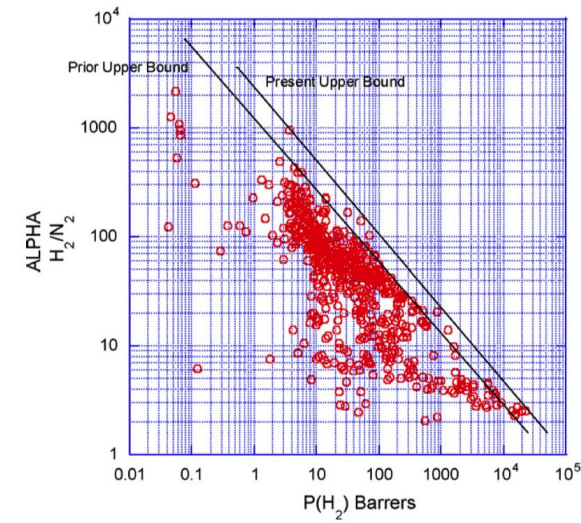
(b) Literature data for α_{H_2/N_2} versus P_{H_2}

Figure 2.10: The relationship between selectivity and permeability for different gas pairs in 2008[Robeson (2008)]

Polyimide (PI) is a typical glassy polymer membrane material, and this material has excellent gas separation performance, thermal stability, and good mechanical properties [Baker (2002)]. The synthesis of polyimide is mainly through the imidization of dicarboxylic anhydrides and diamines. The rigidity of the polymer chain determines diffusion selectivity of membranes, and polymer chain spacing and chain mobility affect the diffusion rate. Lin *et al.* used 6FDA (2,2'-bis(3,4'-dicarboxyphenyl)hexa-fluoropropane diandydride) and mesitylene-diamine (2,3,5,6-tetramethyl-1,4-phenylene-diamine) to prepare 6FDA-durene polyimide membranes. The permeability of CO_2 was about 660 Barrer at 35 °C and 2 atm and decreased with an increase in the feed gas pressure [Lin and Chung (2001)].

Polydimethylsiloxane (PDMS) is a commonly used gas separation membrane material with a high free volume fraction [Firpo et al. (2015); Shi et al. (2006)]. Silicone rubber-like membrane materials have a high permeability coefficient and favorable selectivity especially for the separation of organic vapors and inert gases. Berean et al. (2014) studied the effect of crosslinking temperature on the gas separation performance of PDMS membranes. At a crosslinking temperature of 75 °C, the CH_4 permeability was 1000 Barrer, the N_2 permeability was 590 Barrer, and the CO_2 permeability was 3970 Barrer. The strong stretching vibration of the Si-H bonds at 75 °C led to the decrease of the crosslinking density and ultimately to the increase of the free volume, so gas molecules can transport more easily in the polymer matrix leading to the increase in gas permeability.

Although PDMS membranes show a high gas permeability, the gas selectivity of PDMS membranes is lower than poly(ethylene oxides) based polymers. Polyethylene oxide (PEO) is a general term for polymers with PEO segments and belongs to rubbery polymers [Yave et al. (2011); Shao et al. (2013); Lin and Freeman (2005)]. The PEO segments can interact with CO_2 by a dipole-quadrupole interaction leading to CO_2-philic ability [Yave et al. (2010)]. Low molecular weight PEO is generally difficult to form membranes. However, low molecular weight PEO or polyethylene glycol (PEG) can be used as additives and blended into membranes to increasing CO_2-philic ability as well as adjusting the free volume in membranes. Yave et al. (2009) found

that the fractional free volume increased from 0.125 to 0.133 when the PBEAX membrane had a 50% loading of PEG, and CO_2 permeability increased from around 75 to 150 Barrer. PEG with different molecular weights was blended in PEBAX membranes by Wang et al. (2014) and in cellulose nitrite membranes by Kawakami et al. (1982). They both found that lower molecular weight PEG could benefit CO_2 permeability due to reducing crystallization.

High molecular weight PEO can form membranes, but it has a strong tendency to crystallize, making the CO_2 permeability of the membranes relatively low. Therefore, in order to develop high-performance PEO-based CO_2 separation membranes, it is necessary to simultaneously increase the content of PEO segments, reduce the crystallization of PEO segments, and maintain the mechanical properties of the membranes. At present, methods including crosslinking and copolymerization have been applied in the preparation of PEO-based membranes [Liu et al. (2013); Lin and Freeman (2005)]. Lin et al. (2006) synthesized amorphous, high-molecular-weight, crosslinked, network copolymers using poly(ethylene glycol) diacrylate (PEGDA) and poly(ethylene glycol) methyl ether acrylate (PEGMEA) for CO_2/H_2 separation. The crosslinked structure with EO units both in its backbone and pendant groups resulted in a CO_2 permeability of 400 Barrer at 35 °C and around 17.5 atm. Shao et al. (2013) prepared crosslinked PEO membranes with amino terminated and epoxy terminated PEO. The DSC results showed the crystallization of PEO was effectively controlled leading to a CO_2 permeability of 180 Barrer at 35 °C and 10 atm.
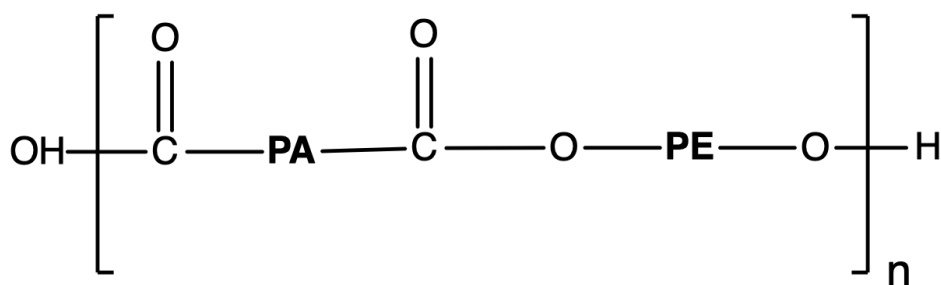
Figure 2.11: General chemical structure of PEBAX copolymer [Bondar et al. (2000)]

Compared with the crosslinked PEO-based polymers, PEO-based copolymers are usually composed of two kinds of segments: the soft segment is a PEO segment and is mainly responsible for the separation performance of the membrane; the hard segment is generally a polyamide (PA), a polyimide (PI), or a polyester (PU) segment, and is mainly responsible for the mechanical properties of the membrane. The general chemical structure is shown in Figure 2.11. PE segments include PEO and poly(tetramethylene oxide) (PTMEO), while PA segments include PA6 and PA12. Different kinds and contents of PA and PE make PEBAX exhibit distinct chemical and physical properties (Table 2.2).

Certain PEBAX membranes have been studied in gas separation, as shown in Table 2.3. Among them, PEBAX 1657 has good hydrophilicity. Besides, it can be dissolved in a mixed solvent of water and ethanol at 80 °C to form a stable polymer solution at room temperature. In order to increase the permselectivity of PEBAX 1657 membranes for carbon capture, various methods have been used. By adding small molecules of polyethylene glycol (PEG) and its derivatives to PEBAX 1657, the content of PEO segments in the membrane can be further increased. The crystallinity degree of PEO can be reduced, and the CO_2 permeability of the membrane can be increased [Car et al. (2008b)]. Besides, blending with other polymers is another option to improve PEBAX 1657 permselectivity. Reijerkerk et al. (2010) blended PEBAX 1657 with poly[dimethylsiloxane-co-methyl(3-hydroxypropyl)siloxane]-graft-poly(ethylene glycol) methyl ether(PDMS-PEG) to combining advantages of two materials and increasing free volume in membranes. Comparing with the pristine PEBAX membranes, the CO_2 permeability of PEBAX/PDMS-PEG(50 wt.%) increased from 98 to 532 Barrer, the CO_2/H_2 selectivity increased from 9.5 to 10.6, while CO_2/CH_4 and CO_2/N_2 selectivity decreased from 16.1 to 10.8 and from 53.2 to 36.1 at 35°C and 4 bar, respectively. Furthermore, PEBAX 1657 can be chemically crosslinked by 2,4-toluylene diisocyanate (TDI) in hexane to adjust membrane structures [Sridhar et al. (2007); Murali et al. (2010)]. Sridhar et al. (2007) found that CO_2 permeance decreased from 3.7 to 0.12 GPU while CO_2/CH_4 selectivity increased from 21.2 to 52.4 as the crosslinking time raised from 0 to 60 min, which was attributed to the compaction pf polymer chains. Moreover,

some salts can be used as additives to enhance membrane permselectivity. Alkali or alkaline-earth metal salts (LiCl, NaCl, KCl, $MgCl_2$, and $CaCl_2$) in PEBAX 1657 could interact with polymer chains to disturbing chain packing [Li et al. (2014)]. The prepared $CaCl_2$-doped membranes had a CO_2 permeability of 2030 Barrer, a CO_2/CH_4 selectivity of 31, and a CO_2/N_2 selectivity of 108 at 298 K and 3 bar. Zhang et al. (2018) prepared the facilitated transport membranes with amino acid salts (sodium glycine) and PEBAX 1657. The presence of sodium glycine also enhanced membrane hydrophilicity and CO_2 solubility in the membranes. Also, some ionic liquid including 1-butyl-3-methylimidazolium trifluoromethanesulfonate ([BMIM][CF_3SO_3]), [emim][BF4], and triethylene tetramine trifluoroacetate ([TETA][Tfa]) has been blended into PEBAX 1657 [Bernardo et al. (2012); Fam et al. (2017); Dai et al. (2016b)]. These ionic liquids can effectively reduce the crystallinity of PEBAX 1657.

In summary, PEBAX 1657 has a good membrane formation property and shows CO_2-philic ability. In order to further improve the permselectivity of the PEBAX 1657 membranes, different approaches have been used in the literature. Many works focused on gas permeation in the PEBAX 1657 based membranes in the dry condition. However, gas permeation in the humid condition needs to be studied as well since gas sources from natural gas sweetening and power generation processes contain a certain amount of water vapor. This study addresses the development of the PEBAX 1657 based membranes and applications for carbon capture in separating CO_2/N_2, CO_2/CH_4, and CO_2/H_2 mixtures in the humid condition. Based on the solution-diffusion mechanism and facilitated transport of CO_2, blending PEBAX 1657 with other materials can adjust membrane structures and create a CO_2 favorable environment in the membranes. Besides, PEBAX 1657 can be fabricated as mixed matrix membranes by blending with some fillers to improve permselectivity, which is described in the next section.

Table 2.2: Composition and properties of PEBAX with different commercial grades

Commercial grade	PA	PE	PE content (wt.%)	Density (g cm^{-3})	T_g (°C)	T_m(PA) (°C)	T_m(PA) (°C)	Reference
1074	PA12	PEO	55	1.09	-55	156	11	[Bondar et al. (2000)]
1657	PA6	PEO	60	1.14	-53	204	49	[Kim et al. (2001)]
2533	PA12	PTMEO	80	1.01	-77	137	12	[Rezac et al. (1997)]
3533	PA12	PTMEO	70	1.01	-72	142	7	[Rezac et al. (1997)]
4011	PA6	PEO	57	1.14	-53	201	13	[Bondar et al. (2000)]
6333	PA12	PTMEO	24.2	1.01	-60	170	None detected	[Rezac et al. (1997)]

PA6 = polyamide 6, PA12 = polyamide 12, PEO = polyethylene oxide, PTMEO = poly(tetramethylene oxide)

Table 2.3: Gas permeability and selectivity of PEBAX with different commercial grades

PEBAX grade	Temperature (°C)	Feed pressre (kPa)	P_{CO_2} (Barrer)	P_{N_2} (Barrer)	P_{CH_4} (Barrer)	P_{H_2} (Barrer)	S_{CO_2/N_2}	S_{CO_2/CH_4}	S_{CO_2/H_2}	Reference
1074	35	1013	120	2.33		12.2	51.5		9.8	[Bondar et al. (2000)]
1074	25	200	64.81		3.2			20.3		[Azizi et al. (2017)]
1657	25	200	82	1.5	4.3		54.7	19.1		[Wu et al. (2014)]
1657	30	100	72			9.1			7.9	[Car et al. (2008a)]
1657	30	100	73	1.4	4	7.5	53	18.3	9.7	[Rahman et al. (2013)]
2533	30	100	240	9.2	30	48	26	8	5	[Rahman et al. (2013)]
2533	21	200	351	10	42		35.1	8.4		[Nafisi and Hagg (2014)]
2533	20	200	234	5.65	29	33	41.4	8.1	7.1	[Ehsani and Pakizeh (2016)]
3533	25	400	132	2		20	61		6.1	[Kim et al. (2001)]
3533*	35	1000	243		42.6			5.7		[Chatterjee et al. (1997)]
4011	35	1000	66	1.17		8.5	56.4		7.8	[Bondar et al. (2000)]
6333*	35	1000	7.4		1.9			3.9		[Chatterjee et al. (1997)]

* The membranes were tested for a mixture gas of $CH_4/CO_2/H_2S$ (70.8/27.9/1.3 vol.%).

33

2.4.3 Mixed matrix membranes

Organic polymer membranes are usually limited by the trade-off relationship between permeability and selectivity, and it is difficult to exceed the Robeson's upper bound. The applications of inorganic membranes are also limited by the inability to prepare continuous, defect-free gas separation membranes, and they are expensive to manufacture as well. Thus, hybrid membranes or mixed matrix membranes (MMMs) have been developed recently [Chung et al. (2007)].
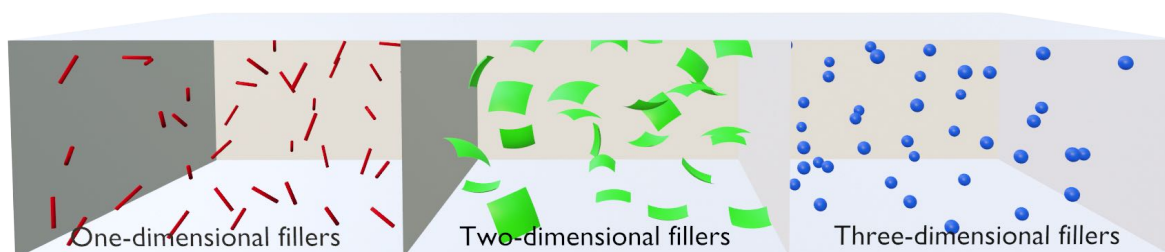
Figure 2.12: Mixed matrix membranes with three kinds of fillers

As shown in Figure 2.12, mixed matrix membranes generally use organic materials as a matrix (continuous phase), and then one or more kinds of fillers (disperse phase) are doped into the organic matrix [Bernardo et al. (2009)]. These fillers include zeolites, carbon molecular sieves, graphene oxide, carbon nanotubes, metal-organic framework compounds (MOFs), covalent organic frameworks (COFs), *etc.* [Chung et al. (2007); Kang et al. (2016)]. Combined with the unique features of polymer materials and the characteristics of fillers, MMMs provides more options for the design and preparation of new high-efficiency membrane materials [Dechnik et al. (2017)]. They also have economic advantages over inorganic membranes, exhibit superior performance over polymer membranes. Although the mixed matrix membrane has many advantages, the actual large-scale manufacture remains a huge challenge. The development of mixed matrix membranes involves various aspects such as how to properly select polymer and inorganic fillers, eliminate or reduce interface defects, and control the filler amount, size and shape [Mahajan and Koros (2000)].

Metal-organic framework compounds (MOFs) are a type of porous material with frameworks that have regular pore sizes and channels, very large specific surface areas, and good thermal stabilities [Erucar et al. (2013)]. Zeolite imidazole framework (ZIF) is an important class of MOFs, which is formed by the connection of transition metal and imidazole ligands [Liu et al. (2012)]. ZIF-7 was embedded into PEBAX 1657 to prepare the mixed matrix composite membrane on a polyacrylonitrile (PAN) support [Li et al. (2013)]. Owing to the addition of ZIF-7, CO_2 permeability of the membranes increased from 72 to 145 Barrer, CO_2/CH_4 selectivity and CO_2/N_2 selectivity was 30 and 97 at 25°C and 3.75 bar. The SEM images showed that the thicknesses of defect-free selective layers were in the range of 498 to 1052 nm, and there were no voids or clusters being observed. Rodenas et al. (2014) used a MOF material (NH_2-MIL-53(Al)) and polyimide (Matrimid 5218) to prepare a mixed matrix membrane. The addition of NH_2-MIL-53(Al) increased the gas permeability by 70%, and the FIB-SEM technique was used to clearly display and analyze the distribution of the MOF particles in the membrane, the main structure of the polymer, and the cavity distribution. Compared with the two-dimensional SEM characterization, this method provided more information and more intuitive evidence to explain the effects of filler on polymer structure.

Graphene oxide (GO), a two-dimensional nanomaterial, has a high specific surface area (>1000 m^2/g), high mechanical property and great thermal stability [Wu et al. (2017)]. The edges and surface of GO have various oxygen-containing groups (epoxy, hydroxyl, and carboxy groups). In order to improve interfacial compatibility between GO and the polymer matrix, poly(2,3-epoxy-1-propanol) (PEP) grafted GO, imidazole functionalized GO, PEG and PEI modified GO were introduced into PEBAX 1657 to fabricate MMMs [Wu et al. (2017); Dai et al. (2016a); Li et al. (2015a)]. Shen et al. (2015) found that the GO laminates with several layers could be formed due to the hydrogen bonds between GO and PEBAX 1657 chains. The molecular-sieving interlayer space can provide fast gas transport pathways, resulting in a CO_2 permeability of 100 Barrer and a CO_2/N_2 selectivity of 91 at 25°C and 0.3 MPa.

One-dimensional materials including carbon nanotubes, titania nanotubes, halloysite nanotubes, and polyaniline (PANI) nanorods or nanofibers have been applied in the preparation of MMMs [Murali et al. (2010); Xin et al. (2015a); Ismail et al. (2011); Zhao et al. (2013,0)]. Comparing with the other two types of fillers, the shape of the one-dimensional materials is beneficial for generating gas transport pathways in the membranes when the fillers are oriented in some specific directions. On the other hand, the presence of these fillers can interfere with the polymer chain distribution and create more free volume. Zhao et al. (2013) claimed that poly(vinylpyrrolidone) (PVP) modified PANI nanorods in the PVAm matrix can facilitate CO_2 transport both in intrachannel and interchannel pathways. Single-walled CNTs (SWCNTs), multi-walled CNT (MWCNTs), carboxyl modified SWCNT, amino-modified MWCNTs, polyzwitterion coated MWCNTs, and N-isopropylacrylamide hydrogel coated MWCNTs has been utilized to fabricate MMMs for carbon capture due to their unique shapes and structures [Cong et al. (2007); Murali et al. (2010); Habibiannejad et al. (2016); Zhao et al. (2014); Liu et al. (2014); Zhang et al. (2016)]. Murali et al. (2010) revealed that the addition of MWCNTs can increase the free volume and hydrophilicity of the PEBAX 1657 membranes. The CO_2 permeability of the PEBAX/MWCNT-5% membrane was 262.15 Barrer which was 4.7-fold of that of the pristine PEBAX membrane. However, the CO_2/N_2 and CO_2/H_2 selectivity were 58.2 and 6.4 at 1 MPa and 30°C which didn't get enhanced comparing with the PEBAX 1657 membranes. Therefore, although the PEBAX 1657 based MMMs showed good gas permeability, the gas selectivity needed to be further improved.

Chapter 3

PVAm/PEBAX blend membranes for carbon capture

3.1 Introduction

Aiming at CO_2/CH_4, CO_2/H_2 and CO_2/N_2 separations, many studies have been conducted in recent years [D'Alessandro et al. (2010); Bernardo et al. (2009)]. As shown in Table 2.1, CO_2 has favorable solubility in water, and its solubility is much higher than other gases (CH_4, N_2 and H_2). Based on the distinct solubility of gases in water, the adjustment of the water environment within membranes can reinforce solubility selectivity and enhance the CO_2 separation performance [Venturi et al. (2018); Deng and Hagg (2010)]. Some poly(ether block amide) copolymers have been successfully commercialized which is known as PEBAX. PEBAX is used to prepare membranes for gas separation by solution casting, melt pressing and melt extrusion [Liu et al. (2013); Chen et al. (2004)]. Many studies have focused on improving the permselectivity of PEBAX membranes. Among a series of PEBAX products, PEBAX 1657 is one of the rubbery copolymers and has been widely used to fabricated CO_2 separation membranes (Figure 3.1). The PEO blocks of PEBAX 1657 can provide gas separation properties due to the favorable affinity

to CO_2, while PA blocks can provide good hydrophilicity and mechanical properties for the membranes. PEBAX 1657 is abbreviated as PEBAX in the following discussion for simplicity.
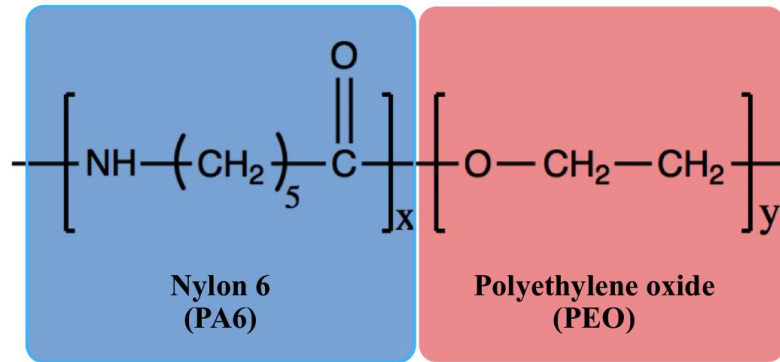
Figure 3.1: Chemical structure of PEBAX 1657
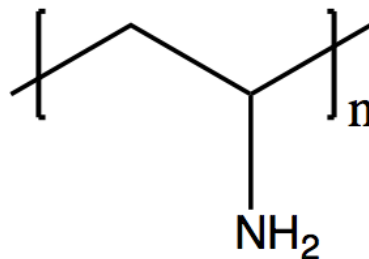
Figure 3.2: Chemical structure of PVAm

Polyvinylamine (PVAm) is a hydrophilic, water-soluble polymer. Besides, it contains a lot of amine groups on the polymer chains (Figure 3.2), so it has been considered as a good material in preparing membranes for carbon capture. Sandru et al. (2009) prepared fixed-site-carrier PVAm membranes by casting on a polysulfone supports. PVAm with high molecular weights (MW 340,000) has a higher CO_2/N_2 selectivity of 197 at 2 bar and 25°C than PVAm with low molecular weights (MW 80,000) due to high densities of carriers. Therefore, PVAm with higher molecular weight was selected in this study. Facilitated transport of CO_2 prevailed in

this membrane, so the CO_2/N_2 selectivity decreased from 197 to 98 when the CO_2 feed partial pressure increased from 0.2 to 1.5 bar. However, the high crystallinity of PVAm limits its applications. Deng and Hagg (2010) physically blended PVAm with polyvinylalcohol (PVA) to improve membrane forming properties by entangling two kinds of polymer chains and obtained a CO_2/N_2 selectivity of 160 (a feed gas pressure of 2 bar, room temperature, a feed gas of CO_2 (10 vol%)/N_2 (90 vol%)). Yi et al. (2006) chose to blend PVAm and polyethylene glycol (PEG) to decrease membrane crystallinity and enhance mechanical properties. When the content of PEG increased from 0 to 30 wt%, CO_2 and CH_4 permeance increased and then decreased, while it showed a CO_2/CH_4 selectivity of 65 at a 10 wt% content of PEG at a temperature of 25°C and a feed gas pressure of 96 cm Hg. The amine groups on the polymer chains were expected to react with CO_2 reversibly and facilitate CO_2 transport as fixed-site carriers. Blending with other materials can be considered as an effective approach to decrease the crystallinity of PVAm.

In this work, PEBAX and PVAm were physically blended to fabricate water-swollen membranes for carbon capture. The addition of PVAm can improve the hydrophilicity of the pristine PEBAX membrane. Besides, the polymer chains of PEBAX and PVAm could tangle to decrease the crystallinity in the membranes. The swelling of the polymer was beneficial to gas permeation due to creating more free volume. Besides, water can act as a plasticizer and build transport pathways for gas molecules in the membranes. Hence, gas molecules can permeate through the blend membranes not only by polymeric matrix but also by these pathways constructed by water. The combination of two polymers can enhance CO_2 solubility in the membranes. The reaction between CO_2 and amine groups on PVAm polymer chains can make membranes more favorable for CO_2 dissolution. The effects of membrane composition on CO_2, N_2, CH_4, and H_2 permeability and CO_2/N_2, CO_2/CH_4, and CO_2/H_2 selectivity were investigated. The effects of feed gas pressure and operating temperature on membrane permselectivity were investigated. The gas mixture permeation through the prepared blend membrane was carried out to evaluate the membrane performance for CO_2/N_2, CO_2/CH_4, and CO_2/H_2 separations, and the stability of the membrane was tested in different conditions.

3.2 Experimental

3.2.1 Materials

PEBAX 1657 was supplied by Arkema Inc. (Philadelphia, PA) in the form of melt-processed pellets (2-3 *mm* in diameter), and PEBAX represents PEBAX 1657 if there is no further specific statement in the following context. Polyvinylamine (PVAm) (Lupamin 9095, MW 340,000) was supplied from BASF company, and the PVAm concentration of Lupamin 9095 is 12.7 wt%. All gases used (nitrogen (N_2), methane (CH_4), hydrogen (H_2), and carbon dioxide (CO_2)) were provided by Praxair Canada Inc. (Mississauga, ON).

3.2.2 Membrane preparation

15 g of PEBAX pellets were placed in a round-bottomed flask. The solvent which was composed of ethanol (252.8 mL) and water (85.5 mL) was added. The mixture was vigorously stirred for 4 h at 80°C in a water bath to dissolve the polymer, and the resulting polymer solution was 5 wt% of PEBAX. The obtained solution was degassed by ultrasonication for 1 h. Then, 22.57 g of the PEBAX solution was cast on a polytetrafluoroethylene (PTFE) plate. The casting area (198 cm^2) was controlled by a frame as shown in Figure 3.3. The plate was placed in a dust-free chamber to evaporate solvent at ambient conditions for 24 h. After carefully peeled off the plate, the PEBAX membrane was collected.

The preparation of the PVAm/PEBAX blend membranes with different contents of PVAm was similar to that of the pristine PEBAX membrane. The compositions of the blend membranes were adjusted by changing the amount of PVAm while keeping the mount of PEBAX unchanged. The mass ratios of PVAm to PEBAX were 0.0064, 0.013, 0.019, and 0.025. The preparation of PVAm/PEBAX(0.025) membrane was taken as an example to describe the preparation of the blend membranes. As shown in Figure 3.3, 15 g of PEBAX pellets were used to prepare polymer solution, and then 2.952 g of Lupamin 9095 was added to the solution. The mixture
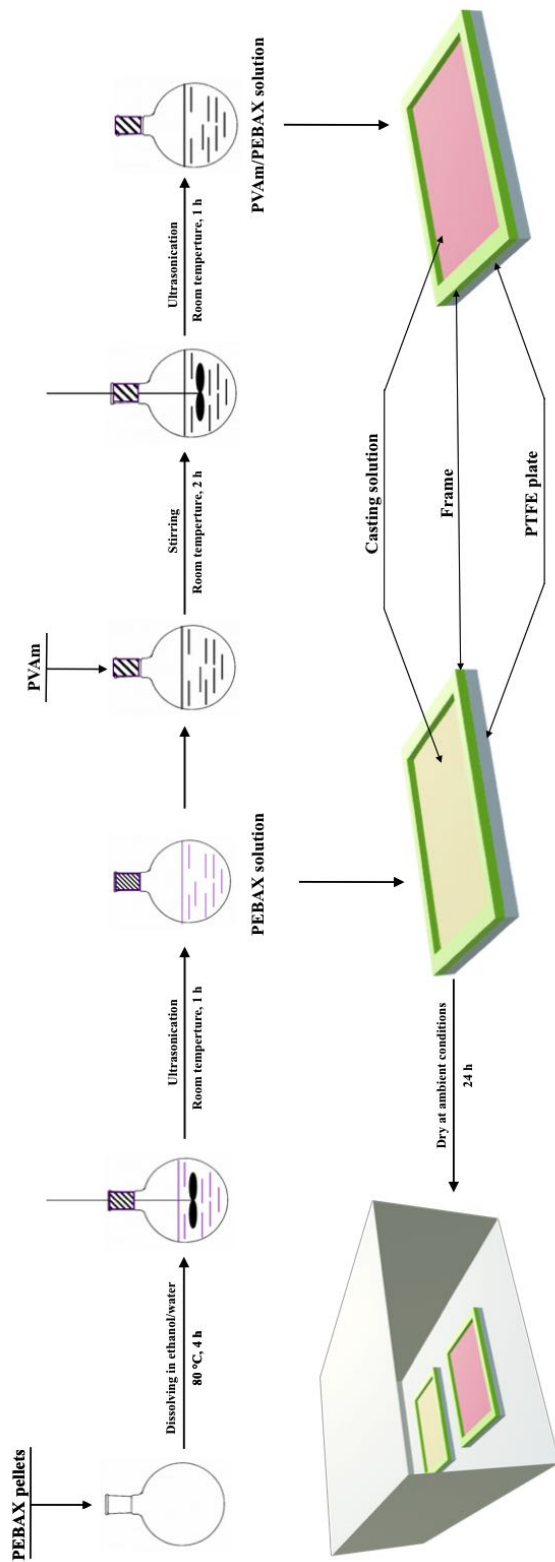
Figure 3.3: The preparation of the PEBAX and PVAm/PEBAX blend membranes

was agitated vigorously at room temperature for further 2 h. Then, the polymer solution was degassed by ultrasonication for 1 h. 22.80 g of the polymer solution was cast on a PTFE flat plate (198 cm^2). After solvent evaporating in a dust-free chamber at ambient conditions for 24 h, the blend membranes were peeled off the plate and collected. The thicknesses of the PEBAX and PVAm/PEBAX blend membranes were in the range of 45.7-63.5 μm in the dry condition, while those of them were in the range of 122.2-166.9 μm in the humid condition. The thicknesses of membranes were measured by a spiral micrometer at ten different places on the membranes.

3.2.3   Membrane swelling degree test

After gas permeation tests, the membranes were weighed using an analytical balance (m_h). Then, the membranes were dried in a vacuum oven at 50°C for 24 h to obtain the weight of membranes in dry conditions (m_d). The degree of swelling of the membranes can be represented by the content of water in the membranes (Equation 3.1):

$$Swelling\ degree = \frac{m_h - m_d}{m_d}$$ (3.1)

where m_h (g) and m_d (g) represents the weights of membranes in humid and dry conditions, respectively. The unit of swelling degree is g water/g polymer.

3.2.4   Gas permeation test

Pure gas permeation

The apparatus of pure gas permeation test used in this study is shown in Figure 3.4. The test equipment included the following: feed gas supply, gas humidification system, membrane cell, temperature control system, bubble flow meter. The feed gas supply system can provide the test gas (CO_2, N_2, CH_4, and H_2). The feed gas pressure was in a range of 200-800 kPa. After passing through the humidifier and getting saturated with water vapor, the relative humidity of the gas

flow was 100%. Then, the feed gas was introduced into the feed side of the membrane cell. The membrane cell was made of stainless steel, and the effective area (A) for permeation is 20.82 cm^2. The membranes were pre-humidified by wet filter paper for two minutes before tests. After wiping out excess water on the surface, the flat membranes were placed into the membrane cell. The temperature of the humidifier and membrane cell was controlled by a thermostatted water bath. After penetrating the membrane, the permeate gas flow rate was measured by a bubble flow meter. The downstream side pressure was kept at the ambient pressure. The retentate valve was closed during the tests.
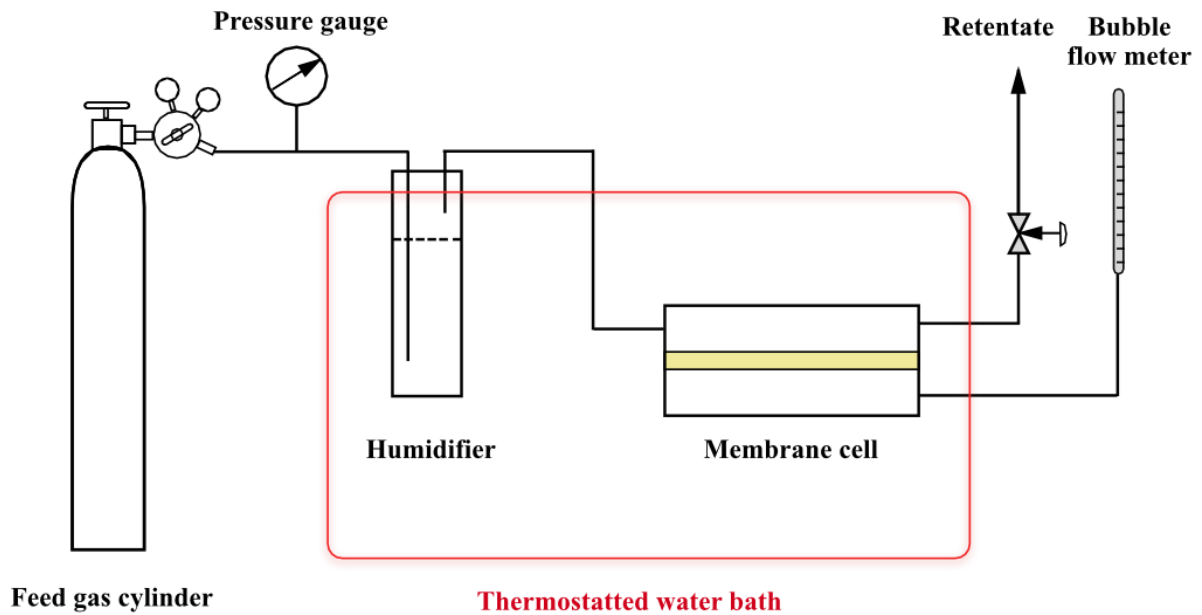
Figure 3.4: Apparatus for pure gas permeation test

The permeability of the membrane can be calculated from:

$$P = \frac{V\,l}{A\,t\,(p_{feed} - p_{perm})} \frac{273.15}{T_0} \frac{p_0}{76} \qquad (3.2)$$

where P is permeability (cm^3 (STP) cm cm^{-2} s^{-1} cm Hg^{-1}), V is the volume of permeate gas (cm^3) measured at ambient conditions (temperature T_0 (K), pressure p_0 (cm Hg)) during a

43

period of time t (s), A is the effective area of the membrane (cm^2), and p_{feed} and p_{perm} ($cm\ Hg$) are the feed pressure and permeate pressure, respectively. The thicknesses of the membranes, l (cm), were measured at ten different locations by a Mitutoyo micrometer and the average values were used. The ideal selectivity (separation factor) α was calculated from:

$$\alpha_{i/j} = \frac{P_i}{P_j} \tag{3.3}$$

Gas mixture permeation

The gas mixture permeation was conducted in a similar way to that of the pure gas permeation test. Figure 3.5 shows a schematic diagram of the gas mixture permeation test apparatus. Two mass flow controllers were used to mix and adjust feed gas composition. A gas chromatography was be used to measure the composition of the gas mixture. The sweeping gas was used to carry the permeate gas into the gas chromatography. For CO_2/N_2 and CO_2/H_2 separation tests, CH_4 was used as the sweeping gas; for CO_2/CH_4 separation tests, N_2 was used as the sweeping gas. The downstream side pressure was kept at the ambient pressure. A bubble flow meter was used to measure the gas flow rate. Both the feed gas and sweeping gas were humidified with water before entering the membrane cell. The gas permeability, P_i, is calculated by:

$$P_i = \frac{V\ l\ x_{perm,i}}{(p_{feed}x_{feed,i} - p_{perm}x_{perm,i})\ A\ t} \frac{273.15}{T_0} \frac{p_0}{76} \tag{3.4}$$

where $x_{feed,i}$ represents the mole fraction of component i in the feed gas, and $x_{perm,i}$ represents the mole fraction of component i in the permeate gas. The membrane selectivity (or ideal separation factor), $\alpha_{i/j}$, was calculated by Equation 3.3. Permeability of the membranes from the same batch showed a relative standard deviation within 9%, which can be considered as the experimental error. The relative standard deviation in gas permeability of the membranes from different batches was within 15%.
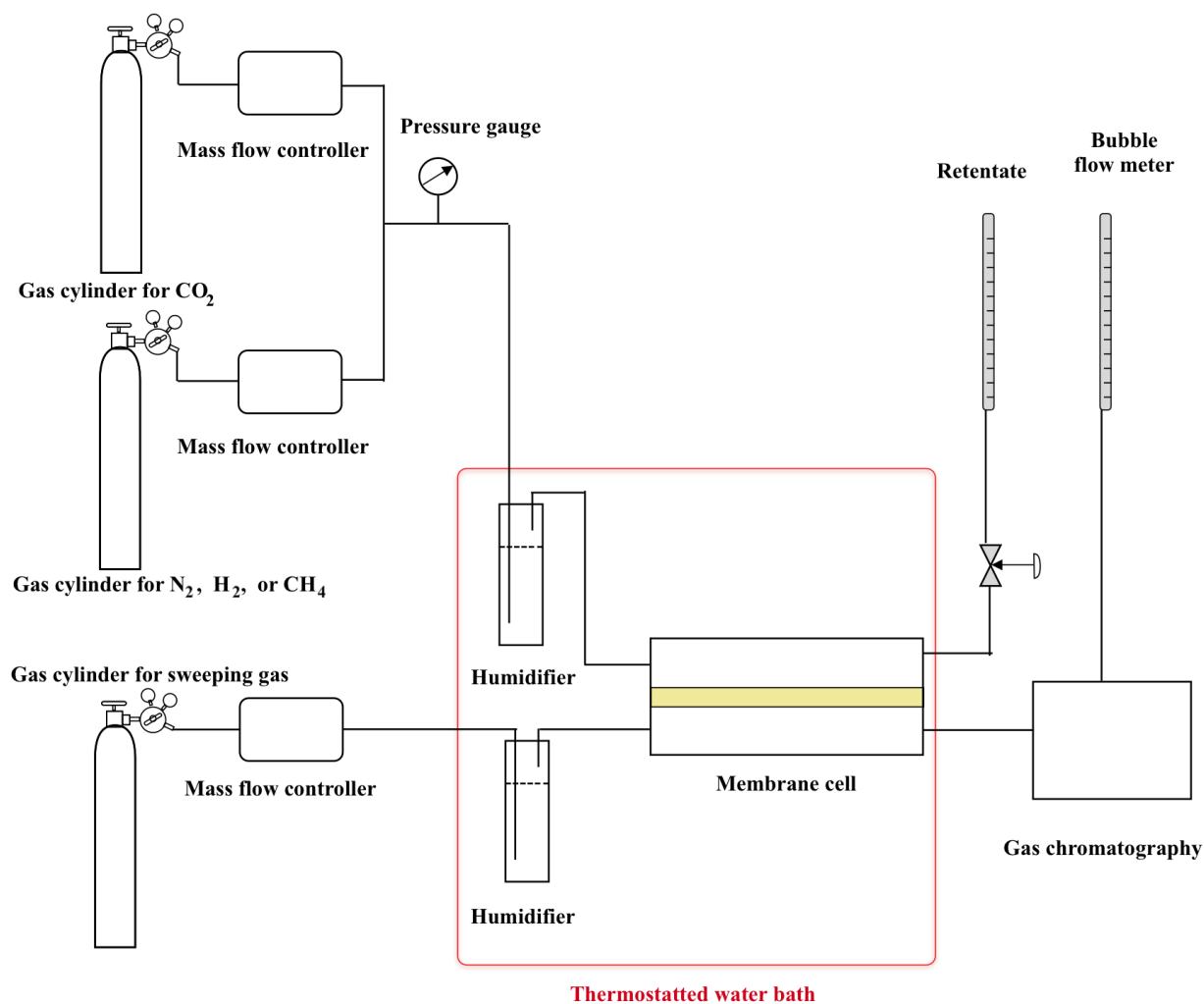
Figure 3.5: Apparatus for gas mixture permeation test

3.3 Results and discussion

3.3.1 Effect of membrane composition

The effects of membrane composition on pure gas permeation are shown in Figures 3.6 and 3.7. The gas separation performance tests were conducted at 303.2 K at a feed gas pressure of 400, 600, 800 kPa. When the PVAm/PEBAX blend membranes were prepared, these water-swollen

membranes became very fragile and difficult to handle in humid conditions if the mass ratio of PVAm/PEBAX (X) was more than 0.025. The main reason was that the excellent hydrophilicity of PVAm made membranes swell excessively and the mechanical property of membranes would be deteriorated dramatically.

As shown in Figure 3.6 (a), CO_2 permeability increased with an increase in the PVAm content in the membrane. The presence of PVAm in membranes not only enhanced the hydrophilicity of the PVAm/PEBAX blend membranes but also provided basic amine groups. The swelling of the membranes was beneficial to CO_2 dissolution because it had high solubility in water [Liu et al. (2008)]. CO_2 can permeate through the membranes by these water pathways easily. Besides, amine groups can also favor CO_2 permeation in membranes due to the acid-basic interaction. Hence, CO_2 permeability increased from 424 to 600 Barrer at a feed gas pressure of 400 kPa when the mass ratio of PVAm/PEBAX increased from 0 to 0.025.

Permeation of N_2, CH_4 and H_2 in PVAm/PEBAX blend membranes occurred via the solution-diffusion mechanism. As shown in Table 3.1, when the contents of PVAm in the blend membranes increased, the water contents increased and the hydrophilicity of blend membranes was improved. The rising of water content in membranes can reduce polymer chain packing and increase free volume. The CH_4 has the largest kinetic diameter among these four gases (0.380 nm), and it is more difficult to diffuse in the membranes. Hence, CH_4 permeability changed quite slightly when the mass ratio of PVAm/PEBAX increased, as shown in Figure 3.6 (c). N_2 (0.364 nm) and H_2 (0.289 nm) can diffuse faster than CH_4 when the membranes became swollen, and thus their permeability increased more than CH_4 permeability. As a result, when the mass ratio of PVAm/PEBAX increased from 0 to 0.025, N_2 and H_2 permeability increased by 30% and 24% under the feed gas pressure of 400 kPa, respectively (Figures 3.6 (b) and (d)).

Table 3.1: The swelling degree of the PVAm/PEBAX blend membranes

Blend ratio (X)	0	0.0064	0.013	0.019	0.025
Swelling degree (g water/g polymer)	1.74	1.86	1.89	1.95	2.22
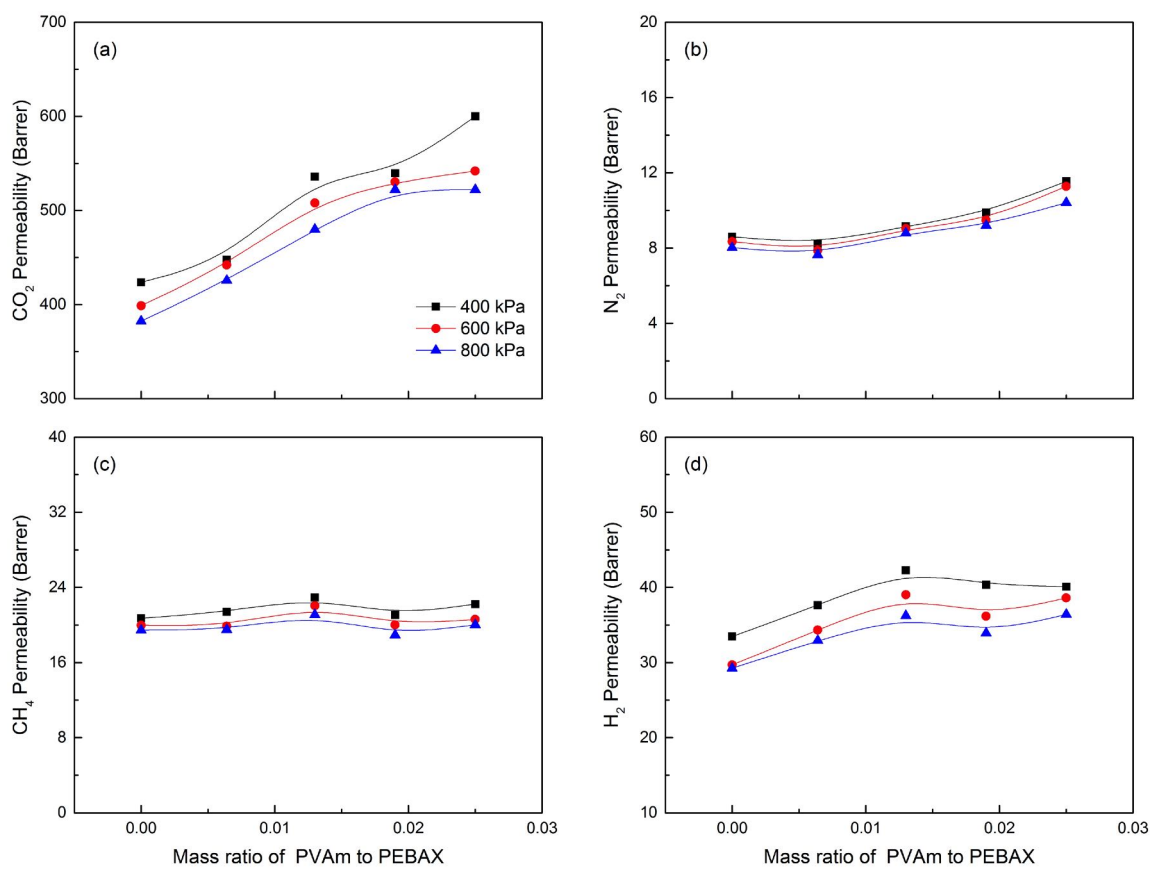
Figure 3.6: Effects of membrane composition on pure gas permeability of CO_2 (a), N_2 (b), CH_4 (c), and H_2 (d) of the PVAm/PEBAX blend membranes

Although the improved hydrophilicity of the blend membranes due to the addition of PVAm is beneficial to CO_2 permeability, the permeability of the other three gases was affected as well. As a result, the size-sieving ability of the polymer chains could be compromised, which was exhibited by the ideal gas selectivity (Figure 3.7). Compared to CO_2/N_2, CO_2/CH_4, and CO_2/H_2 selectivity of the pristine PEBAX membrane, the selectivity of the PVAm/PEBAX blend membranes did not increase significantly in spite of the presence of amino groups in the membranes. In general, when the facilitated transport of CO_2 makes more contributions to CO_2 permeation, it should result in a high selectivity due to the reactions between CO_2 and $-NH_2$. However, the solution-diffusion mechanism was likely to dominate this process. The ideal selectivity of the PVAm/PEBAX(0.025) blend membrane remained comparable with that of the pristine PEBAX membranes.
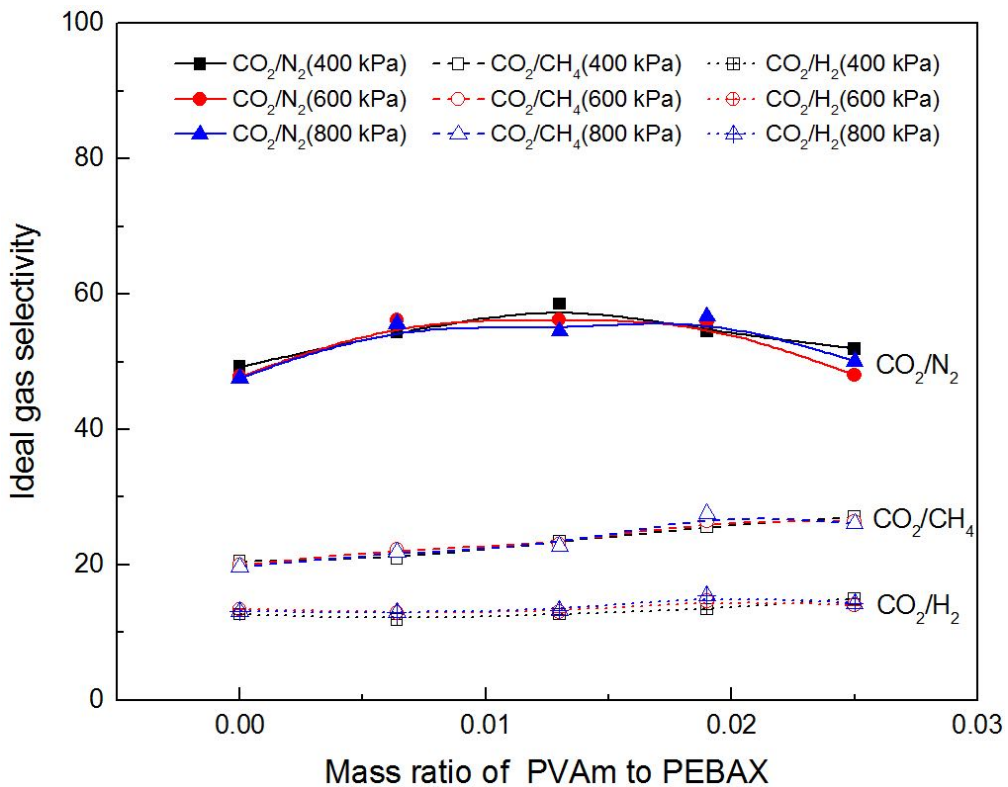
Figure 3.7: Effects of membrane composition on CO_2/N_2, CO_2/CH_4, and CO_2/H_2 selectivity of the PVAm/PEBAX blend membranes
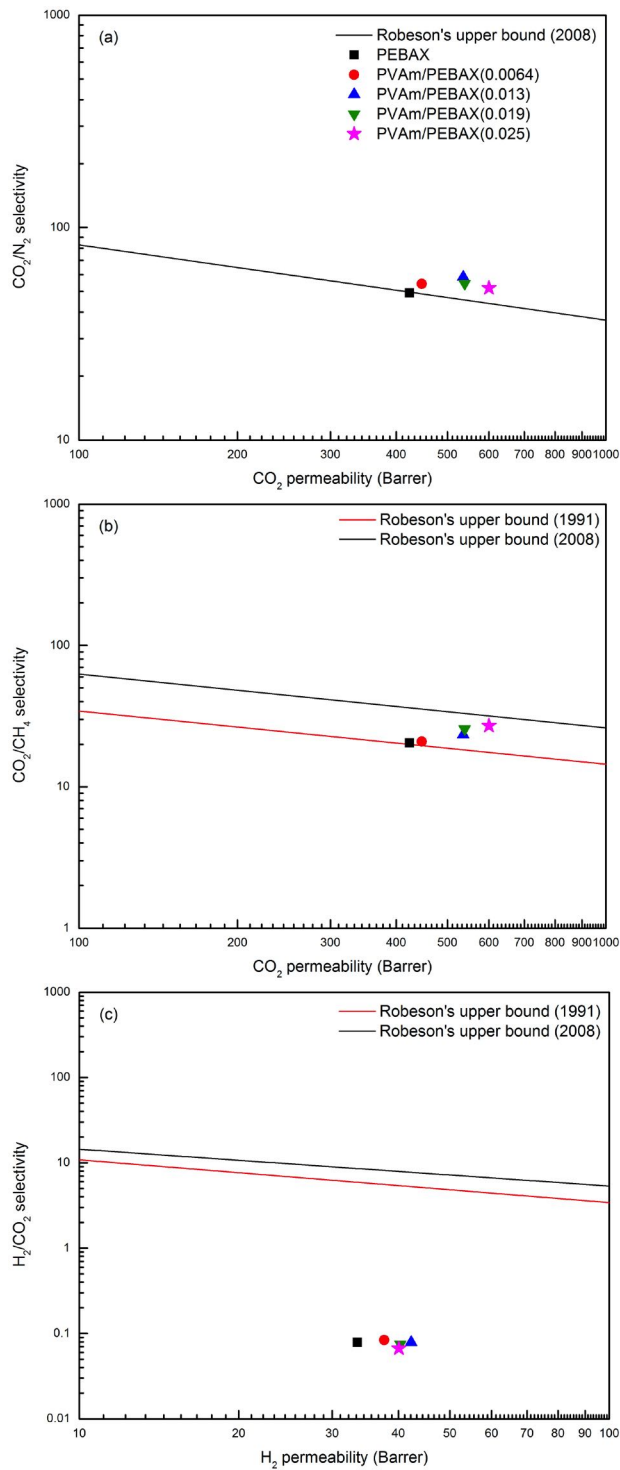
Figure 3.8: Comparison with Robeson's upper bound for CO_2/N_2 (a), CO_2/CH_4 (b), and H_2/CO_2 (c)

The pure gas permeation of the pristine PEBAX and PVAm/PBEAX blend membranes at 303.2 K and 400 kPa were compared with Robeson's upper bound. As shown in Figure 3.8, the pure gas permeation performance for CO_2/N_2 and CO_2/H_2 of all prepared blend membranes exceeded Robeson's upper bound (2008), and the pure gas permeation performance for CO_2/CH_4 only exceeded Robeson's upper bound (1991). The improvement of hydrophilicity due to the addition of PVAm made membranes tended to increase gas permeability rather than gas selectivity. Besides, the PVAm/PEBAX(0.025) blend membrane exhibited good CO_2 permeability (600 Barrer at a feed gas pressure of 400 kPa) among all prepared PVAm/PEBAX blend membranes. Therefore, the PVAm/PEBAX(0.025) blend membrane was selected for further study to determine the effects of other factors (*e.g.*, temperature, feed gas pressure, and feed gas composition) on the gas separation performance of membranes.

3.3.2   Effect of temperature

In order to investigate the effect of temperature on gas permeability and selectivity, the PEBAX and PVAm/PEBAX(0.025) blend membranes were tested for CO_2, N_2, CH_4 and H_2 permeation at temperatures ranging from 303.15 to 341.9 K and feed pressure from 400 to 800 kPa in humid conditions. The results are shown in Figure 3.9 and 3.10.

All pure gas permeability (CO_2, N_2, CH_4 and H_2) of both PEBAX and PVAm/PEBAX(0.025) blend membranes increased with an increase in temperature (Figure 3.9). The kinetic diameter of CO_2 molecule (0.33 nm) is smaller than those of CH_4 molecule (0.38 nm) and N_2 molecule (0.36 nm), which means the diffusion rate of CO_2 is larger than those of CH_4 and N_2. Although the kinetic diameter of H_2 is the smallest among them, the low solubility of H_2 in membranes restricts its transportation. Therefore, the order of gas permeability at a given temperature and pressure was $CO_2>H_2>CH_4>N_2$. As the temperature went up, the solubility of gas molecules in water declined, but the molecular movement could be enhanced dramatically and diffusion rates increased rapidly. Furthermore, the polymer chain mobility was improved at elevated temper-

atures, resulting in decreasing transport resistance. Despite the opposite effects, the diffusion process contributed more than the dissolution process. As a result, the gas permeability in the PEBAX and PVAm/PEBAX(0.025) blend membranes increased with an increase in temperature.
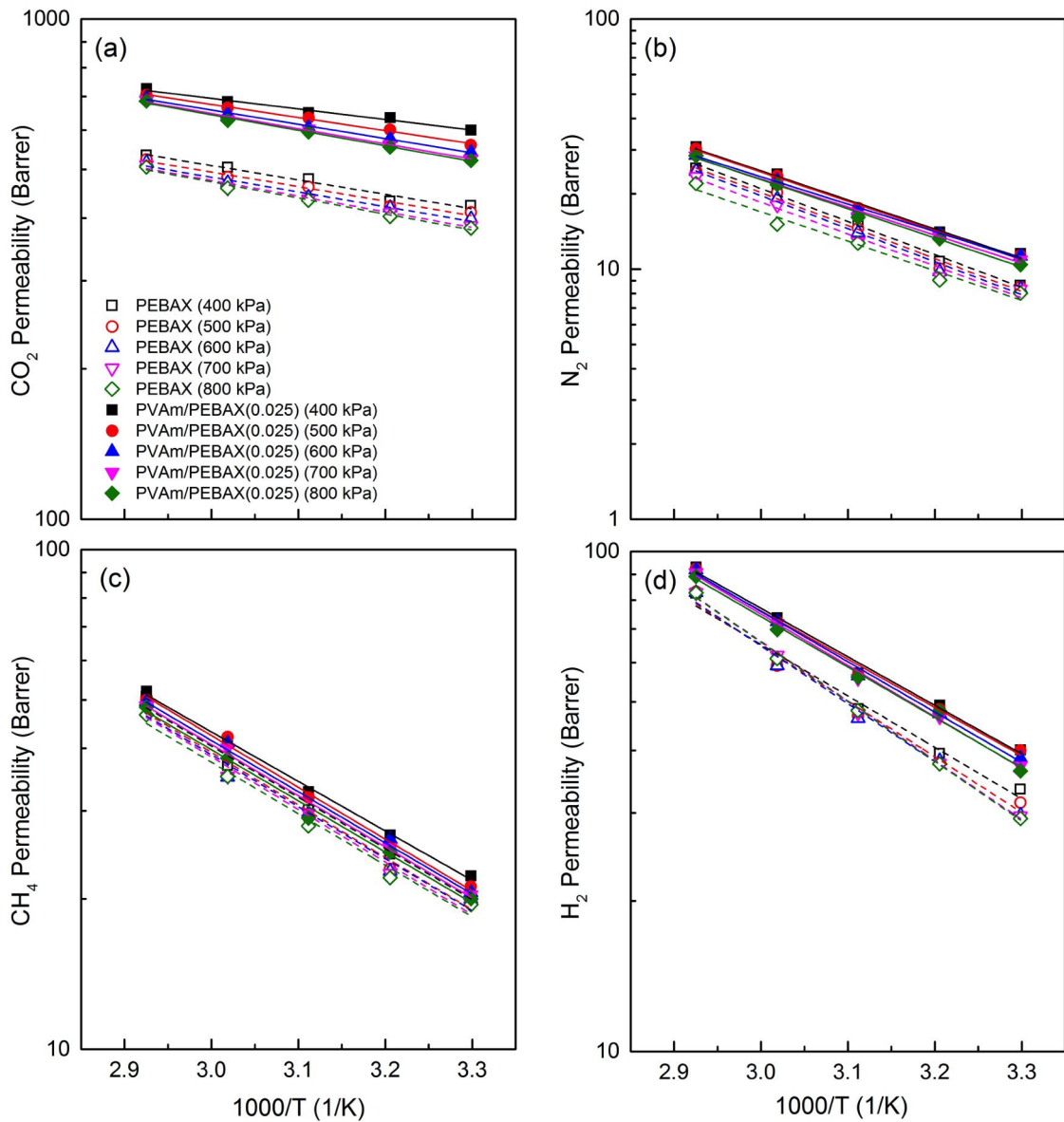
Figure 3.9: Effect of temperature on pure gas permeability of CO_2 (a), N_2 (b), CH_4 (c), and H_2 (d) of the PEBAX and the PVAm/PEBAX(0.025) blend membranes

51
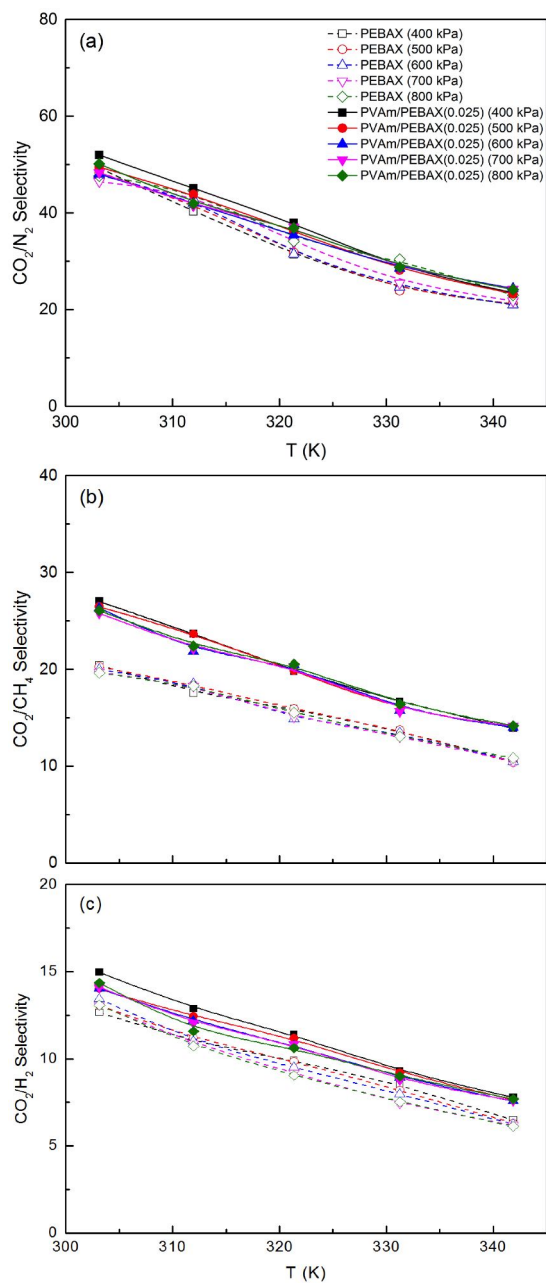
Figure 3.10: Effect of temperature on ideal gas selectivity of CO_2/N_2 (a), CO_2/CH_4 (b), and CO_2/H_2 (c) of the PEBAX and the PVAm/PEBAX(0.025) blend membranes

The temperature dependence of CO_2, N_2, CH_4 and H_2 permeability appeared to be fitted by the Arrhenius equation:

$$P_i = P_{0,\,i}\,exp(-\frac{E_{P,\,i}}{RT}) \qquad (3.5)$$

where $P_{0,\,i}$ is the pre-exponential factor (Barrer), $E_{p,\,i}$ is the activation energy of permeation (kJ/mol), R is ideal gas constant ($kJ/(mol\,K)$), and T is temperature (K). The activation energy for permeation can be calculated by the slopes of the straight lines in Figure 3.9. As shown in in Figure 3.11, the activation energy for N_2, CH_4 and H_2 permeation were larger than that for CO_2 permeation, which indicated that N_2, CH_4 and H_2 permeation was affected by temperature more significantly than CO_2 permeation in both the PEBAX and the PVAm/PEBAX(0.025) blend membranes. As a result, the CO_2/N_2, CO_2/CH_4, and CO_2/H_2 selectivity of the PEBAX membrane and the PVAm/PEBAX(0.025) blend membrane decreased with an increase in temperature (Figure 3.10).

The pressure dependence of the activation energy of permeation is illustrated in Figure 3.11. The activation energy for CO_2, N_2, CH_4, and H_2 permeation in the PVAm/PEBAX(0.025) blend membrane was lower than in the PEBAX membrane. Since the addition of PVAm increased membrane hydrophilicity and loosened the polymer matrix, the energy barrier to overcome for gas permeation through the PVAm/PEBAX(0.025) blend membrane was lowered. The activation energy for N_2, CH_4, and H_2 permeation in both membranes remained almost the same as the feed gas pressure increased from 400 to 800 kPa. However, with an increase in feed gas pressure, the activation energy for CO_2 permeation in the PVAm/PEBAX(0.025) blend membrane experienced an increase from 4.0 to 5.9 kJ/mol. It's attributed to the effects of feed gas pressure on the activation energy for diffusion and the heat for sorption in the membranes, which is needed to further study in the future.
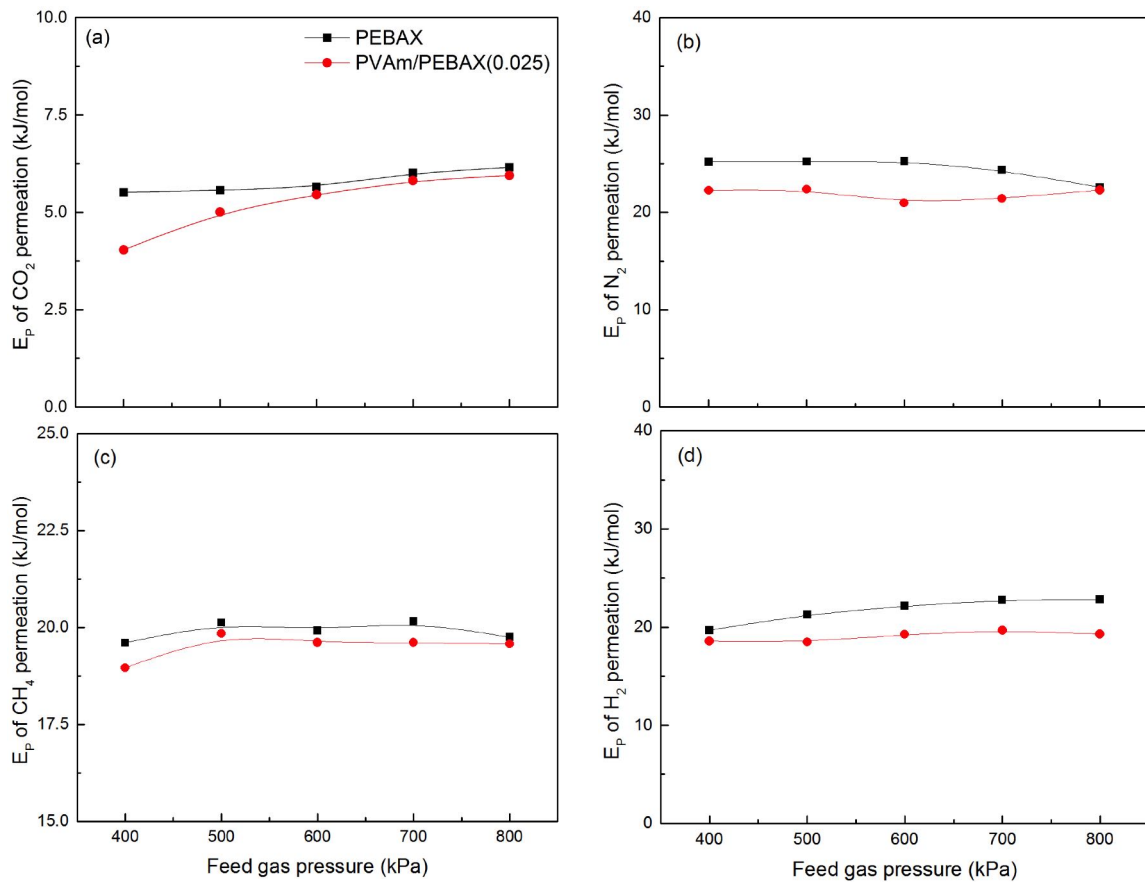
Figure 3.11: Effect of feed gas pressure on the activation energy for CO_2 (a), N_2 (b), CH_4 (c), and H_2 (d) permeation in the PEBAX and the PVAm/PEBAX(0.025) blend membranes

3.3.3 Effect of feed gas pressure

After the discussions about the effects of temperature on pure gas permeation in the previous section, the permeation data was used to describe the effects of feed gas pressure on pure gas permeation. The effects of feed gas pressure on pure gas permeability and ideal gas selectivity of the PEBAX and PVAm/PEBAX(0.025) blend membranes were shown in Figure 3.12 and Figure 3.13, respectively. In general, as the feed pressure increased from 400 to 800 kPa, the CO_2, N_2, CH_4 and H_2 permeability of both the PEBAX and the PVAm/PEBAX(0.025) blend membranes didn't change significantly. Hence, the CO_2/N_2, CO_2/CH_4, and CO_2/H_2 selectivity

of both membranes were hardly affected by feed gas pressure under test conditions. CO_2, N_2, CH_4 and H_2 permeation in both the PEBAX and PVAm/PEBAX(0.025) blend membranes were mainly dominated by solution-diffusion mechanisms.
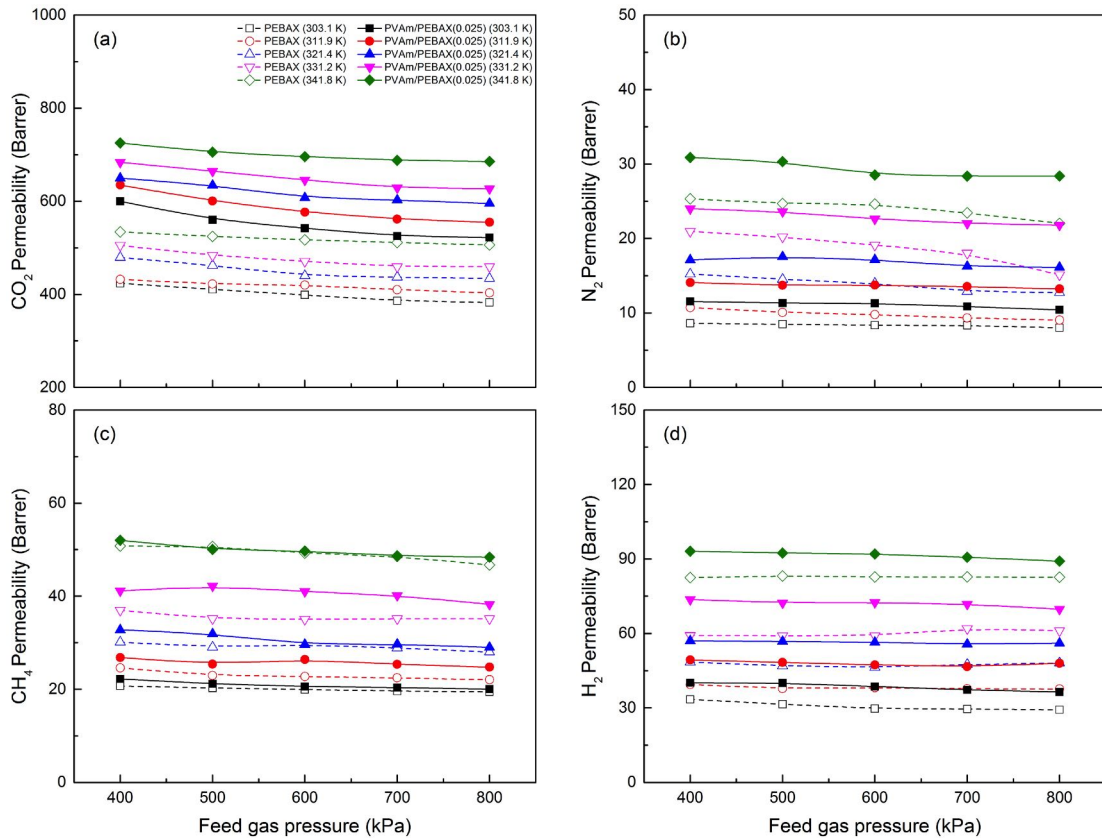
Figure 3.12: Effect of feed gas pressure on pure gas permeability of CO_2 (a), N_2 (b), CH_4 (c), and H_2 (d)
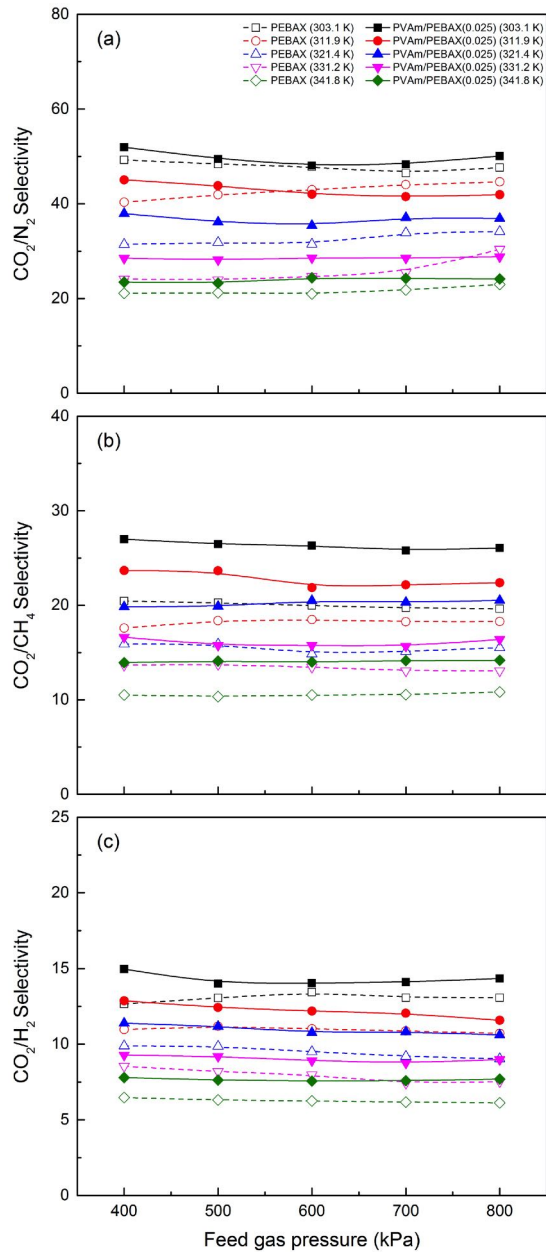
Figure 3.13: Effect of feed gas pressure on ideal gas selectivity of CO_2/N_2 (a), CO_2/CH_4 (b), and CO_2/H_2 (c)

3.3.4 Effect of feed gas composition

The previous work mainly focused on pure gas permeation at different conditions. However, the feed gas to be separated is a mixture. Therefore, it is necessary to study the permeation of binary gas mixtures (CO_2/N_2, CO_2/CH_4, and CO_2/H_2). The effects of feed gas composition on the gas separation performance of the PVAm/PEBAX(0.025) blend membrane were investigated, and the results are shown in Figures 3.14, 3.15, and 3.16. All tests were conducted at feed gas pressure of 400, 600, and 800 kPa and 298 K.

As the mole fraction of CO_2 in the feed gas increased, more CO_2 would be dissolved into the PVAm/PEBAX(0.025) blend membrane. When a large amount of CO_2 dissolved in the membrane, the strong sorption of CO_2 made the polymer chain flexible, and the diffusion of gas molecules across the membrane became easy. This is the so-called CO_2-induced plasticization which can contribute to improving CO_2 diffusivity in the membrane. However, more CO_2 dissolved into membranes resulted in an increase in the concentrations of ionic species, such as carbamates, bicarbonates, protonated amines. Hence, the further dissolution of CO_2 in the membrane was prevented, which is the so-called salting-out effect. Besides, the number of amino groups in membranes was limited, and further increasing the mole fraction of CO_2 in the feed gas would not effectively increase the CO_2 permeability. As a result, CO_2 permeability did not increase dramatically when the mole fraction of CO_2 in the feed gas increased as shown in Figures 3.14 (a), 3.15 (a), and 3.16 (a).

For N_2, CH_4, and H_2 permeation, they only obeyed the solution-diffusion mechanism. The CO_2-induced plasticization effect can not only enhance the CO_2 permeation but also improve the permeation of other gases simultaneously. As shown in Figures 3.14 (b), 3.15 (b), and 3.16 (b), when the mole fraction of CO_2 in the feed gas increased, the N_2 and CH_4 permeability of the PVAm/PEBAX(0.025) blend membrane increased slightly, while the H_2 permeability increased significantly. The H_2 permeability of the PVAm/PEBAX(0.025) blend membrane increased from 37.7 to 74.1 Barrer when the mole fraction of CO_2 in the feed gas increased from 0.08 to 0.87
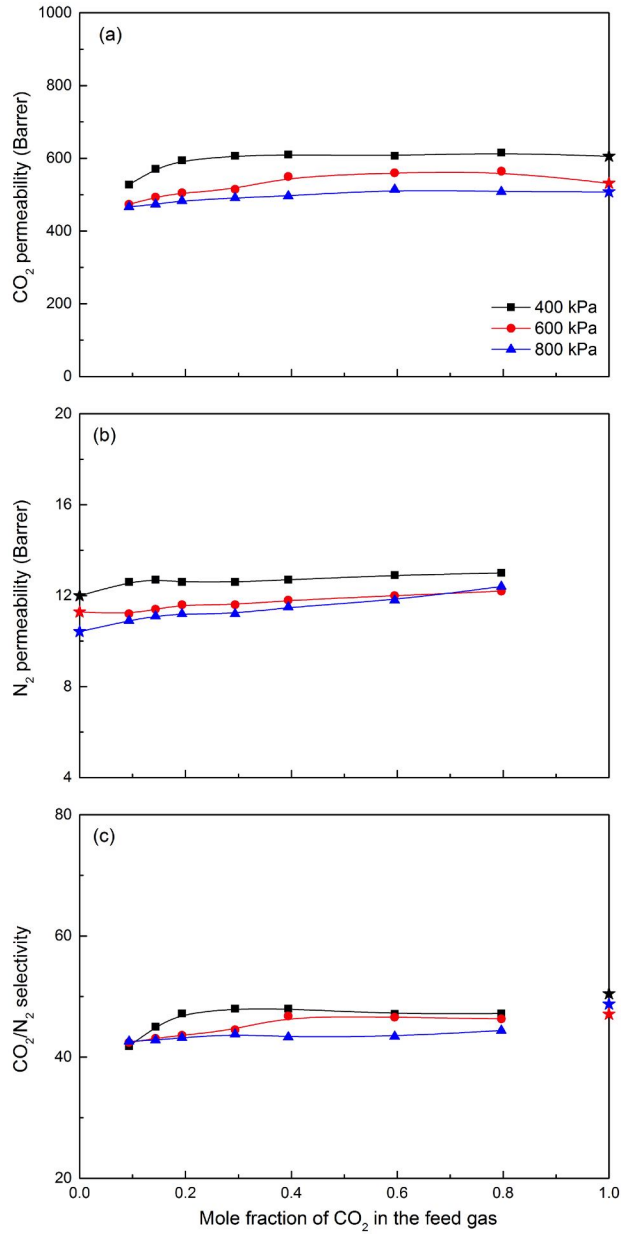
Figure 3.14: Effect of feed gas composition on CO_2 permeability (a), N_2 permeability (b), and CO_2/N_2 selectivity (c) in CO_2/N_2 gas mixture permeation (The symbol star represents pure gas permeability and ideal gas selectivity)
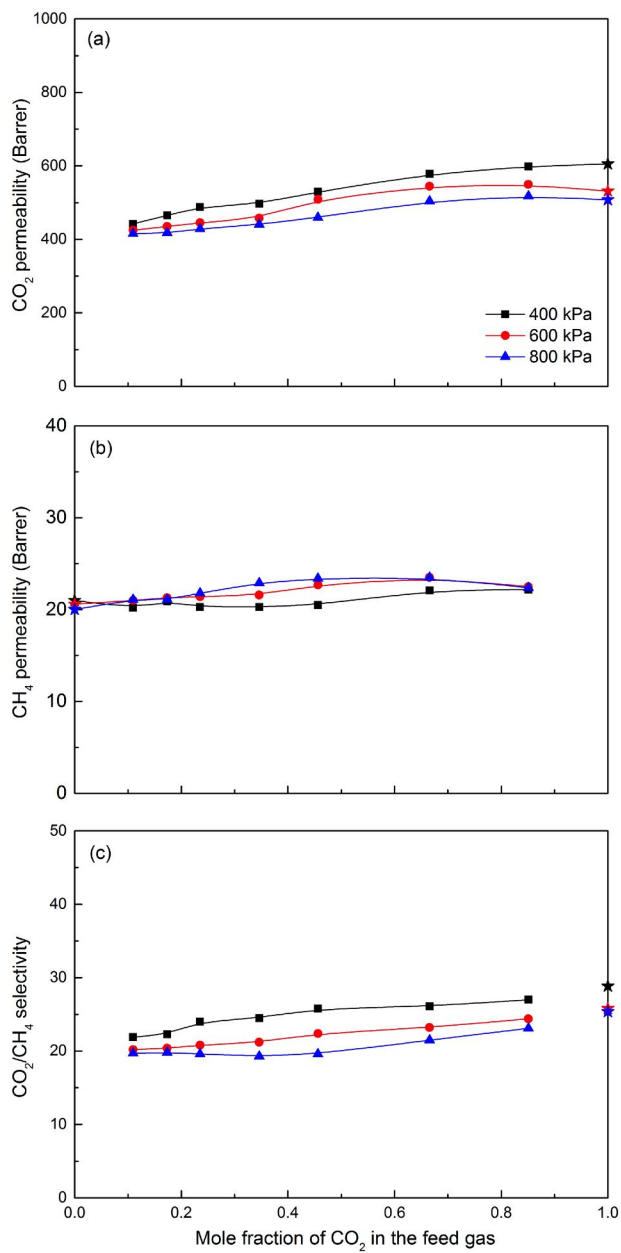
Figure 3.15: Effect of feed gas composition on gas permeability of CO_2 permeability (a), CH_4 permeability (b), and CO_2/CH_4 selectivity (c) in CO_2/CH_4 gas mixture permeation (The symbol star represents pure gas permeability and ideal gas selectivity)
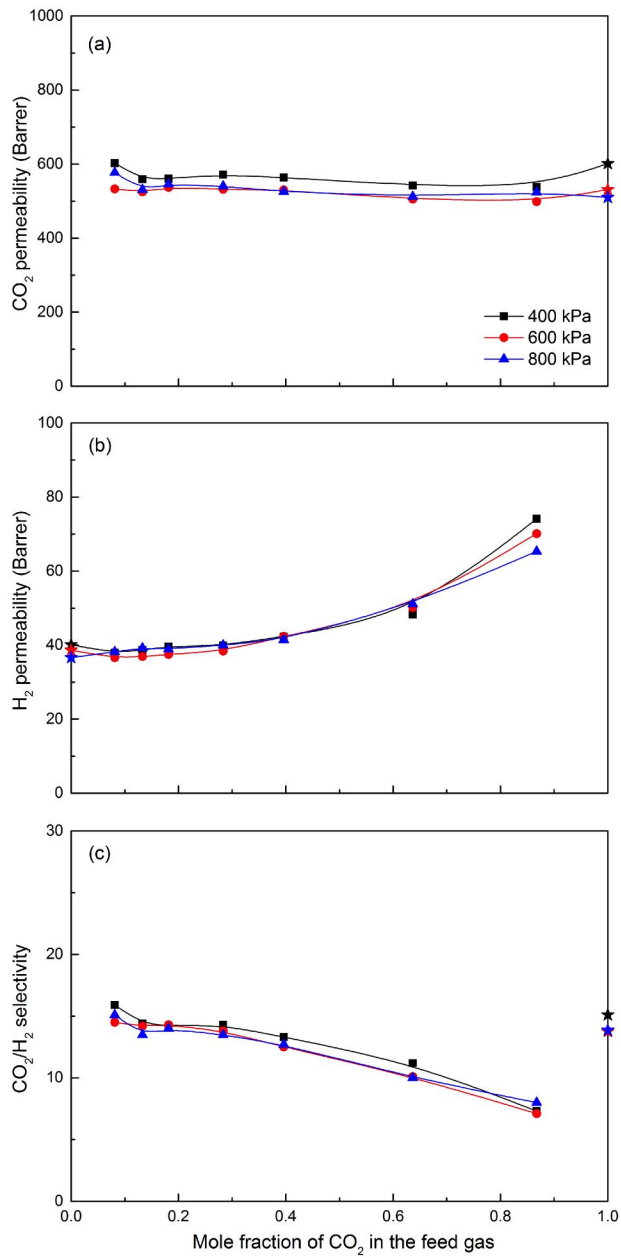
Figure 3.16: Effect of feed gas composition on gas permeability of CO_2 permeability (a), H_2 permeability (b), and CO_2/H_2 selectivity (c) in CO_2/H_2 gas mixture permeation (The symbol star represents pure gas permeability and ideal gas selectivity)

under a feed gas pressure of 400 kPa. Due to the smallest kinetic diameter of H_2 among these three gases (*e.g.*, N_2, CH_4, and H_2), the CO_2-induced plasticization effect allowed the smaller gas molecules to diffuse easily, which indicated that the CO_2-induced plasticization effect impacted H_2 permeation more significantly than N_2 and CH_4 permeation.

The variations in the CO_2, N_2, CH_4, and H_2 permeability of the PVAm/PEBAX(0.025) blend membrane determined the variations in the CO_2/N_2, CO_2/CH_4, and CO_2/H_2 selectivity. As a consequence, with the mole fraction of CO_2 increasing in the feed gas, the CO_2/H_2 selectivity decreased, and the CO_2/N_2 and CO_2/CH_4 selectivity did not show significant changes, as shown in Figures 3.14 (c), 3.15 (c), 3.16 (c). However, the gas selectivity for binary gas separations was lower than the ideal gas selectivity.

3.3.5 Membrane stability

The stability of the membranes is an important factor that determines if the membranes can be used in practical application. The stability of the PVAm/PEBAX(0.025) blend membrane was studied. The feed gas compositions for different systems were CO_2/CH_4 (35/65 vol%), CO_2 /N_2 (14/86 vol%) and CO_2/H_2 (40/60 vol%), which corresponded to carbon emission sources in natural gas sweetening, flue gas, and gas mixture after the water-gas shift reaction, respectively. The membrane was tested at 298 K under a feed gas pressure of 400 kPa every day over three weeks. The feed gas and sweeping gas were not humidified during the first two weeks. After that, it was hydrated for continued tests with humid feed gas and sweeping gas.

As demonstrated in Figures 3.17 (a), 3.18 (a), and 3.19 (a), the CO_2 permeability of the PVAm/PEBAX(0.025) blend membrane decreased more significantly than other gases in dry conditions. Compared with the other three gases, CO_2 solubility in water (1.25 g/kg water) is the highest (Table 2.1). Therefore, when the content of water in the membrane decreased gradually, CO_2 permeability decreased quickly. With the dehydration of the membrane getting worse, the membrane became less swollen resulting in a decrease in N_2, CH_4, and H_2 permeability. Then,

the membrane was wetted and permeation tests continued for one more week, and feed gas and sweeping gas were saturated by water to keep a humid test condition. The CO_2/N_2, CO_2/CH_4, and CO_2/H_2 separation performance of the membrane were stable, and there was no significant decrease in gas permeability and selectivity during the test.
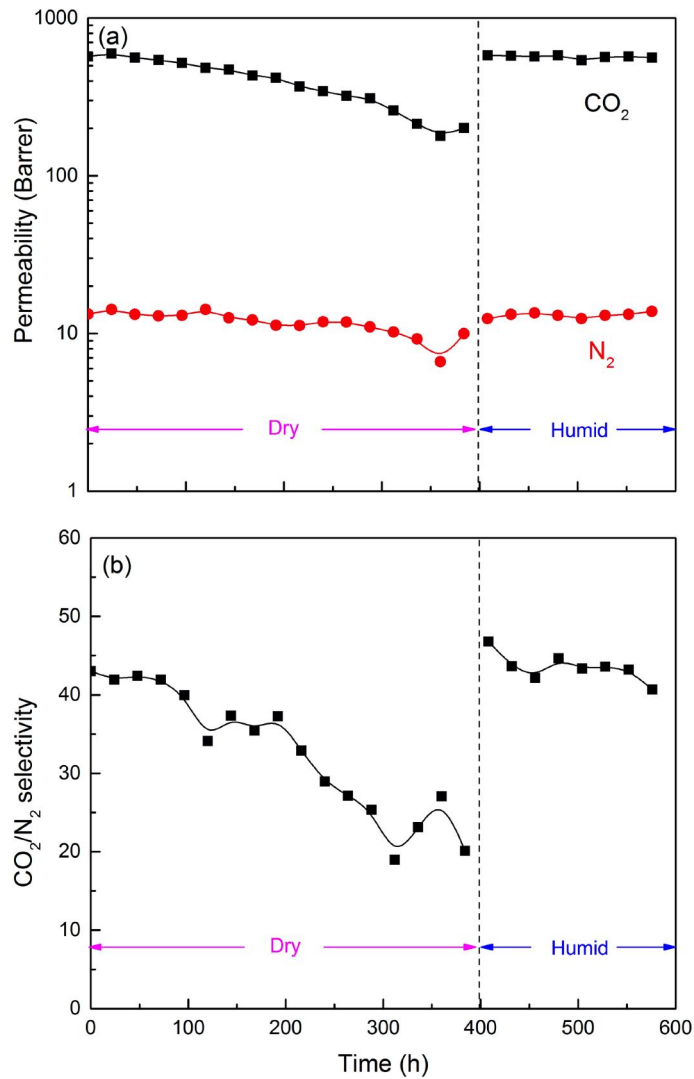
Figure 3.17: Stability of the PVAm/PEBAX(0.025) blend membrane in CO_2/N_2 separation: gas permeability of CO_2 and N_2 (a), CO_2/N_2 selectivity (b)
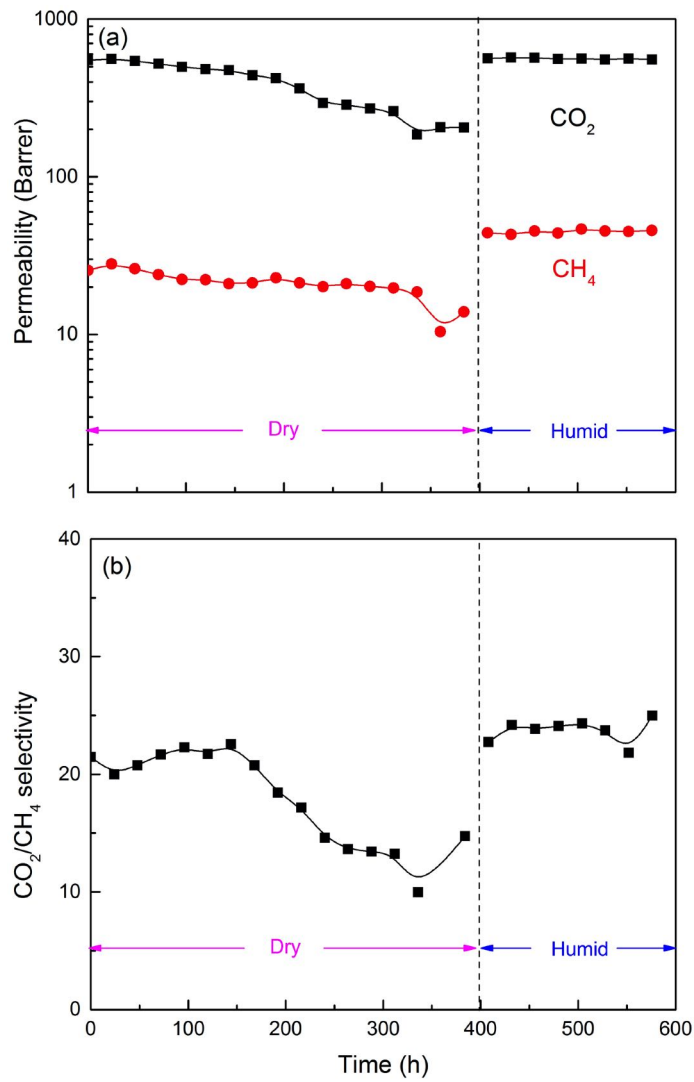
Figure 3.18: Stability of the PVAm/PEBAX(0.025) blend membrane in CO_2 /CH_4 separation: gas permeability of CO_2 and CH_4 (a), CO_2/CH_4 selectivity (b)
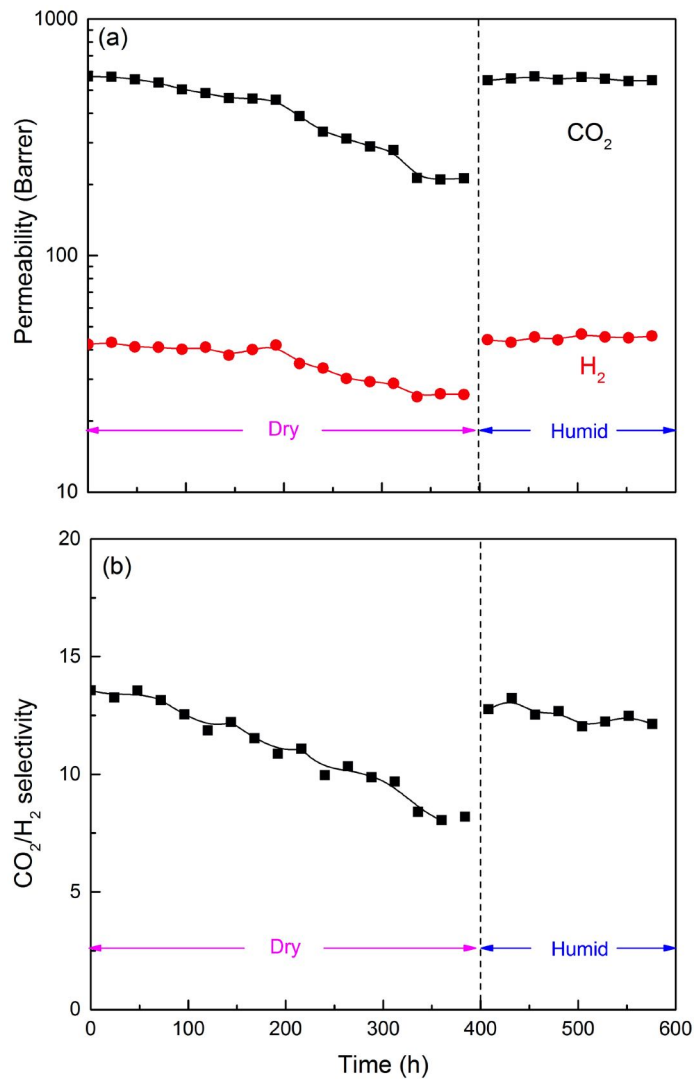
Figure 3.19: Stability of the PVAm/PEBAX(0.025) blend membrane in CO_2 /H_2 separation: gas permeability of CO_2 and H_2 (a), CO_2/H_2 selectivity (b)

3.4 Conclusions

PVAm/PEBAX blend membranes were fabricated by a solution casting method. The combination of PVAm and PEBAX improved membrane hydrophilicity and enhanced CO_2 solubility. Pure gas permeation of CO_2, N_2, CH_4, and H_2 of the PEBAX and the PVAm/PEBAX(0.025) blend membranes at different temperatures and pressures was investigated. The gas mixture permeation for CO_2/N_2, CO_2/CH_4 and CO_2/H_2 and the stability of the PVAm/PEBAX(0.025) blend membrane were studied. The following conclusions can be drawn:

- As the mass ratio of PVAm to PEBAX increased, the CO_2 permeability of the blend membranes increased due to the increase in membrane hydrophilicity. Comparing with the pristine PEBAX membrane, the PVAm/PEBAX(0.025) blend membrane showed a 41% increase in CO_2 permeability, while the CO_2/N_2, CO_2/CH_4 and CO_2/H_2 selectivity remained the same, which were 52, 27, and 15 at 298 K and 400 kPa, respectively.

- The temperature dependence of CO_2, N_2, CH_4, and H_2 permeability followed an Arrhenius type of relationship. As the temperature increased, CO_2, N_2, CH_4, and H_2 permeability of both the PEBAX and PVAm/PEBAX(0.025) blend membranes increased. However, the effect of temperature on CO_2 permeability was less significant than that on other gases, resulting in decreased CO_2/N_2, CO_2/CH_4 and CO_2/H_2 selectivity.

- The feed gas pressure hardly impacted the CO_2, N_2, CH_4, and H_2 permeability of both the PEBAX and PVAm/PEBAX(0.025) membranes.

- The CO_2-induced plasticization effect, the salting-out effect, and limited numbers of amine groups in the PVAm/PEBAX(0.025) blend membrane affected CO_2 permeation. Owing to the different kinetic diameters of N_2, CH_4, and H_2, the CO_2-induced plasticization effect affected H_2 diffusion more significantly than N_2 and CH_4 diffusion, resulting that the CO_2/H_2 selectivity decreased from 15.9 to 7.3 at 400 kPa when the mole fraction of CO_2 in the feed gas increased from 0.08 to 0.87.

- Due to different solubility of CO_2, N_2, CH_4, and H_2 in water, CO_2 was more sensitive to the hydration conditions in the membrane than N_2, CH_4, and H_2. The decrease in water content in the membrane resulted in a decrease in gas permeability. However, when the membrane was humidified again, there was no obvious reduction of gas permeability and selectivity during around a one-week test in humid conditions.

Chapter 4

DEA/PVAm/PEBAX composite membranes for carbon capture

4.1   Introduction

In the previous chapter, the presence of PVAm enhanced membrane hydrophilicity and improved CO_2 permeability. However, there was no chemical crosslinking between PVAm and PEBAX, so the membranes became highly swollen in the high content of PVAm. The decrease in the mechanical property of the membranes made it difficult to handle. A substrate support is a good option to strengthen the mechanical property of membranes, while the surface layer provides separation properties. Besides, a thinner surface layer results in larger gas permeance. Hence, in order to further enhance membrane hydrophilicity by increasing the content of PVAm, PVAm/PEBAX composite membranes were prepared on a polysulfone (PSf) membrane.

PVAm has a high crystallinity due to strong intermolecular interaction [Yi et al. (2006)]. PVAm can be blended with small molecule amines including monoethanolamine (MEA), di-ethanolamine (DEA), N-methyldiethanolamine (MDEA), 2-amino-2-methyl-1-propanol (AMP), ethanediamine (EDA), and piperazine (PIP) (Figure 4.1) to not only reduce crystallinity of the

(a) Monoethanolamine (MEA)

(b) Diethanolamine (DEA)

(c) N-methyldiethanolamine (MDEA)

(d)   2-amino-2-methyl-1-propanol

(AMP)

(e) Ethanediamine (EDA)

(f) Piperazine (PIP)
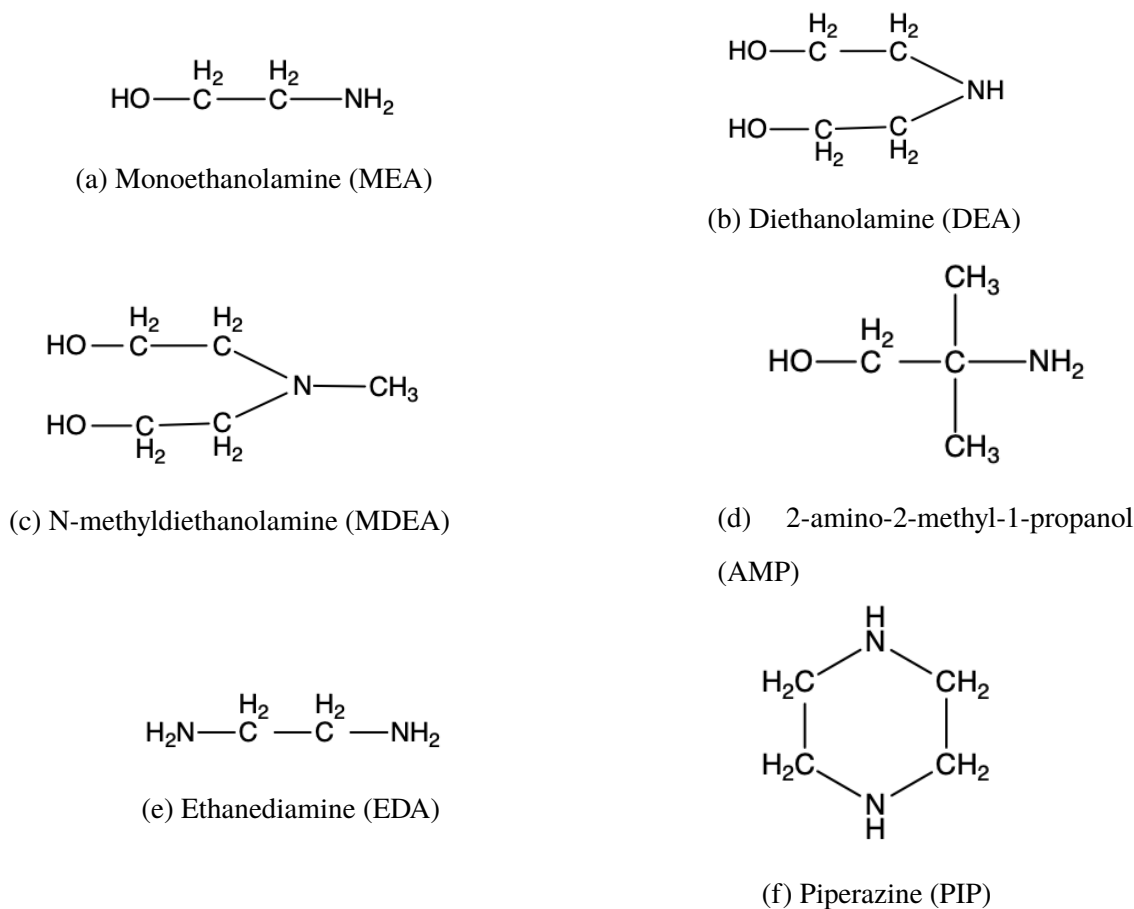
Figure 4.1: Chemical structures of small molecule amines

membranes but also facilitate CO_2 transport [Francisco et al. (2007, 2010); Qiao et al. (2015)]. Qiao et al. (2013) prepared PVAm membranes with PIP to increase amounts of effective carriers and decrease membrane crystallinity. The prepared PVAm-PIP/polysulfone (PSf) composite membrane showed a high CO_2/N_2 selectivity of 277 under a feed pressure of 0.11 MPa in CO_2/N_2 (20/80 by volume) mixed gas separation. Therefore, the addition of small molecule amines is capable of avoiding the crystallinity of PVAm. Moreover, amine groups have been considered as good CO_2 carriers in the membranes due to the reversible reaction with CO_2. Polymers with amine groups act as fixed site CO_2 carriers in the membranes. CO_2 diffuses through the membranes by "hopping" between the amine groups on polymeric chains whose mobility is relatively

limited. Small molecule amines serve as "ferry boats" plying CO_2 between feed side and permeate side. Francisco et al. (2007) fabricated facilitated transport membranes for CO_2/N_2 separation by blending monoethanolamine (MEA), diethanolamine (DEA), N-methyldiethanolamine (MDEA), and 2-amino-2-methyl-1-propanol (AMP) in PVA matrix. Comparing four amines, it was found the reaction rate between amines and CO_2 is moderate, which means DEA can bond with CO_2 easily in the feed side and release CO_2 quickly in the permeate side. Qiao et al. (2015) also used PVAm as fixed carriers and small molecules as mobile carriers (ethanediamine (EDA), piperazine (PIP), MEA and DEA) to prepare composite membranes for CO_2/H_2 separation. The hydrogen bonds between polymeric amines and small molecule amines were expected to stabilize small molecule amines in the polymer matrix. Small molecule amines composing of primary amines, secondary amines, and tertiary amines have different characteristics of interactions with CO_2. Hence, some research works also tried to use more than one small molecule amines in the membranes to increase permselectivity [Hu (2013)].

Although the solution-diffusion mechanism dominates gas permeation in the water-swollen membranes, DEA is still a good substitute of PVAm [Liu et al. (2008)]. On one hand, the molecular weight and viscosity of DEA are smaller than those of PVAm, which can reduce membrane thickness and increase gas permeance. On the other hand, DEA is water-soluble and can move more freely than PVAm in the membranes, and it also can enhance membrane hydrophilicity by hydration. Therefore, DEA was physically blended in the membranes to prepare water-swollen DEA/PVAm/PEBAX composite membranes for CO_2/N_2, CO_2/CH_4 and CO_2/H_2 separations. The effects of membrane composition on pure gas permeation of CO_2, N_2, CH_4, and H_2 were studied. The effects of temperature and feed gas pressure on the pure gas permeation in the PEBAX, PVAm/PEBAX, and DEA/PVAm/PEBAX composite membranes were investigated. The gas mixture permeation in the prepared DEA/PVAm/PEBAX composite membrane for CO_2/N_2, CO_2/CH_4, and CO_2/H_2 separations was studied, and the stability of the membrane was tested during 19 days under humid conditions.

69

4.2   Experimental

4.2.1   Materials

Diethanolamine (DEA) was obtained from Aldrich Co. with a purity of 99%. All other materials used in this study were the same as described in Chapter 3. Polysulfone (PSf) membranes (molecular weight cut-off of about 100,000 Da) were provided by Sepro Membrane Inc.

4.2.2   Membrane preparation

15 g of PEBAX pellets were used to prepare homogeneous PEBAX solution (5 wt%) which was described in the previous chapter. Polysulfone (PSf) substrate was immersed into water for 24 h before casting. 12 g of PEBAX solution was cast on the PSf substrate, and the casting area was controlled by a frame (198 cm^2). The membrane was placed in a dust-free chamber to evaporate solvent at ambient conditions for 48 h, and then the PEBAX composite membrane was collected.

The PVAm/PEBAX composite membranes with different PVAm contents were prepared. The preparation of the PVAm/PEBAX(0.043) composite membrane was used to describe the process. After preparing the PEBAX solution (5 wt%), 0.203 g of Lupamin was added to 11.484 g of PEBAX solution. The solution continued being vigorously stirred for 2 h at room temperature. The PVAm/PEBAX solution was degassed by ultrasonication for 1 h and then cast on a PSf substrate (198 cm^2). After evaporating solvent in a dust-free chamber, the PVAm/PEBAX(0.043) composite membrane was collected. In fabricating the PVAm/PEBAX composite membranes with different PVAm contents, the total mass of polymer used was 0.6 g, and the membrane composition was determined by adjusting the mass fraction of PVAm in the membranes. The obtained composite membranes were designated as PVAm/PEBAX(X), where X (X = 0, 0.021, 0.043, 0.064, 0.10, 0.15) represents the mass fraction of PVAm in the membranes.

The DEA/PVAm/PEBAX composite membranes were prepared by the same solution casting method. The preparation of the DEA(0.20)/PVAm(0.043)/PEBAX composite membrane was

used as an example to describe the process. After obtaining the PVAm/PEBAX polymer solution by the same procedures, 0.15 g of DEA was blended into the polymer solution (11.687 g) under vigorous stirring for 2 h at room temperature. After the same following steps (*e.g.*, degassing, casting, and evaporating solvent), the preparation of the DEA(0.20)/PVAm(0.043)/PEBAX composite membrane was completed. The composition of the composite membranes was controlled by adjusting the mass faction of DEA while keeping the mass of polymer unchanged (0.6 g). The prepared composite membranes were designated as DEA(Y)/PVAm(X)/PEBAX, where Y (Y=0, 0.048, 0.091, 0.20, 0.33, 0.43) represents the mass faction of DEA in the membranes. The effective thicknesses of all prepared membranes (excluding the substrate membrane thickness) were in the range of 13.5-32.2 *μm* in the dry condition and 38.5-77.7 *μm* in the humid condition. The thicknesses of membranes were measured by a micrometer at ten different places on the membranes and the average value was used.

4.2.3 Measurement of contact angle of water

The contact angles of water on the prepared membranes were measured by a contact angle meter (Cam-plus Micro, Tantec Inc.) using the sessile drop (about 3 μL) method. After the water drop contacted the membrane surface, the measurement of water contact angle was completed within 40 s. The membranes were measured at five different places on the surface. The average values of contact angles of water were used, and the relative standard deviations were within 9%.

4.2.4 Gas permeation tests

The pure and gas mixture permeation tests were the same as described in Chapter 3. Gas permeance (J) was used to describe the permeability of the membranes. In pure gas permeation tests, the permeance of the gas through membranes was calculated from:

$$J = \frac{V}{A\,t\,(p_{feed} - p_{perm})} \frac{273.15}{T_0} \frac{p_0}{76} \qquad (4.1)$$

where J is permeance (cm^3 (STP) cm^{-2} s^{-1} cm Hg^{-1}), V is the permeate gas volume (cm^3) measured at ambient conditions (temperature T_0 (K), pressure p_0 (cm Hg)) during a period of time $t(s)$, A is the effective area of the membrane (cm^2), and p_{feed} and p_{perm} (cm Hg) are the feed pressure and permeate pressure, respectively. The unit of permeance is usually expressed as GPU, 1 GPU = 10^{-6} cm^3 (STP) cm^{-2} s^{-1} cm Hg^{-1}). The ideal selectivity (separation factor), $\alpha_{i/j}$, was calculated from:

$$\alpha_{i/j} = \frac{J_i}{J_j} \qquad (4.2)$$

In the gas mixture permeation tests, the permeance of one component i, J_i, was calculated from:

$$J_i = \frac{V\,x_{perm,i}}{(p_{feed}x_{feed,i} - p_{perm}x_{perm,i})\,A\,t} \frac{273.15}{T_0} \frac{p_0}{76} \qquad (4.3)$$

where $x_{feed,i}$ represents the mole fraction of component i in the feed gas, and $x_{perm,i}$ represents the mole fraction of component i in the permeate gas. The membrane selectivity (or separation factor), $\alpha_{i/j}$, was calculated by Equation 4.2. Gas permeance of the composite membranes from the same batch showed a relative standard deviation within 7%, which can be considered as the experimental error. The relative standard deviation in gas permeance of the membranes from different batches was within 16%.

4.3 Results and discussion

4.3.1 Effect of membrane composition

The effects of the mass fraction of PVAm in the membranes on pure gas permeation performance at room temperature and under a feed gas pressure of 700 kPa were studied. PVAm polymer chain contains amine groups which can enhance membrane hydrophilicity and CO_2 solubility. Therefore, as shown in Figure 4.2 (a), CO_2 permeance increased from 6.24 to 9.83 GPU when the mass fraction of PVAm increased from 0 to 0.043. For the permeation of N_2, CH_4, and H_2, the solution-diffusion mechanism dominates the process. As the mass fraction of PVAm increased gradually, the membranes became more swollen and created more free volume. An increase in N_2, CH_4, and H_2 permeance resulted from the enhancement of membrane hydrophilicity when the mass fraction of PVAm increased from 0 to 0.043. However, when the mass fraction of PVAm was higher than 0.043, CO_2, N_2, CH_4, and H_2 permeance of the PVAm/PEBAX composite membranes tended to decline. PVAm has a relatively high crystallinity due to its linearly structured polymer chains [Hu et al. (2012)]. Hence, the polymer chains of PEBAX and PVAm may not be able to be entangled very well resulting in an increase in the crystallinity of the membranes when the mass fraction of PVAm in the membranes increased. High crystallinity of the membranes affected the gas permeation which usually leads to lowering gas permeability [Yi et al. (2006); Yuan et al. (2011); Qiao et al. (2013)]. As a consequence, all gas permeance decreased with an increase in the mass fraction of PVAm in the PVAm/PEBAX composite membranes.

As demonstrated in Figure 4.2 (b), when the content of PVAm in the membranes increased, the ideal selectivity of CO_2/N_2, CO_2/CH_4 and CO_2/H_2 didn't change significantly since the permeance of CO_2, N_2, CH_4, and H_2 at the same extent. Although the membrane structures became looser, the selectivity was unchanged. Compared with the pristine PEBAX membrane, the PVAm/PEBAX(0.043) composite membrane showed a 57.5% increase in CO_2 permeance, while the ideal selectivity remained comparable. Therefore, the PVAm/PEBAX(0.043) composite

membrane was chosen to further study. The PVAm/PEBAX(0.043) composite membrane was abbreviated as the PVAm/PEBAX composite membrane in the following discussion for simplicity.
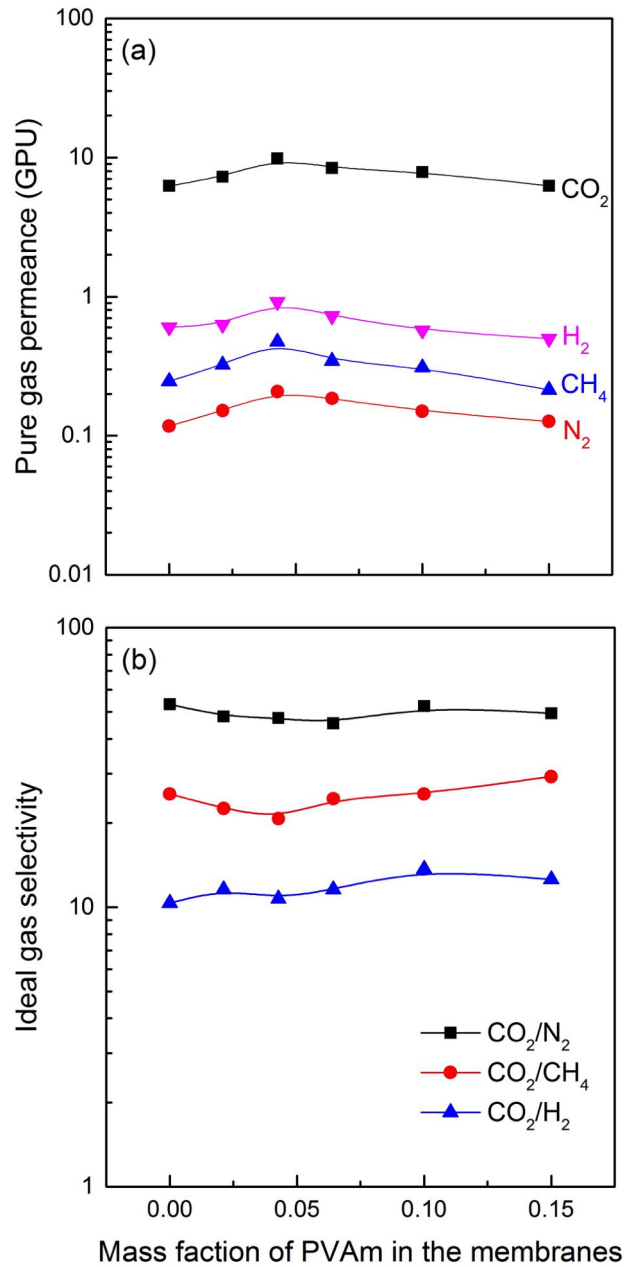
Figure 4.2: Effect of the mass fraction of PVAm in the membranes on the pure gas permeance (a) and the ideal gas selectivity (b) of the PVAm/PEBAX composite membranes

In order to avoid high crystallization of PVAm, small molecule amines (DEA) were blended into the membranes. The effects of the DEA content in membranes were studied, and the results of the pure gas permeation tests of the DEA/PVAm/PEBAX composite membranes at room temperature and under a feed gas pressure of 700 kPa were presented in Figure 4.3. CO_2, N_2, CH_4, and H_2 permeance increased and then decreased as the mass fraction of DEA increased (Figure 4.3 (a)). It is not surprising that all pure gas permeance increased initially with the addition of DEA due to the improving hydrophilicity of the membranes, for instance, CO_2 permeance increased from 9.83 to 12.53 GPU when the mass fraction of DEA increased from 0 to 0.20. Nonetheless, when the mass fraction of DEA exceeded 0.20, CO_2, N_2, CH_4, and H_2 permeance underwent a decrease simultaneously. For CO_2 permeation, as CO_2 was dissolved into the membranes, it would react with amino groups thereby improving CO_2 solubility in the DEA/PVAm/PEBAX composite membranes. The higher contents of DEA in the composite membranes meant more CO_2 could be dissolved, which meant more ions would be generated. The presence of these ions caused the salting-out effect which could reduce CO_2 solubility. Besides, for both CO_2 and inert gas (N_2, CH_4, and H_2) permeation, some transport sites or pathways would be occupied by these ionic species leading to a decrease in gas permeance. Thus, the further increase in the mass fraction of DEA in the membranes cannot ensure the increase in gas permeance due to the opposite effects of membrane swelling and the salting-out effect.

Comparing with N_2, CH_4, and H_2 permeation, CO_2 permeation suffered more than other three gases as the mass fraction of DEA increased. Hence, the selectivity of CO_2/N_2, CO_2/CH_4, and CO_2/H_2 kept unchanged and then decreased to some extent when the mass fraction of DEA increased (Figure 4.3 (b)). Among all the DEA/PVAm/PEBAX composite membranes, the CO_2/N_2, CO_2/CH_4, and CO_2/H_2 selectivity of the DEA(0.20)/PVAm(0.043)/PEBAX composite membrane was 42.3, 22.9, and 12.1, respectively. It was selected to further study the other effects (*e.g.*, temperature, feed gas pressure, feed gas composition). For simplicity, the DEA(0.20)/PVAm(0.043)/PEBAX composite membrane was abbreviated as the DEA/PVAm/PEBAX composite membrane in the following discussion.

Figure 4.3: Effect of the DEA content on the pure gas permeance (a) and the ideal gas selectivity (b) of the DEA(Y)/PVAm(0.043)/PEBAX composite membranes
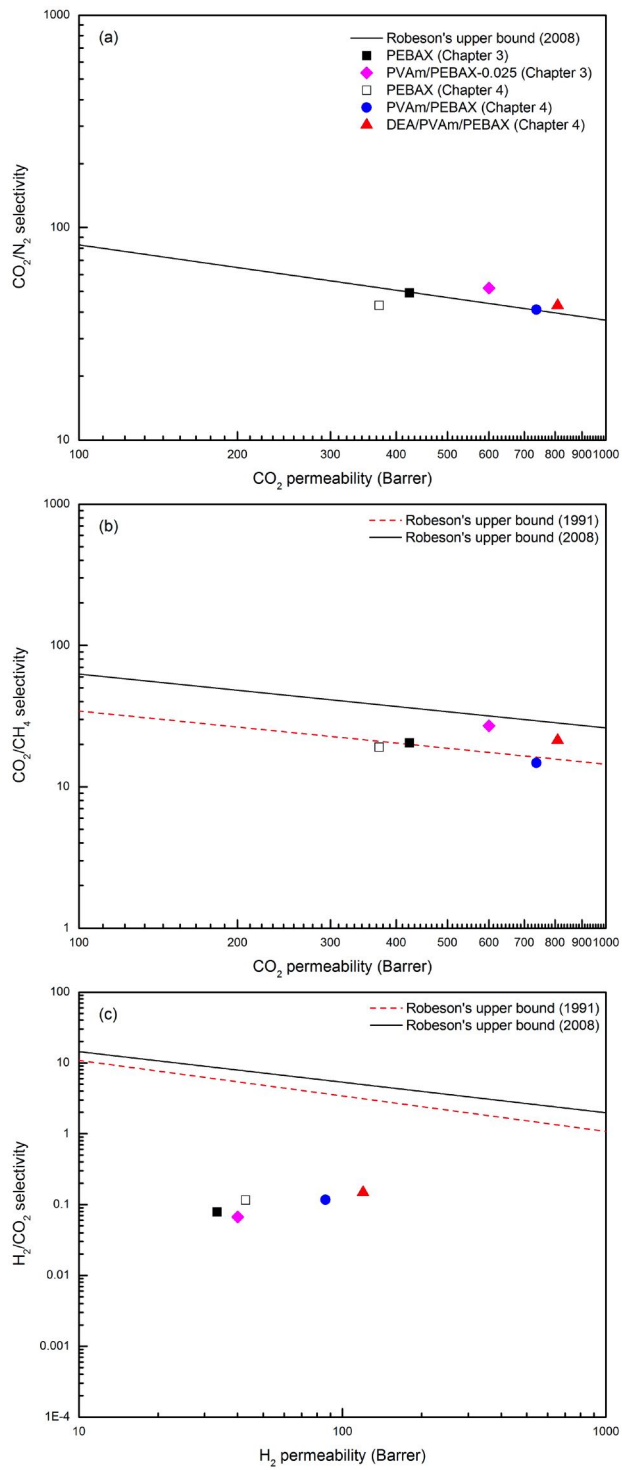
Figure 4.4: Comparison with Robeson's upper bound for CO_2/N_2 (a), CO_2/CH_4 (b), and H_2/CO_2 (c)

Gas permeability of the PEBAX, PVAm/PEBAX, and DEA/PVAm/PEBAX composite membranes was calculated based on the effective thickness which excluded the thickness of the substrate, and the comparison of gas permeation performance with Robeson's upper bound was shown in Figure 4.4. The CO_2 permeability of PEBAX symmetric membrane (Chapter 3) and PEBAX/PSf asymmetric membrane (Chapter 4) showing a difference of 12% which was within the experimental error. As demonstrated in Figure 4.4, gas permeation for CO_2/N_2 and CO_2/H_2 of the DEA/PVAm/PEBAX composite membrane surpassed Robeson's upper bound (2008), but gas permeation for CO_2/CH_4 was between two upper bounds. Water in the membranes can serve as a plasticizer which affects inter space between polymer chains to create more free volume. Besides, water can provide the pathways for gas permeation in the membranes [Liu et al. (2008)]. As shown in Table 4.1, the variations in contact angles of water on the prepared membranes indicated that the hydrophilicity of the membranes was enhanced. As shown in Figure 4.4, improving the hydrophilicity of the membranes by the addition of PVAm or DEA can increase gas permeability. Nonetheless, the structures of the water-swollen membrane became loose, and gas selectivity cannot be improved effectively.

Table 4.1: The contact angles of water on the substrate, PEBAX, PVAm/PEBAX, and DEA/PVAm/PEBAX composite membranes

Membranes	Contact angle of water
Polysulfone substrate	84°
PEBAX	68°
PVAm/PEBAX	55°
DEA/PVAm/PEBAX	38°

4.3.2 Effect of temperature

Figures 4.5, 4.6, and 4.7 show the effects of temperature on the pure gas permeance and the ideal selectivity of the PEBAX, PVAm/PEBAX, and DEA/PVAm/PEBAX composite membranes, respectively. The temperature dependence of CO_2, N_2, CH_4, and H_2 permeance of the PEBAX, PVAm/PEBAX, and DEA/PVAm/PEBAX composite membranes can be fitted by the Arrhenius equation:

$$J_i = J_{0,\,i}\,exp(-\frac{E_{J,\,i}}{RT}) \tag{4.4}$$

where $J_{0,\,i}$ is the pre-exponential factor (GPU), $E_{J,\,i}$ is the activation energy for gas permeation (kJ/mol), R is ideal gas constant ($kJ/(mol\,K)$), and T is temperature (K). The activation energy for CO_2, N_2, CH_4, and H_2 permeation in the PEBAX, PVAm/PEBAX, and DEA/PVAm/PEBAX composite membranes is shown in Figure 4.8.

As demonstrated in Figures 4.5 (a), 4.6 (a), and 4.7 (a), CO_2, N_2, CH_4, and H_2 permeance of the PEBAX, PVAm/PEBAX, and DEA/PVAm/PEBAX composite membranes increased at elevated temperatures. A high temperature can not only accelerate the transport rates of gas molecules through the membranes but also enhance the mobility of polymer chains, resulting in allowing gas molecules to diffuse across the composite membranes easily. Besides, it was evident that N_2, CH_4, and H_2 permeance increased more dramatically than CO_2 permeance when the operating temperature increased from 302 to 342 K since CO_2 had lower activation energy for permeation in the membranes than N_2, CH_4, or H_2 (Figure 4.8). Activation energy for permeation is composed of the heat of sorption and activation energy for diffusion. Generally, gas solubility in water declined at elevated temperatures, and it indicated that the heat of sorption is commonly negative. Due to the strong interactions between CO_2 and the membranes, the heat of sorption for CO_2 was lower than N_2, CH_4, and H_2 [Zhao et al. (2014); Liu et al. (2008)]. Therefore, temperature impacted CO_2 permeation less significantly than N_2, CH_4, and H_2 permeation, resulting that the CO_2/N_2, CO_2/CH_4 and CO_2/H_2 selectivity of all three membranes reduced with increasing temperatures (Figures 4.5 (b), 4.6 (b), and 4.7 (b)). High operating temperature can

contribute to promoting the gas permeance rather than the selectivity of CO_2/N_2, CO_2/CH_4 and CO_2/H_2 in the water-swollen membranes.

As shown in Figure 4.8, when the feed gas pressure increased from 400 to 700 kPa, the activation energy for CO_2, N_2, CH_4, and H_2 permeation in these three membranes did not change. The activation energy for gas permeation indicates the energy barrier for gas permeating through the membranes. Compared with the pristine PEBAX composite membrane, the PVAm/PEBAX composite membrane became more hydrophilic and swollen due to the addition of PVAm. Hence, the energy barrier for gas diffusion in the PVAm/PEBAX composite membrane could be lower than the PEBAX composite membrane. However, when DEA was blended into the membranes, on the one hand, the membrane hydrophilicity increased; on the other hand, DEA would occupy some inter space between polymer chains, resulting that activation energy for gas permeation in the DEA/PVAm/PEBAX composite membrane was higher than the PVAm/PEBAX composite membrane.

Figure 4.5: Effect of temperature on the pure gas permeance (a) and the ideal gas selectivity (b) of the PEBAX composite membrane
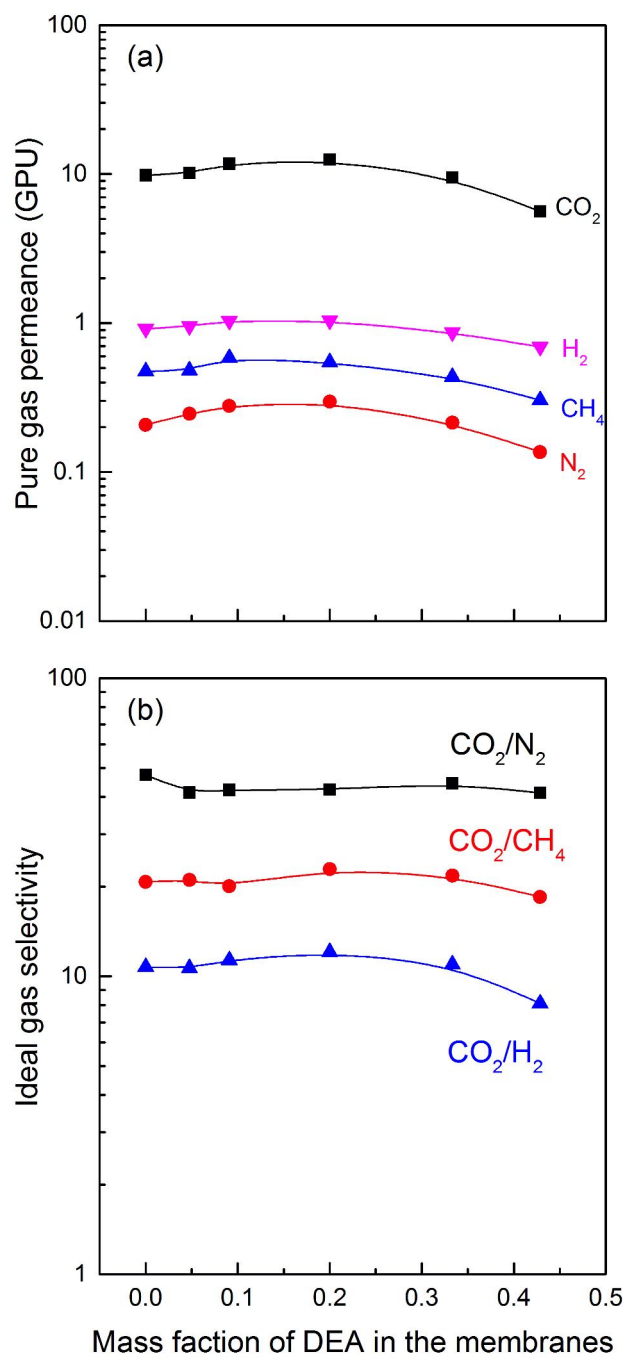
Figure 4.6: Effect of temperature on the pure gas permeance (a) and the ideal gas selectivity (b) of the PVAm/PEBAX composite membrane
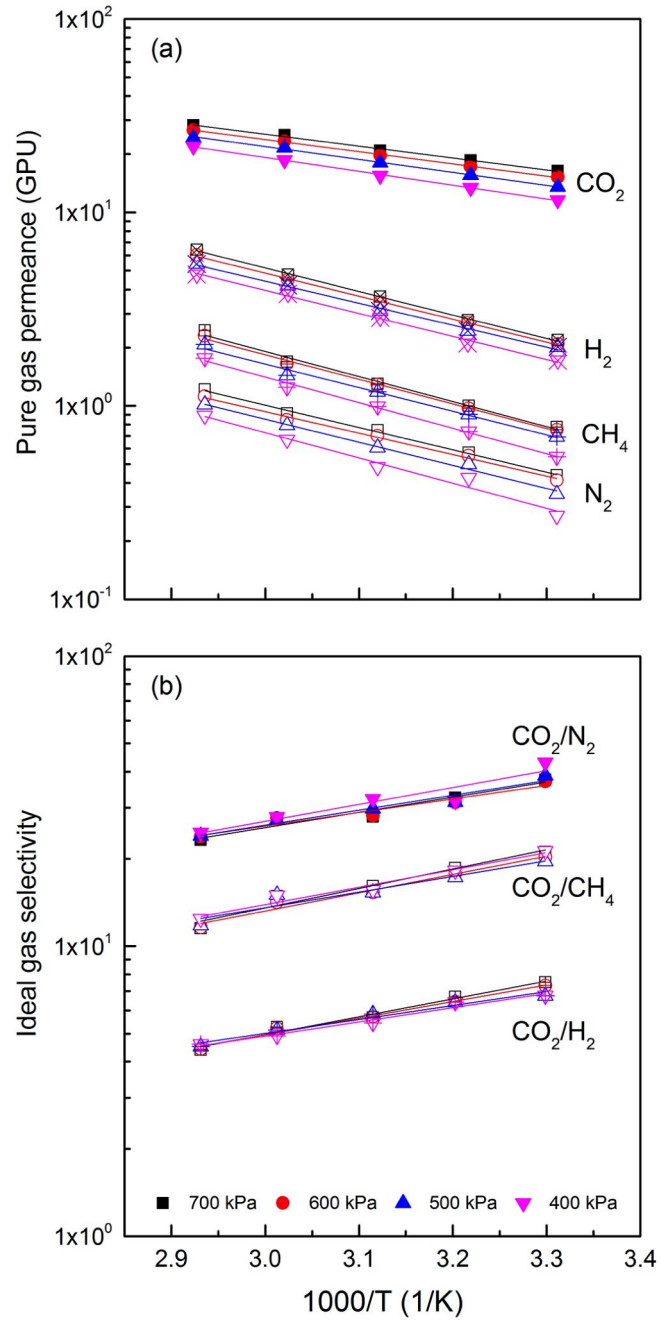
Figure 4.7: Effect of temperature on the pure gas permeance (a) and the ideal gas selectivity (b) of the DEA/PVAm/PEBAX composite membrane
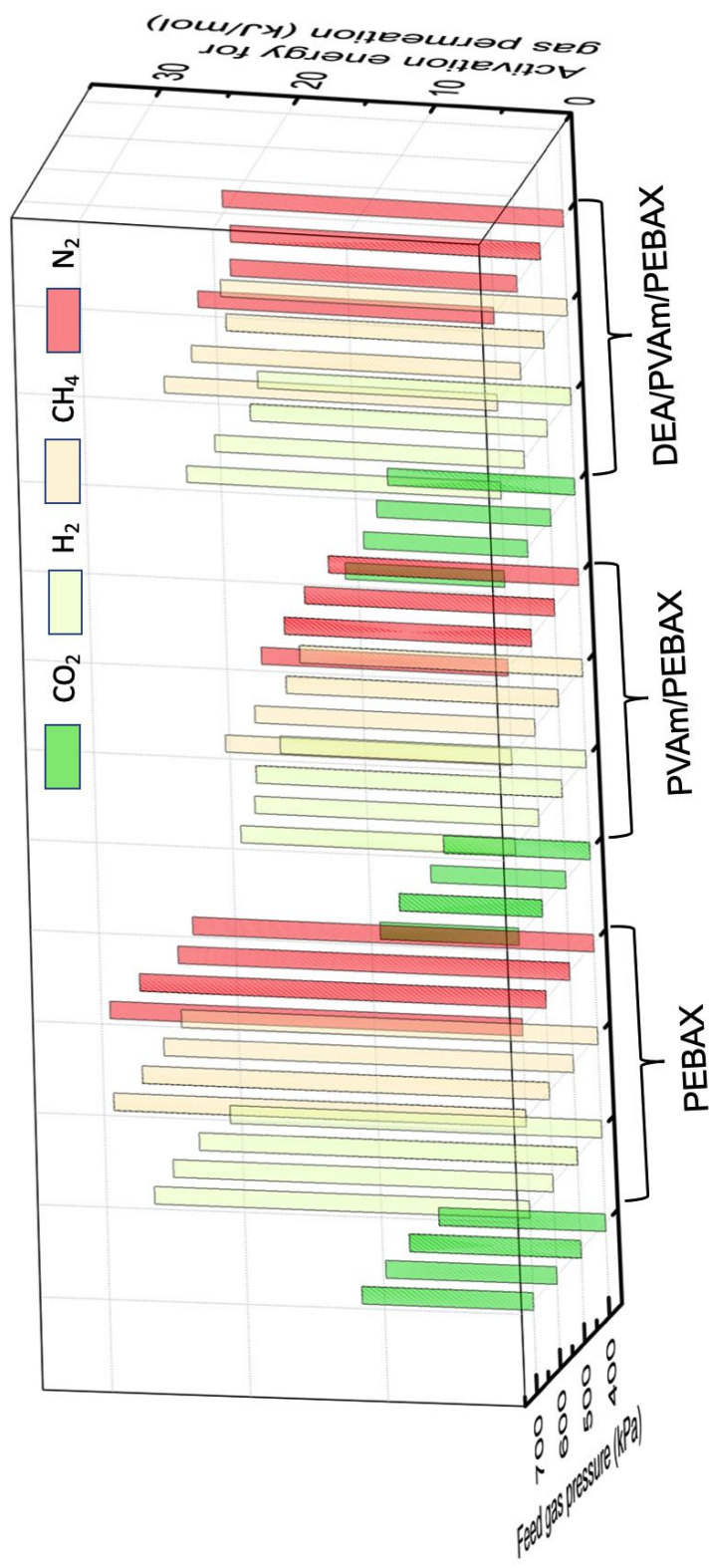
Figure 4.8: Activation energy for pure gas permeation in the PEBAX, PVAm/PEBAX, DEA/PVAm/PEBAX composite membranes under different feed gas pressures

4.3.3 Effect of feed gas pressure

The permeation data has been used to discuss the effects of temperature in the previous section. In this section, the data was used to study the effects of feed gas pressure on the CO_2, N_2, CH_4, and H_2 permeance and the CO_2/N_2, CO_2/CH_4 and CO_2/H_2 selectivity of the PEBAX, PVAm/PEBAX, and DEA/PVAm/PEBAX composite membranes. As shown in Figures 4.9 (a) and 4.10 (a), when the feed gas pressure increased from 400 to 700 kPa, the gas permeance of CO_2, N_2, CH_4, and H_2 and the ideal selectivity of CO_2/N_2, CO_2/CH_4, and CO_2/H_2 remained the same in the PEBAX and the PVAm/PEBAX composite membranes. However, the gas permeance in the DEA/PVAm/PEBAX composite membrane increased (Figure 4.11 (a)). Comparing with the other two membranes, the DEA/PVAm/PEBAX composite membrane had better hydrophilicity, which can be indicated by the contact angles of water on the membranes (Table 4.1). The increase in gas permeance in the DEA/PVAm/PEBAX composite membrane was attributed to the enhanced sorption with escalated pressures in the membrane based on the solution-diffusion mechanism [Kim et al. (2004); Sandru et al. (2010)].

In spite of the presence of amine groups in the PVAm/PEBAX and DEA/PVAm/PEBAX composite membranes, both membranes didn't show a typical feature of the facilitated transport of CO_2. In general, CO_2 permeability or permeance decreases dramatically when feed gas pressure increases for the facilitated transport of CO_2. The number of CO_2 carriers is limited, so when the carriers are consumed and occupied, the CO_2 permeance or permeability can not be improved effectively, which is so-called the CO_2 carrier saturation. However, gas permeation in these three prepared water-swollen membranes was dominated by the solution-diffusion mechanism. Amine groups in the membranes played a role in improving membrane hydrophilicity and CO_2 solubility instead of facilitating CO_2 transport. In comparison among these three composite membranes under various temperatures and feed gas pressures, the addition of amine groups could enhance the membrane hydrophilicity to obtain better gas permeance without significant compromise in gas selectivity.

85
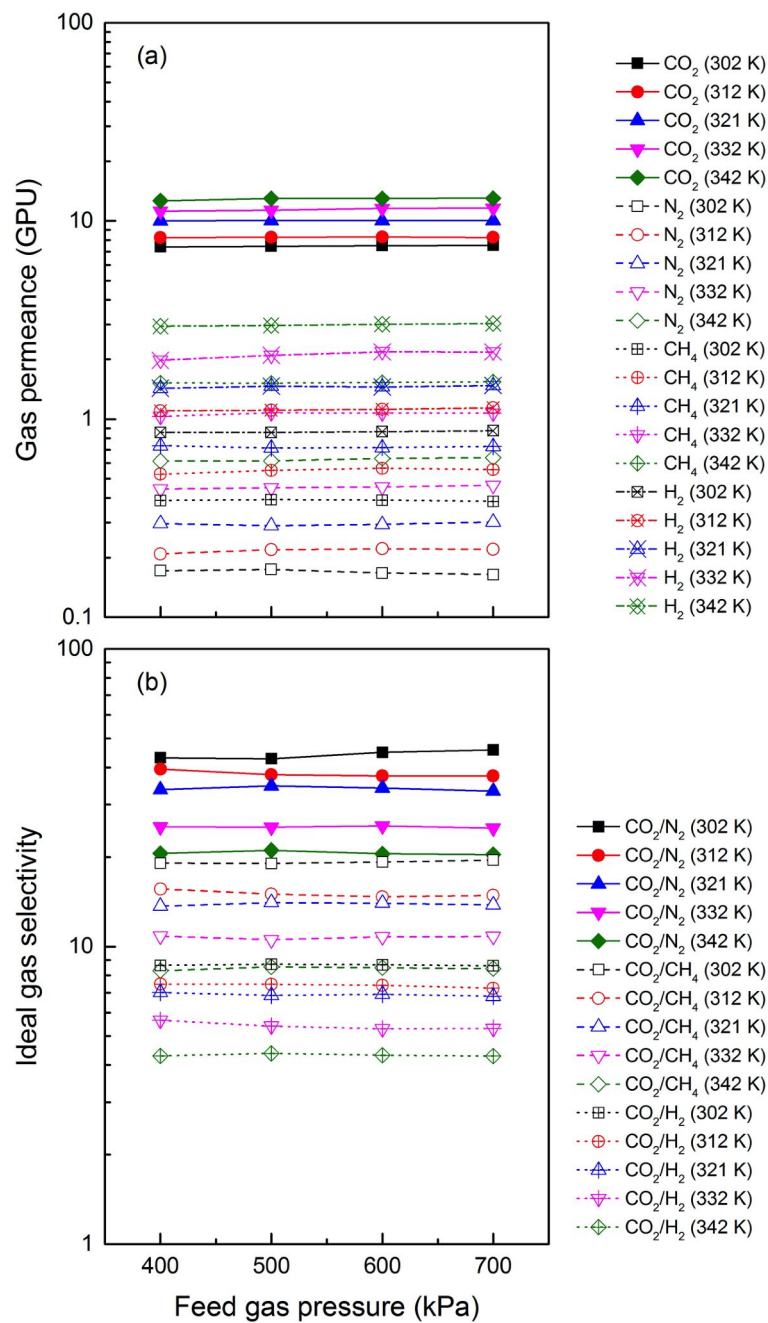
Figure 4.9: Effect of feed gas pressure on the pure gas permeance (a) and the ideal gas selectivity (b) of the PEBAX composite membrane
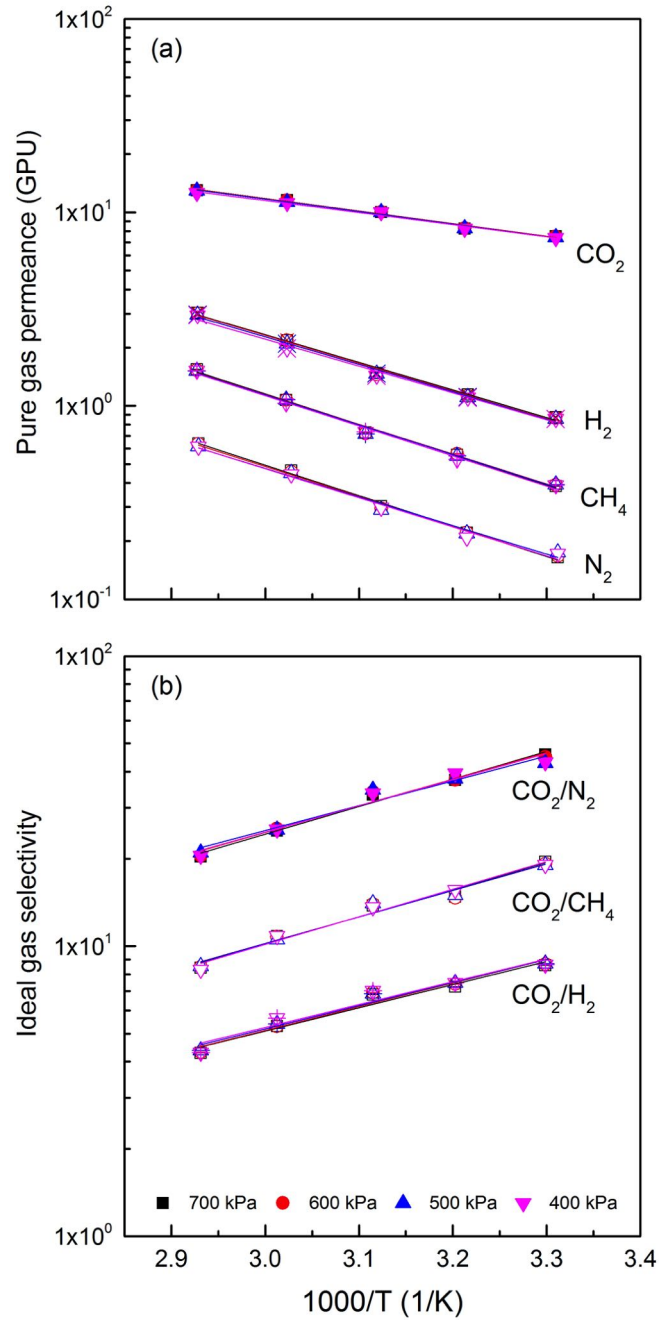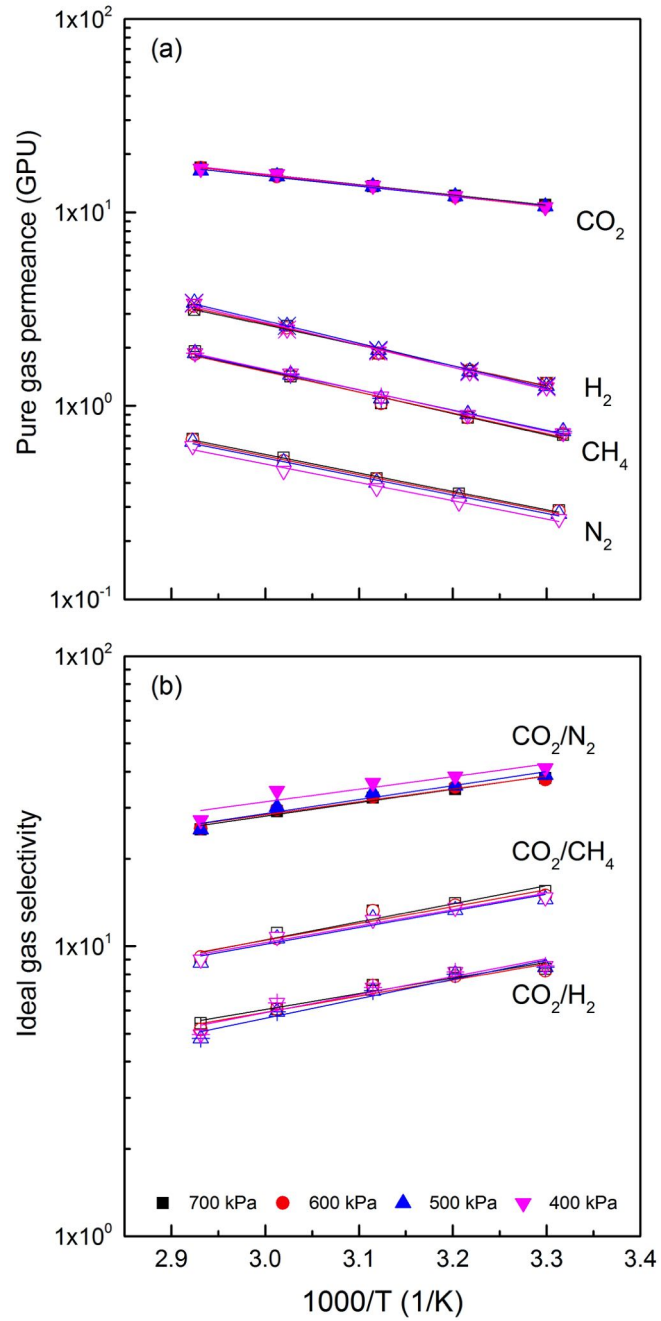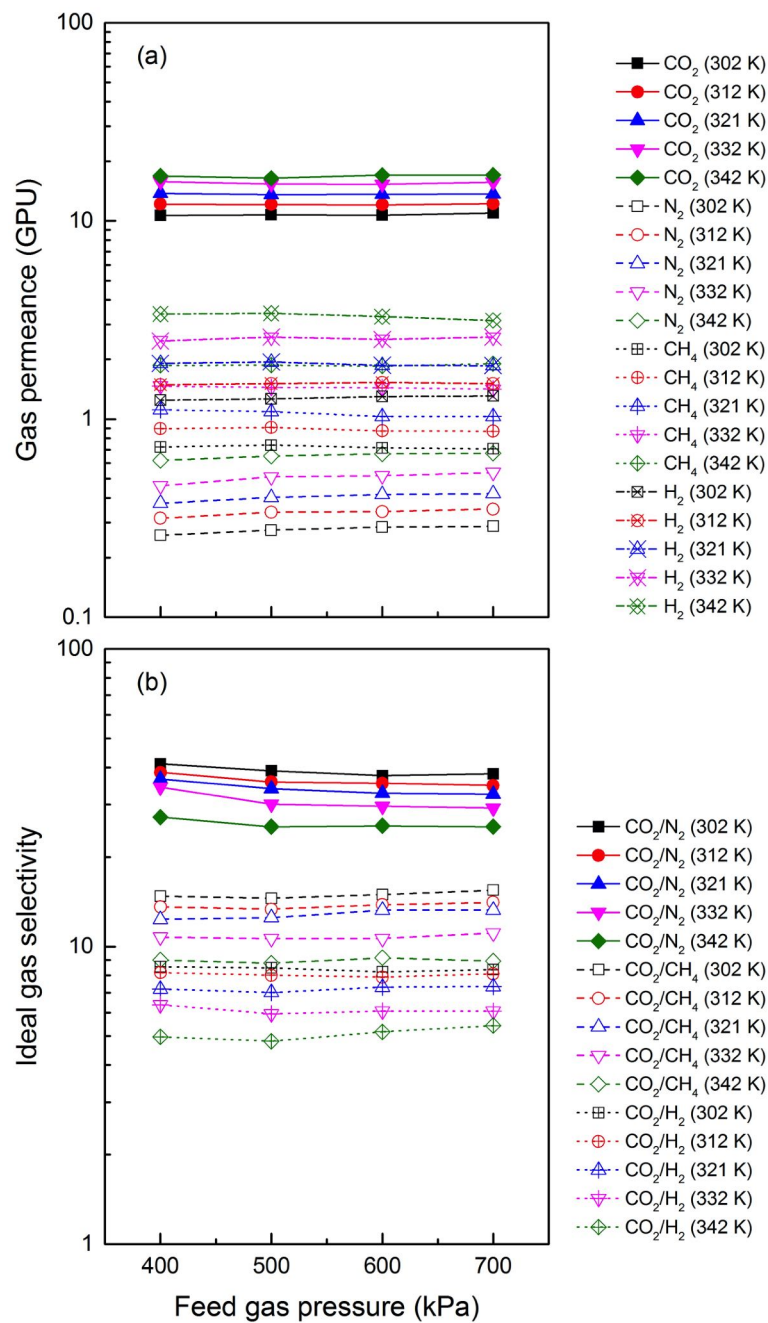
Figure 4.10: Effect of feed gas pressure on the pure gas permeance (a) and the ideal gas selectivity (b) of the PVAm/PEBAX composite membrane
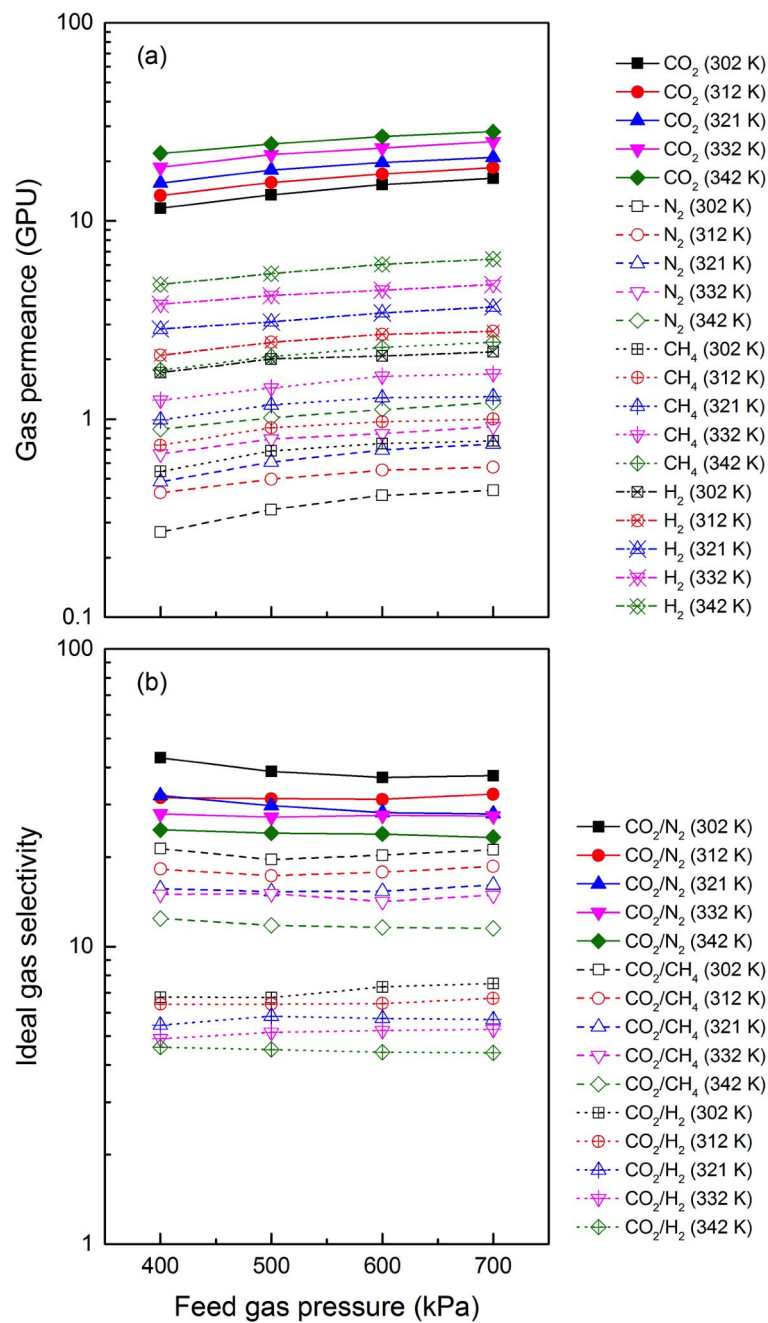
Figure 4.11: Effect of feed gas pressure on the pure gas permeance (a) and the ideal gas selectivity (b) of the DEA/PVAm/PEBAX composite membrane

4.3.4 Effect of feed gas composition

The effects of the mole fraction of CO_2 in feed gas on the separation performance of the DEA/PVAm/PEBAX composite membrane for CO_2/N_2, CO_2/CH_4, and CO_2/H_2 separations under a feed gas pressure of 700 kPa at room temperature were investigated. When two gas components diffuse through the membrane, the permeation behavior of one component may have an influence on the other component, which should be considered in practical application.

When large amounts of CO_2 were dissolved into the membrane, the CO_2-induced plasticization made a contribution to CO_2, N_2, CH_4, and H_2 permeation. In spite of the CO_2-induced plasticization, CH_4, N_2, and H_2 permeation were affected by CO_2 permeation differently in the DEA/PVAm/PEBAX composite membrane. The diffusivity of gas molecules is related to their molecular kinetic diameters. As shown in Figures 4.14 (b) and 4.12 (b), since the molecular kinetic diameter of H_2 (0.289 nm) is smaller than that of N_2 (0.364 nm), H_2 permeance increased by 123%, while N_2 permeance increased by 49.7% when the the mole fraction of CO_2 in feed gas increase from 0 to 0.8. As for CH_4 whose molecular kinetic diameter is the largest among these gases (Table 2.1), its permeance did not change much (Figure 4.13 (b)). Smaller molecule permeation obtained more benefits from the CO_2-induced plasticization than bigger molecule permeation. However, the CO_2/H_2 selectivity decreased more dramatically than the CO_2/N_2 and CO_2/CH_4 selectivity as the mole fraction of CO_2 in feed gas increased (Figures 4.12 (c), 4.13 (c), and 4.14 (c)).

The CO_2-induced plasticization was beneficial to CO_2 diffusion, while the salting-out effect had negative effects on the CO_2 transport due to lowering CO_2 solubility in the membrane. Furthermore, the permeation of CH_4, N_2, and H_2 permeation could affect CO_2 permeation. Since CH_4, N_2, and H_2 occupied part of limited transport sites or pathways in the membrane, CO_2 permeation could be interfered due to the competitive permeation between gas components. As the mole fraction of CO_2 in feed gas increased from 0 to 1, the transport sites initially occupied by the slow gas (CH_4, N_2, and H_2) were replaced by the fast gas (CO_2) gradually
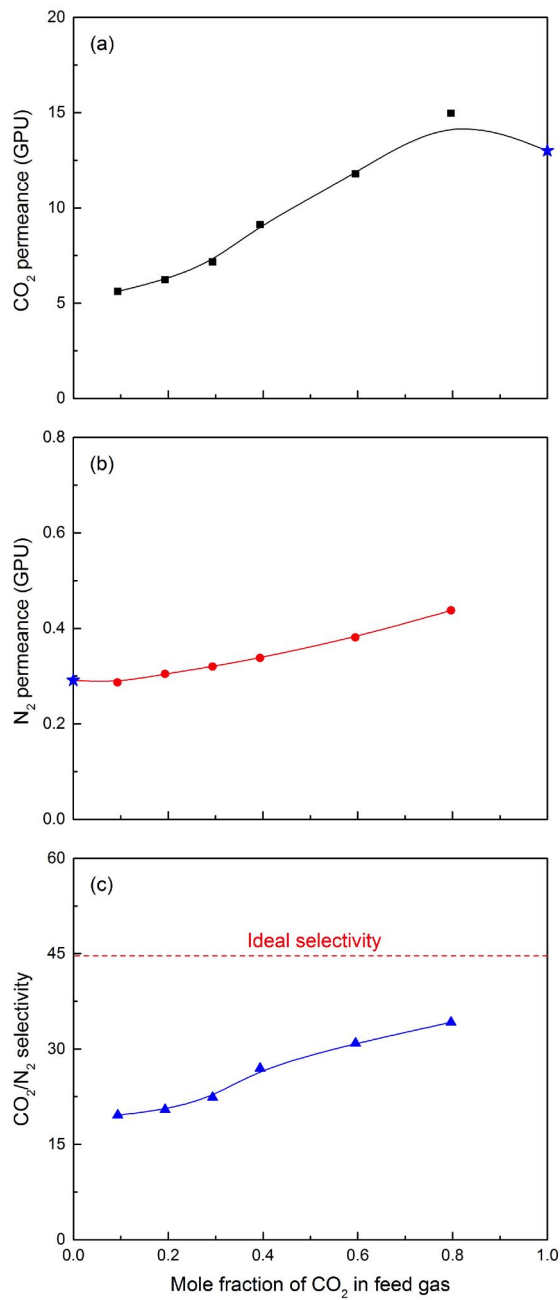
Figure 4.12: Effect of feed gas composition on the CO_2 (a) and N_2 permeance (b) and the CO_2/N_2 selectivity (c) of the DEA/PVAm/PEBAX composite membrane in CO_2/N_2 gas mixture permeation (The symbol stars represent pure gas permeance)
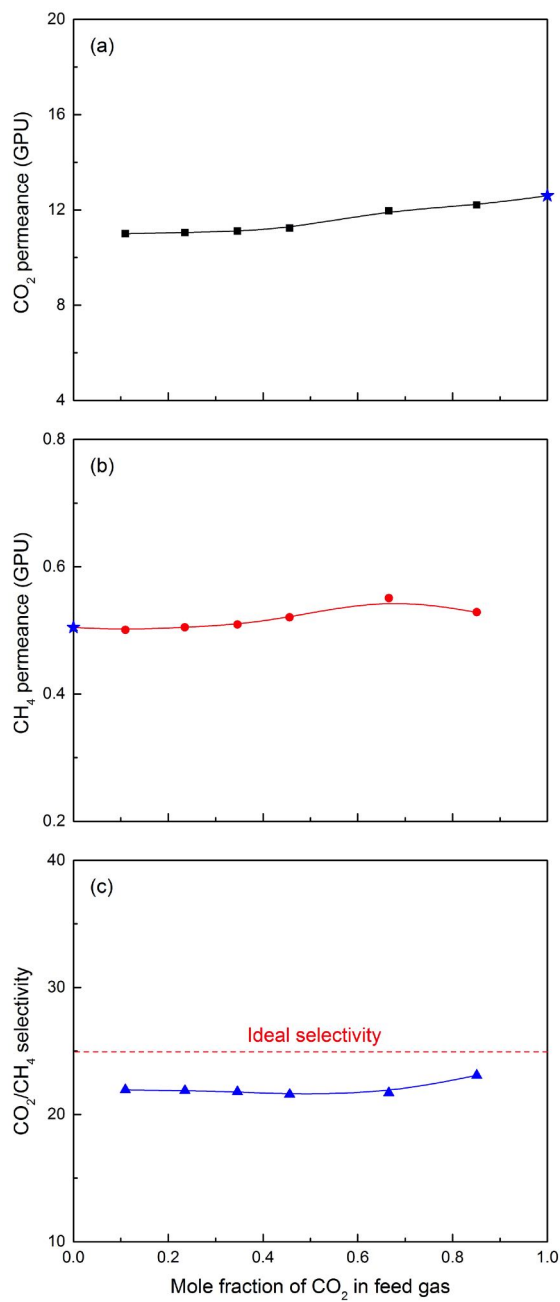
Figure 4.13: Effect of feed gas composition on the CO_2 (a) and CH_4 permeance (b) and the CO_2/CH_4 selectivity (c) of the DEA/PVAm/PEBAX composite membrane in CO_2/CH_4 gas mixture permeation (The symbol stars represent pure gas permeance)
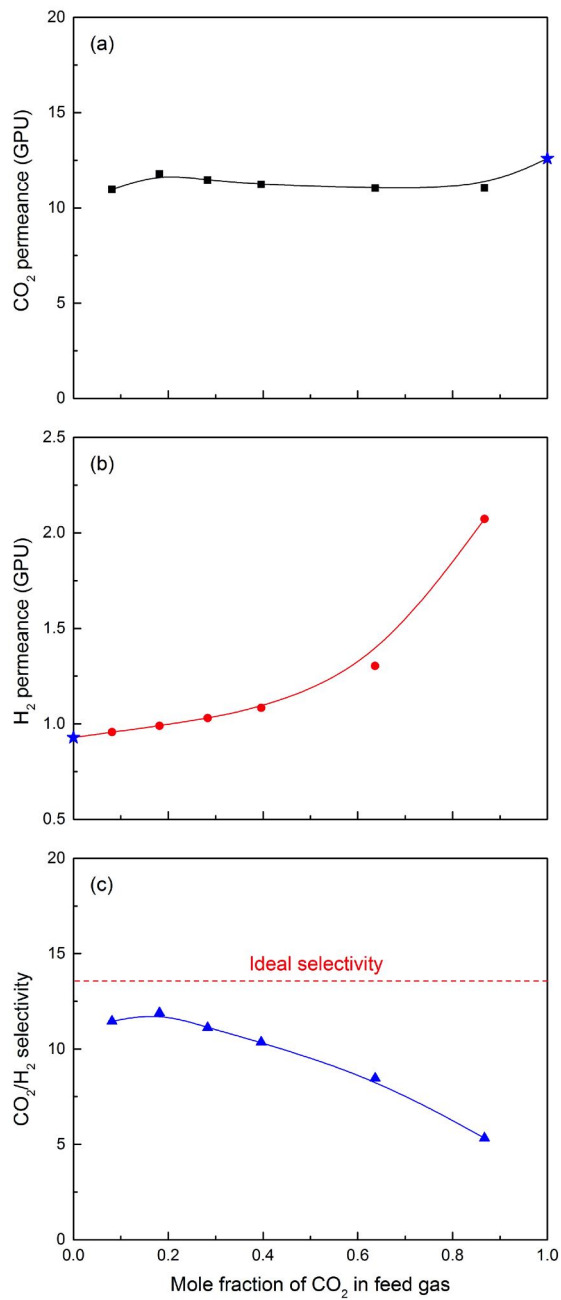
Figure 4.14: Effect of feed gas composition on the CO_2 (a) and H_2 permeance (b) and the CO_2/H_2 selectivity (c) of the DEA/PVAm/PEBAX composite membrane in CO_2/H_2 gas mixture permeation (The symbol stars represent pure gas permeance)

so that CO_2 concentration in the membrane increased. Especially for CO_2/N_2 separation, CO_2 permeance increased by 132%, as demonstrated in Figure 4.12 (a). However, CO_2 permeance remained almost unchanged in CO_2/CH_4 and CO_2/H_2 separations (Figures 4.13 (a) and 4.14 (a)). Apparently, competitive permeation affected CO_2 permeation in CO_2/N_2 separation more significantly than in CO_2/CH_4 and CO_2/H_2 separations. As shown in Figures 4.12 (c) and 4.13 (c), the CO_2/N_2 selectivity increased, while the CO_2/CH_4 selectivity did not change as the mole fraction of CO_2 in feed gas increased, which was attributed to the variations in gas permeance. In all binary gas mixture separations for CO_2/N_2, CO_2/CH_4, and CO_2/H_2, the gas selectivity of the DEA/PVAm/PEBAX composite membrane was lower than the ideal gas selectivity.

4.3.5 Membrane stability

The DEA/PVAm/PEBAX composite membrane was tested for CO_2/N_2 (14 vol% CO_2), CO_2/CH_4 (35 vol% CO_2), and CO_2/H_2 (40 vol% CO_2) separation at a feed gas pressure of 700 kPa and room temperature in humid conditions for 19 days. As shown in Figures 4.15, 4.16, and 4.17, there was no changes in gas permeance and binary gas selectivity. CO_2 permeance maintained 6.1 GPU while CO_2/N_2 selectivity maintained 19.7 in CO_2/N_2 separation, CO_2 permeance maintained 10.6 GPU while CO_2/CH_4 selectivity maintained 21.1 in CO_2/CH_4 separation, and CO_2 permeance maintained 11.5 GPU while CO_2/H_2 selectivity maintained 10.8 in CO_2/H_2 separation. It indicated that the DEA/PVAm/PEBAX composite membrane can maintain its gas separation performance in a long-term test and has a potential of practical industrial applications.
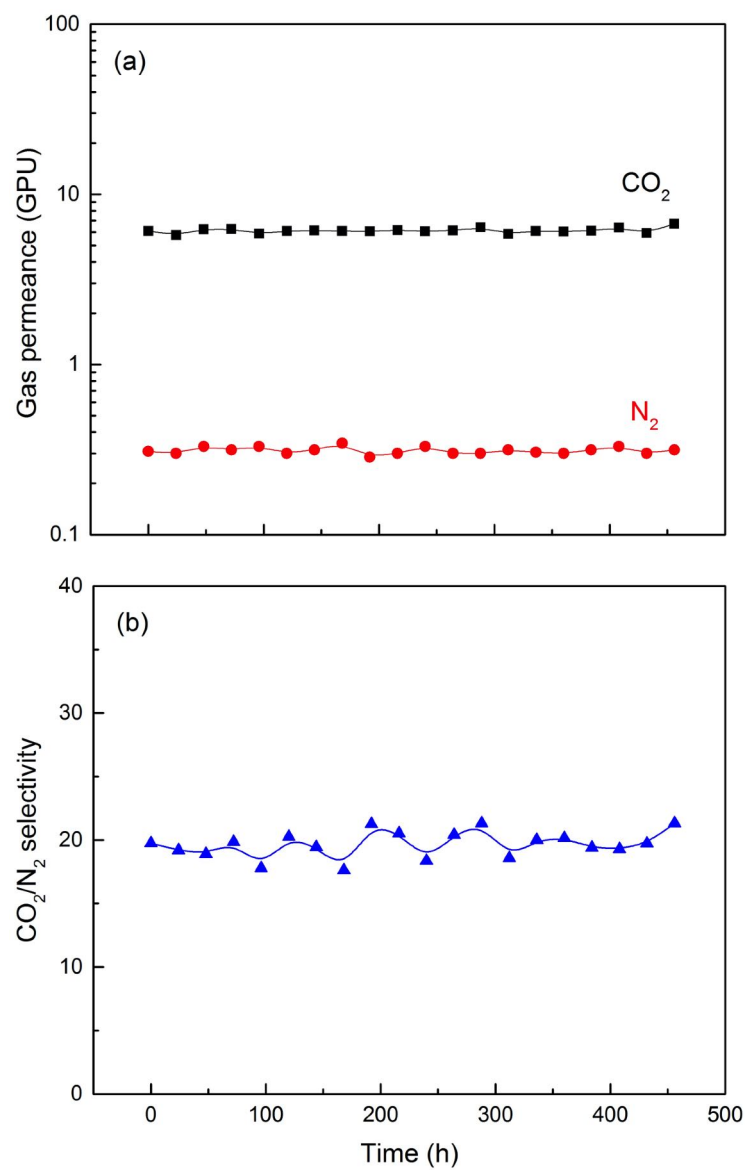
Figure 4.15: Stability of the DEA/PVAm/PEBAX composite membrane in CO_2 /N_2 separation: CO_2 and N_2 permeance (a) and CO_2/N_2 selectivity (b)
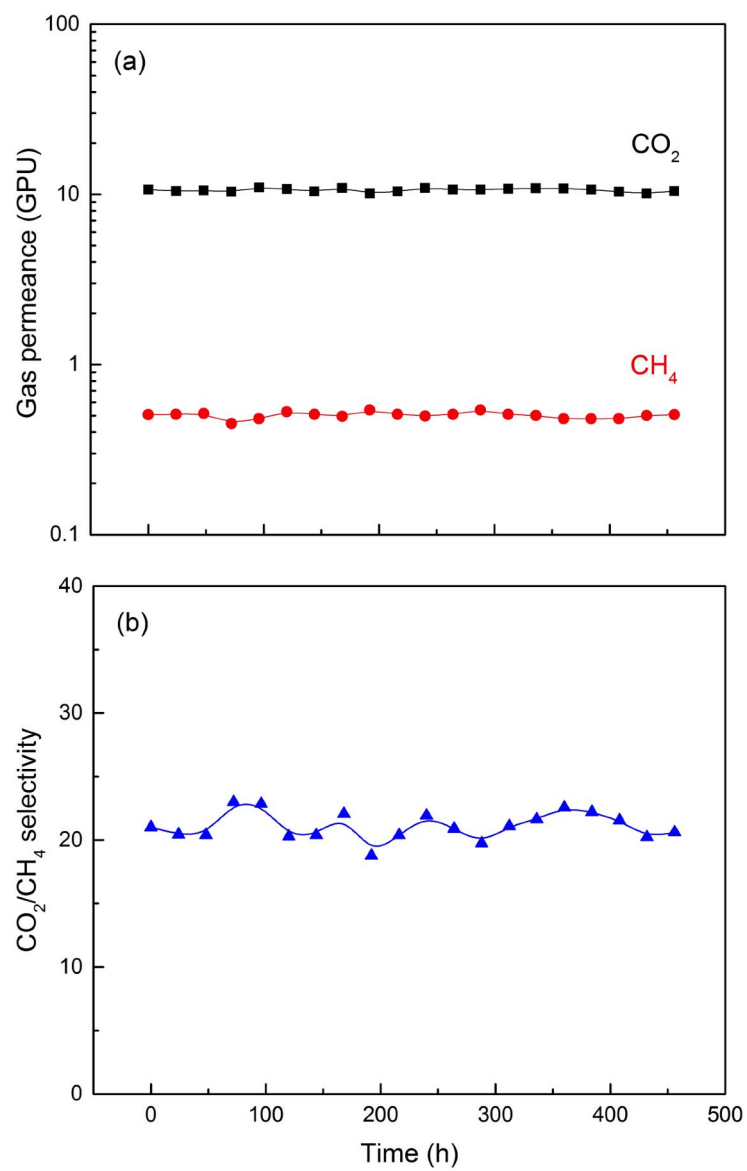
Figure 4.16: Stability of the DEA/PVAm/PEBAX composite membrane in CO_2/CH_4 separation: CO_2 and CH_4 permeance (a) and CO_2/CH_4 selectivity (b)
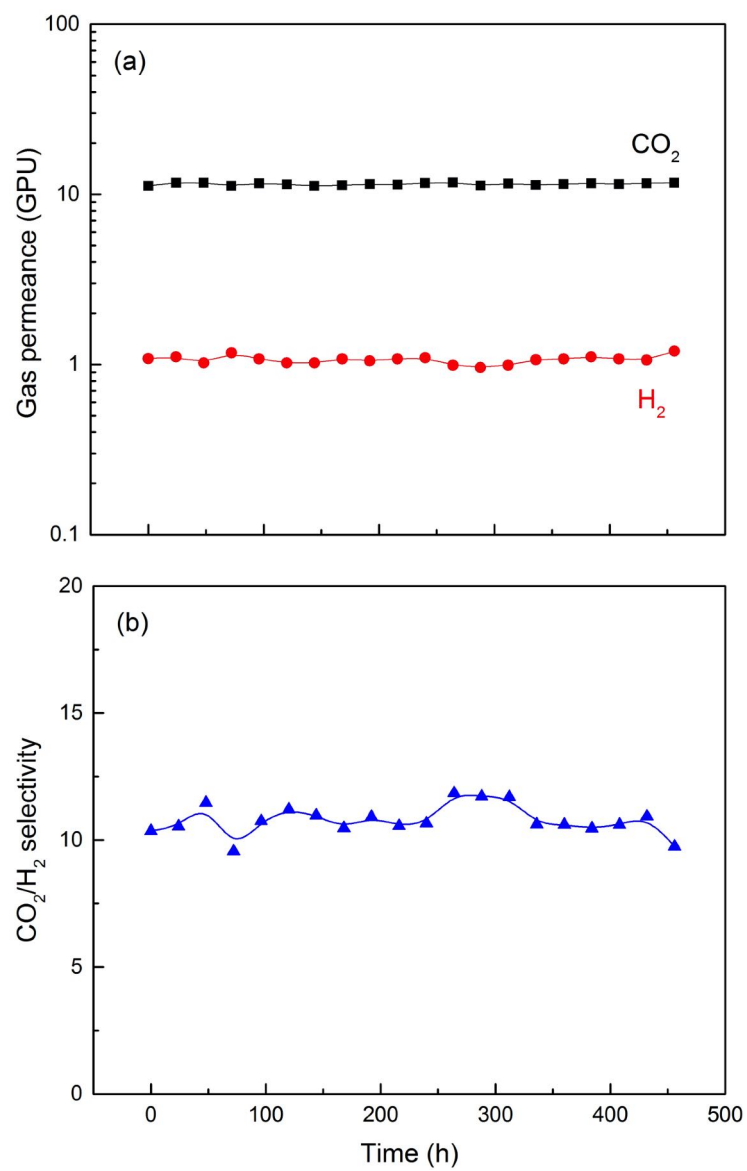
Figure 4.17: Stability of the DEA/PVAm/PEBAX composite membrane in CO_2 /H_2 separation: CO_2 and H_2 permeance (a) and CO_2/H_2 selectivity (b)

4.4 Conclusions

The DEA/PVAm/PEBAX composite membranes were fabricated by a solution casting method on a polysulfone substrate which can provide great mechanical properties for water-swollen membranes. Both pure gas and gas mixture permeation performance was studied and the following conclusions can be drawn:

- The content of PVAm and DEA in the composite membranes affected CO_2, N_2, CH_4, and H_2 permeation due to the improvement of membrane hydrophilicity. When the mass fraction of DEA in the membranes reached 0.20, compared with the PEBAX composite membranes, CO_2 permeance of the DEA containing composite membrane doubled (12.53 GPU), while CO_2/N_2, CO_2/CH_4, and CO_2/H_2 selectivity maintained the same at room temperature and a feed gas pressure of 700 kPa.

- The effects of temperature on the pure gas permeance and the ideal selectivity of the PEBAX, PVAm/PEBAX, and DEA/PVAm/PEBAX composite membranes were studied. In these water-swollen membranes, CO_2, N_2, CH_4, and H_2 permeance increased, and ideal gas selectivity decreased as the temperature raised. The temperature dependence of CO_2, N_2, CH_4, and H_2 permeance can be fitted by an Arrhenius type expression.

- Feed gas pressure did not affect the pure gas permeation performance of the PEBAX and PVAm/PEBAX composite membranes. However, pure gas permeance of the DEA/PVAm/PEBAX composite membrane increased with an increase in feed gas pressure.

- In gas mixture permeation through the DEA/PVAm/PEBAX composite membrane, the CO_2-induced plasticization, the salting-out effect, and competitive permeation contributed to gas permeation simultaneously. The permeation performance of gas mixture in the DEA/PVAm/PEBAX composite membrane was not as good as that of pure gas permeation.

- The stability test of the DEA/PVAm/PEBAX composite membrane indicated that gas

separation performance was retained during 19 days at room temperature and a feed gas pressure of 700 kPa in humid conditions.

Chapter 5

NH$_4$F/PEBAX membranes for carbon capture

5.1 Introduction

As shown in Figure 5.1, gas molecules can permeate through the membranes by two kinds of pathways composed of water and polymer matrix in water-swollen membranes [Liu et al. (2008)]. The diffusion of gas molecules in the membranes is determined by their shaper and size and the free volume and chain mobility of the membranes. In general, smaller gas molecules can diffuse faster. Besides, the structure of the membranes also affects the gas permeation as well. Water can act as a plasticizer to increase the free volume and the polymer chain mobility of the membranes. Hence, the resistance of gas permeation can be effectively reduced. On the other hand, gas molecules can be dissolved into water and utilize the water pathways to permeate across the membranes. Besides, CO_2 can react with amine groups when the membranes are hydrated in the facilitated transport membranes. As a result, the presence of water in the membranes is important.
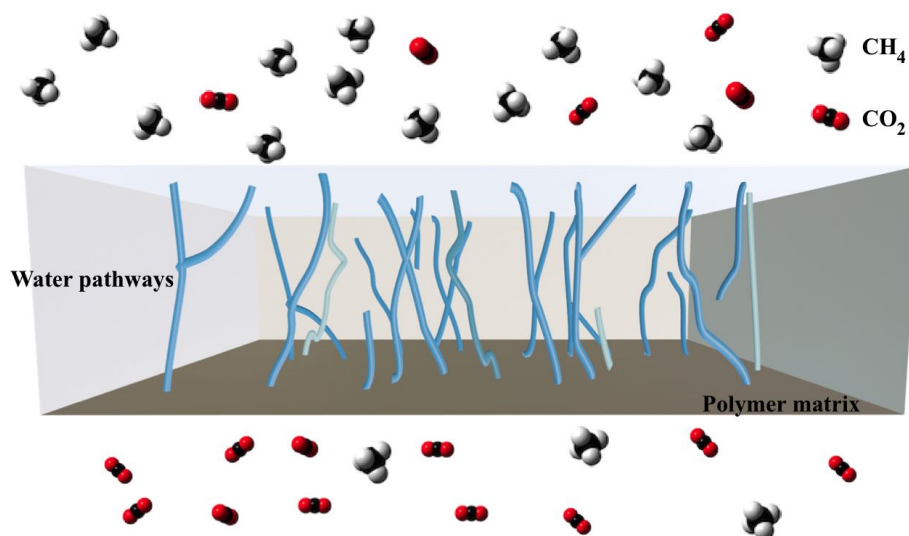
Figure 5.1: Water pathways in the polymer matrix
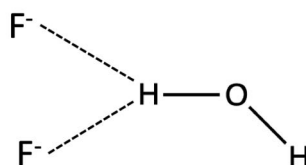
Figure 5.2: Hydrogen bonds between F^- and H_2O

However, the membranes become swollen, and the structures become loosened when the membranes are hydrated. Based on the previous two chapters, increasing membrane hydrophilicity was not able to increase gas selectivity effectively. Hence, the gas selectivity of water-swollen membranes needed to be improved. Polymer blending with salts to prepare polymer electrolyte membranes can be one of the effective approaches to improve membrane selectivity. Li et al. (2014) used different kinds of alkali or alkaline-earth metal salts (LiCl, NaCl, KCl, $MgCl_2$, and $CaCl_2$) with PEBAX to prepared polymer electrolyte membranes. The salts can disturb polymer chain packing to increase the total amounts of water in the membranes and improve CO_2 permeability. It also indicated that the bound water was beneficial to increase gas selectivity due

to the salting-out effect. Kim et al. (2004) prepared PVAm composite membranes by different crosslinking methods including glutaraldehyde, glutaraldehyde and H_2SO_4, NH_4F, glutaraldehyde and NH_4F, and H_2SO_4 or HCl. Among all crosslinking methods, PVAm crosslinked by F^- showed a CO_2/CH_4 selectivity of 1143 at 2 bar and room temperature. It was attributed to hydrogen bonds between F^- and H_2O (Figure 5.2), so these more basic water had a better affinity to CO_2 leading to an increase in CO_2 permeance. Besides, CH_4, N_2, and O_2 can be blocked by these highly polar sites, and their solubility would be reduced due to the salting-out effect. In the study of Zhang and Wang (2012), polyallylamine membranes (PAA) were dipped into NaF, NaCl, and NaBr solution to prepare polymer electrolyte membranes. They found that CO_2 permeance of PAA/NaF (2.8 GPU) was lower than that of PAA/NaCl and PAA/NaBr membranes (3.1 and 3.1 GPU), while CO_2/N_2 selectivity (1400) was much higher than the other two membranes (62 and 51). The salting-out effect affects N_2 permeation more significantly than CO_2 permeation leading to a remarkable increase in gas selectivity. Quinn et al. (1997) and Ji et al. (2010) claimed that CO_2 would react with F^- with the presence of H_2O:

$$2F^- \cdot nH_2O + CO_2 = HF_2^- \cdot (2n\text{-}1)H_2O + HCO_3^-$$
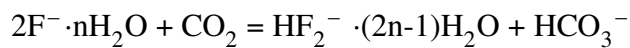
Thus, increasing the amounts of F^- could increase CO_2 solubility in the membranes. They also mentioned that the crystallization of salts could form defects in the membranes which resulted in a decrease in the gas selectivity.

Therefore, F^- can be used to increase CO_2 solubility and gas selectivity. NH_4F/PEBAX polymer electrolyte membranes were prepared for CO_2/N_2, CO_2/CH_4, and CO_2/H_2 separations in this chapter. NH_4F can be considered as an effective additive in the PEBAX membranes to improve membrane permselectivity. The effects of the NH_4F content on permselectivity of the NH_4F/PEBAX membranes were investigated. The effects of temperature and feed gas pressure on the permeability of N_2, CH_4, H_2 and CO_2 and CO_2/N_2, CO_2/CH_4, and CO_2/H_2 selectivity of the PEBAX and NH_4F/PEBAX membranes were investigated. The gas mixture permeation performance of the prepared NH_4F/PEBAX membrane in CO_2/N_2, CO_2/CH_4, and CO_2/H_2 separations was studied, and the membrane stability was tested under humid conditions.

5.2 Experimental

5.2.1 Membrane preparation

Ammonium fluoride (NH_4F) was purchased from Fisher Chemical (purity $\geqslant 98\%$). All other materials used in this study were the same as described in Section 3.2.1. The NH_4F/PEBAX membranes with different mass ratios of NH_4F were fabricated, and the preparation of NH_4F/PEBAX(0.1) was used to describe the membrane preparation. 15 g of PEBAX pellets were used to prepare homogeneous PEBAX solution (6 wt%) by the same method as described in chapter 3. 1.5 g of NH_4F was added to the polymer solution. The casting solution was well mixed by vigorous stirring for 2 h at room temperature. After degassing by ultrasonication for 1 h, 18.9 g of homogeneous casting solution was cast on a glass plate. The casting area was restrained by a frame (12×16.5 cm). The plate was put in a dust-free chamber to evaporate the solvent for 2 days at room temperature. The membrane was peeled off the plate and collected. The prepared membranes were designated as NH_4F/PEBAX(X), where X (X=0, 0.05, 0.075, 0.1, 0.125, 0.15) represents the mass ratio of NH_4F to PEBAX. The thicknesses of membranes were measured by a micrometer at ten different places on the membranes. The thicknesses of all prepared membranes were in the range of 47-53 μm in the dry condition and 67-117 μm in the humid condition.

5.2.2 Gas permeation tests

Both pure gas and gas mixture permeation tests were conducted using the procedure as same as described in Chapter 3. The membranes were pre-humidified by the same method as before, but the time was one minute which was different from the previous chapters. The test method of the membrane swelling degree was the same as described in Chapter 3. The relative standard deviation in gas permeability of the membranes from the same batch was within 5.4% (Appendix A.3), while that from different batches was within 16%.

5.3   Results and discussion

5.3.1   Effect of the NH$_4$F content

The content of NH$_4$F in the NH$_4$F/PEBAX membranes affected gas permeation, and the effects of NH$_4$F to PEBAX mass ratio on pure gas permeation were studied at room temperature and under a feed gas pressure of 500 to 700 kPa.

As shown in Figure 5.3, N$_2$, CH$_4$, H$_2$ and CO$_2$ permeability decreased when the mass ratio of NH$_4$F to PEBAX increased from 0.05 to 0.10. It was attributed to the hydrogen bonds between F$^-$ ions and the hydrogen atom on the polymer chains, which could make the polymer chains compacted leading to a decrease in the free volume. Another reason could be attributed to the decrease of the free water in the membranes which can be indicated by the changes in the membrane swelling degree (Figure 5.6). On one hand, after addition of NH$_4$F, more free water molecules would be stabilized by the hydration of NH$_4$F in the form of NH$_4^+\cdots$OH$_2$ and F$^-\cdots$H$_2$O [Kollman and Kuntz (1976)]. On the other hand, F$^-$ ions have a high electronegativity and can form hydrogen bonds with water molecules. Furthermore, the presence of ionic species could occupy the limited transport sites for gas permeation. Therefore, the salting-out effect due to the presence of ions can decrease the permeability of N$_2$, CH$_4$, H$_2$ and CO$_2$ [Zhang and Wang (2012); Li et al. (2014)]. Therefore, the permeability of N$_2$, CH$_4$, H$_2$ decreased by 28%, 11%, 15%, while CO$_2$ permeability decreased by only 4% when the mass ratio of NH$_4$F to PEBAX increased from 0.05 to 0.1 under a feed gas pressure of 500 kPa. Apparently, the decreasing extent of CO$_2$ permeability was different. As water molecules and F$^-$ ions can form hydrogen bonds, they became more basic due to the high electronegativity of F$^-$ ions [Kim et al. (2004)]. Considering CO$_2$ can be dissolved into water, and the basic environment is beneficial for CO$_2$ dissolution which could compensate for the decrease caused by the salting-out effect. Hence, in spite of the salting-out effect resulting from the addition of NH$_4$F, CO$_2$ permeability reduced less remarkably than the permeability of N$_2$, CH$_4$, and H$_2$. Consequently, CO$_2$/N$_2$, CO$_2$/CH$_4$,

CO_2/H_2 selectivity increased initially with an increase in the mass ratio of NH_4F to PEBAX, as demonstrated in Figure 5.4.

When the mass ratio of NH_4F to PEBAX exceeded 0.1, the polymer electrolyte membranes became more swollen because of the increase of hydrophilicity, as shown in Figure 5.6. The molecular sieving could be weakened when the polymer chain packing is disturbed. As a result, more gas molecules can penetrate the membranes more easily, leading to an increase in gas permeability and a decrease in selectivity, as demonstrated in Figures 5.3 and 5.4. When the mass ratio of NH_4F to PEBAX was 0.1, CO_2/N_2, CO_2/CH_4, and CO_2/H_2 gas pairs had an ideal selectivity of 73.9, 27.6, and 16.0, respectively, at room temperature under a feed gas pressure of 700 kPa. The CO_2 permeability of NH_4F/PEBAX(0.1) membrane (372 Barrer) was higher than that of the pristine PEBAX membrane (329 Barrer). The NH_4F/PEBAX(0.1) membrane was selected to be used in further studies.

The role of water in the membranes was considered as a plasticizer which can adjust the membrane structures. Due to the different swelling degrees of the prepared PEBAX membranes in these three chapters (Figure 5.6), the PEBAX membrane with higher water content resulted in higher CO_2 permeability, as shown in Figure 5.5. Different from the water-swollen membranes containing amine groups, the prepared NH_4F/PEBAX blend membranes tended to increase gas selectivity more obviously than gas permeability. Especially for CO_2/N_2, the ideal gas selectivity of the NH_4F/PEBAX(0.1) membrane increased by 54% comparing with the pristine PEBAX membrane. Both CO_2/N_2 and CO_2/H_2 permeation performance of the NH_4F/PEBAX(0.1) membrane exceeded Robeson's upper bound (2008), and the CO_2/CH_4 permeation performance exceeded Robeson's upper bound (1991).
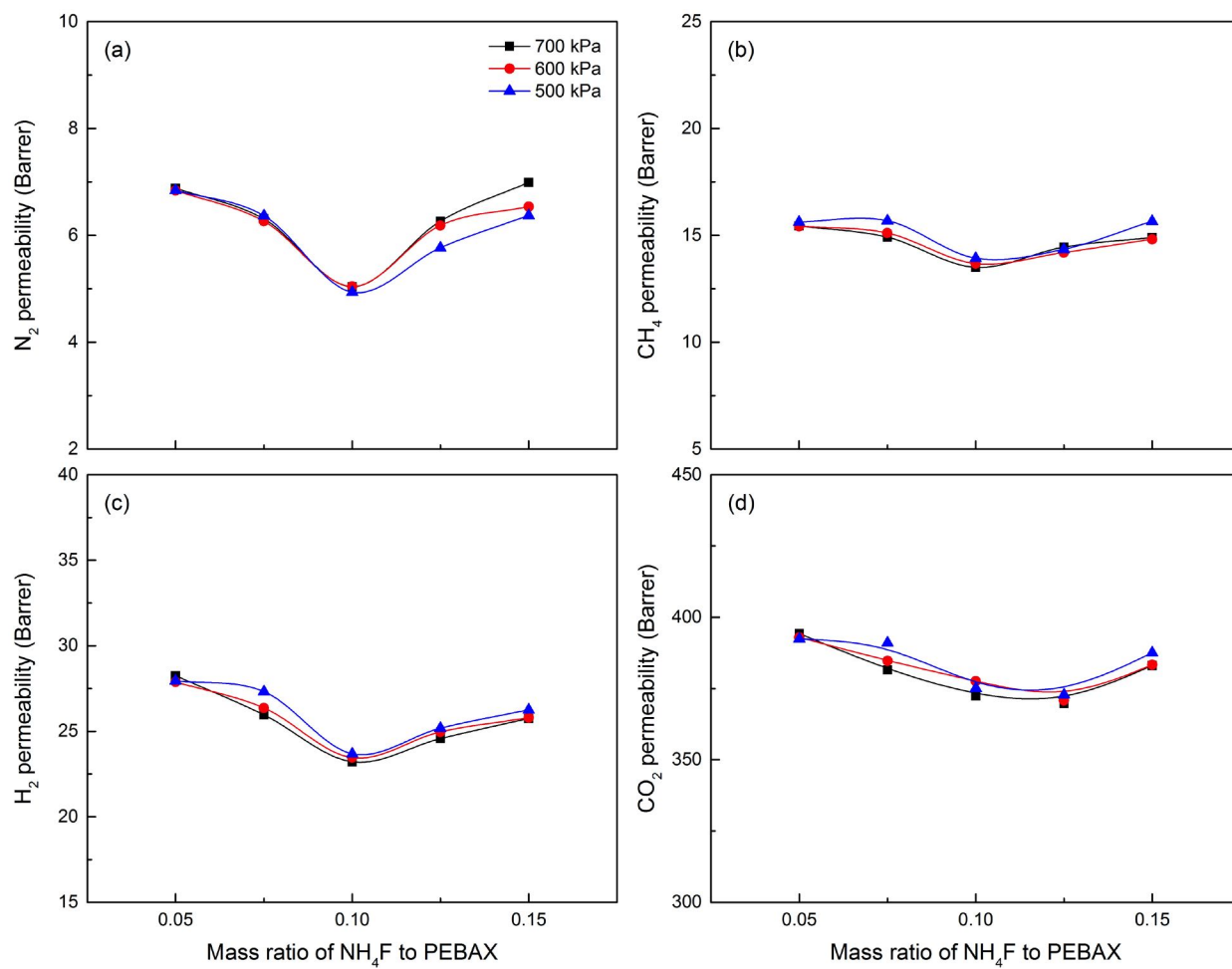
Figure 5.3: Effect of the mass ratio of NH_4F to PEBAX on N_2 (a), CH_4 (b), H_2 (c) and CO_2 permeability (d)
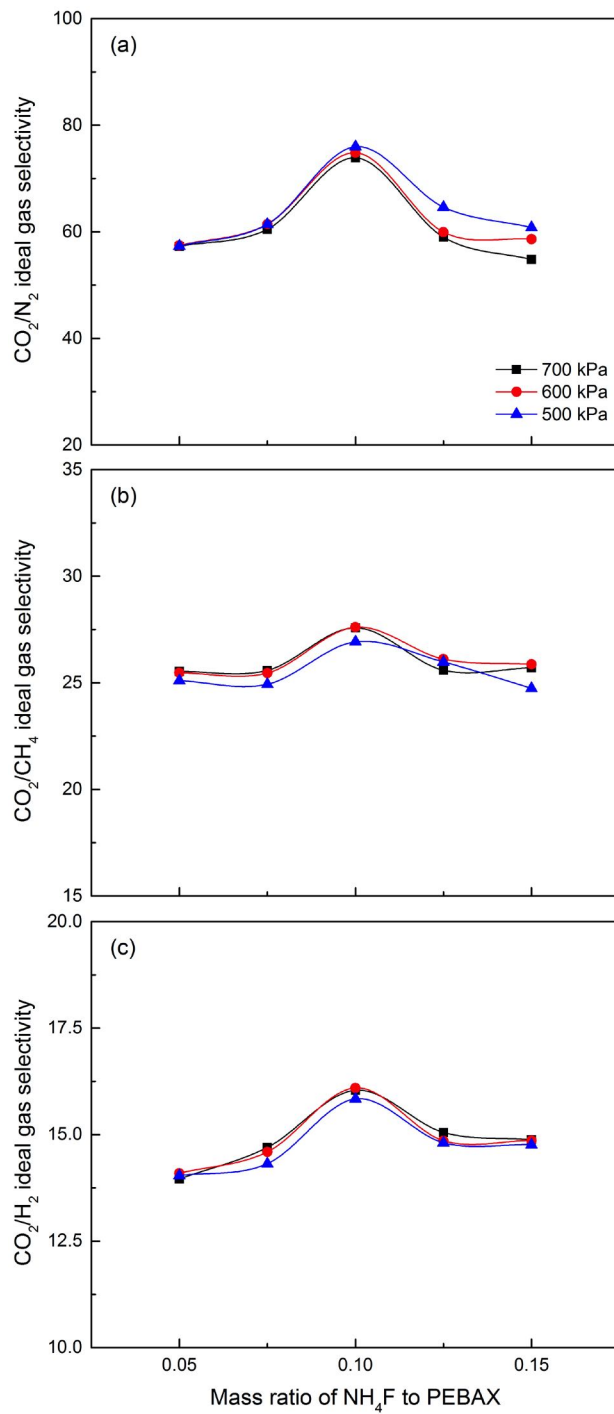
Figure 5.4: Effect of the mass ratio of NH_4F to PEBAX on CO_2/N_2 (a), CO_2/CH_4 (b), CO_2/H_2 ideal selectivity (c)

106
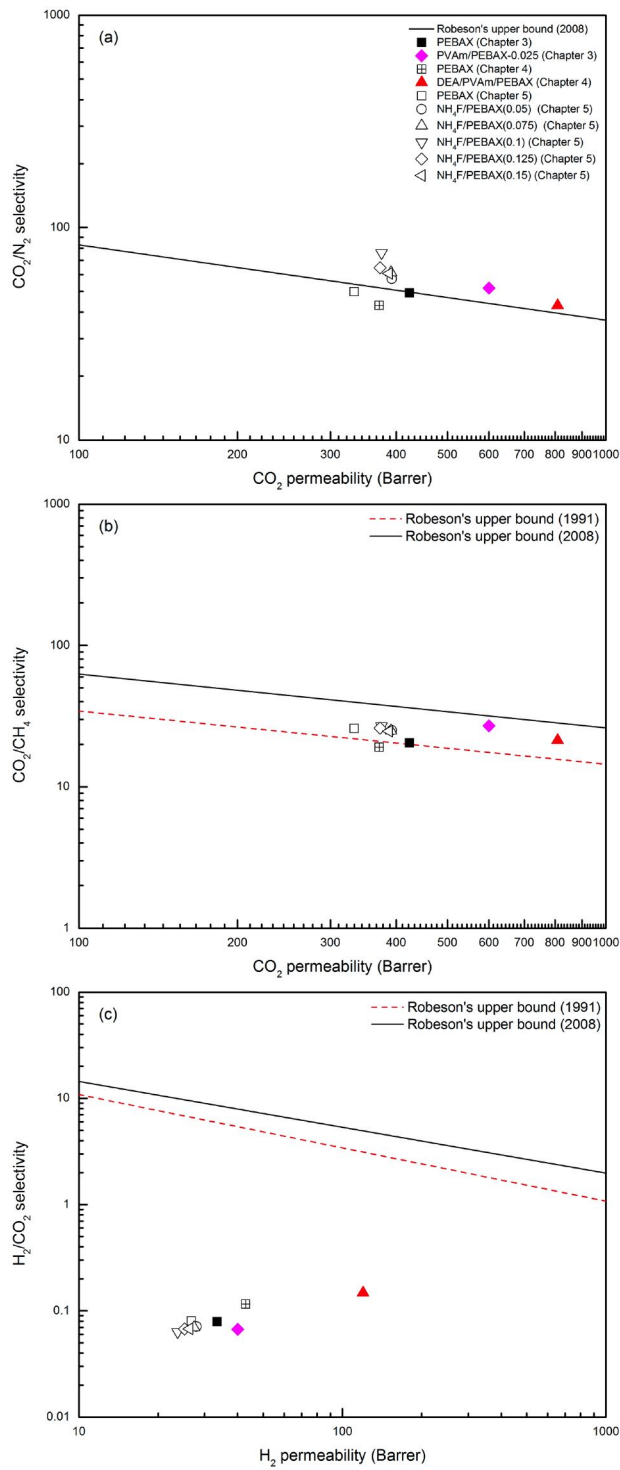
Figure 5.5: Comparison with Robeson's upper bound for CO_2/N_2 (a), CO_2/CH_4 (b), and H_2/CO_2 (c)
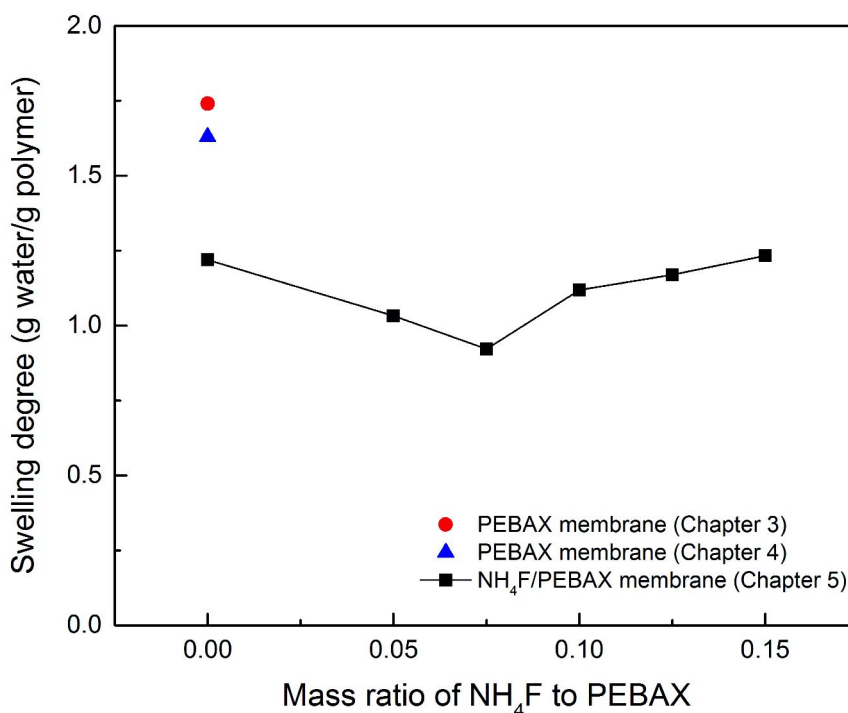
Figure 5.6: Swelling degree of NH_4F/PEBAX membranes

5.3.2 Effect of temperature

The operating temperature is another parameter affects gas permeation. Both the PEBAX and NH_4F/PEBAX(0.1) membranes was tested for pure gas permeation of CO_2, N_2, CH_4, and H_2 at a temperature range from 294 to 342 K under a feed gas pressure range from 300 to 700 kPa in humid conditions. As shown in Figure 5.7, the permeabilities of N_2, CH_4, and H_2 in the NH_4F/PEBAX(0.1) membrane were lower than those of the pristine PEBAX membrane at the same temperature and feed gas pressure, which was attributed to the salting-out effect. Nonetheless, the CO_2 permeability of the NH_4F/PEBAX(0.1) membrane was similar to or higher than that of the pristine PEBAX membrane. As F^- ions made water more basic, the negative influence of the salting-out effect on CO_2 permeability could be offset. As a result, ideal selectivities of CO_2/N_2, CO_2/CH_4, CO_2/H_2 in the NH_4F/PEBAX(0.1) membrane were higher than those in the pristine PEBAX membrane (Figure 5.8).

108

As the temperature increased from 294 to 342 K, N_2, CH_4, H_2, and CO_2 permeability of both the pristine PEBAX and NH_4F/PEBAX(0.1) membranes increased (Figure 5.7). Despite the reduction of gas solubility in water, the increase in gas diffusion in the membranes and polymer chain flexibility resulted in the increase in gas permeability when the temperature increased. The Arrhenius equation can be used to describe the temperature dependence of gas permeability (Equation 3.5). The activation energy for CO_2 permeation in both PEBAX and NH_4F/PEBAX(0.1) membranes was lower than for N_2, CH_4, and H_2 permeation (Figure 5.9), which indicated that the effects of temperature on N_2, CH_4, and H_2 permeability tended to be more significant than CO_2 permeability. Thus, N_2, CH_4, and H_2 permeability decreased more remarkably than CO_2 permeability (Figure 5.7), and ideal selectivities of CO_2/N_2, CO_2/CH_4, CO_2/H_2 in both PEBAX and NH_4F/PEBAX(0.1) membranes decreased when temperature increased (Figure 5.8).

With an increase in the feed gas pressure, there was no change in the activation energy for gas permeation in the PEBAX and the NH_4F/PEBAX(0.1) membranes, as shown in Figure 5.9. Comparing with pristine PEBAX membrane, the activation energy for N_2, H_2, and CO_2 permeation in the NH_4F/PEBAX(0.1) membrane was lower, while the activation energy for CH_4 permeation was similar. The variation in activation energy for gas permeation in the membranes was attributed to the variation in activation energy for diffusion (E_d) and the heat of sorption (ΔH_s). Hence, the influence of the addition of NH_4F in the membrane on E_d and ΔH_s needs to be further studied in future work.

Figure 5.7: Effect of temperature on the pure gas permeability of N_2 (a), CH_4 (b), H_2 (c) and CO_2 (d) of the PEBAX and the $NH_4F/PEBAX(0.1)$ membranes
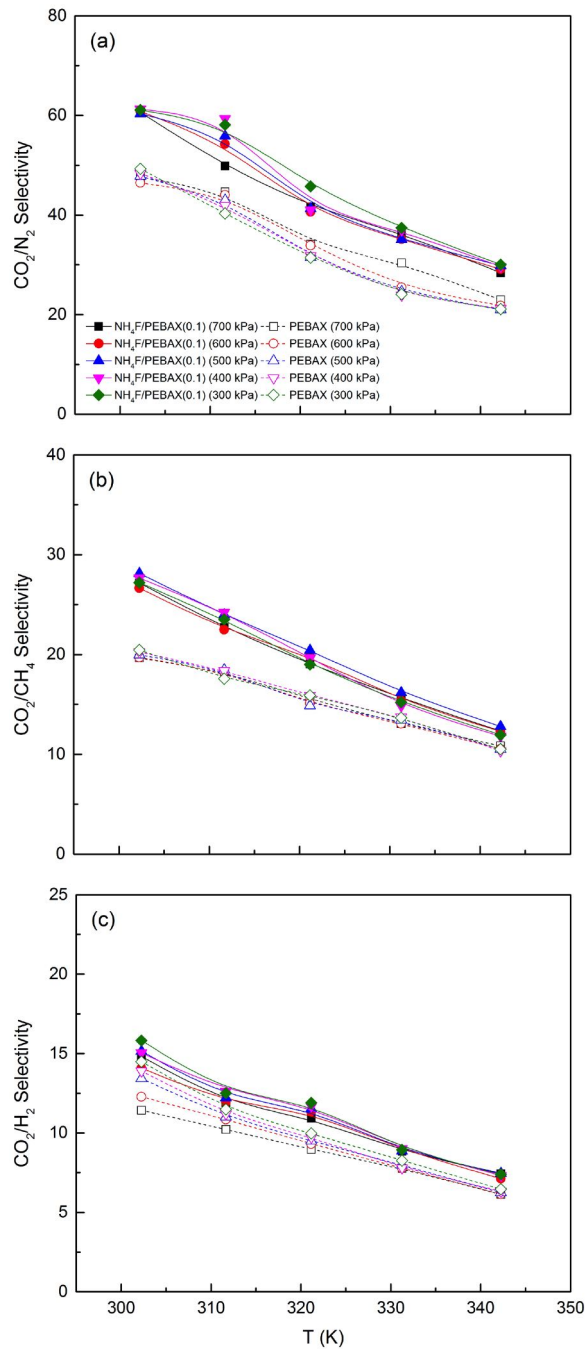
Figure 5.8: Effect of temperature on the CO_2/N_2 (a), CO_2/CH_4 (b), CO_2/H_2 (c) selectivity of the PEBAX and the $NH_4F/PEBAX(0.1)$ membranes
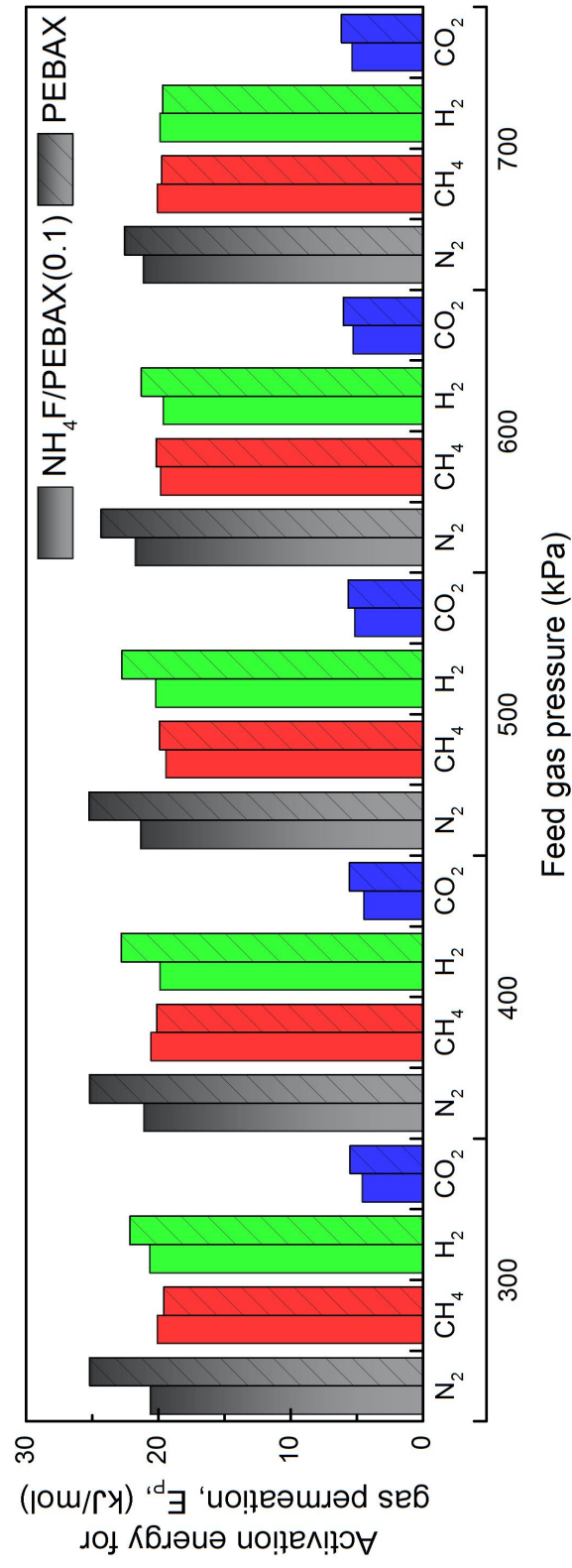
Figure 5.9: Activation energy for pure gas permeation in the PEBAX and the $NH_4F/PEBAX(0.1)$ membranes under different feed gas pressures

5.3.3 Effect of feed gas pressure

The membranes with different contents of NH_4F were tested under a feed gas pressure range of 300 to 700 kPa. Figure 5.10 shows that the feed gas pressure hardly affected the permeabilities of H_2, N_2, CH_4, and CO_2 and the CO_2/N_2, CO_2/CH_4, CO_2/H_2 ideal selectivity for all the membranes. The effects of the feed gas pressure on the pure gas permeation performance of the $NH_4F/PEBAX(0.1)$ membrane were studied at various operating temperatures (Figures 5.11 and 5.12). Similarly, as the feed gas increased from 300 to 700 kPa, the gas permeability and the ideal selectivity didn't change remarkably.

PVAm composite membranes with the addition of NH_4F prepared by Kim et al. (2004) showed a quite high CO_2/CH_4 selectivity of 1143 under 20 °C and 2 bar in humid conditions. The facilitated transport of CO_2 dominated in the membranes. When the feed gas pressure increased further, the selectivity could be deteriorated due to the salting-out effect and carrier saturation [Quinn et al. (1997)]. However, the pressure dependence of CO_2 permeability in the $NH_4F/PEBAX(0.1)$ membrane in this work didn't exhibit the facilitated transport of CO_2, and the solution-diffusion mechanism prevailed in gas permeation through the membrane. It was ascribed that the water in the swollen membranes make membrane structure dilated and loose [Kim et al. (2004); Quinn et al. (1997)]. Hence, feed gas pressure didn't affect much on gas permeation behaviors in the prepared membranes which were determined by the structure of the membranes.
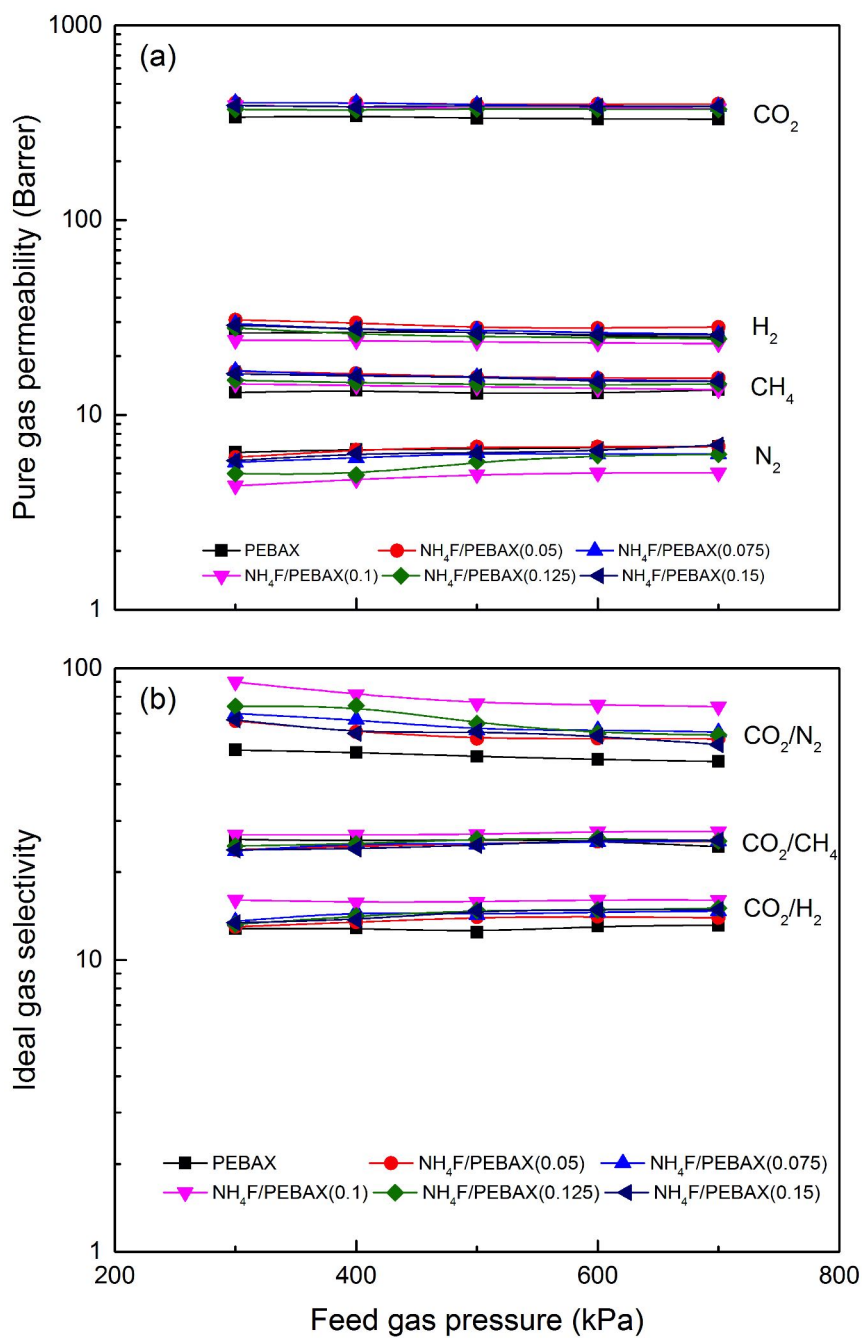
Figure 5.10: Effect of the feed gas pressure on the pure gas permeability (a) and the ideal gas selectivity (b) of the $NH_4F/PEBAX$ blend membranes

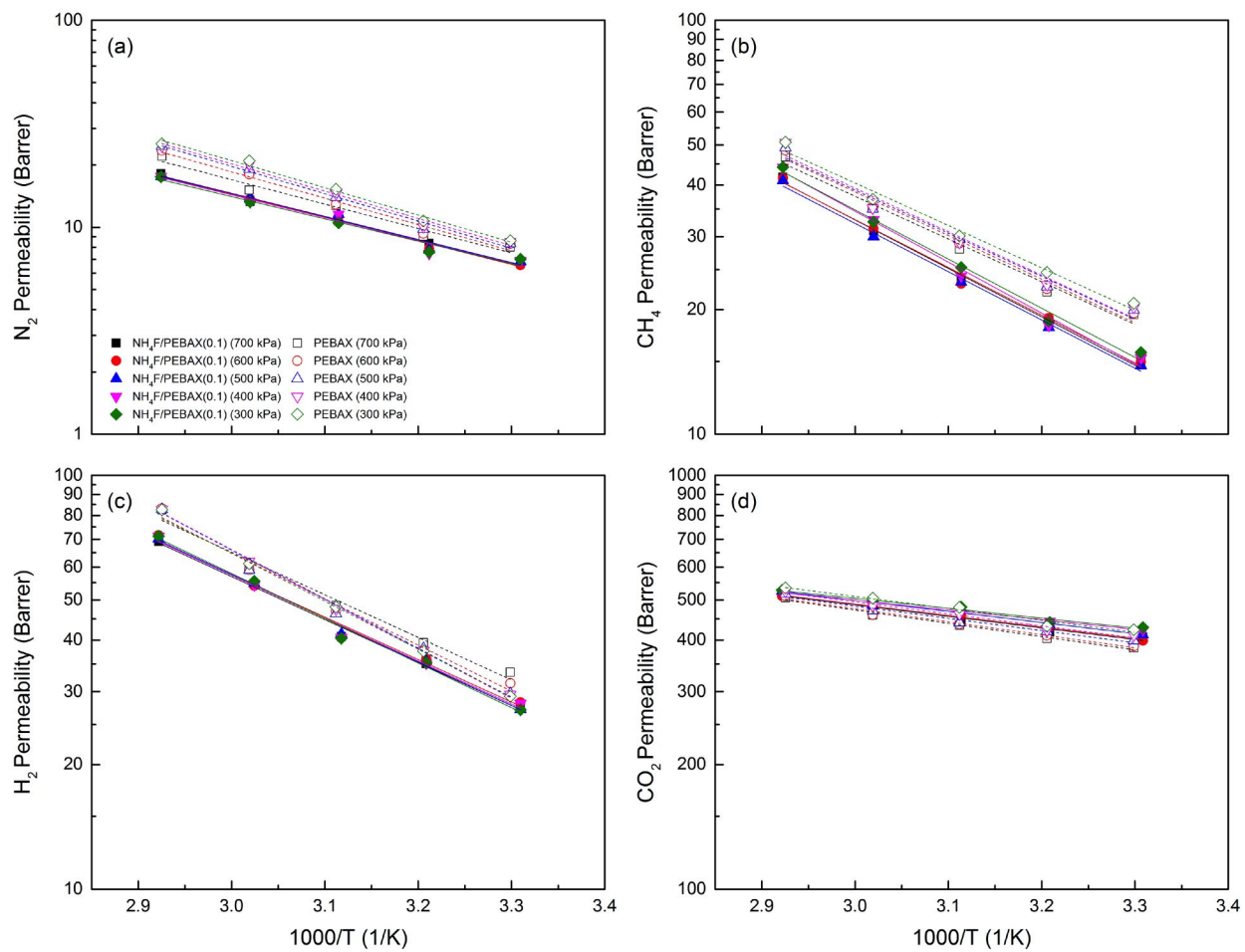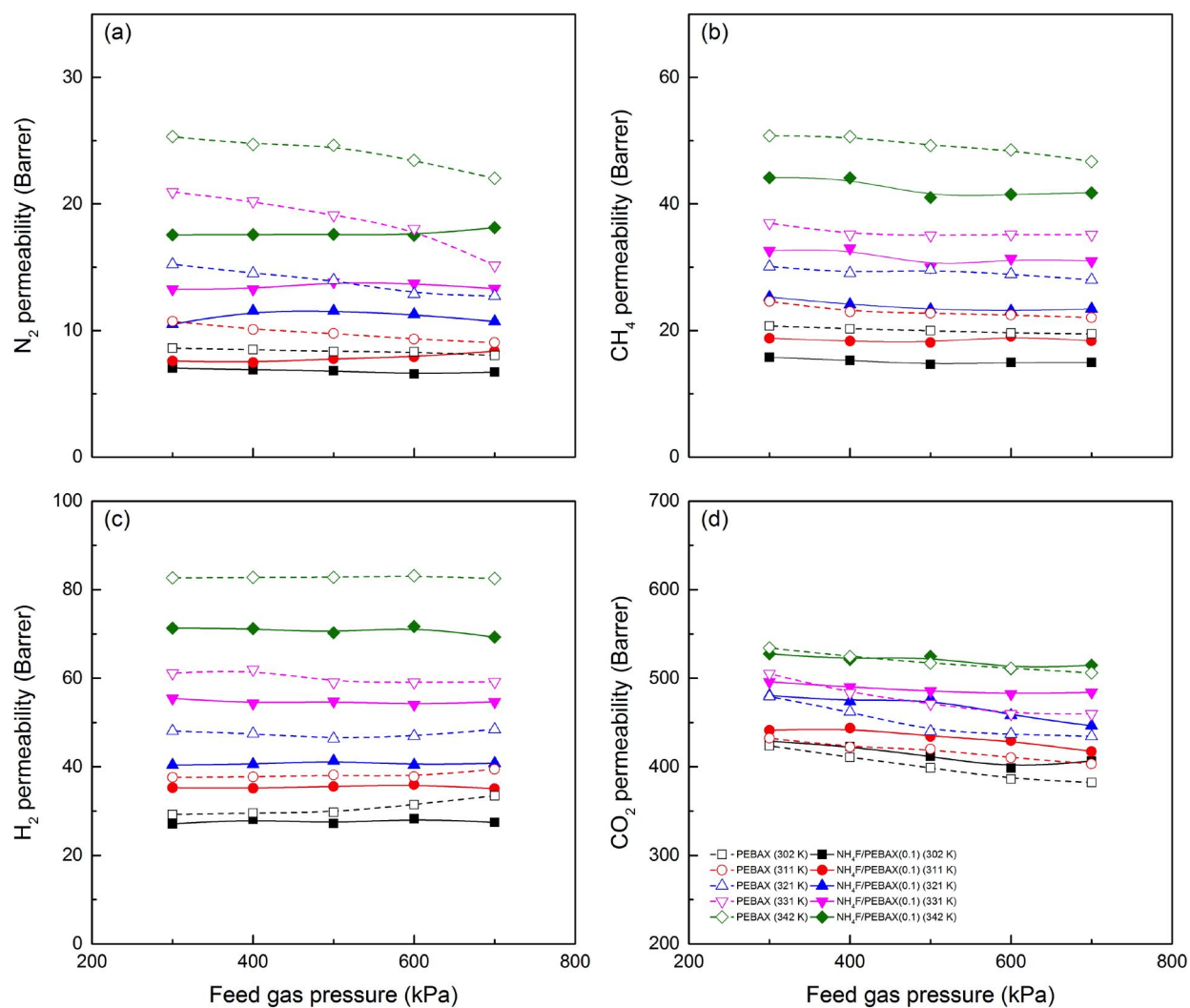Figure 5.11: Effect of feed gas pressure on the pure gas permeability of N_2 (a), CH_4 (b), H_2 (c) and CO_2 (d) of the PEBAX and the $NH_4F/PEBAX(0.1)$ membranes
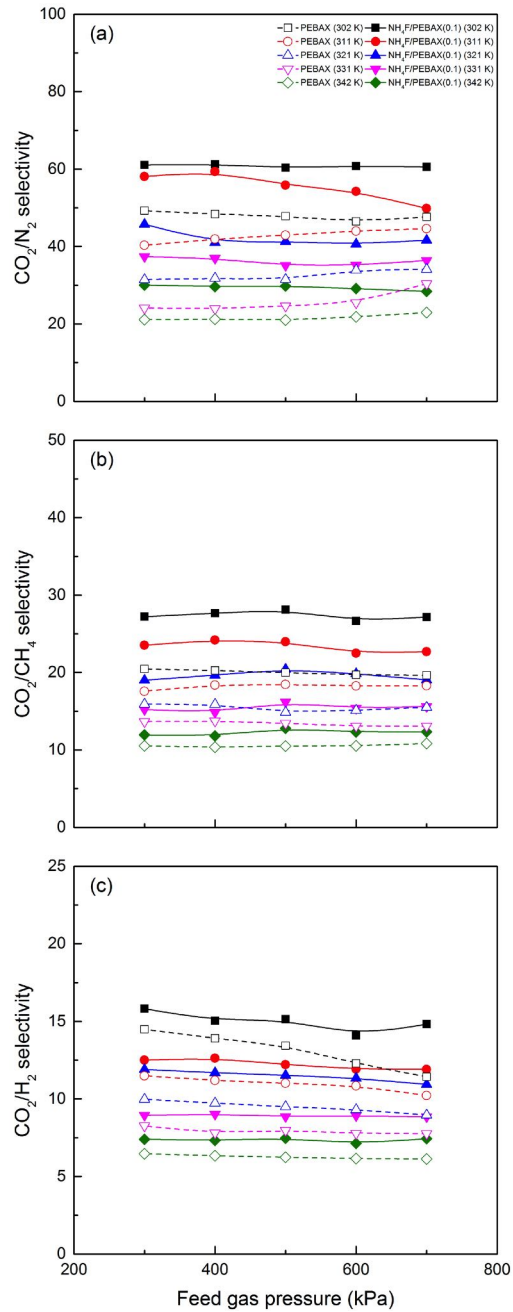
Figure 5.12: Effect of feed gas pressure on the CO_2/N_2 (a), CO_2/CH_4 (b), and CO_2/H_2 (c) selectivity of the PEBAX and the $NH_4F/PEBAX(0.1)$ membranes

5.3.4 Effect of feed gas composition

For gas mixture permeation, when one component permeates through the membrane, the permeation may be affected by the existence of other components due to competitive permeation. Therefore, it is necessary to study the effects of feed gas composition on the gas permeation behavior. The $NH_4F/PEBAX(0.1)$ membrane was tested for CO_2/CH_4, CO_2/N_2, and CO_2/H_2 separations at room temperature and under a feed gas pressure of 700 kPa in humid conditions. As shown in Figure 5.13, the mole fraction of CO_2 in permeate gas was always higher than in feed gas. Besides, when the mole fraction of CO_2 in feed gas increased, more CO_2 diffused across the membrane to the permeate side. Hence, even if CO_2 concentration in binary gas mixtures was low, the membrane was still favorable for CO_2 permeation.

When the mole fraction of CO_2 in the feed gas increased from 0 to 1, the CO_2-induced plasticization due to the strong sorption of CO_2 in the membrane contributed to increasing polymer chain flexibility and intended to increase CH_4, N_2, H_2, and CO_2 permeability. As shown in Figures 5.14 (a), 5.15 (a), and 5.16 (a), the increase in H_2 permeability was most obvious among the slow gases (CH_4, N_2, and H_2). The smallest kinetic diameters of H_2 among them made H_2 diffuse easily in the membrane, resulting that H_2 permeability increased from 23.2 to 50.3 Barrer and CO_2/H_2 selectivity from 13.1 to 6.30 when the mole fraction of CO_2 in the feed gas increased from 0.08 to 0.87 (Figures 5.16 (b) and (c)). As for CO_2 permeation, the salting-out effect prevented further increase in CO_2 permeability. Moreover, the competitive permeation between gas components could also impact CO_2 permeation. As a result, CO_2 permeability remained unchanged in CO_2/H_2 separation, while CO_2 permeability increased in CO_2/CH_4 and CO_2/N_2 separations. As shown in Figures 5.14 (c), 5.15 (c), and 5.16 (c), comparing with CO_2/H_2 selectivity, CO_2/CH_4 and CO_2/N_2 selectivity did not change dramatically since the increase extent of CO_2 permeability and CH_4 or N_2 permeability was similar. However, the gas selectivity of binary gas mixtures was not as good as the ideal selectivity of gas pairs, which reflected that the interactions between gas components or gas molecules and the polymer can affect the gas

permeation in the membrane.

The effect of feed pressure on gas mixture permeation of the $NH_4F/PEBAX(0.1)$ membrane for CO_2/CH_4, CO_2/N_2, and CO_2/H_2 separations was studied. The mole fraction of CO_2 in feed gas was fixed at 14%, 35%, and 40% for CO_2/N_2, CO_2/CH_4, and CO_2/H_2 separations, respectively. As the feed gas pressure increased from 300 to 700 kPa, partial pressure of CO_2 in feed gas increased, but CO_2, N_2, CH_4, and H_2 permeability did not change significantly (Figure 5.17). It indicated that feed gas pressure hardly affected gas mixture permeation in the $NH_4F/PEBAX(0.1)$ membrane which was dominated by the solution-diffusion mechanism, which was in consistent with the results of pure gas permeation under different feed gas pressure.
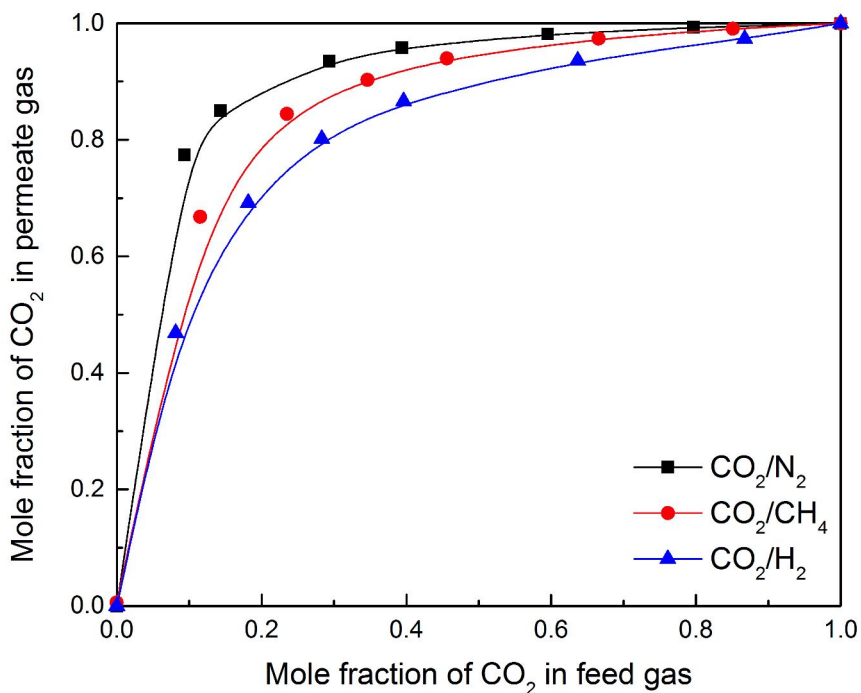
Figure 5.13: Effect of mole fraction of CO_2 in feed gas on mole fraction of CO_2 in permeate gas for CO_2/N_2, CO_2/CH_4, and CO_2/H_2 separations through the $NH_4F/PEBAX(0.1)$ membrane
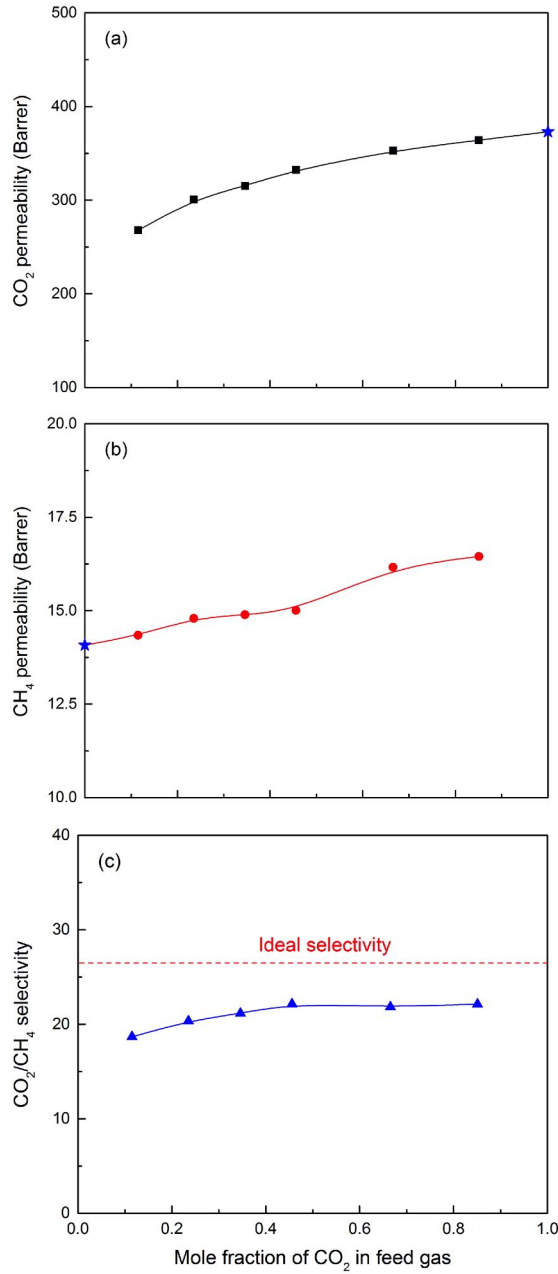
Figure 5.14: Effect of feed gas composition on the CO_2 (a) and CH_4 permeability (b) and the CO_2/CH_4 selectivity (c) of the $NH_4F/PEBAX(0.1)$ membrane in CO_2/CH_4 gas mixture permeation (The star-shape points represent pure gas permeability and ideal gas selectivity)
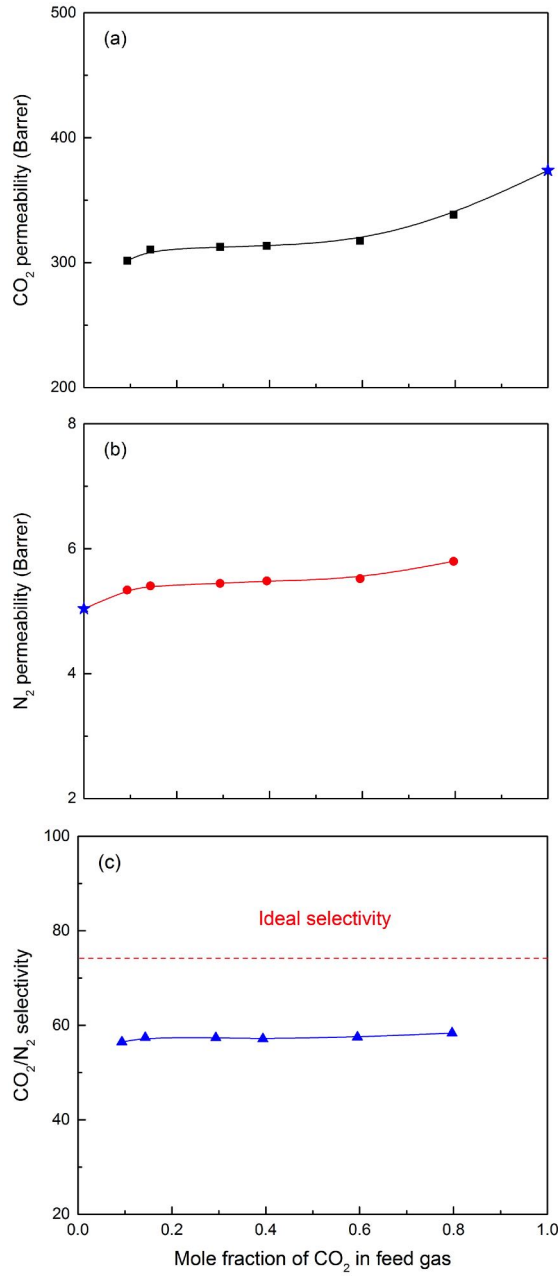
Figure 5.15: Effect of feed gas composition on the CO_2 (a) and N_2 permeability (b) and the CO_2/N_2 selectivity (c) of the $NH_4F/PEBAX(0.1)$ membrane in CO_2/N_2 gas mixture permeation (The star-shape points represent pure gas permeability and ideal gas selectivity)
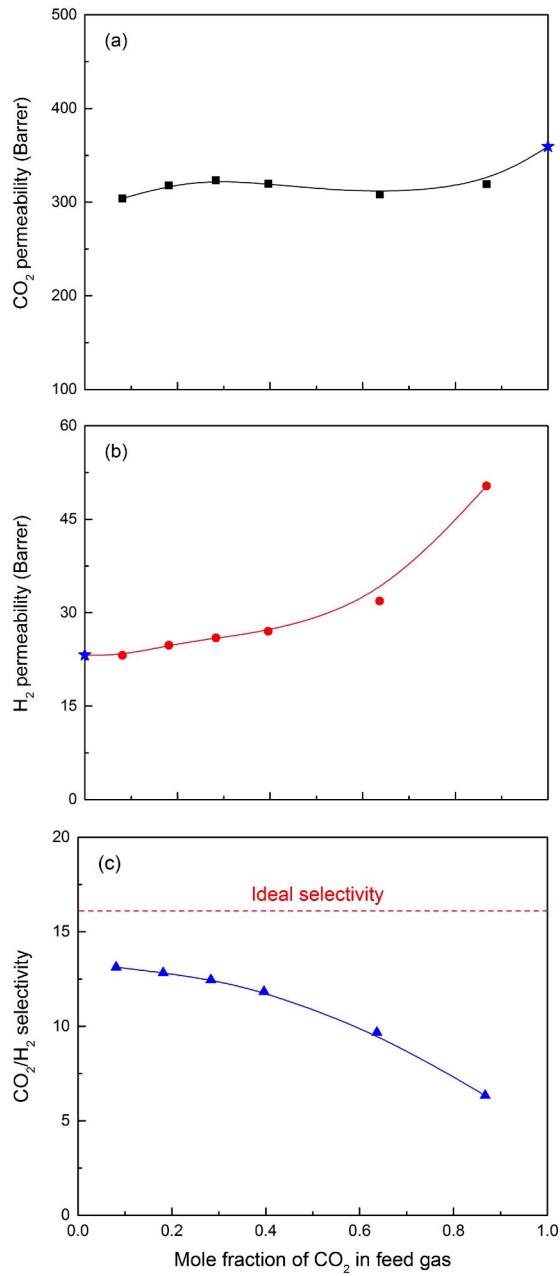
Figure 5.16: Effect of feed gas composition on the CO_2 (a) and H_2 permeability (b) and the CO_2/H_2 selectivity (c) of the $NH_4F/PEBAX(0.1)$ membrane in CO_2/H_2 gas mixture permeation (The star-shape points represent pure gas permeability and ideal gas selectivity)
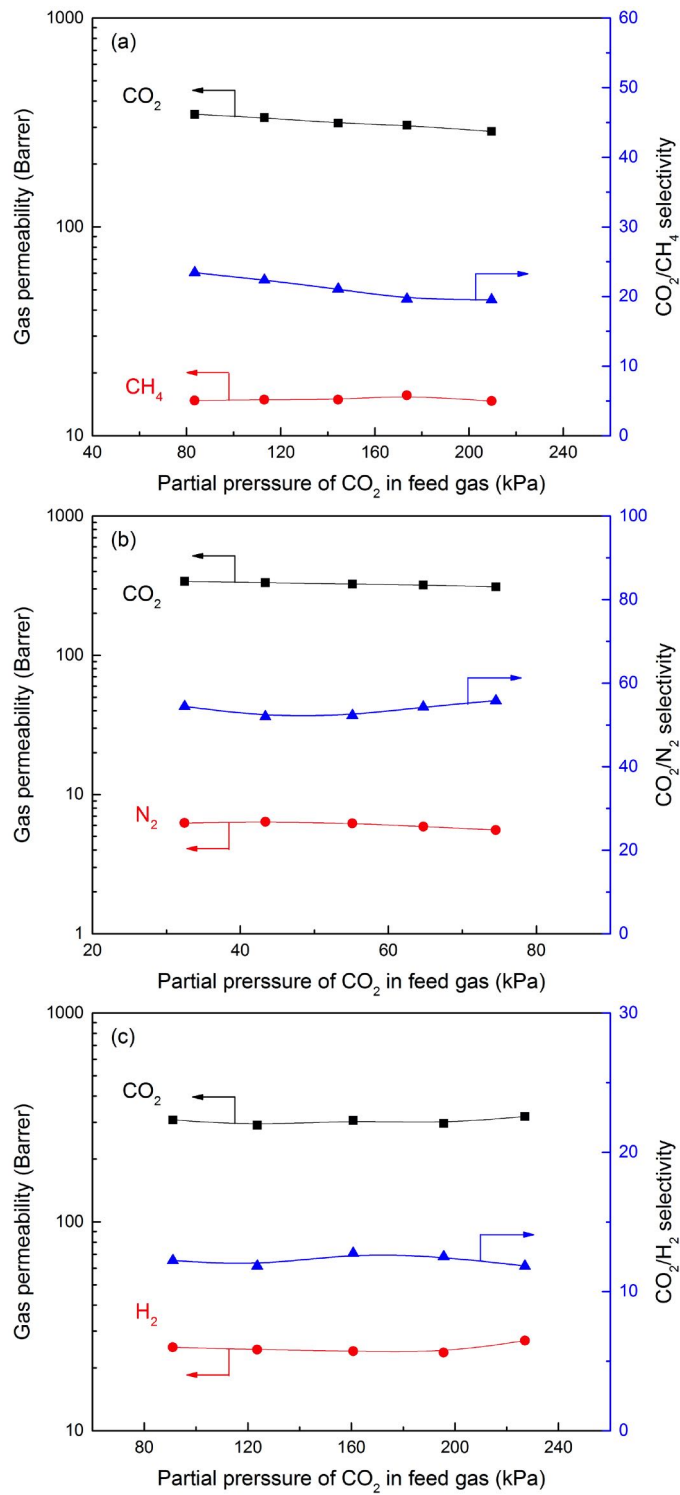
Figure 5.17: Effect of partial pressure of CO_2 in feed gas on gas mixture permeation for CO_2/CH_4 (a), CO_2/N_2 (b), and CO_2/H_2 (c) separations

122

5.3.5 Membrane stability

The $NH_4F/PEBAX(0.1)$ membrane was tested for CO_2/CH_4 (35% CO_2), CO_2/N_2 (14% CO_2), and CO_2/H_2 (40% CO_2) separations at room temperature and under a feed gas pressure of 700 kPa in humid conditions. As shown in Figures 5.18 (a), (b), and (c). The prepared $NH_4F/PEBAX(0.1)$ membrane exhibited no obvious reduction of gas separation performance during an 18-day test: the CO_2 permeability kept around 320 Barrer, while the CO_2/CH_4 selectivity kept around 22 in CO_2/CH_4 separation; the CO_2 permeability kept around 319 Barrer, while the CO_2/N_2 selectivity kept around 58.4 in CO_2/N_2 separation; and the CO_2 permeability kept around 321 Barrer, while the CO_2/H_2 selectivity kept around 12 in CO_2/H_2 separation. Thus, the $NH_4F/PEBAX(0.1)$ membrane showed stable gas separation performance for binary gas mixtures.
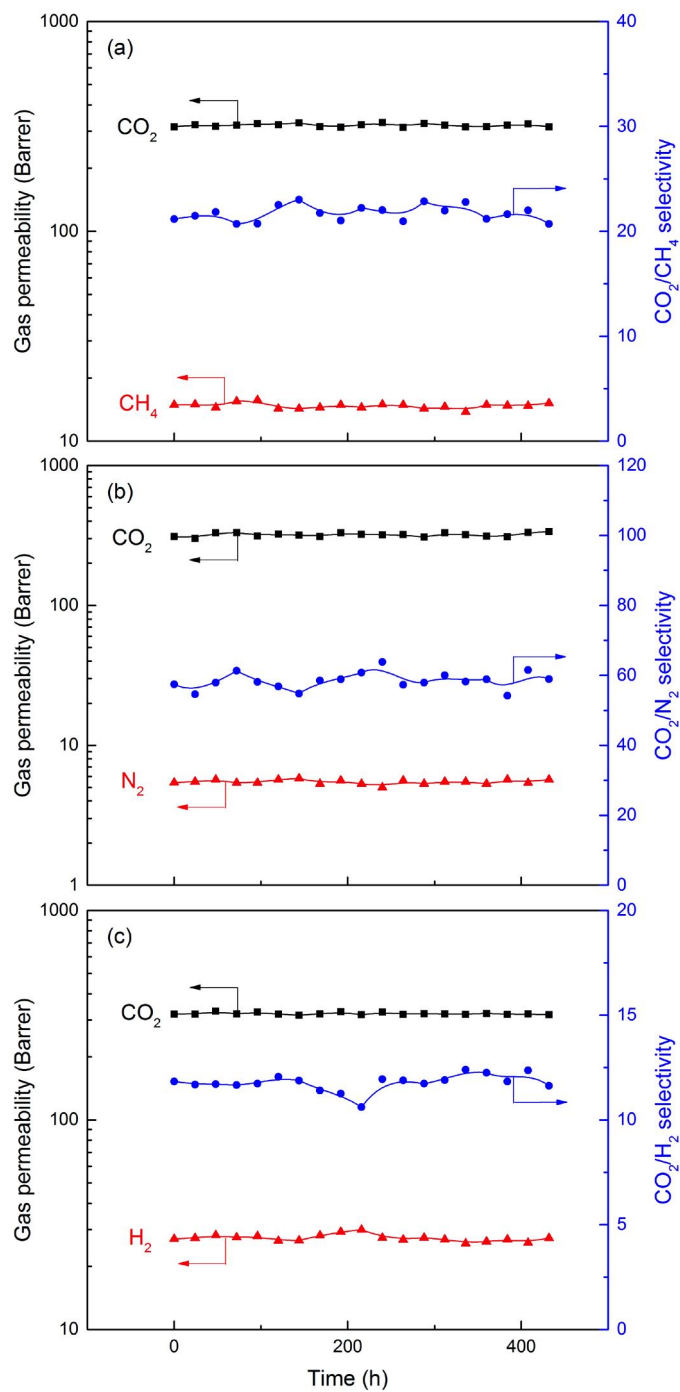
Figure 5.18: Stability of the NH_4F/PEBAX(0.1) membrane in CO_2/CH_4 (a), CO_2/N_2 (b), and CO_2/H_2 (c) separations

124

5.4 Conclusions

In order to increase gas selectivity of the membranes, NH_4F/PEBAX membranes for CO_2/N_2, CO_2/CH_4, and CO_2/H_2 separation were fabricated by a solution casting method. Both pure gas and gas mixture permeation were studied and the following conclusions can be drawn:

- When the mass ratio of NH_4F to PEABX reached 0.1, N_2, CH_4, and H_2 had the lowest permeability (5.04, 13.5, and 23.2 Barrer), while CO_2 permeability (372 Barrer) remained comparable with pristine PEBAX membrane. The salting-out effect affects N_2, CH_4, and H_2 permeation more significantly than CO_2 permeation. Hence, the CO_2/N_2, CO_2/CH_4, and CO_2/H_2 selectivity increased by 54%, 13%, and 22% at room temperature and under a feed gas pressure of 700 kPa, comparing with the pristine PEBAX membranes.

- The NH_4F/PEBAX(0.1) membrane had better ideal gas selectivity than the PEBAX membrane at the same temperature and feed gas pressure. When the temperature increased, CO_2, N_2, CH_4, and H_2 permeability in both membranes increased, while the ideal gas selectivity decreased.

- The feed gas pressure barely affected pure gas permeability and ideal selectivity of all prepared NH_4F/PEBAX(X) membranes. The solution-diffusion mechanism dominated the permeation process instead of the facilitated transport of CO_2.

- When the NH_4F/PEBAX(0.1) membrane was used for gas mixture separation, the CO_2-induced plasticization, the salting-out effect, and competitive permeation affected gas permeation. When feed composition was fixed, the increase in feed gas pressure from 300 to 700 kPa didn't change the permselectivity in CO_2/CH_4, CO_2/N_2, and CO_2/H_2 separations.

- The gas mixture separation performance of the NH_4F/PEBAX(0.1) membrane in CO_2/CH_4, CO_2/N_2 and CO_2/H_2 separations was stable during an 18-day test.

Chapter 6

MWCNT-PDA-PEI/PEBAX membranes for carbon capture

6.1 Introduction

Gas permeability and selectivity of polymeric membranes usually have a "trade-off" relationship. When the gas permeability of a membrane is high, the gas selectivity is usually low, and *vice versa*. Many studies have focused on the breakthrough of the Robeson's upper bound of gas separation performance to achieve high permselectivity [Robeson (1991, 2008)]. Mixed matrix membranes (MMMs) have attracted more and more attention recently due to the potential to break the upper bound. These membranes are composed of a polymer matrix (continuous phase) and fillers (disperse phase), as shown in Figure 6.1. MMMs combine advantages of different materials: the polymer matrix provides good gas permeability, while the fillers can enhance the selectivity of membranes [Chung et al. (2007)].

126
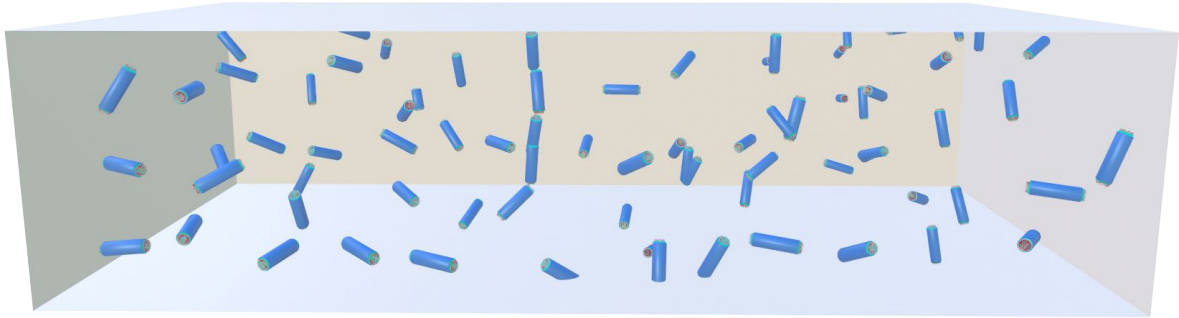
Figure 6.1: Structure of mixed matrix membranes
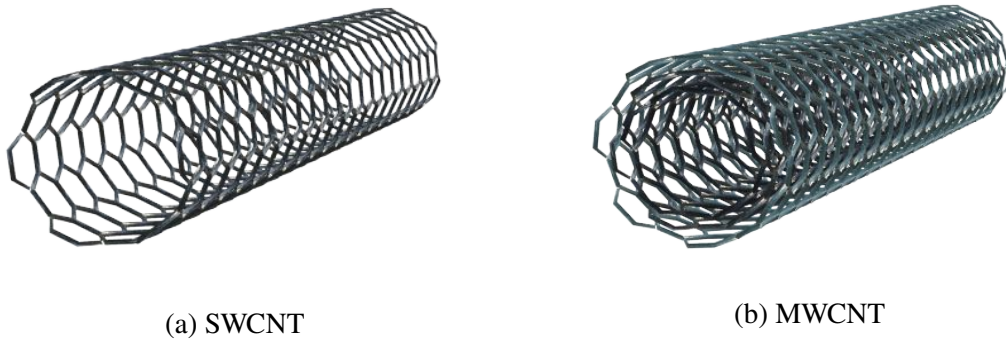
(a) SWCNT

(b) MWCNT

Figure 6.2: Schematic illustration of carbon nanotubes

The fillers in MMMs can disturb the polymer chain packing, adjust the free volume of the polymer, and even offer transport passageways for gas permeation in the membranes owing to their inherent structures [Hu et al. (2012); Zhang et al. (2016); Zhao et al. (2013)]. Besides, in order to improve the affinity to CO_2, the fillers have been modified with some functional groups ($-NH_2$, $-COOH$, $-OH$, and $-SO_3H$) which can be considered as CO_2 carriers to facilitate transport of CO_2 in the membrane [Ansaloni et al. (2015); Li et al. (2015b); Xin et al. (2015b); Ma et al. (2015)]. Carbon nanotubes (CNTs) have the advantages of smooth surface, high aspect ratio (> 1000), high mechanical strength and thermal stability [Kim et al. (2007); Murali et al. (2010)]. CNTs can be single-walled (SWCNTs) and multi-walled (MWCNTs) (Figure 6.2). From both the molecular dynamic simulations and experimental observations, the gas transport rate in the

CNTs can be quite high due to the smooth inner walls [Sholl and Johnson (2006)]. Cong et al. (2007) found that MWCNTs can increase CO_2 permeability more effectively than SWCNTs in the brominated poly(2,6-diphenyl-1,4-phenylene oxide) membranes. However, both of them did not improve CO_2/N_2 selectivity.

The fillers are surrounded by polymers, and the interface between polymer and fillers can form different morphologies [Chung et al. (2007)]. The strong interactions between them can reduce polymer chain flexibility and lead to polymer chain rigidification. The formation of undesirable defects or voids could increase gas permeability but decrease the selectivity of membranes. Besides, MWCNTs tend to be aggregated to form bundles owing to the strong van der Waals attraction or hydrogen bonds among the tubes. Thus, chemical modification of MWCNTs can be considered as an effective and feasible method to achieve good dispersion and decrease interfacial defects in membranes. In this study, MWCNTs were functionalized chemically, as shown in Figure 6.3. Initially, MWCNTs were modified by polydopamine (PDA) through the self-polymerization of dopamine in weak alkaline solution. The obtained MWCNT-PDA particles were expected to improve interfacial compatibility to introduce some amine groups. Furthermore, branched polyethylenimine (PEI) with numerous amine groups was grafted on the surface of MWCNT-PDA. The catechol groups on PDA can react with amine groups on PEI by the Michael addition and Schiff base reactions. The grafting of PEI can not only improve interfacial compatibility further but also contribute more CO_2 carriers. Therefore, the MWCNT-PDA-PEI particles were blended with PEBAX to fabricate MMMs. The effects of membrane composition on N_2, CH_4, H_2, and CO_2 permeation were investigated. The effects of temperature and feed gas pressure on gas permeability and ideal selectivity of the prepared membranes were studied. The gas mixture permeation of the MWCNT-PDA-PEI/PEBAX membrane for CO_2/N_2, CO_2/CH_4, and CO_2/H_2 separations was studied, and the membrane stability was tested for 22 days.
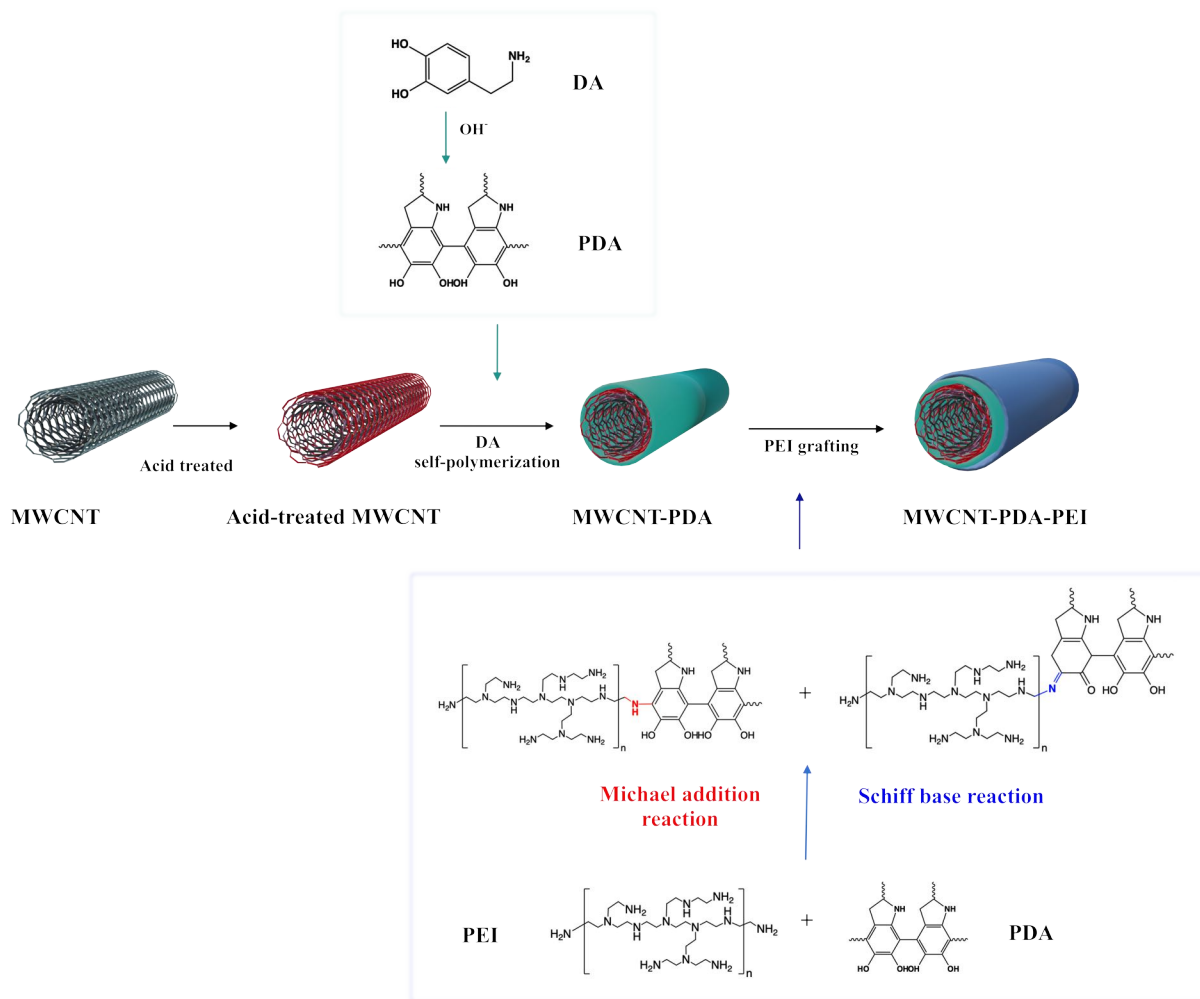
Figure 6.3: Schematic illustration of modification of MWCNTs

6.2 Experimental

6.2.1 Materials

Multi-walled carbon nanotubes (MWCNTs) (purity 95%, diameter of 20-40 nm, length of 1-2 μm) were supplied by Shenzhen Nanotech Ltd., China. Branched polyethylenimine (PEI, average MW 25,000), dopamine hydrochloride (DA), and tris(hydroxymethyl)aminomethane (Tris) were purchased from Sigma-Aldrich. $NH_3 \cdot H_2O$ (28-30 wt%), hydrochloric acid (36.5-38.0 wt%), nitric acid (70 wt%), and sulfuric acid (98 wt%) were purchased from Fisher Scientific. Other materials were the same as described in the previous chapter.

6.2.2 Preparation of particles

Purification of MWCNTs

An acid solution composed of nitric acid (100 mL) and sulfuric acid (300 mL) was prepared. Two grams of MWCNTs were added to the acid solution with stirring in a round-bottom flask. Then, the mixture was ultra-sonicated for 1 h to disperse MWCNTs, followed by refluxing at 90°C for 3 h. After dilution with DI water, acid-treated MWCNTs were separated by centrifugation at 8000 r/min for 15 min. After thorough rinsing with DI water several times until the liquid became neutral, the acid-treated MWCNTs were dried in a vacuum oven at 80 °C for 24 h.

Modification of MWCNTs by PDA

0.969 g of Tris was added to 800 mL of DI water in a round-bottom flask with stirring. The pH value of the Tris solution was adjusted to 8.5 by HCl and $NH_3 \cdot H_2O$. 1.981 g of DA and 0.8 g of MWCNTs were added to the Tris solution sequentially. The mixture was dispersed by ultra-sonication in an ice water bath for 1 h. Then, DA was allowed to polymerize on the surface

of the acid-treated MWCNTs at room temperature for 18 h. The polydopamine (PDA) modified MWCNTs (MWCNT-PDA) were filtered with a microfiltration membrane (nominal pore size 0.2 μm) under vacuum. MWCNT-PDA particles were washed by DI water until the liquid became neutral. The filtrate was dried in a vacuum oven at 80 °C for 24 h.

Modification of MWCNT-PDA by PEI

The MWCNT-PDA particles were further modified by PEI. 0.5 g of MWCNT-PDA and 3.0 g of PEI were added to 100 mL DI water in a round-bottom flask with stirring. Then, the mixture was stirred vigorously at 60 °C for 10 h. The catechol groups on PDA can react with amine groups on PEI by the Michael addition reaction and Schiff base reaction. The PEI modified MWCNT-PDA particles (MWCNT-PDA-PEI) were filtered. After being washed with DI water several times until the liquid became neutral, the MWCNT-PDA-PEI particles were dried in a vacuum oven at 80°C for 24 h.

6.2.3 Membrane preparation

The PEBAX solution (5 wt%) was prepared by the same method as described in Chapter 3. The MWCNT/PEBAX(X) membranes with different mass ratio of MWCNTs to PEBAX (X, X = 0, 0.02, 0.04, 0.06, and 0.08) were prepared by a solution casting method. The preparation of the MWCNT/PEBAX(0.08) membrane was used as an example to describe this process. 0.56 g of the acid-treated MWCNTs and 7 g of the PEBAX pellets were added to the mixture solvent of DI water (40 mL) and ethanol (118 mL). After ultrasonication for 4 h, the mixture was stirred at 80°C for 4 h to produce a homogeneous casting solution. 3 mL of the casting solution was cast on a PTFE plate, and the casting area was fixed by a frame (48.7 cm^2). The plate was placed in a dust-free chamber to evaporate the solvent in ambient conditions after 48 h. The MWCNT/PEBAX(0.08) membrane was peeled off the plate carefully and collected.

The MWCNT-PDA/PEBAX(0.08) and MWCNT-PDA-PEI/PEBAX(0.08) membranes were fabricated by blending the MWCNT-PDA and MWCNT-PDA-PEI particles in PEBAX, respectively. The preparation process was the same as described above. The thicknesses of membranes were measured by a spiral micrometer at ten different places on the membranes, and the average value was used. The thicknesses of all prepared membranes were in the range of 8-13 μm in dry conditions and 27-41 μm in humid conditions.

6.2.4   Gas permeation tests

Both pure gas and gas mixture permeation tests were conducted by the same methods which were described in Chapter 3. All membranes were placed in a container with constant humidity for 4 days at room temperature before the permeation tests. The membrane swelling degree was measured by the same method as described in Chapter 3. Gas permeability of the membranes from the same batch showed a relative standard deviation within 6% which was considered as the experimental error. The relative standard deviation in gas permeability of the membranes from different batches was within 16%.

6.3   Results and discussion

6.3.1   Effect of membrane composition

The prepared MWCNT/PEBAX(X) membranes were tested under a feed gas pressure from 300 to 700 kPa at room temperature. As shown in Figure 6.4 (a), when the mass ratio of MWCNTs to PEBAX increased, the permeability of N_2, CH_4, H_2 and CO_2 increased. The blend of MWCNTs in the membranes adjusted the polymer chain packing and created more free volume for gas molecule permeation. Besides, MWCNTs were randomly dispersed in the polymeric matrix, and the inner diameter of MWCNTs (20-40 nm) is large enough to allow the gas molecules to pass

through quickly, which was determined by the dispersion orientation in the membranes. If the MWCNTs could be distributed vertically to the surface of the membranes, they could form fast transport pathways for gas permeation in the membranes. As a result, N_2, CH_4, H_2 and CO_2 permeability increased as the mass ratio of MWCNTs to PEBAX increased.

Although all gas permeability increased, the extent of the permeability increase was different, which can be indicated by the CO_2/N_2, CO_2/CH_4, and CO_2/H_2 selectivity. As shown in Figure 6.4 (b), CO_2/CH_4 and CO_2/H_2 selectivity of all MWCNT/PEBAX(X) membranes seemed to be similar, but the CO_2/N_2 selectivity of MWCNT/PEBAX(X) membranes (X = 0.02, 0.04, 0.06, and 0.08) increased by around 38% than that of the pristine PEBAX membranes. According to the solution-diffusion model, permeability selectivity (P_i/P_j) was determined by diffusivity selectivity (D_i/D_j) and solubility selectivity (S_i/S_j) (Equation 2.5):

$$\alpha_{i,j} = \frac{P_i}{P_j} = \frac{S_i}{S_j}\frac{D_i}{D_j} \qquad (2.5)$$

The diffusivity selectivity is related to the kinetic diameter difference of gas molecules. The kinetic diameter difference of CO_2/H_2 (0.041 nm) and CO_2/CH_4 (0.05 nm) were larger than that of CO_2/N_2 (0.034 nm) from Table 2.1. Nonetheless, the critical temperature of CO_2 (304.2 K) was higher than that of N_2 (126.2 K), which indicated that the improvement of CO_2/N_2 solubility selectivity is more effective than that of diffusivity selectivity in order to increasing permeability selectivity [Ramasubramanian et al. (2013); Wang et al. (2014)]. Therefore, a 38% of increase in CO_2/N_2 selectivity could be attributed to the increase of solubility selectivity with the presence of MWCNTs.

In fact, excessive addition of MWCNTs can increase transport tortuosity due to random dispersion, and more tortuous permeation pathways in the membranes resulted in the decrease in gas permeability and the increase in gas selectivity [Hu (2013); Ordonez et al. (2010); Ismail et al. (2011)]. High contents of fillers in the MMMs may decrease the gas selectivity due to filler aggregation and microvoids between fillers and polymer matrix [Kim et al. (2007)]. Hence,
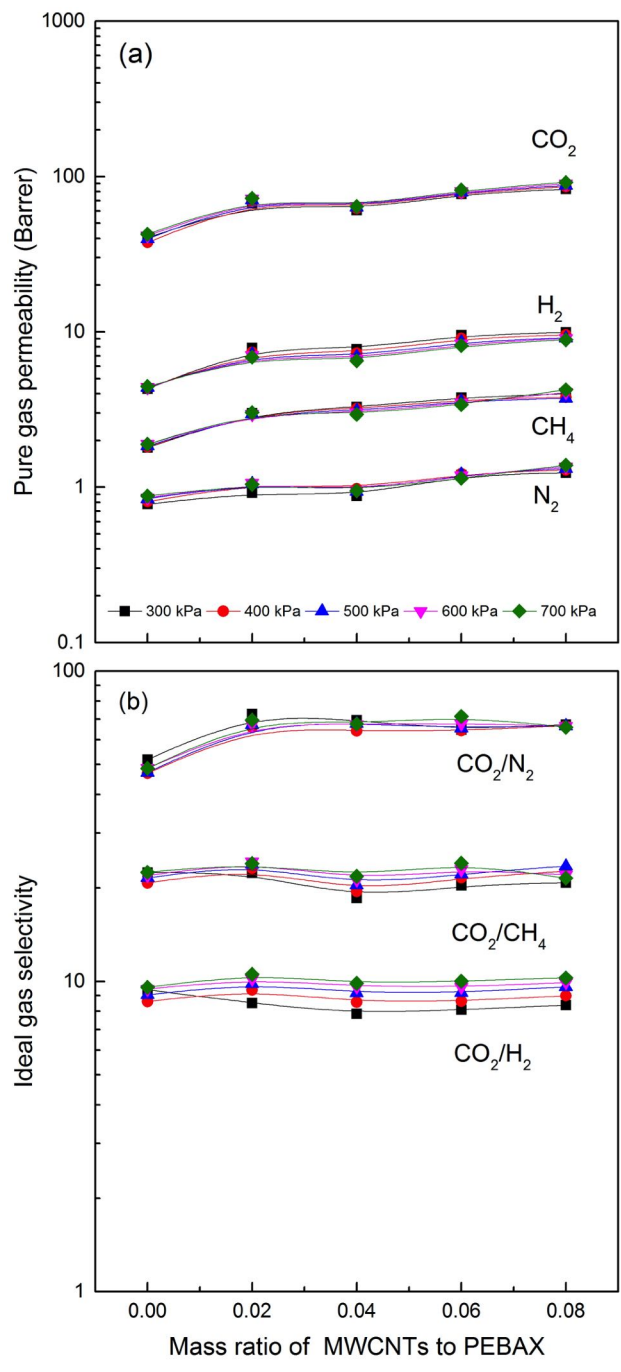
Figure 6.4: Effect of the MWCNT content in the membranes on the pure gas permeability (a) and the ideal gas selectivity (b)

the MWCNT/PEBAX(0.08) membrane was chosen for further study. In order to further improve the gas selectivity, MWCNTs were modified by PDA and PEI subsequently. Comparing with the acid-treated MWCNTs, the surface of MWCNT-PDA and MWCNT-PDA-PEI contains more functional groups which can interact with CO_2. The interfacial compatibility between inorganic fillers (MWCNTs) and polymeric matrix (PEBAX) could be improved, which was beneficial for the decrease of interfacial defects. Also, the interface would form polymer chain rigidification. The polymer chains in the vicinity of fillers became less flexible for gas diffusion leading to a decrease in gas permeability. Therefore, the permeability of N_2, CH_4, and H_2 decreased after the modification of MWCNTs by PDA and PEI (Figures 6.5 (b), (c), and (d)).

In spite of polymer chain rigidification, CO_2 permeability increased by 19% comparing the MWCNT-PDA-PEI/PEBAX(0.08) membrane with the MWCNT/PEBAX(0.08) membrane under a feed gas pressure of 300 kPa, which was attributed to the PEI modification (Figure 6.5 (a)). Since PEI contains numerous and different kinds of amine groups on the polymer chains, amine groups can react with CO_2 reversibly to facilitate CO_2 transport. N_2, CH_4, and H_2 can not react with amine groups, and their permeation only obeys the solution-diffusion mechanism. As shown in Figure 6.8, as the swelling degrees of PEBAX membranes which were prepared in these four chapters increased, gas permeability increased while gas selectivity kept almost unchanged (Figure 6.7). Besides, the membranes prepared in Chapter 6 had lower gas permeabilities than the water-swollen membranes prepared in previous chapters. Water in the membranes can not only improve gas diffusion due to making membrane swollen but also participate in the reversible reaction between CO_2 and amine groups. As shown in Figure 6.7, pure gas permeation performance in the MWCNT-PDA-PEI/PEBAX(0.08) membrane exceeded Robeson's upper bound (2008) except for CO_2/CH_4. Comparing with the pristine PEBAX membrane, the CO_2/N_2, CO_2/CH_4, and CO_2/H_2 selectivity (107, 26, and 11) of the MWCNT-PDA-PEI/PEBAX(0.08) membrane increased by 106%, 18%, and 20% under a feed gas pressure of 300 kPa, respectively (Figure 6.6).
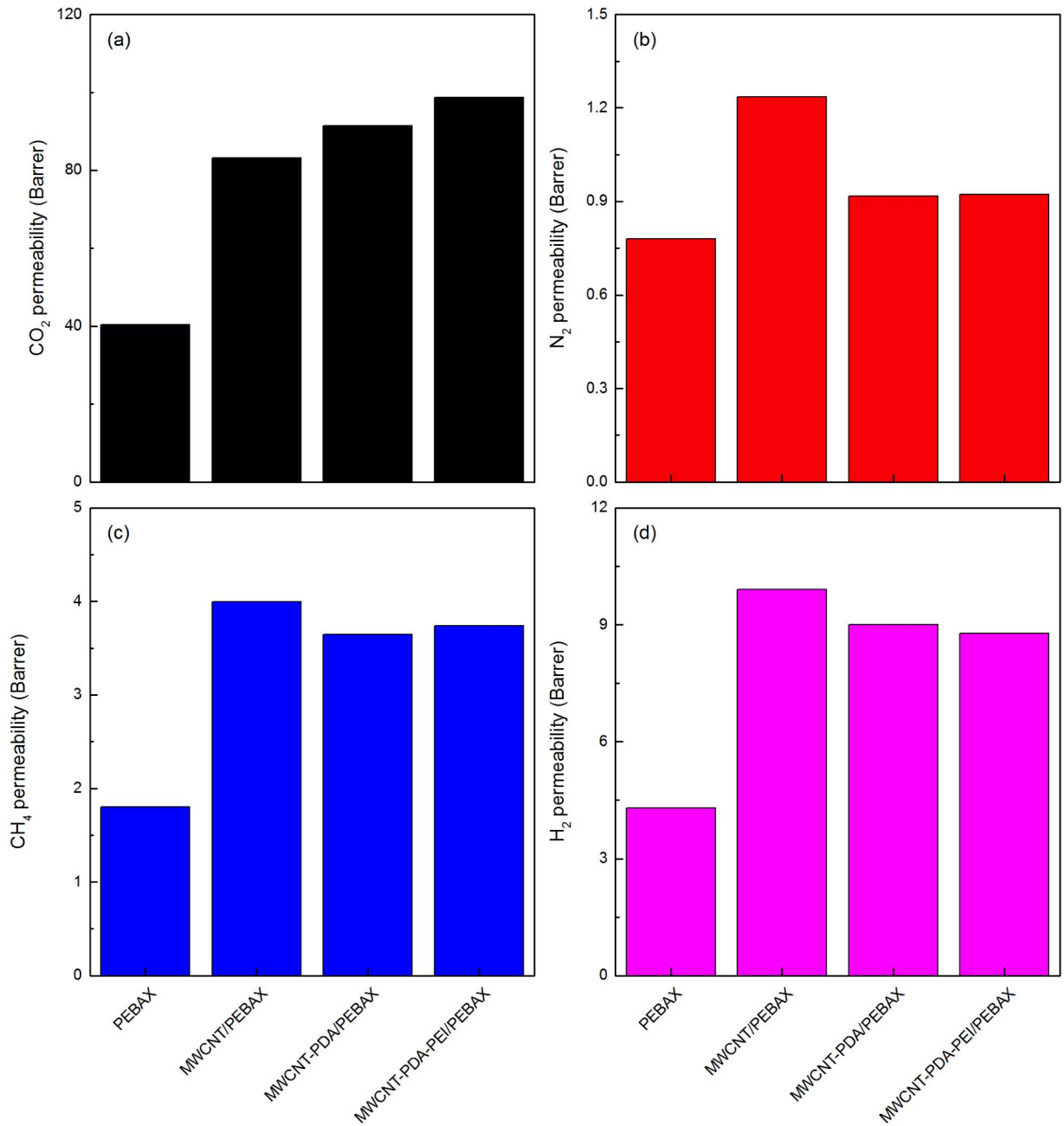
Figure 6.5: Effect of modified MWCNTs on the pure gas permeability of CO_2 (a), CH_4 (b), H_2 (c) and N_2 (d)
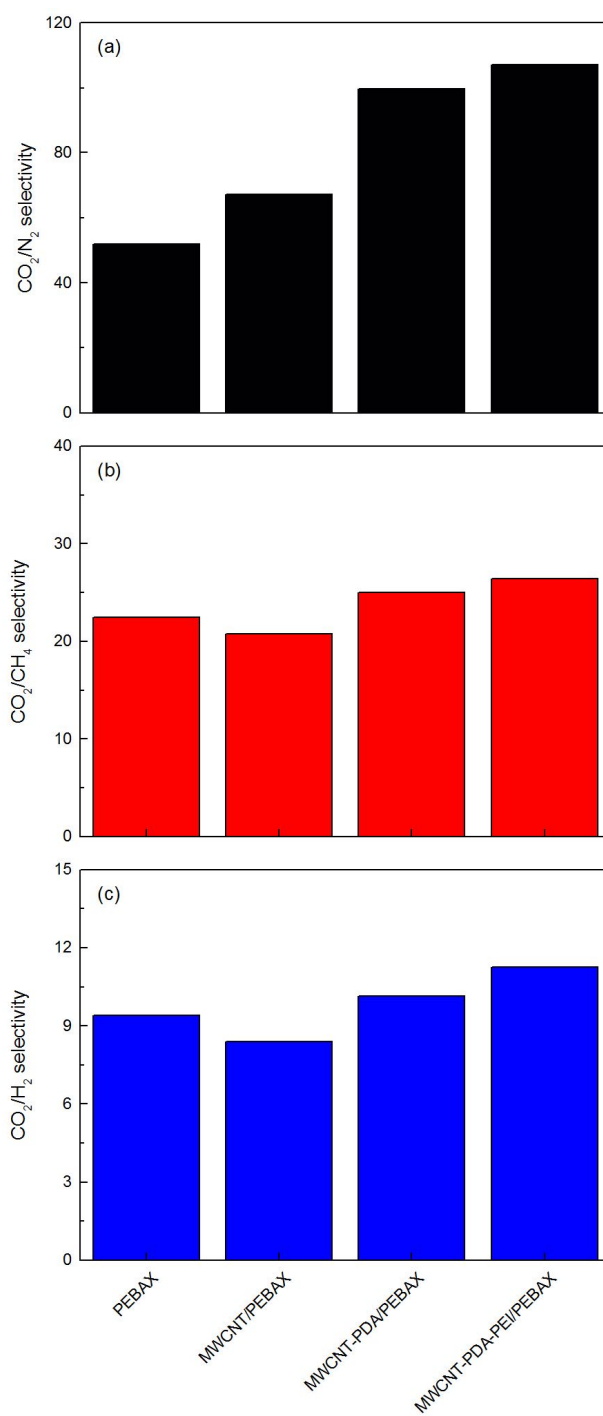
Figure 6.6: Effect of modified MWCNTs on the CO_2/N_2 (a), CO_2/CH_4 (b), CO_2/H_2 (c) selectivity
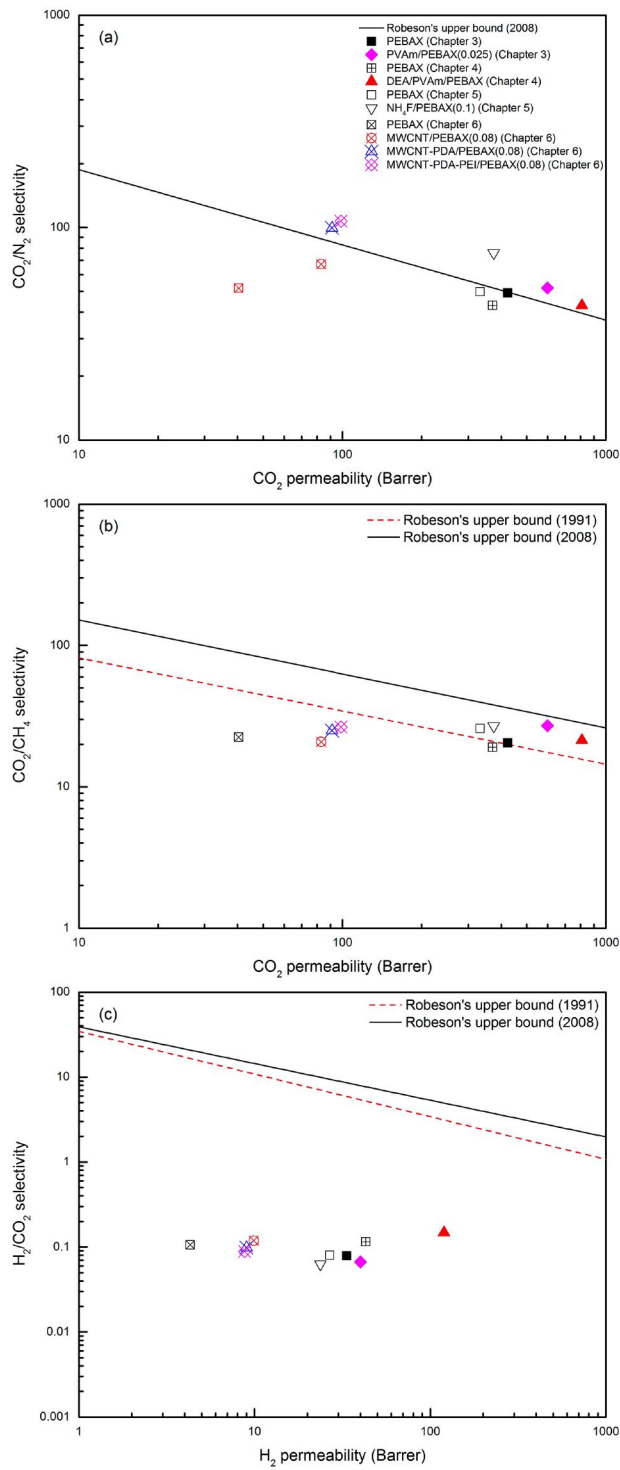
Figure 6.7: Comparison with Robeson's upper bound for CO_2/N_2 (a), CO_2/CH_4 (b), and H_2/CO_2 (c)
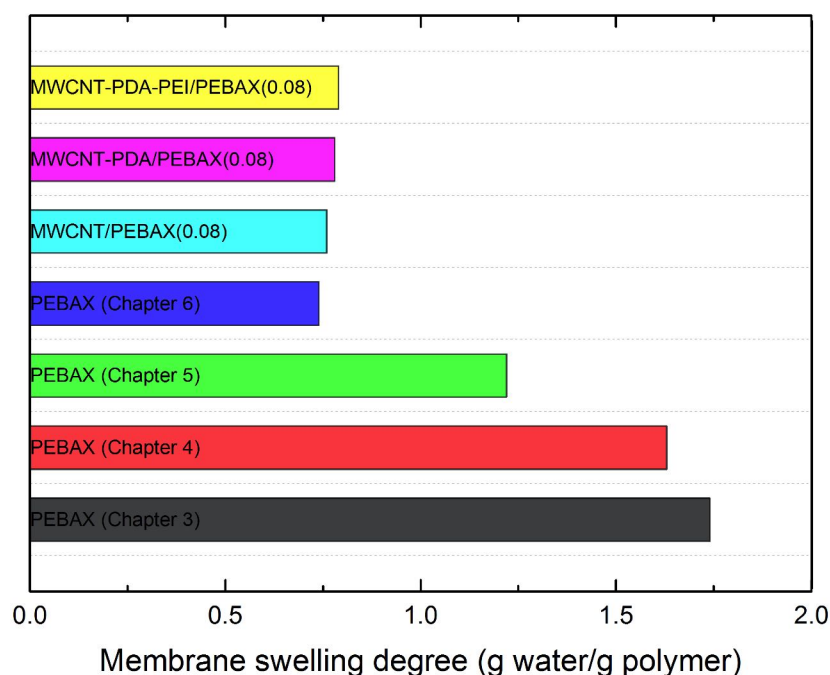
Figure 6.8: Comparison of swelling degrees of membranes

6.3.2 Effect of temperature

The effects of operating temperature on pure gas permeation of the PEBAX and MWCNT-PDA-PEI/PEBAX(0.08) membranes under a feed gas pressure from 300 to 700 kPa were studied. The results were shown in Figures 6.9 and 6.10. As the operating temperature raised from 294 to 342 K, the N_2, CH_4, H_2 and CO_2 permeability of both membranes increased, while the CO_2/N_2, CO_2/CH_4, and CO_2/H_2 selectivity decreased. Increasing temperature increases gas molecule movement so that gas solubility in the water tends to decrease. However, the diffusivity of gas molecule and polymer chain mobility increased at elevated temperatures, which could offset the decrease in gas permeability due to the diminishment of solubility. For CO_2 permeation in the MWCNT-PDA-PEI/PEBAX(0.08) membrane, it was dominated by not only the solution-diffusion mechanism but also the facilitated transport of CO_2. The increasing temperature could accelerate the reaction rate between CO_2 and amine groups and the diffusion rate of CO_2-amine complexes. As a consequence, N_2, CH_4, H_2 and CO_2 permeability increased at higher temperatures.

However, as observed in Figure 6.10, higher temperatures tended to decrease the gas selectivity of both membranes. The opposite effects of temperature on gas permeability and selectivity need to be considered in practical applications. The relationship between temperature and permeability could be fitted by the Arrhenius type expression (Equation 3.5). As shown in Figure 6.11, the activation energy for the N_2, CH_4, and H_2 permeation were higher than that for CO_2 permeation in both the PEBAX and MWCNT-PDA-PEI/PEBAX(0.08) membranes. It indicated that N_2, CH_4, and H_2 permeation were more sensitive to the change of temperature than CO_2 permeation in both membranes, resulting that the CO_2/N_2, CO_2/CH_4, and CO_2/H_2 selectivity of both membranes decreased with increasing temperatures, as shown in Figure 6.10. The ideal selectivity of the MWCNT-PDA-PEI/PEBAX(0.08) membrane was higher than that of the pristine PEBAX membrane due to the facilitated transport of CO_2. Feed gas pressure hardly affected the activation energy for gas permeation in both membranes in the test range of 300-700 kPa. The activation energy for gas permeation can imply the energy barrier which needs to be overcome for gas molecules to penetrate the membranes. It was observed that the activation energy for N_2 permeation in the MWCNT-PDA-PEI/PEBAX(0.08) membrane was higher than that in the pristine PEBAX membrane, while the activation energy for CH_4 and H_2 permeation were lower.

Figure 6.9: Effect of temperature on the pure gas permeability of N_2 (a), CH_4 (b), H_2 (c) and CO_2 (d) of the PEBAX and the MWCNT-PDA-PEI/PEBAX(0.08) membranes

Figure 6.10: Effect of temperature on the CO_2/N_2 (a), CO_2/CH_4 (b), CO_2/H_2 (c) selectivity of the PEBAX and the MWCNT-PDA-PEI/PEBAX(0.08) membranes
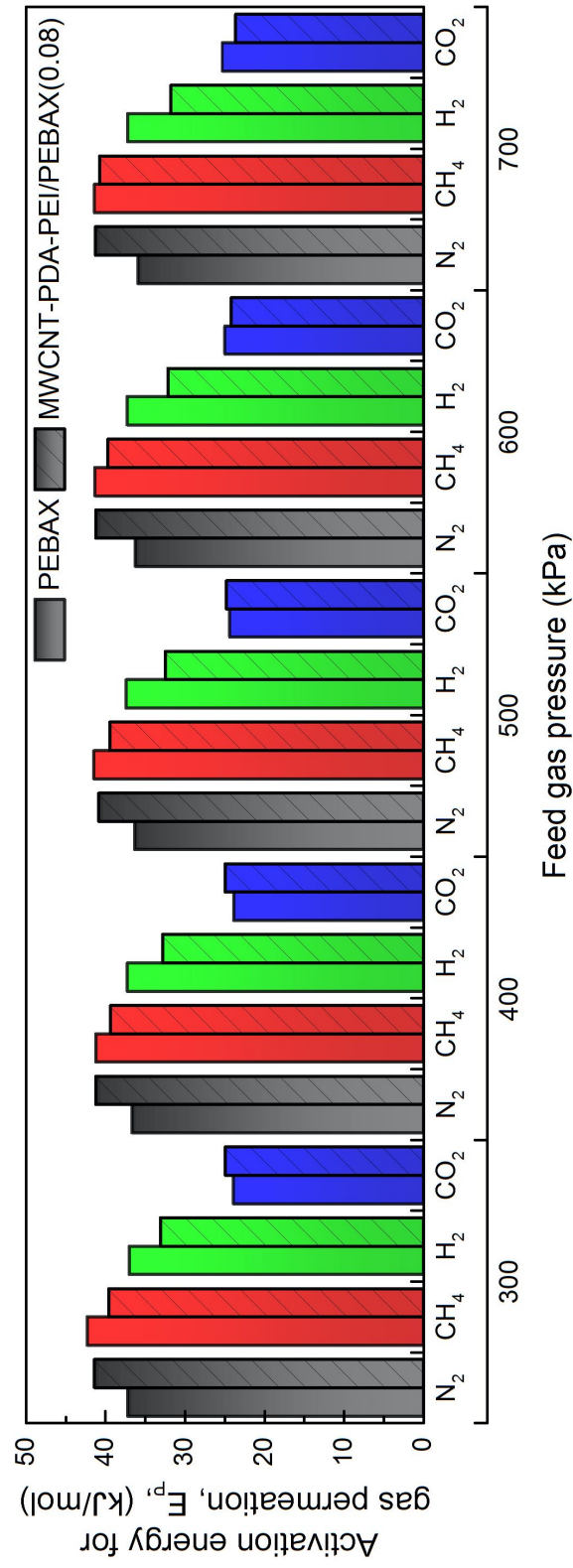
Figure 6.11: Activation energy for pure gas permeation in the PEBAX and the MWCNT-PDA-PEI/PEBAX(0.08) membranes under different feed gas pressures

6.3.3 Effect of feed gas pressure

The gas permeation data was studied with respect to the effects of feed gas pressure of the pure gas permeation of the MWCNT-PDA-PEI/PEBAX(0.08) membrane, the MWCNT-PDA/PEBAX(0.08) membrane, and the MWCNT/PEBAX(X) membranes. As shown in Figure 6.12 (a), as the feed gas pressure increased from 142 to 700 kPa, CO_2 permeability decreased from 211 to 92 Barrer. When the feed gas pressure increased, more CO_2 would be dissolved into the MWCNT-PDA-PEI/PEBAX(0.08) membrane. Nonetheless, the amounts of amine groups which acted as CO_2 carriers were limited. Once most of the amine groups were occupied by CO_2 leading to the carrier saturation, it would cause a decrease in CO_2 permeability. When feed gas pressure became high enough, the facilitated transport of CO_2 could not be as effective as under a low gas pressure. The solution-diffusion mechanism was more dominant under elevated feed gas pressures.

The permeation of N_2, CH_4, and H_2 in the MWCNT-PDA-PEI/PEBAX(0.08) membrane obeyed the solution-diffusion mechanism. The feed gas pressure hardly changed their permeabilities, as shown in Figure 6.12 (a). The N_2, CH_4, and H_2 flux were quite low and could not be measured when the feed gas pressure was under 300 kPa. There was no variation in the ideal gas selectivities of CO_2/N_2, CO_2/CH_4, and CO_2/H_2 in the MWCNT-PDA-PEI/PEBAX(0.08) membrane in the test range from 300 to 700 kPa (Figure 6.12 (b)). As shown in Figures 6.13, 6.14, and 6.15, the pure gas permeation of the MWCNT/PEBAX(X) membranes, the MWCNT-PDA/PEBAX(0.08) membrane, and the MWCNT-PDA-PEI/PEBAX(0.08) membranes under different conditions were barely impacted by feed gas pressure in the test range from 300 to 700 kPa. The solution-diffusion mechanism prevailed in these membranes. The pure gas permeation of the MWCNT-PDA-PEI/PEBAX(0.08) membrane was still better than that of the PEBAX membrane under the same conditions.
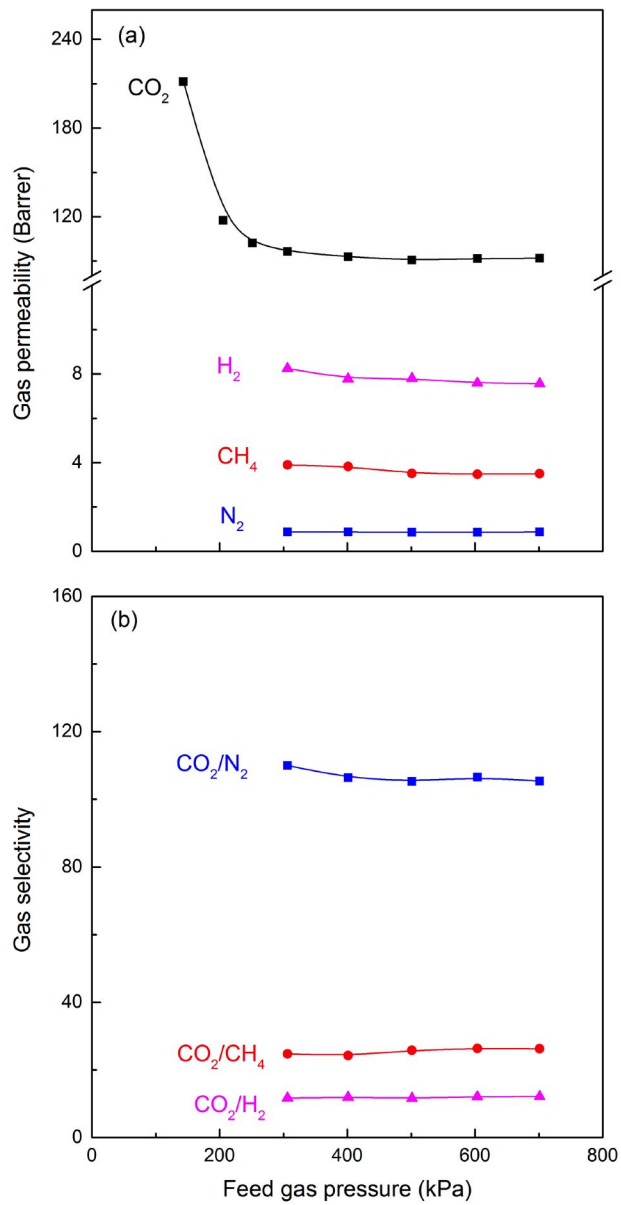
Figure 6.12: Effect of feed gas pressure on the pure gas permeability of N_2, CH_4, H_2 and CO_2 (a) and the ideal gas selectivity of CO_2/N_2, CO_2/CH_4, and CO_2/H_2 (b) of the MWCNT-PDA-PEI/PEBAX(0.08) membranes
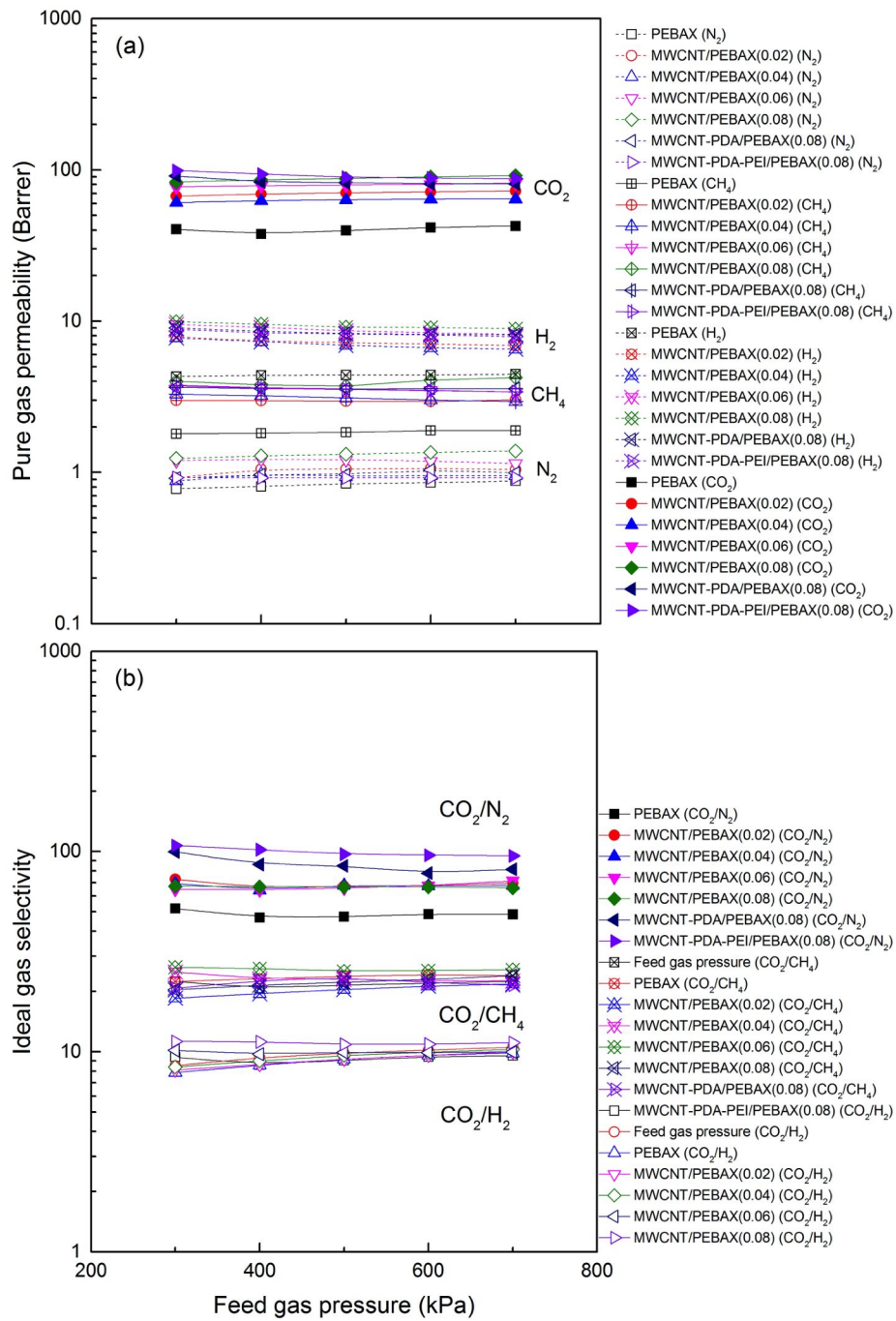
Figure 6.13: Effect of the feed gas pressure on the pure gas permeability (a) and the ideal gas selectivity (b) of the PBEAX/MWCNT(X), MWCNT-PDA/PEBAX(0.08), MWCNT-PDA-PEI/PEBAX(0.08) membranes
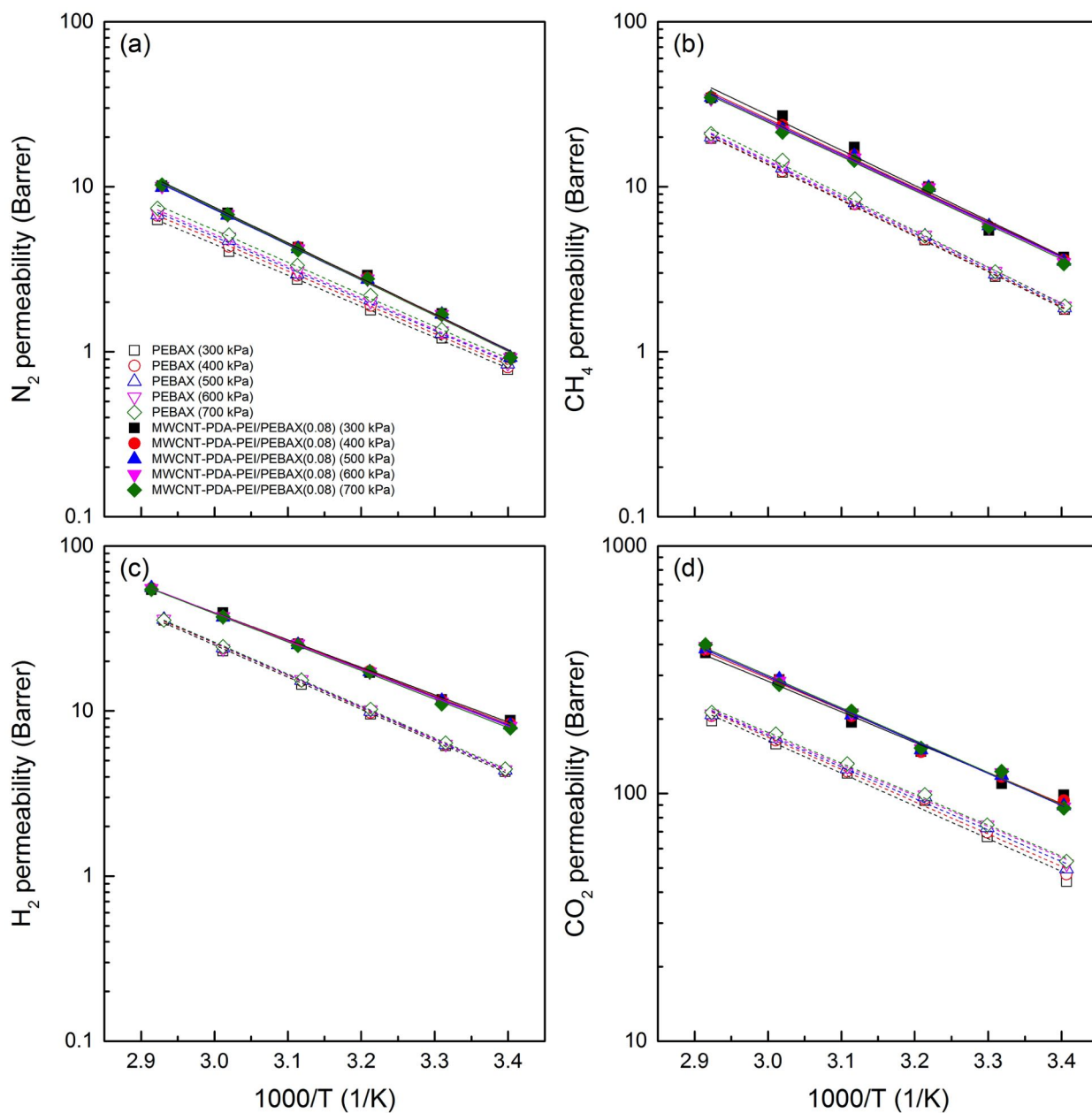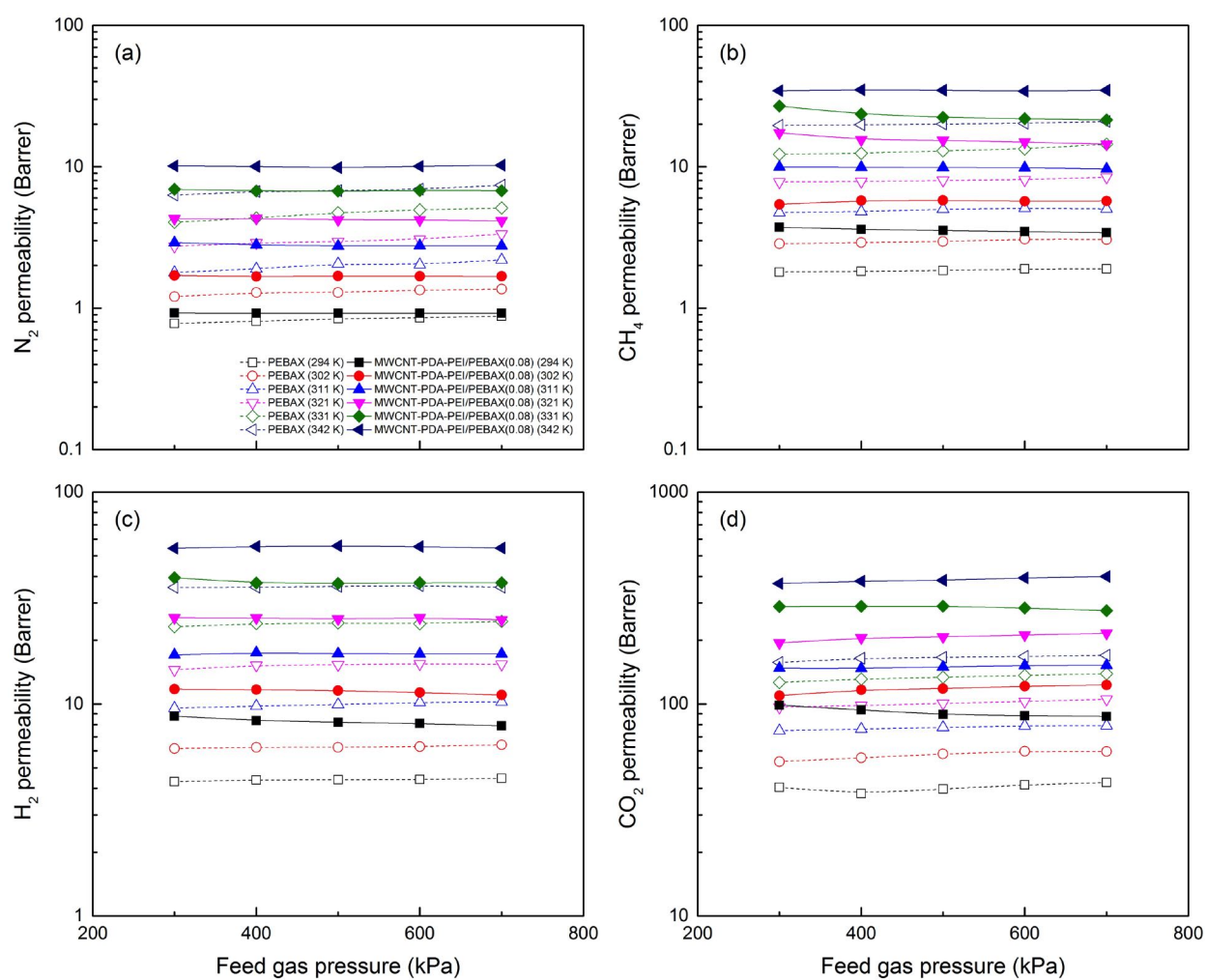
Figure 6.14: Effect of feed gas pressure on the pure gas permeability of N_2 (a), CH_4 (b), H_2 (c) and CO_2 (d) of the PEBAX and MWCNT-PDA-PEI/PEBAX(0.08) membranes at different temperatures
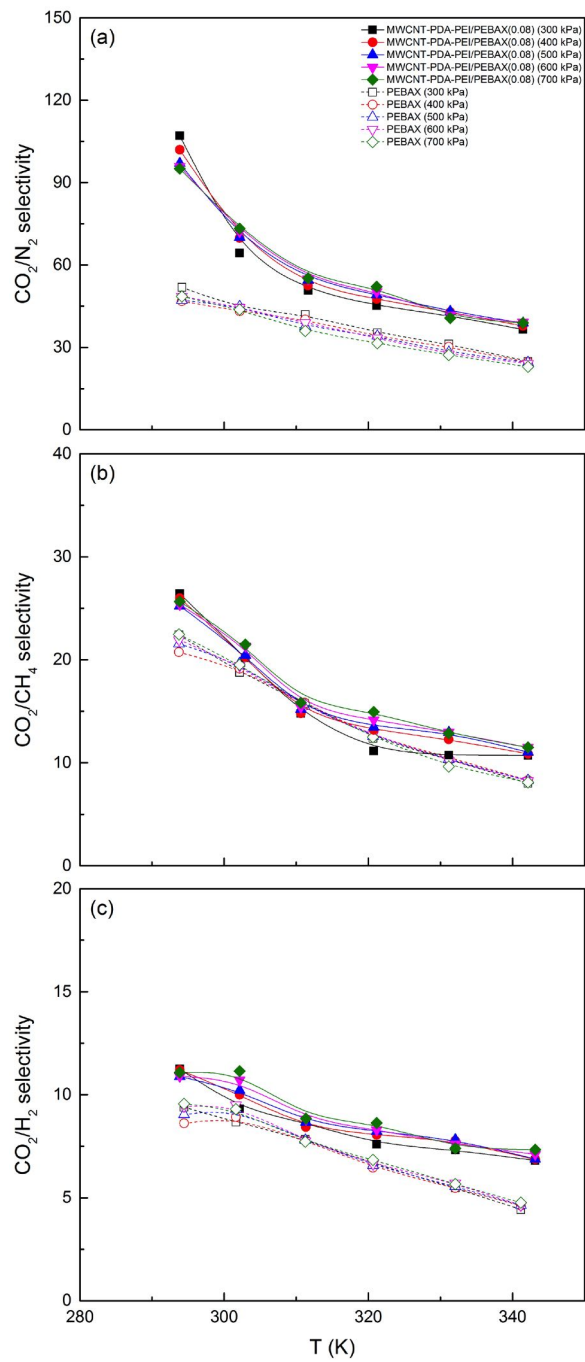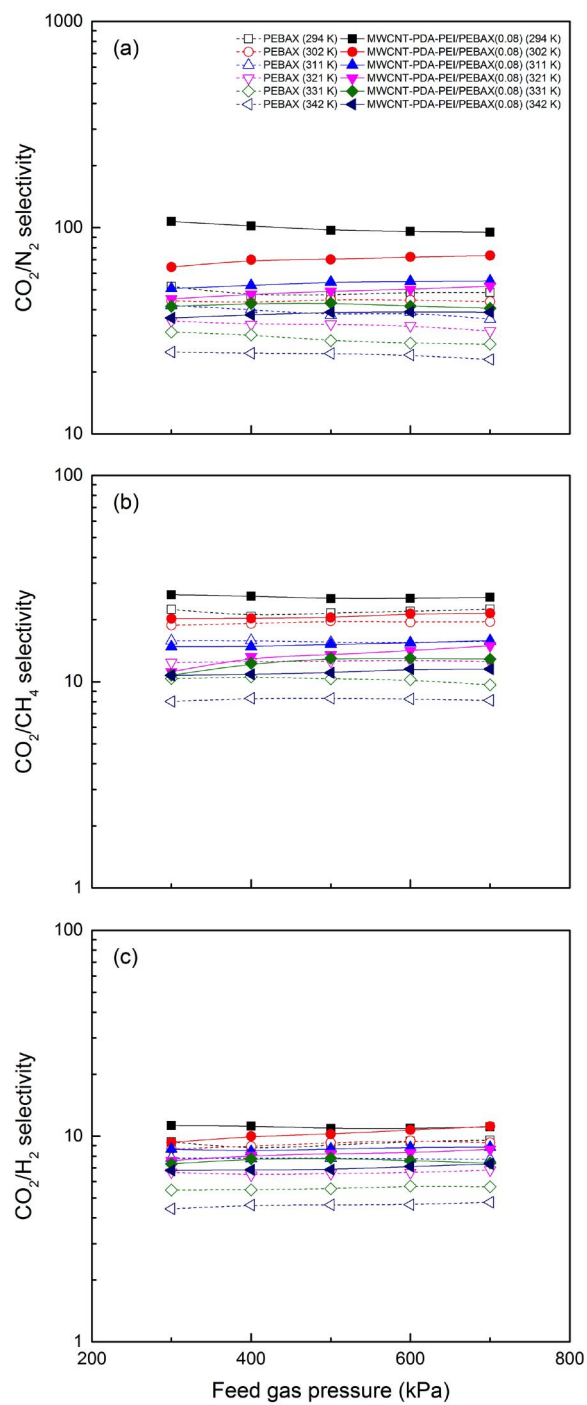
Figure 6.15: Effect of feed gas pressure on the CO_2/N_2 (a), CO_2/CH_4 (b), and CO_2/H_2 (c) selectivity of the PEBAX and MWCNT-PDA-PEI/PEBAX(0.08) membranes at different temperatures

148

6.3.4 Effect of feed gas composition

The MWCNT-PDA-PEI/PEBAX(0.08) membrane was tested for CO_2/N_2, CO_2/CH_4, and CO_2/H_2 separations at room temperature under a feed gas pressure of 300 kPa. CO_2 permeation was more preferential than the permeation of slow gases (N_2, CH_4, and H_2) in the membrane. Thus, as shown in Figure 6.16, the mole factions of CO_2 in permeate gas in CO_2/N_2, CO_2/CH_4, and CO_2/H_2 separations were higher than in feed gas. As demonstrated in Figures 6.17, the partial permeation flux of CO_2 increased, while the partial permeation flux of slow gases decreased as the mole faction of CO_2 in feed gas increased. However, the partial permeation flux of CO_2 was much higher than slow gases, so the total permeation flux (N_{total}) in CO_2/N_2, CO_2/CH_4, and CO_2/H_2 separations increased with an increase in CO_2 content in feed gas.

Since the reactions between CO_2 and amine groups were dependent on the CO_2 concentration, as the mole fraction of CO_2 in feed gas increased, more CO_2 would be dissolved into the membrane resulting in the increase in CO_2 concentration in the membrane. Besides, the CO_2-induced plasticization enhanced CO_2 diffusion. However, the salting-out effect due to the hydration of CO_2 with water and the reactions with amine groups limited CO_2 solubility. Consequently, as shown in Figures 6.18 (a), 6.19 (a), and 6.20 (a), when the mole fraction of CO_2 in the feed gas increased, CO_2 permeability of the MWCNT-PDA-PEI/PEBAX(0.08) membrane in the CO_2/N_2, CO_2/CH_4, and CO_2/H_2 separations increased by 27%, 61%, and 11%, respectively. Moreover, the partial permeation flux of CO_2 in CO_2/CH_4 separation was obviously lower than in CO_2/N_2 and CO_2/H_2 separations, as shown in Figure 6.17 (b). The extent of the increase in CO_2 permeability was different, which was attributed to competitive permeation between two components when they penetrated the membrane. It seemed that gas molecules with larger kinetic diameter impacted CO_2 permeation more obviously.

Similarly, CO_2 permeation affected N_2, CH_4, and H_2 permeation in the membrane as well. Although the solubility of slow gases was lowered owing to the salting-out effect, the gas diffusion was improved by the CO_2-induced plasticization. As a result, N_2, CH_4, and H_2

permeability increased with an increase in the mole fraction of CO_2 in the feed gas (Figures 6.18 (b), 6.19 (b), and 6.20 (b)). Furthermore, the CO_2-induced plasticization allowed smaller gas molecules to permeate the membrane more easily, H_2 permeability increased more than N_2 and CH_4 permeability. As a result, the selectivity of CO_2/N_2 and CO_2/CH_4 of the MWCNT-PDA-PEI/PEBAX(0.08) membrane didn't change as remarkably as the CO_2/H_2 selectivity which decreased by 48.3% when the mole fraction of CO_2 in the feed gas increased, as shown in Figures 6.18 (c), 6.19 (c), and 6.20 (c). Hence, multiple effects including the CO_2-induced plasticization, salting-out effect, and competitive permeation impacted gas permeation in the membrane. All gas selectivity of the MWCNT-PDA-PEI/PEBAX(0.08) membrane was lower than the ideal selectivity for which there were no interactions between gas components.
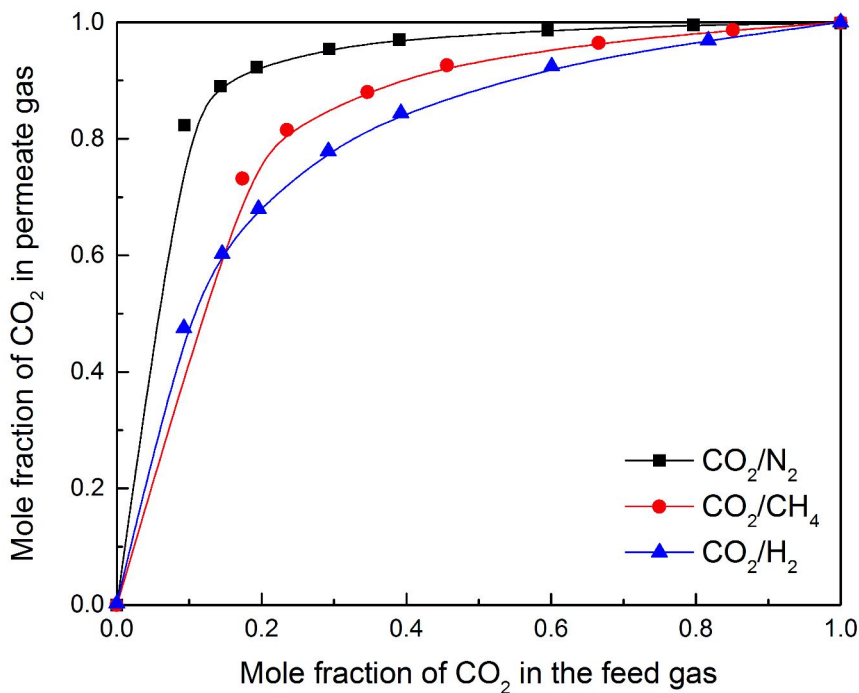
Figure 6.16: Effect of mole fraction of CO_2 in feed gas on mole fraction of CO_2 in permeate gas for CO_2/N_2, CO_2/CH_4, and CO_2/H_2 separations in the MWCNT-PDA-PEI/PEBAX(0.08) membrane
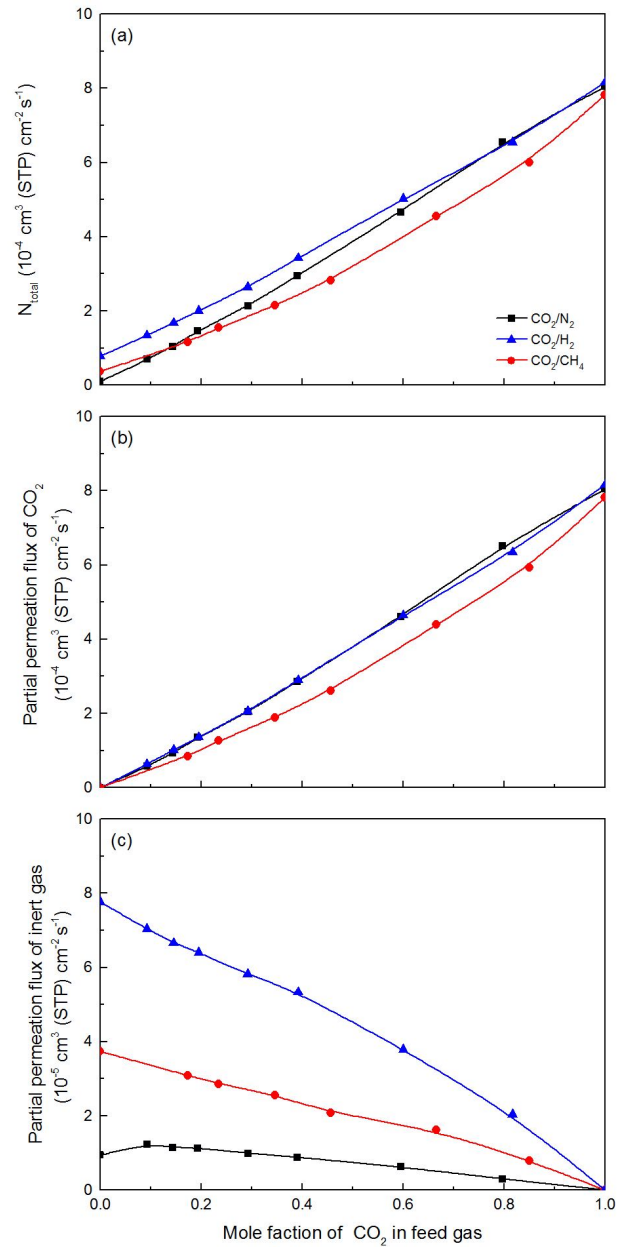
Figure 6.17: Effect of mole fraction of CO_2 in feed gas on total permeation flux (a), partial permeation flux of CO_2 (b), and partial permeation flux of N_2, CH_4, and H_2 (c) for CO_2/N_2, CO_2/CH_4, and CO_2/H_2 separations in the MWCNT-PDA-PEI/PEBAX(0.08) membrane
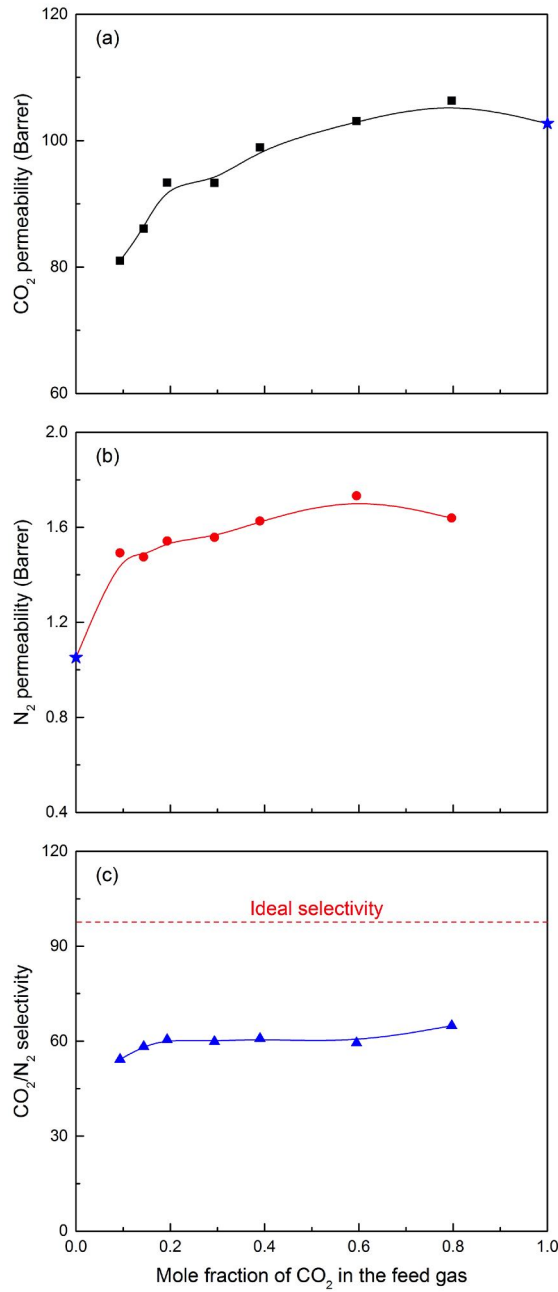
Figure 6.18: Effect of feed gas composition on the CO_2 (a) and N_2 permeability (b) and CO_2/N_2 selectivity (c) of the MWCNT-PDA-PEI/PEBAX(0.08) membrane in CO_2/N_2 gas mixture permeation (The star-shape points represent pure gas permeability and ideal gas selectivity)
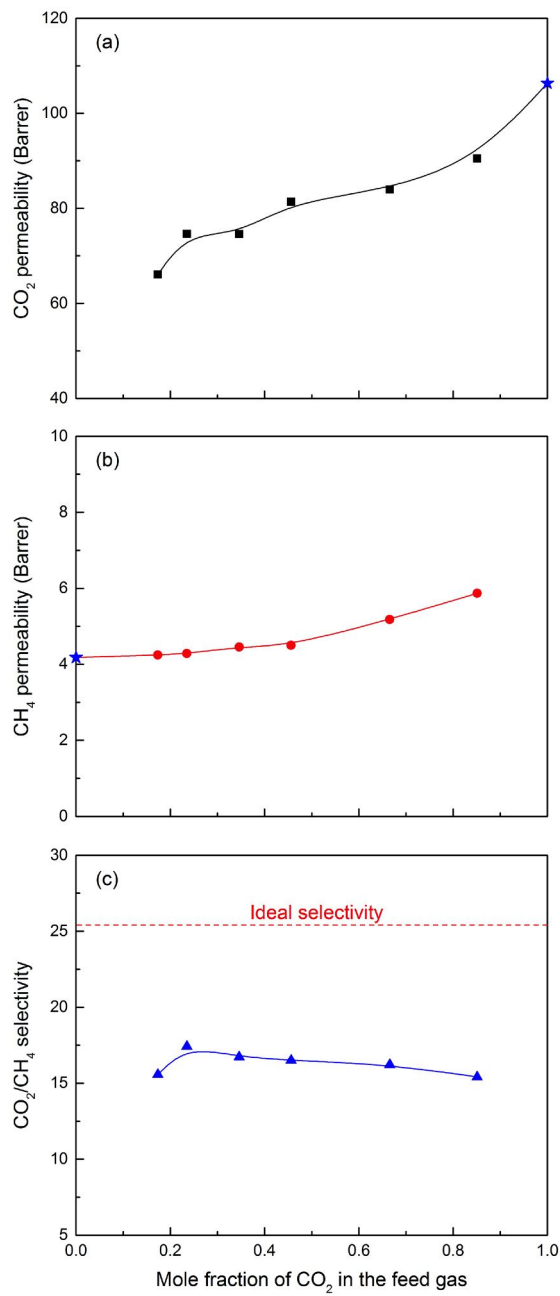
Figure 6.19: Effect of feed gas composition on the CO_2 (a) and CH_4 permeability (b) and CO_2/CH_4 selectivity (c) of the MWCNT-PDA-PEI/PEBAX(0.08) membrane in CO_2/CH_4 gas mixture permeation (The star-shape points represent pure gas permeability and ideal gas selectivity)
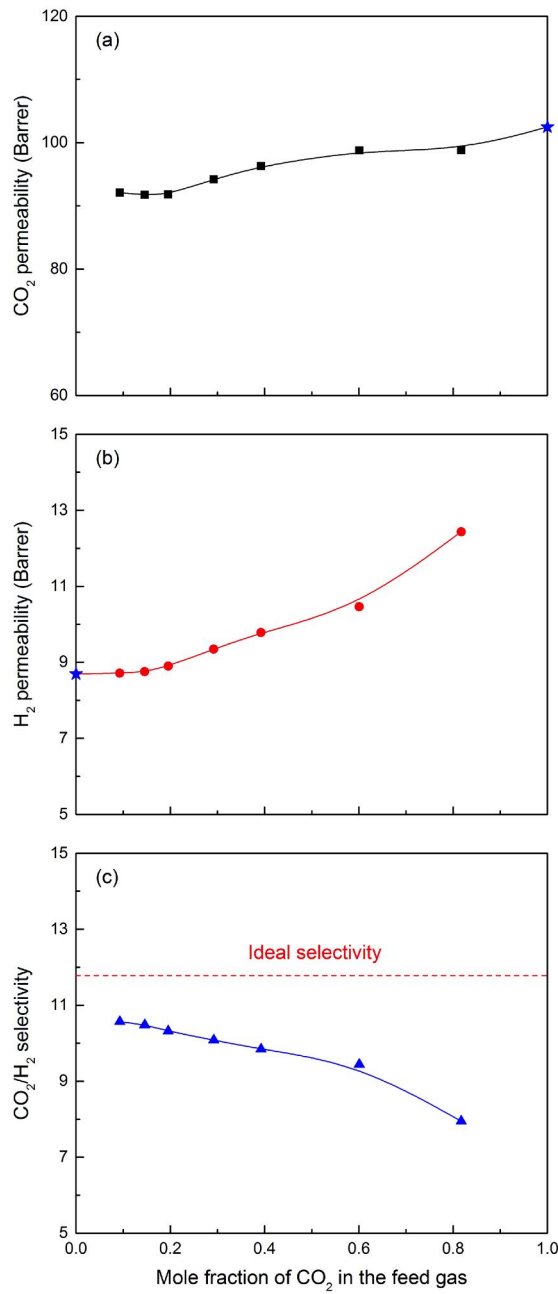
Figure 6.20: Effect of feed gas composition on the CO_2 (a) and H_2 permeability (b) and CO_2/H_2 selectivity (c) of the MWCNT-PDA-PEI/PEBAX(0.08) membrane in CO_2/H_2 gas mixture permeation (The star-shape points represent pure gas permeability and ideal gas selectivity)

154

6.3.5 Membrane stability

The stability of a membrane over a long-term operating period is another aspect which needs to be studied. The MWCNT-PDA-PEI/PEBAX(0.08) membrane was tested for 22 days at room temperature under a feed pressure of 300 kPa in the humid condition. The composition of the feed gas was CO_2/N_2: 14vol%/86vol%, CO_2/CH_4: 35vol%/65vol%, and CO_2/H_2: 40vol%/60vol%. As shown in Figures 6.21, 6.22, and 6.23, there was no significant variation in the gas separation performance of the MWCNT-PDA-PEI/PEBAX(0.08) membrane in the 22-day test. The CO_2 permeability was around 87 Barrer, while the CO_2/N_2 selectivity was 58.6 in CO_2/N_2 separation; the CO_2 permeability was around 74.8 Barrer, while the CO_2/CH_4 selectivity was 16.9 in CO_2/CH_4 separation; the CO_2 permeability was 97 Barrer, while the CO_2/H_2 selectivity was 9.8 in CO_2/H_2 separation.
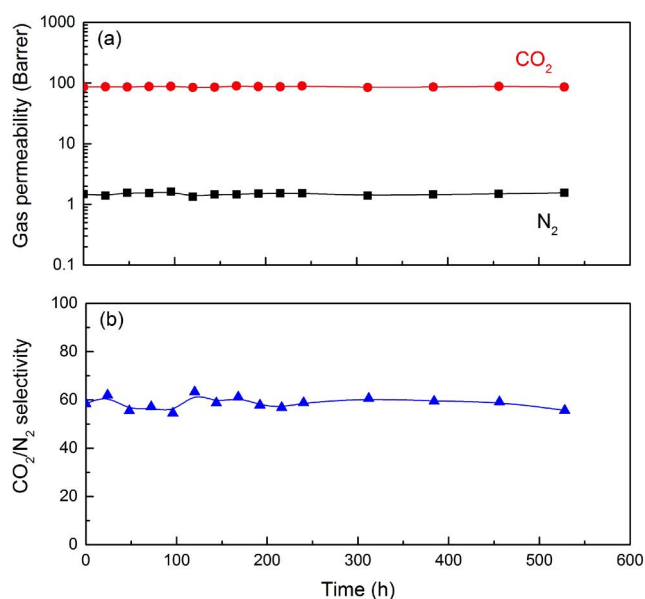
Figure 6.21: Stability of the MWCNT-PDA-PEI/PEBAX(0.08) membrane in CO_2/N_2 separation: CO_2 and N_2 permeability (a) and CO_2/N_2 selectivity (b)
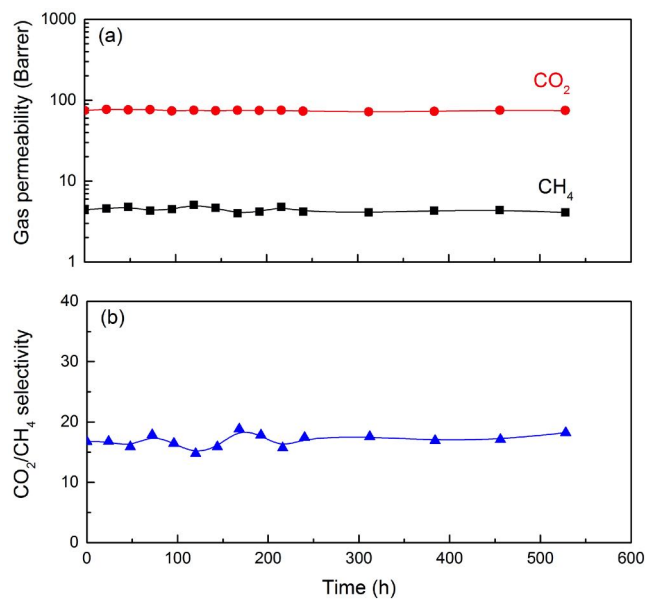
Figure 6.22: Stability of the MWCNT-PDA-PEI/PEBAX(0.08) membrane in CO_2/CH_4 separation: CO_2 and CH_4 permeability (a) and CO_2/CH_4 selectivity (b)
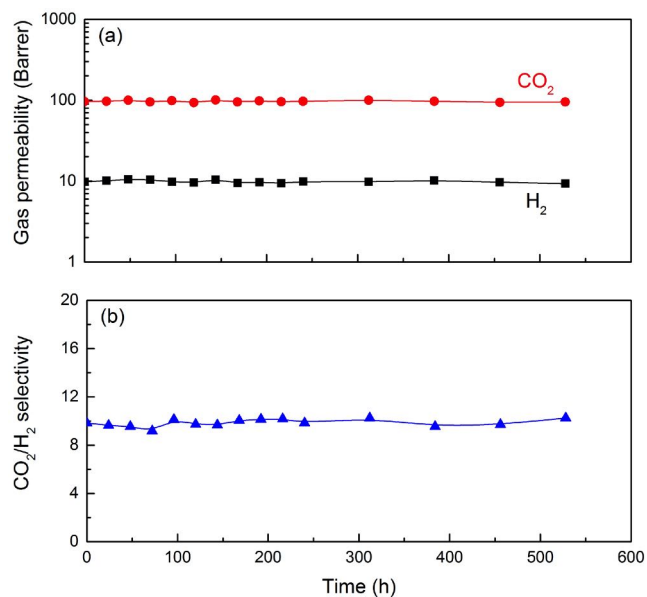
Figure 6.23: Stability of the MWCNT-PDA-PEI/PEBAX(0.08) membrane in CO_2/H_2 separation: CO_2 and H_2 permeability (a) and CO_2/H_2 selectivity (b)

6.4 Conclusions

The MWCNTs were chemically modified by PDA and PEI sequentially to prepare the MWCNT-PDA-PEI particles. Mixed matrix membranes were fabricated using MWCNTs based fillers (acid-treated MWCNTs, MWCNT-PDA, MWCNT-PDA-PEI) and PEBAX as a polymer matrix. The MWCNT-PDA-PEI can not only adjust the membrane structures but also facilitate CO_2 transport. Pure gas permeation for N_2, CH_4, H_2, and CO_2 and gas mixture permeation for CO_2/N_2, CO_2/CH_4, and CO_2/H_2 in the prepared membranes at various conditions were studied. The following conclusions can be drawn:

- The CO_2 permeability of the MWCNT-PDA-PEI/PEBAX(0.08) membrane was 2.4-fold of that of the pristine PEBAX membrane, while CO_2/N_2, CO_2/CH_4, and CO_2/H_2 selectivity increased by 106%, 18%, and 20% at room temperature under a feed gas pressure of 300 kPa in humid conditions, respectively.

- The temperature dependency of gas permeability of both the PEBAX and MWCNT-PDA-PEI/PEBAX(0.08) membranes followed the Arrhenius relation. The gas permeability of both membranes increased with temperature, while the ideal gas selectivity decreased owing to that temperature impacted less significantly on CO_2 permeation than the permeation of N_2, CH_4, and H_2.

- The fabricated MWCNT-PDA-PEI/PEBAX(0.08) membrane showed facilitated transport of CO_2 under low feed gas pressure due to the reaction between CO_2 with amine groups. However, the solution-diffusion mechanism was dominant under high feed gas pressures.

- The gas mixture permeation of the MWCNT-PDA-PEI/PEBAX(0.08) membrane for CO_2/N_2, CO_2/CH_4, and CO_2/H_2 separations was investigated. The gas permeation in the membrane was impacted by the CO_2-induced plasticization, the salting-out effect, and competitive permeation. CH_4 permeation affected CO_2 permeation more obviously than N_2 and H_2 permeation.

- The MWCNT-PDA-PEI/PEBAX(0.08) membrane was tested for CO_2/N_2, CO_2/CH_4, and CO_2/H_2 separations, and the membrane performance was stable at room temperature under a feed pressure of 300 kPa during a 22-day test.

Chapter 7

General Conclusions, Contributions and Recommendations

7.1 General conclusions

PEBAX-based membranes for CO_2/N_2, CO_2/CH_4, and CO_2/H_2 separations were prepared and studied. Different strategies were applied in order to improve the permselectivity of the pristine PEBAX membranes. The following conclusions can be drawn from this research and contributions to original research are as follows:

7.1.1 Improvement of CO_2 permeability in the water-swollen membranes

1. The water-swollen PVAm/PEBAX blend membranes were fabricated by a solution casting method. The hydrophilicity of membranes was enhanced due to the addition of PVAm. Owing to the increase of CO_2 solubility in the membranes, the fabricated PVAm/PEBAX(0.025) blend membrane showed a CO_2 permeability of 600 Barrer and CO_2/N_2, CO_2/CH_4 and CO_2/H_2 selectivity of 52.0, 26.9, and 14.9 at 298 K and 400 kPa.

The temperature dependence of CO_2, N_2, CH_4, and H_2 permeability appeared to follow Arrhenius equation. The feed gas pressure barely impacted the permselectivity of all prepared membranes in the test range of 400-800 kPa. The mixture gas permeation performance of the PVAm/PEBAX(0.025) blend membrane was studied. Due to the CO_2-induced plasticization effect, N_2, CH_4, and H_2 permeability increased when the mole fraction of CO_2 in the feed gas increased. The CO_2/N_2, CO_2/CH_4 and CO_2/H_2 selectivities were lower than their ideal gas selectivities. During the membrane stability test, when the PVAm/PEBAX(0.025) blend membrane became less hydrated, the CO_2 permeability decreased obviously. However, when the membrane was humidified again, the permselectivity was recovered.

2. The DEA/PVAm/PEBAX composite membranes were fabricated on polysulfone substrates. Instead of increasing the PVAm content in membranes, small molecule amines, DEA, were added in the membranes, which was beneficial for increasing CO_2 solubility. The DEA/PVAm/PEBAX composite membrane showed a CO_2 permeance of 12.53 GPU, while the while CO_2/N_2, CO_2/CH_4, CO_2/H_2 selectivity maintained the same as the PEBAX composite membranes at room temperature and a feed gas pressure of 700 kPa.

The pure gas permeance of CO_2, N_2, CH_4, and H_2 and the CO_2/N_2, CO_2/CH_4, CO_2/H_2 ideal selectivity of the PEBAX, PVAm/PEBAX, and DEA/PVAm/PEBAX composite membranes were affected by temperature. The gas permeance increased, while gas selectivity decreased at higher temperatures. The temperature dependence of CO_2, N_2, CH_4, and H_2 permeance can be fitted by an Arrhenius type expression. The activation energy for gas permeation in the DEA/PVAm/PEBAX composite membrane was higher than in the PVAm/PEBAX composite membranes. The feed gas pressure hardly affected the pure gas permeance in the PEBAX and PVAm/PEBAX composite membranes. However, the pure gas permeance of the DEA/PVAm/PEBAX composite membrane increased with elevated feed gas pressure. The prepared PVAm/PEBAX and DEA/PVAm/PEBAX composite membranes didn't show the facilitated transport of CO_2. The solution-diffusion mechanism

160

dominated the permeation process in these membranes. The CO_2-induced plasticization, the salting-out effect, and competitive permeation affected mixture gas permeation performance in the DEA/PVAm/PEBAX composite membrane. The DEA/PVAm/PEBAX composite membrane was stable and exhibited no dramatic reduction of mixture gas permeation performance during 19 days at room temperature and a feed gas pressure of 700 kPa in humid conditions.

7.1.2 Improvement of gas selectivity by enhancing the salting-out effect

The NH_4F/PEBAX membranes were prepared for CO_2/N_2, CO_2/CH_4, and CO_2/H_2 separation by a solution casting method. The effects of membrane composition on pure gas permeation performance were studied. The NH_4F/PEABX(0.1) membrane showed the lowest N_2, CH_4, and H_2 permeability (5.04, 13.5, and 23.2 Barrer) and CO_2 permeability (372 Barrer) remained comparable in the test range. Hence, the CO_2/N_2, CO_2/CH_4, and CO_2/H_2 ideal selectivity were 73.9, 27.6, and 16.0 at room temperature under a feed gas pressure of 700 kPa. The influence of the salting-out effect on N_2, CH_4, and H_2 permeation was more significant than CO_2 permeation. The NH_4F/PEABX(0.1) membrane was in favor of CO_2 dissolution resulting from the strong interaction between F^- and H_2O.

As the operating temperature increased, the permeabilities of CO_2, N_2, CH_4, and H_2 in the PEBAX and NH_4F/PEBAX(0.1) membranes increased, while the ideal gas selectivity of CO_2/N_2, CO_2/CH_4, and CO_2/H_2 decreased. Nonetheless, the NH_4F/PEBAX(0.1) membrane had better ideal gas selectivity than the pristine PEBAX membrane. The activation energy for gas permeation in the NH_4F/PEBAX(0.1) membrane was lower than in the PEBAX membrane resulting from the salting-out effect and the enhancement of hydrophilicity. The effect of feed gas pressure on the pure gas permeability and the ideal gas selectivity of all prepared NH_4F/PEBAX(X) membranes was negligible in the test range from 300 to 700 kPa. The solution-diffusion mechanism made more contributions to the permeation process instead of the facilitated of CO_2. The mixture gas

permeation in the $NH_4F/PEBAX(0.1)$ membrane was studied. The CO_2-induced plasticization affected H_2 permeation more significantly than the permeation of CH_4 and N_2 so that CO_2/H_2 selectivity decreased from 13.1 to 6.3. At a given composition of the feed gas, the permselectivity of the membrane did not show significant variation with an increase in feed gas pressure from 300 to 700 kPa. During an 18-day stability test, the $NH_4F/PEBAX(0.1)$ membrane was shown to be stable for CO_2/CH_4, CO_2/N_2 and CO_2/H_2 separations.

7.1.3 Improvement of gas permselectivity by facilitated transport of CO_2

Mixed matrix membranes were fabricated by embedding the MWCNT-based fillers (acid-treated MWCNTs, MWCNT-PDA, MWCNT-PDA-PEI) into PEBAX polymer matrix. MWCNT-PDA-PEI can not only impact polymer chain distribution but also facilitate CO_2 transport in the membranes. With a mass ratio of MWCNT-PDA-PEI to PEABX of 0.08, CO_2 permeability of the MWCNT-PDA-PEI/PEBAX(0.08) membrane increased by 144%, while CO_2/N_2, CO_2/CH_4, and CO_2/H_2 selectivity was 106%, 18%, and 20% higher than pristine PEBAX membrane at room temperature under a feed gas pressure of 300 kPa in humid conditions.

The temperature dependence of gas permeability of both the PEBAX and MWCNT-PDA-PEI/PEBAX(0.08) membranes could be fitted by an Arrhenius type expression. The activation energy for N_2 permeation in the MWCNT-PDA-PEI/PEBAX(0.08) membrane was higher than that in the PEBAX membrane, which indicated that the energy barrier for N_2 permeation to overcome was higher. The effects of feed gas pressure on pure gas permeation were studied. The facilitated transport of CO_2 due to the reaction between CO_2 with amine groups was exhibited in the MWCNT-PDA-PEI/PEBAX(0.08) membrane under low pressures. At higher CO_2 pressures, CO_2 carriers were gradually occupied and consumed. Thus, the solution-diffusion mechanism prevailed and the feed gas pressure affected pure gas permeability slightly under high pressures. In the separation of CO_2/N_2, CO_2/CH_4, and CO_2/H_2 by the MWCNT-PDA-PEI/PEBAX(0.08) membrane, the permeation of one component would affect that of the other component resulting

162

from the CO_2-induced plasticization, salting-out effect, and competitive permeation. No significant variation in the separation performance of the MWCNT-PDA-PEI/PEBAX(0.08) membrane was observed at room temperature and 300 kPa during a 22-day test.

7.1.4   Comparison with Robeson's upper bound

The CO_2/N_2 permeation performance of some typical membranes was compared with Robeson's upper bound (2008). Two water-swollen membranes including the PVAm/PEBAX(0.025) membrane and the DEA/PVAm/PEBAX composite membranes tended to increase the CO_2 permeability due to enhancement of membrane hydrophilicity. Although the structures of membranes became loose because of water, the two membranes maintain a comparable CO_2/N_2 selectivity with the PEBAX membrane. Hence, the improvement of membrane hydrophilicity is beneficial for increasing gas permeability rather than selectivity. Compared with four membranes, water-swollen membranes with the addition of PVAm and DEA showed better gas permeability. The salting-out effect derived from the addition of NH_4F can decreased the N_2, CH_4, and H_2 permeability of the NH_4F/PEBAX(0.1) membrane. The CO_2 permeability increased since the interaction between H_2O and F^- made water become more basic. The facilitated transport of CO_2 owing to the reaction between CO_2 and NH_2 on MWCNT-PDA-PEI improved CO_2/N_2 selectivity of the MWCNT-PDA-PEI/PEBAX(0.08) membrane as compared to the PEBAX membrane (Chapter 6). Except for the PEBAX membranes, the PVAm/PEBAX(0.025), DEA/PVAm/PEBAX composite, NH_4F/PEBAX(0.1), and MWCNT-PDA-PEI/PEBAX(0.08) membranes for CO_2/N_2 permeation exceeded Robeson's upper bound (2008). Compared with water-swollen membranes with polymeric and small molecule amines, the NH_4F/PEBAX(0.1) and MWCNT-PDA-PEI/PEBAX(0.08) membranes exhibited better gas selectivity.

The CO_2/CH_4 permeation performance of the PEBAX membrane, the PVAm/PEBAX(0.025) blend membrane, the DEA/PVAm/PEBAX composite membrane, and the NH_4F/PEBAX(0.1) membrane only broke Robeson's upper bound (1991). The CO_2/H_2 permeation performance of all

prepared membranes broke Robeson's upper bound (2008). Compared with the pristine PEBAX membranes, the CO_2/CH_4 and CO_2/H_2 selectivity increased less than the CO_2/N_2 selectivity. The PVAm/PEBAX(0.025), the DEA/PVAm/PEBAX composite, the NH_4F/PEBAX(0.1), and the MWCNT-PDA-PEI/PEBAX(0.08) membranes were more suitable for CO_2/N_2 separation. As for CO_2/CH_4 and CO_2/H_2 separations, these membranes had higher CO_2 permeability and kept the CO_2/CH_4 and CO_2/H_2 comparable with the pristine PEBAX membranes.

7.2   Contributions to original research

Four types of PEBAX-based composite membranes were prepared in this thesis research. With the addition of polymeric amines (PVAm) and small molecule amines (DEA), PVAm/PBEAX blend membranes and DEA/PVAm/PEBAX composite membranes were prepared to increase gas permeability. The polymer electrolyte membranes with the blend of NH4F were fabricated to enhance the gas selectivity. Amine modified MWCNTs (MWCNT-PDA-PEI) and PEBAX were used to prepare mixed matrix membranes to improve both gas permeability and selectivity. All prepared membranes were tested for CO_2/N_2, CO_2/CH_4, and CO_2/H_2 separations.

7.3   Recommendations for future work

7.3.1   Investigation of gas diffusivity and solubility of in the membranes

Different kinds of additives (PVAm, DEA, NH_4F, and MWCNT-PDA-PEI) were blended into the membranes to improve different aspects of membranes. They can adjust membrane structures and affect the gas permeation. The effects of the addition of these additives on gas permeability were studied in this thesis research. The solution-diffusion mechanism was used to describe the gas permeation in the membranes prepared in this study:

$$P = DS \qquad (2.10)$$

Since the variations of gas permeability were from the variations of diffusivity and solubility, the effects of the addition of these additives on diffusivity and solubility under various temperatures and pressures need to be further investigated. The diffusivity coefficient can be measured by a time-lag method [Liu et al. (2008)]. Since the gas permeability was obtained in this thesis research, the solubility coefficient can be calculated by Equation 2.10. It would provide more details about the influence of the additives on membrane structures and gas permeation performance and can help determine the materials of polymer and additives for different separation systems.

7.3.2 Improvement of gas selectivity of water-swollen membranes

The PVAm/PEBAX blend membranes and the DEA/PVAm/PEBAX composite membranes showed good CO_2 permeability or permeance, while there was little improvement in the CO_2/N_2, CO_2/CH_4, and CO_2/H_2 selectivity, which was attributed to the membrane swelling. The solution-diffusion mechanism dominated the permeation process. The crosslinking the membranes can effectively make the membrane structures more compacted. The crosslinking agents include glutaraldehyde, NH_4F, and acid [Kim et al. (2004)]. It is suggested to study the effects of crosslinking on the gas permeation performance of the membranes. The gas selectivity is expected to be improved by adjusting membrane structures.

7.3.3 Development of polymer electrolyte membranes with different salts

The NH_4F/PEBAX(0.1) can improve the CO_2/N_2, CO_2/CH_4, and CO_2/H_2 selectivity, but the CO_2 permeability didn't increase remarkably. The interaction between F^- and H_2O can make water more basic resulting in increased CO_2 solubility. F^- has the highest electronegativity among all halogens [Zhang and Wang (2012)]. However, the choices of cations of the salts need to be studied. Alkali metal salts (Li^+, Na^+, K^+), alkaline-earth metal salts (Mg^{2+}, Ca^{2+}), and transition metal salts (Zn^{2+}, Ag^+) should be taken into consideration. Especially for K^+ and Zn^{2+}, they exhibited facilitated transport of CO_2 in some membranes [Li and Chung (2008); Oh et al.

165

(2013)]. The combination of the advantages of cations and anions could surpass the Robeson's upper bound. The further development and study of polymer electrolyte membranes are needed to achieve both high permeability and selectivity.

7.3.4 Development of hollow fiber membranes with PEBAX and MWCNT-PDA-PEI

MWCNT-PDA-PEI/PEBAX(0.08) MMMs showed excellent permselectivity for CO_2/N_2, CO_2/CH_4, and CO_2/H_2 permeation. The acid treatment of MWCNTs in this study followed the procedures from literature [Hu (2013)]. However, acid types, treatment time, and treatment temperature can affect the surface morphology of MWCNTs, so it needs to be further studied [Mazov et al. (2012)]. Moreover, the flat symmetric membranes were prepared by a solution casting method. In industrial applications, membranes are usually packed into a module including plate and frame module, spiral wound module, and hollow fiber module. Hollow fiber module has a higher packing density and can withstand high pressures. For practical applications of the MWCNT-PDA-PEI/PEBAX MMMs, hollow fiber membranes need to be developed by dip coating the solution on a hollow fiber substrate. The thin surface layer of MWCNT-PDA-PEI/PEBAX can achieve high gas permeance, but the defects should be eliminated. Therefore, the effects of coating solution concentration and coating times on the gas permeation performance need to be studied.

References

Ansaloni, L., Zhao, Y. N., Jung, B. T., Ramasubramanian, K., Baschetti, M. G., and Ho, W. S. W. (2015). Facilitated transport membranes containing amino-functionalized multi-walled carbon nanotubes for high-pressure CO_2 separations. *Journal of Membrane Science*, 490:18–28.

Azizi, N., Mohammadi, T., and Behbahani, R. M. (2017). Synthesis of a new nanocomposite membrane (PEBAX-1074/PEG-400/TiO_2) in order to separate CO_2 from CH_4. *Journal of Natural Gas Science and Engineering*, 37:39–51.

Bachu, S. (2008). CO_2 storage in geological media: Role, means, status and barriers to deployment. *Progress in Energy and Combustion Science*, 34(2):254–273.

Baker, R. W. (2002). Future directions of membrane gas separation technology. *Industrial & Engineering Chemistry Research*, 41(6):1393–1411.

Baker, R. W. (2012). *Membrane Technology and Applications*. John Wiley & Sons Ltd., Chichester, West Sussex, United Kingdom, 3rd edition.

Basu, S., Cano-Odena, A., and Vankelecom, I. F. J. (2011). MOF-containing mixed-matrix membranes for CO_2/CH_4 and CO_2/N_2 binary gas mixture separations. *Separation and Purification Technology*, 81(1):31–40.

Berean, K., Ou, J. Z., Nour, M., Latham, K., McSweeney, C., Paull, D., Halim, A., Kentish, S., Doherty, C. M., Hill, A. J., and Kalantar-zadeh, K. (2014). The effect of crosslinking

temperature on the permeability of PDMS membranes: Evidence of extraordinary CO_2 and CH_4 gas permeation. *Separation and Purification Technology*, 122:96–104.

Bernardo, P., Drioli, E., and Golemme, G. (2009). Membrane gas separation: A review/state of the art. *Industrial & Engineering Chemistry Research*, 48(10):4638–4663.

Bernardo, P., Jansen, J. C., Bazzarelli, F., Tasselli, F., Fuoco, A., Friess, K., Izak, P., Jarmarova, V., Kacirkova, M., and Clarizia, G. (2012). Gas transport properties of PEBAX®/room temperature ionic liquid gel membranes. *Separation and Purification Technology*, 97:73–82.

Biswal, B. P., Chaudhari, H. D., Banerjee, R., and Kharul, U. K. (2016). Chemically stable covalent organic framework (COF)-polybenzimidazole hybrid membranes: Enhanced gas separation through pore modulation. *Chemistry*, 22(14):4695–4699.

Bondar, V. I., Freeman, B. D., and Pinnau, I. (2000). Gas transport properties of poly(ether-b-amide) segmented block copolymers. *Journal of Polymer Science Part B-Polymer Physics*, 38(15):2051–2062.

Caplow, M. (1968). Kinetics of carbamate formation and breakdown. *Journal of the American Chemical Society*, 90(24):6795–6803.

Car, A., Stropnik, C., Yave, W., and Peinemann, K.-V. (2008a). PEBAX®/polyethylene glycol blend thin film composite membranes for CO_2 separation: Performance with mixed gases. *Separation and Purification Technology*, 62(1):110–117.

Car, A., Stropnik, C., Yave, W., and Peinemann, K. V. (2008b). PEG modified poly(amide-b-ethylene oxide) membranes for CO_2 separation. *Journal of Membrane Science*, 307(1):88–95.

Chatterjee, G., Houde, A. A., and Stern, S. A. (1997). Poly(ether urethane) and poly(ether

urethane urea) membranes with high H_2S/CH_4 selectivity. *Journal of Membrane Science*, 135(1):99–106.

Chen, J. C., Feng, X. S., and Penlidis, A. (2004). Gas permeation through poly(ether-b-amide) (PEBAX 2533) block copolymer membranes. *Separation Science and Technology*, 39(1):149–164.

Chen, S. L., Zhou, T. T., Wu, H., Wu, Y. Z., and Jiang, Z. Y. (2017). Embedding molecular amine functionalized polydopamine submicroparticles into polymeric membrane for carbon capture. *Industrial & Engineering Chemistry Research*, 56(28):8103–8110.

Choi, S., Drese, J. H., and Jones, C. W. (2009). Adsorbent materials for carbon dioxide capture from large anthropogenic point sources. *ChemSusChem*, 2(9):796–854.

Chung, T. S., Jiang, L. Y., Li, Y., and Kulprathipanja, S. (2007). Mixed matrix membranes (MMMs) comprising organic polymers with dispersed inorganic fillers for gas separation. *Progress in Polymer Science*, 32(4):483–507.

Cong, H. L., Zhang, J. M., Radosz, M., and Shen, Y. Q. (2007). Carbon nanotube composite membranes of brominated poly(2,6-diphenyl-1,4-phenylene oxide) for gas separation. *Journal of Membrane Science*, 294(1-2):178–185.

Dai, Y., Ruan, X. H., Yan, Z. J., Yang, K., Yu, M., Li, H., Zhao, W., and He, G. H. (2016a). Imidazole functionalized graphene oxide/PEBAX mixed matrix membranes for efficient CO_2 capture. *Separation and Purification Technology*, 166:171–180.

Dai, Z. D., Bai, L., Hval, K. N., Zhang, X. P., Zhang, S. J., and Deng, L. Y. (2016b). PEBAX®/TSIL blend thin film composite membranes for CO_2 separation. *Science China-Chemistry*, 59(5):538–546.

D'Alessandro, D. M., Smit, B., and Long, J. R. (2010). Carbon dioxide capture: prospects for new materials. *Angew Chem Int Ed Engl*, 49(35):6058–6082.

169

Dechnik, J., Gascon, J., Doonan, C. J., Janiak, C., and Sumby, C. J. (2017). Mixed-matrix membranes. *Angew Chem Int Ed Engl*, 56(32):9292–9310.

Deng, L. Y. and Hagg, M. B. (2010). Swelling behavior and gas permeation performance of PVAm/PVA blend fsc membrane. *Journal of Membrane Science*, 363(1-2):295–301.

Deng, L. Y., Kim, T. J., and Hagg, M. B. (2009). Facilitated transport of CO_2 in novel PVAm/PVA blend membrane. *Journal of Membrane Science*, 340(1-2):154–163.

Descamps, C., Bouallou, C., and Kanniche, M. (2008). Efficiency of an integrated gasification combined cycle (IGCC) power plant including CO_2 removal. *Energy*, 33(6):874–881.

Donaldson, T. L. and Nguyen, Y. N. (1980). Carbon-dioxide reaction-kinetics and transport in aqueous amine membranes. *Industrial & Engineering Chemistry Fundamentals*, 19(3):260–266.

Du, N. Y., Park, H. B., Dal-Cin, M. M., and Guiver, M. D. (2012). Advances in high permeability polymeric membrane materials for CO_2 separations. *Energy & Environmental Science*, 5(6):7306–7322.

Ehsani, A. and Pakizeh, M. (2016). Synthesis, characterization and gas permeation study of ZIF-11/PEBAX® 2533 mixed matrix membranes. *Journal of the Taiwan Institute of Chemical Engineers*, 66:414–423.

Erucar, I., Yilmaz, G., and Keskin, S. (2013). Recent advances in metal-organic framework-based mixed matrix membranes. *Chem Asian J*, 8(8):1692–1704.

Fam, W., Mansouri, J., Li, H. Y., and Chen, V. (2017). Improving CO_2 separation performance of thin film composite hollow fiber with PEBAX® 1657/ionic liquid gel membranes. *Journal of Membrane Science*, 537:54–68.

Figueroa, J. D., Fout, T., Plasynski, S., McIlvried, H., and Srivastava, R. D. (2008). Advances in CO_2 capture technology-the U.S. Department of Energy's Carbon Sequestration Program. *International Journal of Greenhouse Gas Control*, 2(1):9–20.

Firpo, G., Angeli, E., Repetto, L., and Valbusa, U. (2015). Permeability thickness dependence of polydimethylsiloxane (PDMS) membranes. *Journal of Membrane Science*, 481:1–8.

Francisco, G. J., Chakma, A., and Feng, X. S. (2007). Membranes comprising of alkanolamines incorporated into poly(vinyl alcohol) matrix for CO_2/N_2 separation. *Journal of Membrane Science*, 303(1-2):54–63.

Francisco, G. J., Chakma, A., and Feng, X. S. (2010). Separation of carbon dioxide from nitrogen using diethanolamine-impregnated poly(vinyl alcohol) membranes. *Separation and Purification Technology*, 71(2):205–213.

Habibiannejad, S. A., Aroujalian, A., and Raisi, A. (2016). PEBAX-1657 mixed matrix membrane containing surface modified multi-walled carbon nanotubes for gas separation. *Rsc Advances*, 6(83):79563–79577.

Hu, S. Y., Zhang, Y. F., Lawless, D., and Feng, X. S. (2012). Composite membranes comprising of polyvinylamine-poly(vinyl alcohol) incorporated with carbon nanotubes for dehydration of ethylene glycol by pervaporation. *Journal of Membrane Science*, 417:34–44.

Hu, Y. (2013). *PVAm-PVA Composite Membranes Incorporated with Carbon Nanotubes and Molecular Amines for Gas Separation and Pervaporation*. University of Waterloo, Waterloo, Ontario, Canada.

Huang, J., Zou, J., and Ho, W. S. W. (2008). Carbon dioxide capture using a CO_2-selective facilitated transport membrane. *Industrial & Engineering Chemistry Research*, 47(4):1261–1267.

Husain, S. and Koros, W. J. (2007). Mixed matrix hollow fiber membranes made with modified HSSZ-13 zeolite in polyetherimide polymer matrix for gas separation. *Journal of Membrane Science*, 288(1-2):195–207.

Ismail, A. F., Hashemifard, S. A., and Matsuura, T. (2011). Facilitated transport effect of ag+ ion exchanged halloysite nanotubes on the performance of polyetherimide mixed matrix membrane for gas separation. *Journal of Membrane Science*, 379(1-2):378–385.

Jeon, Y. W. and Lee, D. H. (2015). Gas membranes for CO_2/CH_4 (biogas) separation: A review. *Environmental Engineering Science*, 32(2):71–85.

Ji, P. F., Cao, Y. M., Jie, X. M., and Yuan, Q. A. (2010). Fabrication of polymer/fluoride-containing salts blend composite membranes for CO_2 separation. *Journal of Natural Gas Chemistry*, 19(6):560–566.

Kang, Z. X., Peng, Y. W., Qian, Y. H., Yuan, D. Q., Addicoat, M. A., Heine, T., Hu, Z. G., Tee, L., Guo, Z. G., and Zhao, D. (2016). Mixed matrix membranes (MMMs) comprising exfoliated 2D covalent organic frameworks (COFs) for efficient CO_2 separation. *Chemistry of Materials*, 28(5):1277–1285.

Kawakami, M., Iwanaga, H., Hara, Y., Iwamoto, M., and Kagawa, S. (1982). Gas permeabilities of cellulose nitrate poly(ethylene glycol) blend membranes. *Journal of Applied Polymer Science*, 27(7):2387–2393.

Kentish, S., Scholes, C., and Stevens, G. (2008). Carbon dioxide separation through polymeric membrane systems for flue gas applications. *Recent Patents on Chemical Engineeringe*, 1(1):52–66.

Kim, J. H., Ha, S. Y., and Lee, Y. M. (2001). Gas permeation of poly(amide-6-b-ethylene oxide) copolymer. *Journal of Membrane Science*, 190(2):179–193.

172

Kim, S., Chen, L., Johnson, J. K., and Marand, E. (2007). Polysulfone and functionalized carbon nanotube mixed matrix membranes for gas separation: Theory and experiment. *Journal of Membrane Science*, 294(1-2):147–158.

Kim, T. J., Li, B. A., and Hagg, M. B. (2004). Novel fixed-site-carrier polyvinylamine membrane for carbon dioxide capture. *Journal of Polymer Science Part B-Polymer Physics*, 42(23):4326–4336.

Kollman, P. and Kuntz, I. (1976). Hydration of ammonium fluoride. *Journal of the American Chemical Society*, 98(22):6820–6825.

Koros, W. J. and Fleming, G. K. (1993). Membrane-based gas separation. *Journal of Membrane Science*, 83(1):1–80.

Kunze, C. and Spliethoff, H. (2012). Assessment of oxy-fuel, pre- and post-combustion-based carbon capture for future IGCC plants. *Applied Energy*, 94:109–116.

Lee, J. H., Hong, J., Kim, J. H., Kang, Y. S., and Kang, S. W. (2012). Facilitated CO_2 transport membranes utilizing positively polarized copper nanoparticles. *Chem Commun*, 48(43):5298–5300.

Lewis, J. (2018). Gas separation membranes: Polymeric and inorganic by af ismail, kc khulbe, and t. matsuura. *Chemical Engineering Education*, 52(3):223.

Li, S., Wang, Z., Yu, X., Wang, J., and Wang, S. (2012). High-performance membranes with multi-permselectivity for CO_2 separation. *Adv Mater*, 24(24):3196–3200.

Li, T., Pan, Y. C., Peinemann, K. V., and Lai, Z. P. (2013). Carbon dioxide selective mixed matrix composite membrane containing ZIF-7 nano-fillers. *Journal of Membrane Science*, 425:235–242.

Li, X., Cheng, Y., Zhang, H., Wang, S., Jiang, Z., Guo, R., and Wu, H. (2015a). Efficient CO_2 capture by functionalized graphene oxide nanosheets as fillers to fabricate multi-permselective mixed matrix membranes. *ACS Appl Mater Interfaces*, 7(9):5528–5537.

Li, X. Q., Jiang, Z. Y., Wu, Y. Z., Zhang, H. Y., Cheng, Y. D., Guo, R. L., and Wu, H. (2015b). High-performance composite membranes incorporated with carboxylic acid nanogels for CO_2 separation. *Journal of Membrane Science*, 495:72–80.

Li, Y. and Chung, T. S. (2008). Highly selective sulfonated polyethersulfone (spes)-based membranes with transition metal counterions for hydrogen recovery and natural gas separation. *Journal of Membrane Science*, 308(1-2):128–135.

Li, Y., Chung, T. S., and Kulprathipanja, S. (2007). Novel ag+-zeolite/polymer mixed matrix membranes with a high CO_2/CH_4 selectivity. *Aiche Journal*, 53(3):610–616.

Li, Y. F., Xin, Q. P., Wu, H., Guo, R. L., Tian, Z. Z., Liu, Y., Wang, S. F., He, G. W., Pan, F. S., and Jiang, Z. Y. (2014). Efficient CO_2 capture by humidified polymer electrolyte membranes with tunable water state. *Energy & Environmental Science*, 7(4):1489–1499.

Lin, H. and Freeman, B. D. (2004). Gas solubility, diffusivity and permeability in poly(ethylene oxide). *Journal of Membrane Science*, 239(1):105–117.

Lin, H., Van Wagner, E., Freeman, B. D., Toy, L. G., and Gupta, R. P. (2006). Plasticization-enhanced hydrogen purification using polymeric membranes. *Science*, 311(5761):639–642.

Lin, H. Q. and Freeman, B. D. (2005). Materials selection guidelines for membranes that remove CO_2 from gas mixtures. *Journal of Molecular Structure*, 739(1-3):57–74.

Lin, W. H. and Chung, T. S. (2001). Gas permeability, diffusivity, solubility, and aging characteristics of 6fda-durene polyimide membranes. *Journal of Membrane Science*, 186(2):183–193.

Liu, J., Thallapally, P. K., McGrail, B. P., Brown, D. R., and Liu, J. (2012). Progress in adsorption-based CO_2 capture by metal-organic frameworks. *Chem Soc Rev*, 41(6):2308–2322.

Liu, L., Chakma, A., and Feng, X. (2004). Preparation of hollow fiber poly(ether block amide)/polysulfone composite membranes for separation of carbon dioxide from nitrogen. *Chemical Engineering Journal*, 105(1-2):43–51.

Liu, L., Chakma, A., and Feng, X. S. (2008). Gas permeation through water-swollen hydrogel membranes. *Journal of Membrane Science*, 310(1-2):66–75.

Liu, S. L., Shao, L., Chua, M. L., Lau, C. H., Wang, H., and Quan, S. (2013). Recent progress in the design of advanced peo-containing membranes for CO_2 removal. *Progress in Polymer Science*, 38(7):1089–1120.

Liu, Y., Peng, D., He, G., Wang, S., Li, Y., Wu, H., and Jiang, Z. (2014). Enhanced CO_2 permeability of membranes by incorporating polyzwitterion@CNT composite particles into polyimide matrix. *ACS Appl Mater Interfaces*, 6(15):13051–13060.

Liu, Y., Ye, Q., Shen, M., Shi, J., Chen, J., Pan, H., and Shi, Y. (2011). Carbon dioxide capture by functionalized solid amine sorbents with simulated flue gas conditions. *Environ Sci Technol*, 45(13):5710–5716.

Loeb, S. (1981). *The Loeb-Sourirajan membrane: How it came about*. ACS Publications.

Ma, J., Ying, Y., Yang, Q., Ban, Y., Huang, H., Guo, X., Xiao, Y., Liu, D., Li, Y., Yang, W., and Zhong, C. (2015). Mixed-matrix membranes containing functionalized porous metal-organic polyhedrons for the effective separation of CO_2-CH_4 mixture. *Chem Commun*, 51(20):4249–4251.

MacDowell, N., Florin, N., Buchard, A., Hallett, J., Galindo, A., Jackson, G., Adjiman, C. S., Williams, C. K., Shah, N., and Fennell, P. (2010). An overview of CO_2 capture technologies. *Energy & Environmental Science*, 3(11):1645–1669.

Mahajan, R. and Koros, W. J. (2000). Factors controlling successful formation of mixed-matrix gas separation materials. *Industrial & Engineering Chemistry Research*, 39(8):2692–2696.

Mazov, I., Kuznetsov, V. L., Simonova, I. A., Stadnichenko, A. I., Ishchenko, A. V., Romanenko, A. I., Tkachev, E. N., and Anikeeva, O. B. (2012). Oxidation behavior of multiwall carbon nanotubes with different diameters and morphology. *Applied Surface Science*, 258(17):6272–6280.

McMichael, A. J., Woodruff, R. E., and Hales, S. (2006). Climate change and human health: present and future risks. *Lancet*, 367(9513):859–869.

Meldon, J. H., Stroeve, P., and Gregoire, C. E. (2011). Facilitated transport of carbon dioxide: A review. *Chemical Engineering Communications*, 16(1-6):263–300.

Millward, A. R. and Yaghi, O. M. (2005). Metal-organic frameworks with exceptionally high capacity for storage of carbon dioxide at room temperature. *J Am Chem Soc*, 127(51):17998–9.

Murali, R. S., Sridhar, S., Sankarshana, T., and Ravikumar, Y. V. L. (2010). Gas permeation behavior of PEBAX-1657 nanocomposite membrane incorporated with multiwalled carbon nanotubes. *Industrial & Engineering Chemistry Research*, 49(14):6530–6538.

Nafisi, V. and Hagg, M. B. (2014). Development of dual layer of ZIF-8/PEBAX-2533 mixed matrix membrane for CO_2 capture. *Journal of Membrane Science*, 459:244–255.

Oh, J. H., Kang, Y. S., and Kang, S. W. (2013). Poly(vinylpyrrolidone)/KF electrolyte membranes for facilitated CO_2 transport. *Chem Commun*, 49(86):10181–10183.

Ordonez, M. J. C., Balkus, K. J., Ferraris, J. P., and Musselman, I. H. (2010). Molecular sieving realized with ZIF-8/Matrimid® mixed-matrix membranes. *Journal of Membrane Science*, 361(1-2):28–37.

Pera-Titus, M. (2014). Porous inorganic membranes for CO_2 capture: present and prospects. *Chem Rev*, 114(2):1413–1492.

Qiao, Z., Wang, Z., Yuan, S., Wang, J., and Wang, S. (2015). Preparation and characterization of small molecular amine modified PVAm membranes for CO_2/H_2 separation. *Journal of Membrane Science*, 475:290–302.

Qiao, Z. H., Wang, Z., Zhang, C. X., Yuan, S. J., Zhu, Y. Q., Wang, J. X., and Wang, S. C. (2013). PVAm-PIP/PS composite membrane with high performance for CO_2/N_2 separation. *Aiche Journal*, 59(1):215–228.

Quinn, R., Laciak, D. V., and Pez, G. P. (1997). Polyelectrolyte-salt blend membranes for acid gas separations. *Journal of Membrane Science*, 131(1-2):61–69.

Rahman, M. M., Filiz, V., Shishatskiy, S., Abetz, C., Neumann, S., Bolmer, S., Khan, M. M., and Abetz, V. (2013). PEBAX$^{®}$ with PEG functionalized poss as nanocomposite membranes for CO_2 separation. *Journal of Membrane Science*, 437:286–297.

Ramasubramanian, K., Zhao, Y., and Winston Ho, W. S. (2013). CO_2 capture and H_2 purification: Prospects for CO_2-selective membrane processes. *AIChE Journal*, 59(4):1033–1045.

Raupach, M. R., Marland, G., Ciais, P., Le Quere, C., Canadell, J. G., Klepper, G., and Field, C. B. (2007). Global and regional drivers of accelerating CO_2 emissions. *Proc Natl Acad Sci U S A*, 104(24):10288–10293.

Reijerkerk, S. R., Knoef, M. H., Nijmeijer, K., and Wessling, M. (2010). Poly(ethylene glycol) and poly(dimethyl siloxane): Combining their advantages into efficient CO_2 gas separation membranes. *Journal of Membrane Science*, 352(1-2):126–135.

Rezac, M. E., John, T., and Pfromm, P. H. (1997). Effect of copolymer composition on the solubility and diffusivity of water and methanol in a series of polyether amides. *Journal of Applied Polymer Science*, 65(10):1983–1993.

Rezakazemi, M., Amooghin, A. E., Montazer-Rahmati, M. M., Ismail, A. F., and Matsuura, T. (2014). State-of-the-art membrane based CO_2 separation using mixed matrix membranes

(MMMs): An overview on current status and future directions. *Progress in Polymer Science*, 39(5):817–861.

Robeson, L. M. (1991). Correlation of separation factor versus permeability for polymeric membranes. *Journal of Membrane Science*, 62(2):165–185.

Robeson, L. M. (2008). The upper bound revisited. *Journal of Membrane Science*, 320(1-2):390–400.

Rochelle, G. T. (2009). Amine scrubbing for CO_2 capture. *Science*, 325(5948):1652–1654.

Rodenas, T., van Dalen, M., Garcia-Perez, E., Serra-Crespo, P., Zornoza, B., Kapteijn, F., and Gascon, J. (2014). Visualizing MOF mixed matrix membranes at the nanoscale: Towards structure-performance relationships in CO_2/CH_4 separation over NH2-MIL-53(Al)@PI. *Advanced Functional Materials*, 24(2):249–256.

Rumble, J. (1977). *CRC handbook of chemistry and physics*. CRC handbook of chemistry and physics. Boca Raton, Fla. : CRC Press, Boca Raton, Fla. Cleveland, Ohio, 100 edition.

Saeed, M. and Deng, L. Y. (2015). CO_2 facilitated transport membrane promoted by mimic enzyme. *Journal of Membrane Science*, 494:196–204.

Sandru, M., Haukebo, S. H., and Hagg, M. B. (2010). Composite hollow fiber membranes for CO_2 capture. *Journal of Membrane Science*, 346(1):172–186.

Sandru, M., Kim, T. J., and Hagg, M. B. (2009). High molecular fixed-site-carrier PVAm membrane for CO_2 capture. *Desalination*, 240(1-3):298–300.

Shao, L., Low, B. T., Chung, T.-S., and Greenberg, A. R. (2009). Polymeric membranes for the hydrogen economy: Contemporary approaches and prospects for the future. *Journal of Membrane Science*, 327(1-2):18–31.

Shao, L., Quan, S., Cheng, X. Q., Chang, X. J., Sun, H. G., and Wang, R. G. (2013). Developing cross-linked poly(ethylene oxide) membrane by the novel reaction system for H_2 purification. *International Journal of Hydrogen Energy*, 38(12):5122–5132.

Shen, J., Liu, G., Huang, K., Jin, W., Lee, K. R., and Xu, N. (2015). Membranes with fast and selective gas-transport channels of laminar graphene oxide for efficient CO_2 capture. *Angew Chem Int Ed Engl*, 54(2):578–582.

Shen, J., Zhang, M., Liu, G., Guan, K., and Jin, W. (2016). Size effects of graphene oxide on mixed matrix membranes for CO_2 separation. *AIChE Journal*, 62(8):2843–2852.

Shen, J. N., Yu, C. C., Zeng, G. N., and van der Bruggen, B. (2013). Preparation of a facilitated transport membrane composed of carboxymethyl chitosan and polyethylenimine for CO_2/N_2 separation. *Int J Mol Sci*, 14(2):3621–3638.

Shi, Y. T., Burns, C. M., and Feng, X. S. (2006). Poly(dimethyl siloxane) thin film composite membranes for propylene separation from nitrogen. *Journal of Membrane Science*, 282(1-2):115–123.

Shieh, J. J., Chung, T. S., Wang, R., Srinivasan, M. P., and Paul, D. R. (2001). Gas separation performance of poly(4-vinylpyridine)/polyetherimide composite hollow fibers. *Journal of Membrane Science*, 182(1-2):111–123.

Sholl, D. S. and Johnson, J. K. (2006). Materials science. making high-flux membranes with carbon nanotubes. *Science*, 312(5776):1003–1004.

Sridhar, S., Suryamurali, R., Smitha, B., and Aminabhavi, T. M. (2007). Development of crosslinked poly(ether-block-amide) membrane for CO_2/CH_4 separation. *Colloids and Surfaces a-Physicochemical and Engineering Aspects*, 297(1-3):267–274.

Suer, M. G., Bac, N., and Yilmaz, L. (1994). Gas permeation characteristics of polymer-zeolite mixed matrix membranes. *Journal of Membrane Science*, 91(1-2):77–86.

Venturi, D., Grupkovic, D., Sisti, L., and Baschetti, M. G. (2018). Effect of humidity and nanocellulose content on polyvinylamine-nanocellulose hybrid membranes for CO_2 capture. *Journal of Membrane Science*, 548:263–274.

Wang, S. F., Liu, Y., Huang, S. X., Wu, H., Li, Y. F., Tian, Z. Z., and Jiang, Z. Y. (2014). PEBAX-PEG-MWCNT hybrid membranes with enhanced CO_2 capture properties. *Journal of Membrane Science*, 460:62–70.

Wang, S. F., Liu, Y., Zhang, M. W., Shi, D. D., Li, Y. F., Peng, D. D., He, G. W., Wu, H., Chen, J. F., and Jiang, Z. Y. (2016). Comparison of facilitated transport behavior and separation properties of membranes with imidazole groups and zinc ions as CO_2 carriers. *Journal of Membrane Science*, 505:44–52.

Ward, W. J., Browall, W. R., and Salemme, R. M. (1976). Ultrathin silicone-polycarbonate membranes for gas separation processes. *Journal of Membrane Science*, 1(1):99–108.

Wijmans, J. G. and Baker, R. W. (1995). The solution-diffusion model - a review. *Journal of Membrane Science*, 107(1-2):1–21.

Wu, H., Li, X. Q., Li, Y. F., Wang, S. F., Guo, R. L., Jiang, Z. Y., Wu, C., Xin, Q. P., and Lu, X. (2014). Facilitated transport mixed matrix membranes incorporated with amine functionalized MCM-41 for enhanced gas separation properties. *Journal of Membrane Science*, 465:78–90.

Wu, Y., Jia, P., Xu, L., Chen, Z., Xiao, L., Sun, J., Zhang, J., Huang, Y., Bielawski, C. W., and Geng, J. (2017). Tuning the surface properties of graphene oxide by surface-initiated polymerization of epoxides: An efficient method for enhancing gas separation. *ACS Appl Mater Interfaces*, 9(5):4998–5005.

Xiao, S., Feng, X., and Huang, R. Y. M. (2007). Synthesis and properties of 6FDA-MDA copolyimide membranes: Effects of diamines and dianhydrides on gas separation and pervaporation properties. *Macromolecular Chemistry and Physics*, 208(24):2665–2676.

Xin, Q. P., Gao, Y. Y., Wu, X. Y., Li, C. D., Liu, T. Y., Shi, Y., Li, Y. F., Jiang, Z. Y., Wu, H., and Cao, X. Z. (2015a). Incorporating one-dimensional aminated titania nanotubes into sulfonated poly(ether ether ketone) membrane to construct CO_2-facilitated transport pathways for enhanced CO_2 separation. *Journal of Membrane Science*, 488:13–29.

Xin, Q. P., Liu, T. Y., Li, Z., Wang, S. F., Li, Y. F., Li, Z., Ouyang, J. Y., Jiang, Z. Y., and Wu, H. (2015b). Mixed matrix membranes composed of sulfonated poly(ether ether ketone) and a sulfonated metal-organic framework for gas separation. *Journal of Membrane Science*, 488:67–78.

Xiong, L., Gu, S., Jensen, K. O., and Yan, Y. S. (2014). Facilitated transport in hydroxide-exchange membranes for post-combustion CO_2 separation. *ChemSusChem*, 7(1):114–116.

Yang, H., Xu, Z., Fan, M., Gupta, R., Slimane, R. B., Bland, A. E., and Wright, I. (2008). Progress in carbon dioxide separation and capture: a review. *J Environ Sci (China)*, 20(1):14–27.

Yave, W., Car, A., Peinemann, K. V., Shaikh, M. Q., Ratzke, K., and Faupel, F. (2009). Gas permeability and free volume in poly(amide-b-ethylene oxide)/polyethylene glycol blend membranes. *Journal of Membrane Science*, 339(1-2):177–183.

Yave, W., Huth, H., Car, A., and Schick, C. (2011). Peculiarity of a CO_2-philic block copolymer confined in thin films with constrained thickness: "a super membrane for CO_2-capture". *Energy & Environmental Science*, 4(11):4656–4661.

Yave, W., Szymczyk, A., Yave, N., and Roslaniec, Z. (2010). Design, synthesis, characterization and optimization of PTT-b-PEO copolymers: A new membrane material for CO_2 separation. *Journal of Membrane Science*, 362(1-2):407–416.

Yegani, R., Hirozawa, H., Teramoto, A., Himei, H., Okada, O., Takigawa, T., Ohmura, N., Matsumiya, N., and Matsuyama, H. (2007). Selective separation of CO_2 by using novel facilitated transport membrane at elevated temperatures and pressures. *Journal of Membrane Science*, 291(1-2):157–164.

Yi, C. H., Wang, Z., Li, M., Wang, J. X., and Wang, S. C. (2006). Facilitated transport of CO_2 through polyvinylamine/polyethlene glycol blend membranes. *Desalination*, 193(1-3):90–96.

Yu, C. H., Huang, C. H., and Tan, C. S. (2012). A review of CO_2 capture by absorption and adsorption. *Aerosol and Air Quality Research*, 12(5):745–769.

Yu, K. M., Curcic, I., Gabriel, J., and Tsang, S. C. (2008). Recent advances in CO_2 capture and utilization. *ChemSusChem*, 1(11):893–899.

Yuan, S., Wang, Z., Qiao, Z., Wang, M., Wang, J., and Wang, S. (2011). Improvement of CO_2/N_2 separation characteristics of polyvinylamine by modifying with ethylenediamine. *Journal of Membrane Science*, 378(1-2):425–437.

Zhang, H., Guo, R., Hou, J., Wei, Z., and Li, X. (2016). Mixed-matrix membranes containing carbon nanotubes composite with hydrogel for efficient CO_2 separation. *ACS Appl Mater Interfaces*, 8(42):29044–29051.

Zhang, H. Y., Tian, H. L., Zhang, J. L., Gun, R. L., and Li, X. Q. (2018). Facilitated transport membranes with an amino acid salt for highly efficient CO_2 separation. *International Journal of Greenhouse Gas Control*, 78:85–93.

Zhang, L. Z. and Wang, R. (2012). Salting-out effect on facilitated transport membranes for CO_2 separation: From fluoride salt to polyoxometalates. *Rsc Advances*, 2(25):9551–9554.

Zhao, D., Ren, J. Z., Li, H., Li, X. X., and Deng, M. C. (2014). Gas separation properties of poly(amide-6-b-ethylene oxide)/amino modified multi-walled carbon nanotubes mixed matrix membranes. *Journal of Membrane Science*, 467:41–47.

Zhao, D., Ren, J. Z., Wang, Y., Qiu, Y. T., Li, H., Hua, K. S., Li, X. X., Ji, J. M., and Deng, M. C. (2017). High CO_2 separation performance of PEBAX[®]/CNTs/GTA mixed matrix membranes. *Journal of Membrane Science*, 521:104–113.

Zhao, D. Y., Cleare, K., Oliver, C., Ingram, C., Cook, D., Szostak, R., and Kevan, L. (1998). Characteristics of the synthetic heulandite-clinoptilolite family of zeolites. *Microporous and Mesoporous Materials*, 21(4-6):371–379.

Zhao, J., Wang, Z., Wang, J., and Wang, S. (2012). High-performance membranes comprising polyaniline nanoparticles incorporated into polyvinylamine matrix for CO_2/N_2 separation. *Journal of membrane science*, 403:203–215.

Zhao, S., Wang, Z., Qiao, Z. H., Wei, X., Zhang, C. X., Wang, J. X., and Wang, S. C. (2013). Gas separation membrane with CO_2-facilitated transport highway constructed from amino carrier containing nanorods and macromolecules. *Journal of Materials Chemistry A*, 1(2):246–249.

Appendix A

Sample calculations

A.1   Sample calculations for pure gas permeation

Pure gas permeability

Membrane: PVAm/PEBAX(0.025) blend membranes

Membrane area (A): 20.82 cm^2

Membrane thickness (l): 0.0125 cm

Room temperature (T_0): 295.75 K

Ambient pressure (p_0): 76.3 cm Hg

Feed gas pressure (p_{feed}): 226.3 cm Hg

Permeate pressure (p_{perm}): 76.3 cm Hg

Permeate flow rate of CO_2 (V/t): 0.0170 cm^3/s

The permeability of CO_2:

$$P = \frac{V\,l}{A\,t\,(p_{feed} - p_{perm})} \frac{273.15}{T_0} \frac{p_0}{76}$$

$$= \frac{0.0170 \times 0.0125}{20.82 \times (226.3 - 76.3)} \frac{273.15}{295.75} \frac{76.3}{76}$$

$$= 6.29 \times 10^{-8} \ cm^3 \ (STP) \ cm \ cm^{-2} \ s^{-1} \ cm \ Hg^{-1}$$

$$= 629 \ Barrer$$

The permeability of N_2 (11.8 Barrer) at the same conditions can be calculated by the same method.

Ideal gas selectivity

The ideal selectivity of CO_2/N_2 can be calculated by the permeability ratio of CO_2 to N_2:

$$\alpha_{CO_2/N_2} = \frac{P_{CO_2}}{P_{N_2}}$$

$$= \frac{629}{11.8}$$

$$= 53.3$$

A.2 Sample calculations for mixture gas permeation

Gas permeability

Membrane: PVAm/PEBAX(0.025) blend membranes

Mole fraction of CO_2 in feed gas: $x_{feed,\ CO_2}$=0.14

Mole fraction of CO_2 in permeate gas: $x_{perm,\ CO_2}$=0.85

Mole fraction of CO_2 in downstream flow: y'_{CO_2}=0.13

Mole fraction of N_2 in feed gas: $x_{feed,\ N_2}$=0.86

Mole fraction of N_2 in permeate gas: $x_{perm,\ N_2}$=0.15

Mole fraction of N_2 in downstream flow: y'_{N_2}=0.023

Membrane area (A): 20.82 cm^2

Membrane thickness (l): 0.0157 cm

Room temperature (T_0): 294.3 K

Ambient pressure (p_0): 76.1 cm Hg

Feed gas pressure (p_{feed}): 602.6 cm Hg

Permeate pressure (p_{perm}): 76.3 cm Hg

Permeate flow rate (V/t): 0.0054 cm^3/s

The permeability of CO_2:

$$
\begin{aligned}
P_{CO_2} &= \frac{V\ l\ x_{perm,CO_2}}{(p_{feed}x_{feed,CO_2} - p_{perm}y'_{CO_2})\ A\ t} \frac{273.15}{T_0} \frac{p_0}{76} \\
&= \frac{0.0054 \times 0.0157 \times 0.85}{(602.6 \times 0.14 - 76.3 \times 0.13)\ 20.82} \frac{273.15}{294.3} \frac{76.1}{76} \\
&= 4.23 \times 10^{-8}\ cm^3\ (STP)\ cm\ cm^{-2}\ s^{-1}\ cm\ Hg^{-1} \\
&= 423\ Barrer
\end{aligned}
$$

The permeability of N_2:

$$
\begin{aligned}
P_{N_2} &= \frac{V\ l\ x_{perm,N_2}}{(p_{feed}x_{feed,N_2} - p_{perm}y'_{N_2})\ A\ t} \frac{273.15}{T_0} \frac{p_0}{76} \\
&= \frac{0.0054 \times 0.0157 \times 0.15}{(602.6 \times 0.86 - 76.3 \times 0.023)\ 20.82} \frac{273.15}{294.3} \frac{76.1}{76} \\
&= 1.13 \times 10^{-9}\ cm^3\ (STP)\ cm\ cm^{-2}\ s^{-1}\ cm\ Hg^{-1} \\
&= 11.3\ Barrer
\end{aligned}
$$

Selectivity

The selectivity of CO_2/N_2 can be calculated by the permeability ratio of CO_2 to N_2:

$$
\begin{aligned}
\alpha_{CO_2/N_2} &= \frac{P_{CO_2}}{P_{N_2}} \\
&= \frac{423}{11.3} \\
&= 37.5
\end{aligned}
$$

A.3 Sample calculations for experimental errors

Membrane: $NH_4F/PEBAX(0.1)$ blend membrane

Operating temperature: 298.15 K

Feed gas pressure: 700 kPa

The permeability of N_2 was tested three times under the same conditions: 5.04, 4.86, 5.12 Barrer

The average value of N_2 permeability:

$$
P(N_2) = \frac{5.04 + 4.86 + 5.12}{3} = 5.01 \; Barrer \tag{A.1}
$$

The standard deviation (SD) is:

$$
SD_{P(N_2)} = \left[\frac{(5.04 - 5.01)^2 + (4.86 - 5.01)^2 + (5.12 - 5.01)^2}{3 - 1} \right]^{\frac{1}{2}} = 0.13 \; Barrer \tag{A.2}
$$

The relative standard deviation (RSD) is:

$$
RSD = \frac{0.13}{5.01} \times 100\% = 2.66\% \tag{A.3}
$$

The N_2 permeability of the $NH_4F/PEBAX(0.1)$ blend membrane was 5.01±0.13 Barrer. The N_2 permeabilities of the blend membranes with different mass ratios of $NH_4F/PEBAX$ can be calculated by the same method. The relative standard deviation in gas permeability was within 5.4%. The effect of membrane composition on N_2 permeability is shown in Figure A.1.
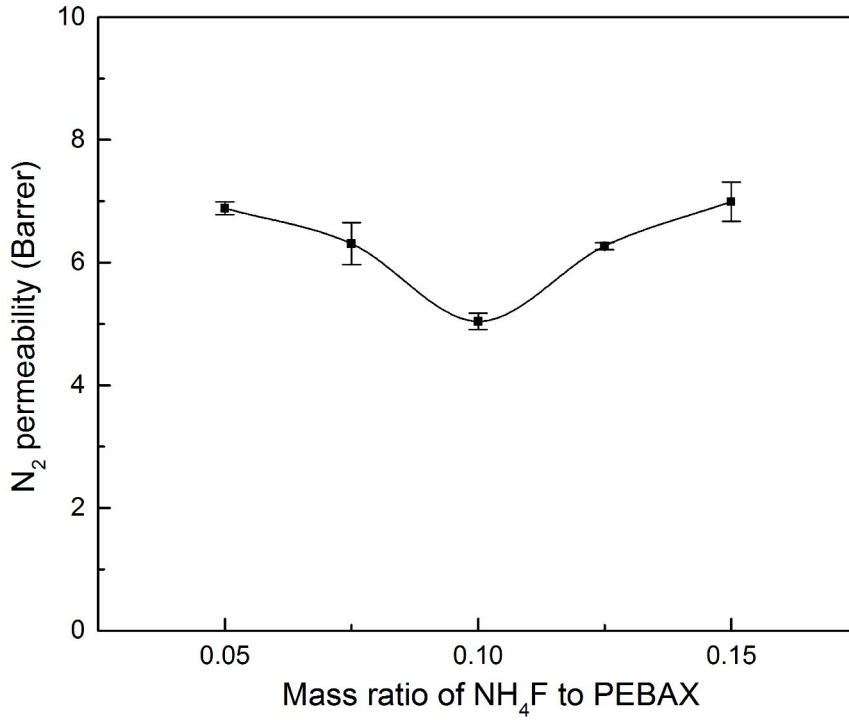
Figure A.1: The effect of membrane composition on N_2 permeability

A.4 Sample calculations for activation energy

The temperature dependence of gas permeability can be fitted by Arrhenius law expression:

$$P_i = P_{0,i} \, exp(-\frac{E_{P,i}}{RT}) \qquad (3.5)$$

Activation energy for gas permeation ($E_{P,i}$) can be obtained from the relationship between $log(P_i)$ and $1/T$ based on the following equations:

$$log(P_i) \quad = \quad log(P_{0,i}) - \frac{E_{P,i}}{ln(10)R}\frac{1}{T} \qquad (A.4)$$

$$Slope \quad = \quad -\frac{E_{P,i}}{ln(10)R} \qquad (A.5)$$

$$E_{P,i} \quad = \quad -Slope \times R \times ln(10) \qquad (A.6)$$

The NH_4F/PEBAX(0.1) membrane was tested for CO_2 permeation at a temperature range from 303.2 to 341.8 K under a feed gas pressure of 700 kPa. The result is shown in Table A.1:

Table A.1: P_{CO_2} of the $NH_4F/PEBAX(0.1)$ membrane at various temperatures

T (K)	P_{CO_2} (Barrer)	1000/T	$log(P_{CO_2})$
302.2	407	3.3	2.61
311.6	417	3.2	2.62
321.1	446	3.1	2.65
331.2	484	3.0	2.68
342.3	515	2.9	2.71

The value of slope can be obtained by the linear regression of the plot of $log(P_i)$ against $1000/T$:

$$Slope = -\frac{E_{P,\,i}}{ln(10)R} = -0.28$$

The activation energy for CO_2 permeation in the $NH_4F/PEBAX(0.1)$ membrane:

$$E_{P,\,i} = -Slope \times R \times ln(10) = -(-0.28) \times 8.314 \times ln(10) = 5.24\ kJ/mol$$